frontiers | Research Topics

Antimicrobial resistance and modern therapeutics approaches

Edited by
Mingkai Li and Rizwan Shahid

Published in
Frontiers in Pharmacology

ISSN 1664-8714
ISBN 978-2-8325-6077-8
DOI 10.3389/978-2-8325-6077-8

About Frontiers

Frontiers is more than just an open access publisher of scholarly articles: it is a pioneering approach to the world of academia, radically improving the way scholarly research is managed. The grand vision of Frontiers is a world where all people have an equal opportunity to seek, share and generate knowledge. Frontiers provides immediate and permanent online open access to all its publications, but this alone is not enough to realize our grand goals.

Frontiers journal series

The Frontiers journal series is a multi-tier and interdisciplinary set of open-access, online journals, promising a paradigm shift from the current review, selection and dissemination processes in academic publishing. All Frontiers journals are driven by researchers for researchers; therefore, they constitute a service to the scholarly community. At the same time, the *Frontiers journal series* operates on a revolutionary invention, the tiered publishing system, initially addressing specific communities of scholars, and gradually climbing up to broader public understanding, thus serving the interests of the lay society, too.

Dedication to quality

Each Frontiers article is a landmark of the highest quality, thanks to genuinely collaborative interactions between authors and review editors, who include some of the world's best academicians. Research must be certified by peers before entering a stream of knowledge that may eventually reach the public - and shape society; therefore, Frontiers only applies the most rigorous and unbiased reviews. Frontiers revolutionizes research publishing by freely delivering the most outstanding research, evaluated with no bias from both the academic and social point of view. By applying the most advanced information technologies, Frontiers is catapulting scholarly publishing into a new generation.

What are Frontiers Research Topics?

Frontiers Research Topics are very popular trademarks of the *Frontiers journals series*: they are collections of at least ten articles, all centered on a particular subject. With their unique mix of varied contributions from Original Research to Review Articles, Frontiers Research Topics unify the most influential researchers, the latest key findings and historical advances in a hot research area.

Find out more on how to host your own Frontiers Research Topic or contribute to one as an author by contacting the Frontiers editorial office: frontiersin.org/about/contact

Antimicrobial resistance and modern therapeutics approaches

Topic editors

Mingkai Li — Air Force Medical University, China

Rizwan Shahid — Alberta Health Services, Canada

Citation

Li, M., Shahid, R., eds. (2025). *Antimicrobial resistance and modern therapeutics approaches*. Lausanne: Frontiers Media SA. doi: 10.3389/978-2-8325-6077-8

Table of contents

frontiers | Frontiers in Pharmacology

TYPE Original Research
PUBLISHED 15 November 2023
DOI 10.3389/fphar.2023.1260632

OPEN ACCESS

EDITED BY
Zul Kamal,
Shaheed Benazir Bhutto University, Pakistan

REVIEWED BY
Islam M. Ghazi,
Long Island University-Brooklyn, United States
Matthias Gerhard Vossen,
Medical University of Vienna, Austria

*CORRESPONDENCE
Silvia Gómez-Zorrilla,
sgomezzorrilla@psmar.cat

†These authors share senior authorship

RECEIVED 18 July 2023
ACCEPTED 23 October 2023
PUBLISHED 15 November 2023

CITATION
Rodríguez-Alarcón A, Sanz de Mena M, Alanti SS, Echeverría-Esnal D, Sorli L, Sendra E, Benítez-Cano A, Membrilla E, Cots F, Güerri-Fernández R, Adalia R, Horcajada JP, Escolano F, Grau S and Gómez-Zorrilla S (2023), A retrospective case-control study to evaluate the use of beta-lactam desensitization in the management of penicillin-allergic patients: a potential strategy for Antimicrobial Stewardship Programs. *Front. Pharmacol.* 14:1260632. doi: 10.3389/fphar.2023.1260632

A retrospective case-control study to evaluate the use of beta-lactam desensitization in the management of penicillin-allergic patients: a potential strategy for Antimicrobial Stewardship Programs

Alicia Rodríguez-Alarcón[1], Manuela Sanz de Mena[2], Soukaina Sara Alanti[2], Daniel Echeverría-Esnal[1], Luisa Sorli[2,3], Elena Sendra[2], Adela Benítez-Cano[4], Estela Membrilla[5], Francesc Cots[6], Robert Güerri-Fernández[2,3], Ramón Adalia[4], Juan Pablo Horcajada[2,3], Fernando Escolano[4], Santiago Grau[1,3†] and Silvia Gómez-Zorrilla[2,3*†] on behalf of PROA-PSMAR

[1]Pharmacy Service, Hospital del Mar, Infectious Pathology and Antimicrobial Research Group (IPAR), Hospital del Mar Research Institute, Universitat Autònoma de Barcelona (UAB), Universitat Pompeu Fabra (UPF), Barcelona, Spain, [2]Infectious Diseases Service, Hospital del Mar, Infectious Pathology and Antimicrobials Research Group (IPAR), Hospital del Mar Research Institute, Universitat Autònoma de Barcelona (UAB), Universitat Pompeu Fabra (UPF), Barcelona, Spain, [3]Center for Biomedical Research in Infectious Diseases Network (CIBERINFEC), Instituto de Salud Carlos III, Madrid, Spain, [4]Department of Anesthesiology and Surgical Intensive Care, Hospital del Mar, Parc de Salut Mar. Hospital del Mar Research Institute, Barcelona, Spain, [5]Surgery Service, Parc de Salut Mar. IHospital del Mar Research Institute, Barcelona, Spain, [6]Management Control Department, Hospital del Mar-Parc de Salut Mar, Barcelona, Spain

Introduction: Penicillin allergy labels (PAL) are common in the hospital setting and are associated with worse clinical outcomes. Desensitization can be a useful strategy for allergic patients when alternative options are suboptimal or not available. The aim was to compare clinical outcomes of patients with PAL managed with antibiotic desensitization vs. those who received alternative non-beta-lactam antibiotic treatments.

Methods: A retrospective 3:1 case-control study was performed between 2015–2022. Cases were adult PAL patients with infection who required antibiotic desensitization; controls were PAL patients with infection managed with an alternative antibiotic treatment. Cases and controls were adjusted for age, sex, infection source, and critical or non-critical medical services.

Results: Fifty-six patients were included: 14 in the desensitization group, 42 in the control group. Compared to the control group, desensitized PAL patients had more comorbidities, with a higher Charlson index (7.4 vs. 5; p = 0.00) and more infections caused by multidrug-resistant (MDR) pathogens (57.1% vs. 28.6%; p = 0.05). Thirty-day mortality was 14.3% in the desensitized group, 28.6% in the control group (p = 0.24). Clinical cure occurred in 71.4% cases and 54.8% controls (p = 0.22). Four control patients selected for MDR strains after alternative

treatment; selection of MDR strains did not occur in desensitized patients. Five controls had antibiotic-related adverse events, including *Clostridioides difficile* or nephrotoxicity. No antibiotic-related adverse events were found in the study group. In multivariate analysis, no differences between groups were observed for main variables.

Conclusion: Desensitization was not associated with worse clinical outcomes, despite more severe patients in this group. Our study suggests that antibiotic desensitization may be a useful Antimicrobial Stewardship tool for the management of selected PAL patients.

KEYWORDS

antibiotic desensitization, penicillins, beta-lactams, antimicrobial stewardship programs, hypersensitivity, allergy

1 Introduction

Antibiotic hypersensitivity is the most commonly reported class of drug hypersensitivity (Wong et al., 2019; Macy, 2020). A high percentage of the population (15%–20%) carries a penicillin allergy label (PAL) (Blumenthal et al., 2017; Rose et al., 2020). Indeed, penicillin allergy is the leading reported antibiotic allergy and accounts for more than half of all antibiotic allergies (Macy, 2020).

Beta-lactams are among the most commonly prescribed antibiotics with numerous clinical indications and are considered the first-line therapy in many bacterial infections (Categorisation, 2019). Alternative treatments used instead of beta-lactam antibiotics in patients with PAL are less effective, are often associated with a higher frequency of adverse effects, provide unnecessary exposure to broad-spectrum antibiotics with the attendant risk of selection of multidrug-resistant (MDR) microorganisms, and are also associated with increased costs (Blumenthal et al., 2018; Blumenthal et al., 2019a; Castells et al., 2019; Shenoy et al., 2019; Blumenthal et al., 2020).

Published studies exploring the management of PAL patients are increasing (Trubiano et al., 2016; Trubiano et al., 2017a; Trubiano et al., 2017b; Rose et al., 2020; Wijnakker et al., 2023; Stone et al., 2020; Ramsey and Mustafa, 2023). Early de-labelling of PAL patients is strongly supported as one of the main actions in Antimicrobial Stewardship Programs (ASP) to avoid unnecessary use of broad-spectrum antibiotics in low-risk allergic patients and to promote the administration of first-line treatment at an early stage of infection (Wijnakker et al., 2023; Ramsey and Mustafa, 2023). There are some strategies available to remove an allergy label, such as skin tests and oral provocation, as well as obtaining a complete allergy history (Trubiano et al., 2016; Trubiano et al., 2017a; Trubiano et al., 2017b; Rose et al., 2020; Stone et al., 2020). Although less widespread, antibiotic desensitization is an option in patients with confirmed or high-risk penicillin allergy (Habib et al., 2015; Paño-Pardo et al., 2022; Rodríguez-Alarcón et al., 2022). The mechanism of desensitization is to induce tolerance to the drug by administering increasing concentrations of the diluted antibiotic and to prevent anaphylaxis due to inhibition of IgE cross-linking and mast cell degranulation. For this reason, desensitization is indicated only for Ig E-mediated allergic reactions (Blumenthal et al., 2019a; Castells et al., 2019). This strategy is only useful at the time of active infection. When antibiotic treatment is stopped, it should be performed again (Rodríguez-Alarcón et al., 2022).

Prior study suggest that desensitization is well tolerated, even in complex patients with high comorbidity scores (Rodríguez-Alarcón et al., 2022). In clinical practice, the most common indications for desensitization are absence of alternative therapeutic options and therapeutic failure (Rodríguez-Alarcón et al., 2022).

We hypothesized that PAL patients who are managed with alternative non-beta-lactam antibiotic treatments have worse outcomes than those who are desensitized and treated with beta-lactams. To the best of our knowledge, this is the first study to assess this issue in a cohort of PAL patients. Previous studies have noted that prolongation of hospitalization, surgical site infection and treatment failure are costly outcomes that are increased in PAL patients (Huang et al., 2018; Stone et al., 2020). However, studies comparing desensitization to alternative treatments in PAL patients are lacking.

We conducted a 3:1 case-control study to compare the clinical outcomes and mortality of PAL patients with infection who were managed with antibiotic desensitization vs. those who were not desensitized and received alternative non-beta-lactam antibiotic treatment.

2 Materials and methods

2.1 Study design and participants

A retrospective 3:1 case-control study was conducted at a tertiary care university hospital in Barcelona (Spain), between 2015 and 2022. All adult PAL patients who required antibiotic desensitization for treatment of the infections during the study period were considered cases. In these cases, patients were managed with beta-lactam desensitization and subsequently given a beta-lactam antibiotic. They were identified through electronic medical records. The control group consisted of PAL patients with a clinical infection who required antibiotic therapy and were potentially eligible to receive a desensitization but were managed with alternative antibiotic treatment based on physician decision. The controls were selected per case, adjusted for age, sex, infection source and critical versus non-critical medical services. Controls were included consecutively starting from the initial day of the study period until the required sample size was reached.

Patients with loss to 30-day follow up or with missing data in the study outcomes were excluded. STROBE guidelines were used to report the study (Supplementary Table S1).

2.2 Desensitization protocol

An Infectious Diseases physician prescribed desensitization in selected patients. The selection was made from patients with severe or life-threatening infections for whom the physician considered that alternative treatment was not available or was suboptimal and could compromise the patient's life expectancy due to the source of infection (e.g., central nervous system) or microbiology (Shenoy et al., 2019; Paño-Pardo et al., 2022). In addition, these patients had to meet one of the following criteria: a) patients with confirmed allergy and the results of previous skin tests positive for penicillin; b) a history of immediate hypersensitivity reactions (including anaphylactic reaction); c) PAL with unconfirmed hypersensitivity, but in a compromised clinical situation and in need of penicillin or a penicillin-related antibiotic (Shenoy et al., 2019). These indications were stipulated based on the non-availability of assessment by allergist during the hospitalization of patients in our center.

Since desensitization strategies carry the risk of complications, all patients were transferred to an intensive care unit (ICU) and were strictly monitored and followed during the procedure. The physicians who supervised desensitization were properly trained for the procedure and the nursing team followed a checklist provided by the pharmacy department (Chen et al., 2019; Rodríguez-Alarcón et al., 2022). Desensitization bags were prepared in sterile laminar flow cabinets in the pharmacy, following predefined protocols for each antibiotic (Rodríguez-Alarcón et al., 2022). Desensitization was not associated with a delay in the administration of antibiotic therapy, since the patient received desensitization within the first few hours after it was prescribed. If the procedure had to be delayed, the patient received a single dose of the alternative antibiotic agent before desensitization to avoid delays in antibiotic administration.

2.3 Data collection and definitions

Demographic, clinical and epidemiological data were collected from hospital medical and nursing records as follows: age and sex; comorbidities and severity of underlying diseases assessed using the age-adjusted Charlson comorbidity index (Charlson et al., 1987; Charlson et al., 1994). Individual matching of three controls, whenever possible, was used with each case. Case and control groups were adjusted for age, sex, infection source (endocarditis, endovascular, intraabdominal, pancreaticobiliary, skin and soft tissue (SST), respiratory and central nervous system) and critical care vs. non-critical care unit patients. The definitions for specific types of infection were based on Centers for Disease Control and Prevention criteria (CDC/NHSN, 2020). Disease severity was calculated using quick SOFA (Seymour et al., 2016) on the day of the desensitization procedure in the study group, and on the day of initiation of alternative treatment in the control group, adjusted for the previously mentioned criteria. The MDR profile was defined according to current international standard definitions (Magiorakos et al., 2012).

Data on allergy history included date of allergy diagnosis (unknown date of allergy diagnosis, less than 1 year, 1–5 years, more than 10 years, childhood). Date of allergy diagnosis was defined as unknown when a patient had an allergy label but did not remember when they were diagnosed. Medical confirmation of allergy, skin prick and/or intradermal testing, clinical manifestations of allergy and antibiotic involved were also collected. All patients with a delayed-type allergic reaction, such as Toxic epidermal necrolysis (TEN), belonged to the control group, as desensitization is not indicated in these patients because it is not IgE-mediated.

Data on the desensitization procedure (indication, antibiotic involved, duration, completion, reactions) were recorded as previously described (Rodríguez-Alarcón et al., 2022). Desensitization costs were calculated including antibiotic cost plus materials for preparation (bags, serums and syringes), human resources in pharmacy (pharmacy technician) and the cost of a 4-h process in an intensive care unit based on critical unit bed-day cost in Spain which is estimated to be 1,250€/day (Rodríguez Villar and Barrientos Yuste, 2014).

2.4 Outcomes and follow-up

The primary outcome variable was clinical cure. Secondary outcomes were 30-day all-cause mortality, infection-related mortality, infection-related hospital days, adverse events related to antibiotic therapy, and hospital readmission at 30 days.

Clinical cure was considered when all signs and symptoms of infection were completely resolved on the day of hospital discharge. Our study included patients with different infectious syndromes, in which length of hospitalization, duration of treatment and/or time to clinical cure can vary depending on the source of infection. For this reason, we performed a second analysis, considering clinical cure at end of treatment (EOT), defined as the resolution of all signs and symptoms of infection at the end of antimicrobial therapy.

Infection-related hospital days was defined as days from the onset of the infection until the end of infection, considered to be discontinuation of antibiotic treatment if the antibiotic was stopped during hospitalization, or hospital discharge if the patient did not finish antibiotic treatment before leaving the hospital.

Hospital readmission was assessed within 30 days of hospital discharge. Patients were followed up to 30 days.

2.5 Statistical analysis

It was not possible to calculate the sample size due to the small number of desensitization cases, since desensitization was only prescribed in selected patients. Based on recommendations from studies conducted in rare diseases, the case-control ratio of 1:3 was chosen precisely to increase the precision of the statistical analysis (Iwagami and Shinozaki, 2022). Continuous quantitative variables are presented as means and standard deviation (SD), and categorical variables as number of cases and percentages. The Student's t-test or Mann-Whitney U test were applied to compare continuous variables, and Fisher's exact test or Pearson's $\chi 2$ test to contrast categorical variables, as appropriate. All p-values were 2-tailed, and statistical significance was set at <0.05. Logistic regression models adjusted for potential confounders were fitted to assess the impact of antibiotic desensitization on outcomes (clinical cure, hospital readmission, mortality). Statistical analysis was performed using SPSS v.25.

TABLE 1 Demographic, clinical and epidemiological data.

Demographic	Desensitized group N = 14	Control group N = 42	*p*-value
Female	9 (64.3)	22 (52.4)	0.32
Male	5 (35.7)	20 (47.6)	0.32
Age, m (SD)	72.8 (±7.5)	73.5 (±13.8)	0.49
Comorbidities			
CHARLSON, m (SD)	7.4 (±3.3)	5 (±2.3)	0.01
Diabetes mellitus	5 (35.7)	11 (26.2)	0.36
Respiratory disease	8 (57.1)	11 (26.2)	0.04
Heart disease	6 (42.9)	12 (28.6)	0.25
Chronic kidney disease	5 (35.7)	5 (11.9)	0.05
Liver disease	3 (21.4)	3 (7.1)	0.16
Solid malignancy	5 (35.7)	10 (23.8)	0.29
Haematological neoplasm	0 (0)	1 (2.4)	0.75
Neurological disease	5 (35.7)	4 (9.5)	0.03
Critical care unit	5 (35.7)	13 (31)	0.49
Infection source			0.78
-Pulmonary	2 (14.3)	11 (26.2)	
-Intraabdominal	3 (21.4)	8 (19)	
-SST	2 (14.3)	7 (16.7)	
-Pancreaticobiliary	1 (7.1)	6 (14.3)	
-Endovascular	2 (14.3)	4 (9.5)	
-Endocarditis	3 (21.4)	3 (7.1)	
-Central nervous system	1 (7.1)	3 (7.1)	
Infection data			
Hospital-acquired	5 (35.7)	20 (47.6)	0.32
Community-acquired	9 (64.3)	22 (52.4)	0.32
Post-surgical infection	5 (35.7)	16 (38.1)	0.57
Bloodstream infection	10 (71.4)	22 (52.4)	0.17
QuickSOFA, m (SD)	0.9 (±0.9)	0.9 (±0.9)	0.84
Polymicrobial	6 (42.9)	11 (26.2)	0.19
MDR pathogens[a]	8 (57.1)	12 (28.6)	0.05

Data are presented as *n* (%), unless otherwise specified. SST: skin and soft tissue. quickSOFA: quick Sequential Organ Failure Assessment. MDR: multidrug-resistant.
[a]At least one MDR pathogen present in cultures. Statistical significance at $p < 0.05$.

2.6 Ethical approval

The study design was revised and approved by the Clinical Research Ethical Committee of Parc de Salut Mar (CEIC Parc de Salut Mar, registration no. 2021/9829/I). The need for written consent to participate in the study was waived due to the observational and retrospective nature of the study. However, patients who were desensitized provided written informed consent prior to the desensitization procedure, as required by standard clinical practice.

3 Results

Fifty-six patients were included: 14 in the desensitization group and 42 in the control group. The demographic, clinical and

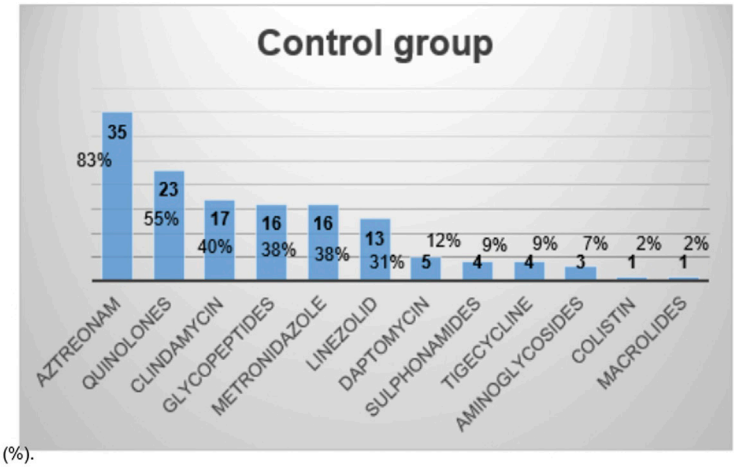

FIGURE 1
Alternative non-beta-lactam treatment administered to non-desensitized group.

TABLE 2 Primary and secondary outcomes.

	Desensitized group N = 14	Control group N = 42	*p*-value
30-day all-cause mortality	2 (14.3)	12 (28.6)	0.24
In-hospital mortality	2 (14.3)	11 (26.2)	0.30
Infection-related mortality	2 (14.3)	9 (21.4)	0.44
Clinical cure (hospital discharge)	10 (71.4)	23 (54.8)	0.22
30-day hospital readmission	5 (35.7)	7 (16.7)	0.13
Antibiotic-related adverse events	0 (0)	5 (11.9)	0.22

Data are presented as *n* (%), unless otherwise specified. Statistical significance at $p < 0.05$.

epidemiological data are shown in Table 1. The results of desensitization were published in a previous study (Rodríguez-Alarcón et al., 2022).

No statistically significant differences in allergy data were found between groups: the dates of allergy diagnosis were as follows: unknown 41 patients (73.2%), in childhood in 3 (5.4%), more than 10 years earlier in 5 (8.9%), between 1 and 5 years earlier in 3 (5.4%), and less than 1 year earlier in 4 (7.1%). Previous clinical manifestations associated with the allergy were: unknown 34 (60.7%), rash 13 (23.2%), anaphylaxis 3 (5.4%), others 6 (10.7%) (uvular edema, dizziness, TEN).

The indications for desensitization in the study group were a lack of available alternative treatment options, failure of non-beta-lactam treatment, or the need to optimize treatment in severe infections (Rodríguez-Alarcón et al., 2022).

Regarding antibiotic treatment, Figure 1 includes alternative non-beta-lactam treatment received by control group. Table 2 shows differences in primary and secondary outcomes between the two groups.

Twelve patients were readmitted to hospital within 30 days, and five were infection-related (two in the desensitized group and three in the control group). With respect to selection of MDR strains, none of the desensitized patients who did not previously have a MDR isolate, selected MDR pathogens after being readmitted. In contrast, four patients in the control group who did not previously have MDR pathogens, selected an MDR strain after readmission. Moreover, antibiotic-related adverse events occurred only in the control group. These were: nephrotoxicity in two patients (both related to vancomycin treatment), *Clostridioides difficile* infection in one patient, hepatotoxicity in one patient (related to teicoplanin treatment), and gastrointestinal disorders in one patient (related to levofloxacin treatment).

Univariate and multivariate analysis of the main outcome are shown in Table 3. No differences in clinical cure were observed at hospital discharge between desensitized patients and those who received an alternative treatment after adjusting for potential confounding variables. No statistically significant differences in clinical cure at EOT were found.

For secondary outcomes, 30-day all-cause mortality and 30-day hospital readmission between desensitized patients and the control group were included in the adjusted analysis (Tables 4, 5, respectively).

Number of infection-related hospital days were 36.4 (±22.4) in the desensitization group and 16.1 (±17.9) in the control group ($p = 0.00$). In the multiple regression model, there were associations with

TABLE 3 Univariate and multivariate analysis of variables predicting clinical cure.

Overall cohort (*n* = 56, clinical cure = 33)						
	Clinical cure (N = 33)	Non-clinical cure (N = 23)	Unadjusted OR (95% CI)	*p*-value	Adjusted OR (95% CI)	*p*-value
Age	73.85 (±12.01)	72.51 (±13.38)	0.97 (0.92–1.03)	0.36	0.98 (0.93–1.03)	0.49
Male	13 (39.4)	12 (52.2)	0.72 (0.19–2.73)	0.63		
CHARLSON index	6.06 (±2.77)	4.96 (±2.69)	1.36 (0.97–1.92)	0.07	1.30 (0.97–1.75)	0.08
Pulmonary disease	11 (33.3)	8 (34.8)	0.57 (0.12–2.79)	0.49		
Chronic kidney disease	5 (15.2)	5 (21.7)	0.17 (0.02–1.28)	0.09	0.24 (0.042–1.43)	0.12
Desensitization	10 (30.3)	4 (17.4)	0.38 (0.07–2.21)	0.28	0.54 (0.11–2.62)	0.45
Post-surgical infection	13 (39.4)	8 (34.8)	1.58 (0.36–6.88)	0.54		
Bloodstream infection	19 (57.6)	13 (56.5)	1.30 (0.30–5.60)	0.72		
QuickSOFA	0.70 (±0.81)	1.22 (±1.08)	0.42 (0.19–0.89)	0.02	0.47 (0.24–0.92)	0.03
Polymicrobial	10 (30.3)	7 (30.4)	0.77 (0.14–4.19)	0.76		
MDR microorganisms	11 (33.3)	9 (39.1)	0.45 (0.09–2.23)	0.33		

Data are presented as *n* (%), unless otherwise specified. OR: odds ratio, CI: confidence interval. quickSOFA: quick Sequential Organ Failure Assessment. MDR: multidrug-resistant. Statistical significance at $p < 0.05$.

TABLE 4 Univariate and multivariate analysis of variables predicting 30-day all-cause mortality.

Overall cohort (*n* = 56, 30-day all-cause mortality = 14)						
	Mortality (N = 14)	Non-mortality (N = 42)	Unadjusted OR (95% CI)	*p*-value	Adjusted OR (95% CI)	*p*-value
Age, m (SD)	68.05 (±12.8)	75.05 (±12.0)	0.95 (0.89–1.01)	0.10	0.95 (0.89–1.01)	0.09
Male	5 (35.7)	20 (47.6)	0.29 (0.06–1.54)	0.15	0.36 (0.08–1.59)	0.18
CHARLSON index, m (SD)	5.29 (±2.8)	5.71 (±2.8)	1.03 (0.77–1.37)	0.85	1.07 (0.82–1.39)	0.61
Pulmonary disease	4 (28.6)	15 (35.7)	1.34 (0.22–7.99)	0.75		
Chronic kidney disease	3 (21.4)	7 (16.7)	1.94 (0.26–14.35)	0.52		
Desensitization	2 (14.3)	12 (28.6)	3.09 (0.38–25.06)	0.29	2.83 (0.42–19.25)	0.29
Post-surgical infection	6 (42.9)	15 (35.7)	1.33 (0.29–6.06)	0.71		
Bloodstream infection	7 (50.0)	25 (59.5)	0.63 (0.11–3.56)	0.60		
QuickSOFA, m (SD)	1.36 (±1.0)	0.76 (±0.9)	2.04 (0.93–4.46)	0.07	1.82 (0.89–3.68)	0.09
Polymicrobial	3 (21.4)	14 (33.3)	0.67 (0.07–6.22)	0.72		
MDR pathogens	4 (28.6)	16 (38.1)	0.86 (0.10–7.33)	0.89	0.61 (0.13–2.89)	0.53

Data are presented as *n* (%), unless otherwise specified. OR: odds ratio, CI: confidence interval. quickSOFA: quick Sequential Organ Failure Assessment. MDR: multidrug-resistant. Statistical significance at $p < 0.05$.

age ($p = 0.01$) and CHARLSON ($p < 0.00$), but not with desensitization ($p = 0.36$).

The cost of the desensitization procedure was estimated to be approximately 250.50€ per patient. The cost of hospitalization between groups (desensitization and control groups) was not compared.

4 Discussion

The present study describes in some detail the clinical characteristics and outcomes of PAL patients with infections who were managed with beta-lactam desensitization followed by beta-lactams compared to those with infection who were treated with

TABLE 5 Univariate and multivariate analysis of variables predicting 30-day hospital readmission.

Overall cohort (*n* = 56, 30-day hospital readmission = 12)						
	Readmission (N = 12)	No readmission (N = 44)	Unadjusted OR (95% CI)	*p*-value	Adjusted OR (95% CI)	*p*-value
Age	77.66 (±7.8)	72.11 (±13.3)	1.04 (0.93–1.17)	0.47		
Male	5 (35.7)	20 (47.6)	0.43 (0.05–3.76)	0.45		
CHARLSON index	8.50 (±3.1)	4.80 (±2.1)	2.29 (1.29–4.07)	0.00	1.91 (1.27–2.86)	0.00
Pulmonary disease	4 (28.6)	15 (35.7)	6.41 (0.63–65.00)	0.12	2.73 (0.50–14.79)	0.24
Chronic kidney disease	3 (21.4)	7 (16.7)	0.19 (0.01–4.28)	0.29	0.45 (0.05–3.94)	0.47
Desensitization	2 (14.3)	12 (28.6)	1.51 (0.06–40.23)	0.80	1.71 (0.20–14.27)	0.62
Post-surgical infection	6 (42.9)	15 (35.7)	0.50 (0.04–5.52)	0.57		
Bloodstream infection	7 (50.0)	25 (59.5)	1.59 (0.13–19.87)	0.72		
QuickSOFA	1.00 (±0.8)	0.89 (±0.9)	0.58 (0.17–1.94)	0.37		
Polymicrobial	3 (21.4)	14 (33.3)	0.24 (0.01–5.64)	0.38		
MDR microorganisms	4 (28.6)	16 (38.1)	0.58 (0.05–6.17)	0.65		

Data are presented as *n* (%), unless otherwise specified. OR: odds ratio, CI: confidence interval. quickSOFA: quick Sequential Organ Failure Assessment. MDR: multidrug-resistant. Statistical significance at $p < 0.05$.

alternative antibiotic therapy. In our study, desensitized patients had higher severity of underlying diseases as assessed by the Charlson comorbidity index. It may be assumed that physicians preferred to use a beta-lactam antibiotic in more complicated patients. Nevertheless, the desensitized group was not associated with worse clinical outcomes (clinical cure, mortality, readmissions) in adjusted analysis. Furthermore, desensitized patients had fewer adverse antibiotic events, including *C. difficile* infection and MDR selection.

Desensitization allows patients to receive more optimal treatments with higher clinical cure rates and lower mortality. In a study carried out in 2020, allergy-labelled patients who received alternative treatments were more likely to die in hospital (Krah et al., 2021). Another study evaluating mortality in recorded penicillin allergy found that that label was associated with a 14% increased risk of death, a result that is potentially modifiable by allergy testing to remove the label and better antibiotic prescribing (Blumenthal et al., 2019b). We observed a non-statistically significant trend toward clinical cure in desensitized patients. Mortality rates in our study were almost twice as high in the non-desensitized group (29% vs. 14%), which is consistent with the literature above.

Despite the fact that the desensitized group had more comorbidities, including respiratory, kidney and neurological diseases, the mortality rates in this group were lower and clinical cure was higher, although no statistically significant differences were observed, probably due to the small sample size. The study group had more severe infections, with more bloodstream or polymicrobial infections and MDR microorganisms, the latter with statistically significant differences.

Desensitization was not independently associated with hospital readmission. Duration of hospitalization attributable to infection was longer in the desensitization group; in the adjusted analysis, it was related to age and Charlson index, but desensitization was not independently associated.

It should be noted that, despite the small sample size, the desensitization group did not select for MDR pathogens, whereas the control group did. These data should be interpreted with caution due to the small number amount of patients, but are nevertheless consistent with previous data suggesting that PAL patients treated with alternative antibiotics are more likely to have MDR infections or to be colonized with an MDR organism (Blumenthal et al., 2018; Blumenthal et al., 2019a; Castells et al., 2019; Shenoy et al., 2019; Blumenthal et al., 2020; Stone et al., 2020; Krah et al., 2021). This may be due to the broader spectrum of alternative treatments. In our cohort, we observed that the non-desensitized group frequently received broad-spectrum antibiotics. Our study suggests that this problem could be partially avoided by desensitizing patients with penicillin allergy as part of the activity of ASP.

Another interesting finding is that desensitization did not cause any adverse events related to the desensitized antibiotic, confirming that this strategy is safe. The use of alternative treatments poses a risk of antibiotic-related adverse events such as nephrotoxicity or *C. difficile*, which could complicate the course of infection. Previous studies also suggest that the use of alternative treatments in PAL patients is associated with an increased risk of adverse events (Castells et al., 2019). A high comorbidity index and chronic kidney disease did not induce antibiotic-related adverse events in the study group, which is an important finding because patients with renal insufficiency, who cannot take certain alternative treatments due to their nephrotoxicity, may be a suitable group for desensitization.

The studies carried out so far have been mainly descriptive with small sample sizes (González-García et al., 2021; Rodríguez-Alarcón et al., 2022). Based on current evidence, desensitization should be used as a last resort in the management of PAL patients. The results observed, both in our study and in the literature, provide support that this strategy can be used safely in selected patients. Our study suggests that PAL patients with severe infections for which there are no alternative options available or in whom an alternative antibiotic treatment has failed, may benefit from desensitization. Patients with serious or life-threatening infections in whom the use of alternative antibiotics may be associated with a worse clinical outcome than the use of beta-lactams are also potential candidates for receipt of desensitization. Nevertheless, it should be borne in mind that this is not a risk-free practice since it must be performed in a strictly monitored area such as the ICU, prepared in a sterile cabinet, and the desensitization procedure must be restarted if it is interrupted, or the antibiotic needs to be re-administered. Nevertheless, the time spent in the ICU is usually short (hours) and standardized protocols can be created to prevent certain risks.

In our study, one of the most commonly used antibiotics in the control group was aztreonam, a monobactam class antibiotic with good activity against gram-negative bacteria but has no activity against gram-positive or anaerobic bacteria (Ramsey and MacGowan, 2016). Although aztreonam has a beta-lactam ring, it does not have a bicyclic structure and can be safely administered in patients with penicillin or cephalosporin allergy, with the exception of ceftazidime (Castells et al., 2019). Ceftazidime and aztreonam have identical side chains and clinical cross-reactivity may occur between these antibiotics (Castells et al., 2019; Wijnakker et al., 2023). As aztreonam contains a beta-lactam ring, its inclusion in the control group may have introduced a bias toward better treatment efficacy than if only non-beta-lactam alternative antibiotics had been included. The decision to include aztreonam as an alternative treatment was based on the fact that it is not generally considered a first-line antibiotic (Ramsey and MacGowan, 2016).

The study has certain limitations derived from the fact that the results are based on a retrospective, single-center, case series study. Second, the sample size of the study group was small, due to the prescription of desensitization in selected patients. A 1:3 ratio was selected to increase the precision of the statistical analysis, based on the recommendations of studies applied in rare diseases (Iwagami and Shinozaki, 2022). Future studies with larger samples are required to confirm the optimal methodology to analyze the matter in this study. Third, due to the retrospective nature of the study and the fact that allergy testing was not routinely performed at our center, the penicillin allergy label was not confirmed in all patients, and some of them had an allergy diagnosis of more than 10 years. Confirmation that IgE-mediated hypersensitivity was still present at the time of desensitization was not possible either due to laboratory delays. While we are aware that it would be ideal to confirm allergy prior to desensitization, there are also certain differences between countries in terms of accessibility to allergists (Paño-Pardo et al., 2022), and in the context of a life-threatening infection where the patient is unstable, a full allergy anamnesis is difficult to make. If it is not possible to carry out a thorough allergy evaluation at the time, desensitization is justified even when the allergy label cannot be confirmed, especially in patients with serious and active life-threatening infections, to avoid delaying beta-lactam administration if the patient can realistically benefit from it for the treatment of their infection (Shenoy et al., 2019; Paño-Pardo et al., 2022). Although a good attempt was made to adjust fully for few covariates, the final number of events was low, which restricts the accuracy of some estimates. There were differences in the baseline characteristics between the two study groups; more specifically, the desensitization group had higher comorbidity scores and more drug-resistant infections and these patients were also more likely to be selected for the desensitization procedure. Although it would have been interesting to conduct an economic analysis to compare the groups, this was not possible due to the retrospective nature of the study and the fact that it was impossible to obtain certain data, especially for patients during the COVID-19 pandemics. This is why we only calculated the approximate cost of desensitization.

Several strengths of this study can be highlighted. Recent interventions have focused on the process and outcomes of de-labelling through a thorough history taking, skin testing and oral challenge, but we explored a unique aspect of antibiotic allergy management: desensitization. To our knowledge, this is the first study to compare the clinical characteristics and outcomes of PAL patients treated with beta-lactams after desensitization versus those managed with alternative options. Beta-lactams are the first-line treatment in many bacterial infections and alternative non beta-lactam treatments are often less effective and associated with more adverse effects. This study provided evidence that desensitization was effective, safe, and not associated with worse clinical cure. Due to the small sample size, the results should be interpreted with caution, but the lack of robust studies in the literature makes our study an interesting starting point to present desensitization as an available option to consider in selected PAL patients that is both effective and safe. Finally, antibiotic desensitization was conducted in severely ill patients with high comorbidity scores, some of them with life-threatening infections. Despite this, the desensitization strategy in our cohort proved to be safe, with no adverse events associated with either desensitization or beta-lactams.

We believe that this study can serve as the basis for a prospective study with desensitization as the intervention.

To conclude, despite higher comorbidity scores and MDR infections, desensitization of PAL patients was not associated with worse clinical cure, higher hospital readmissions or higher mortality rates when compared to PAL patients treated with alternative antibiotics. Our results suggest that antibiotic desensitization could be a useful tool in Antimicrobial Stewardship Programs for the management of selected patients allergic to antibiotics.

Data availability statement

The original contributions presented in the study are included in the article/Supplementary Material, further inquiries can be directed to the corresponding author.

Ethics statement

The study design was revised and approved by the Clinical Research Ethical Committee of Parc de Salut Mar (CEIC Parc de Salut Mar, registration no. 2021/9829/I). The need for written consent to participate in the study was waived due to the observational and retrospective nature of the study. However, patients who were desensitized provided written informed consent prior to the desensitization procedure, as required by standard clinical practice.

Author contributions

AR-A: Conceptualization, Data curation, Formal Analysis, Investigation, Methodology, Resources, Validation, Writing–original draft, Writing–review and editing. MS: Writing–review and editing, Data curation, Investigation, Resources, Validation. SA: Writing–review and editing, Investigation, Methodology, Resources, Validation. DE-E: Formal Analysis, Investigation, Methodology, Validation, Writing–review and editing. LS: Investigation, Methodology, Visualization, Writing–review and editing. ES: Data curation, Investigation, Methodology, Resources, Validation, Writing–review and editing. AB-C: Investigation, Resources, Validation, Writing–review and editing. EM: Investigation, Resources, Validation, Writing–review and editing. FC: Data curation, Methodology, Resources, Writing–review and editing. RG-F: Investigation, Methodology, Resources, Writing–review and editing. RA: Methodology, Supervision, Validation, Writing–review and editing. JH: Validation, Writing–review and editing. FE: Validation, Visualization, Writing–original draft, Writing–review and editing, Investigation, Methodology, Resources, Supervision. SG: Conceptualization, Data curation, Formal Analysis, Funding acquisition, Investigation, Methodology, Resources, Supervision, Validation, Visualization, Writing–original draft, Writing–review and editing. SG-Z: Conceptualization, Data curation, Formal Analysis, Funding acquisition, Investigation, Methodology, Resources, Supervision, Validation, Writing–original draft, Writing–review and editing.

Funding

The author(s) declare financial support was received for the research, authorship, and/or publication of this article. This study was carried out as a part of our routine work.

Acknowledgments

We would like to thank Janet Dawson for English editing and Enric García-Alzorriz for providing the necessary resource consumption data. This study is part of Alicia Rodriguez's PhD program in Medicine of the Universitat Autònoma de Barcelona (Spain). Silvia Gómez-Zorrilla has received research grants unrelated with this study from the Spanish Society of Infectious Diseases and Clinical Microbiology (SEIMC) to support her research and the project "PI21/00509" funded by Instituto de Salud Carlos III (ISCIII) and co-funded by the European Union.

Conflict of interest

The authors declare that the research was conducted in the absence of any commercial or financial relationships that could be construed as a potential conflict of interest.

Publisher's note

Supplementary material

The Supplementary Material for this article can be found online at: https://www.frontiersin.org/articles/10.3389/fphar.2023.1260632/full#supplementary-material

References

Blumenthal, K. G., Kuper, K., Schulz, L. T., Bhowmick, T., Postelnick, M., Lee, F., et al. (2020). Association between penicillin allergy documentation and antibiotic use. *JAMA Intern Med.* 180 (8), 1120–1122. doi:10.1001/jamainternmed.2020.2227

Blumenthal, K. G., Lu, N., Zhang, Y., Li, Y., Walensky, R. P., and Choi, H. K. (2018). Risk of meticillin resistant *Staphylococcus aureus* and *Clostridium difficile* in patients with a documented penicillin allergy: population based matched cohort study. *BMJ* 361 (June), k2400. doi:10.1136/bmj.k2400

Blumenthal, K. G., Lu, N., Zhang, Y., Walensky, R. P., and Choi, H. K. (2019b). Recorded penicillin allergy and risk of mortality: a population-based matched cohort study. *J. Gen. Intern Med.* 34 (9), 1685–1687. doi:10.1007/s11606-019-04991-y

Blumenthal, K. G., Peter, J. G., Trubiano, J. A., and Phillips, E. J. (2019a). Antibiotic allergy. *Lancet* 393 (10167), 183–198. doi:10.1016/S0140-6736(18)32218-9

Blumenthal, K. G., Wickner, P. G., Hurwitz, S., Pricco, N., Nee, A. E., Laskowski, K., et al. (2017). Tackling inpatient penicillin allergies: assessing tools for antimicrobial stewardship. *J. Allergy Clin. Immunol.* 140 (1), 154–161. doi:10.1016/j.jaci.2017.02.005

Castells, M., Khan, D. A., and Phillips, E. (2019). Penicillin allergy. *N. Engl. J. Med.* 381, 2338–2351. doi:10.1056/NEJMra1807761

Categorisation, E. M. A. (2019). Of antibiotics in the European Union. *Eur. Med. Agence.* 31 (December), 1–73.

CDC/NHSN (2020). Surveillance definitions for specific type of infections. *Surveill. Defin*, 1–24.

Charlson, M., Szatrowski, T. P., Peterson, J., and Gold, J. (1994). Validation of a combined comorbidity index. *J. Clin. Epidemiol.* 47 (11), 1245–1251. doi:10.1016/0895-4356(94)90129-5

Charlson, M. E., Pompei, P., Ales, K. L., and MacKenzie, C. R. (1987). A new method of classifying prognostic comorbidity in longitudinal studies: development and validation. *J. Chronic Dis.* 40 (5), 373–383. doi:10.1016/0021-9681(87)90171-8

Chen, X. J. C., Fong, K., Altshuler, D., Dubrovskaya, Y., Louie, E., Amoroso, N., et al. (2019). Evaluation of pharmacy-developed antibiotic desensitization protocols. *Ann. Pharmacother.* 53 (3), 229–251. doi:10.1177/1060028018801959

González-García, R., Albanell-Fernández, M., Aranda, L., Gelis, S., Bartra, J., Soy Muner, D., et al. (2021). Evaluation of desensitization protocols to betalactam antibiotics. *J. Clin. Pharm. Ther.* 47 (June), 592–599. doi:10.1111/jcpt.13578

Habib, G., Lancellotti, P., Antunes, M. J., Bongiorni, M. G., Casalta, J. P., Del Zotti, F., et al. (2015). 2015 ESC Guidelines for the management of infective endocarditis: the task force for the management of infective endocarditis of the European society of eardiology (ESC). Endorsed by: European association for cardio-thoracic surgery (EACTS), the European association of nuclear medicine (EANM). *Eur. Heart J.* 36 (44), 3075–3128. doi:10.1093/eurheartj/ehv319

Huang, K. H. G., Cluzet, V., Hamilton, K., and Fadugba, O. (2018). The impact of reported beta-lactam allergy in hospitalized patients with hematologic malignancies requiring antibiotics. *Clin. Infect. Dis.* 67 (1), 27–33. doi:10.1093/cid/ciy037

Iwagami, M., and Shinozaki, T. (2022). Introduction to matching in case-control and cohort studies. *Ann. Clin. Epidemiol.* 4 (2), 33–40. doi:10.37737/ace.22005

Krah, N. M., Jones, T. W., Lake, J., and Hersh, A. L. (2021). The impact of antibiotic allergy labels on antibiotic exposure, clinical outcomes, and healthcare costs: a systematic review. *Infect. Control Hosp. Epidemiol.* 42 (5), 530–548. doi:10.1017/ice.2020.1229

Macy, E. (2020). Addressing the epidemic of antibiotic "allergy" over-diagnosis. *Ann. Allergy, Asthma Immunol.* 124 (6), 550–557. Available from. doi:10.1016/j.anai.2019.12.016

Magiorakos, A. P., Srinivasan, A., Carey, R. B., Carmeli, Y., Falagas, M. E., Giske, C. G., et al. (2012). Multidrug-resistant, extensively drug-resistant and pandrug-resistant bacteria: an international expert proposal for interim standard definitions for acquired resistance. *Clin. Microbiol. Infect.* 18 (3), 268–281. doi:10.1111/j.1469-0691.2011.03570.x

Paño-Pardo, J. R., Rodilla, E. M., Sacristan, S. C., Saldaña, J. L.C., Párraga, L. P., León, J. L. D. P., et al. (2022). Management of patients with suspected or confirmed antibiotic allergy. Executive summary of guidance from the Spanish Society of Infectious Diseases and Clinical Microbiology (SEIMC), the Spanish Society of Allergy and Clinical Immunology (SEAIC), the Spanish Society of Hospital Pharmacy (SEFH) and the Spanish Society of Intensive Medicine and Coronary Care Units (SEMICYUC). *Enferm Infecc Microbiol Clin (Engl Ed).* 41 (3), 181–186. doi:10.1016/j.eimce.2022.08.010

Ramsey, A., and Mustafa, S. (2023). The penicillin allergy decision rule - something new for penicillin allergy. *JAMA Intern Med.* 183 (9), 953–954. doi:10.1001/jamainternmed.2023.3936

Ramsey, C., and MacGowan, A. P. (2016). A review of the pharmacokinetics and pharmacodynamics of aztreonam. *J. Antimicrob. Chemother.* 71 (10), 2704–2712. doi:10.1093/jac/dkw231

Rodríguez-Alarcón, A., Barceló-Vidal, J., Echeverría-Esnal, D., Sorli, L., Güerri-Fernández, R., Ramis Fernández, S. M., et al. (2022). Antibiotic desensitization as a potential tool in antimicrobial stewardship programs: retrospective data analysis and systematic literature review. *Expert Rev. Anti Infect. Ther.* 20 (11), 1491–1500. doi:10.1080/14787210.2022.2122443

Rodríguez Villar, S., and Barrientos Yuste, R. M. (2014). Long-term admission to the intensive care unit: a cost-benefit analysis. *Rev. Esp. Anestesiol. Reanim.* 61 (9), 489–496. doi:10.1016/j.redar.2014.02.008

Rose, M. T., Slavin, M., and Trubiano, J. (2020). The democratisation of de-labelling: a review of direct oral challenge in adults with low-risk penicillin allergy. *Expert Rev. Anti Infect. Ther.* 8 (11), 1143–1153. doi:10.1080/14787210.2020.1792775

Seymour, C. W., Liu, V. X., Iwashyna, T. J., Brunkhorst, F. M., Rea, T. D., Scherag, A., et al. (2016). Assessment of clinical criteria for sepsis for the third international consensus definitions for sepsis and septic shock (sepsis-3). *JAMA - J. Am. Med. Assoc.* 315 (8), 762–774. doi:10.1001/jama.2016.0288

Shenoy, E. S., Macy, E., Rowe, T., and Blumenthal, K. G. (2019). Evaluation and management of penicillin allergy: a review. *JAMA - J. Am. Med. Assoc.* 321 (2), 188–199. doi:10.1001/jama.2018.19283

Stone, C. A., Trubiano, J., Coleman, D. T., Rukasin, C. R., and Phillips, E. J. (2020). The challenge of de-labeling penicillin allergy. *Allergy* 75 (2), 273–288. doi:10.1111/all.13848

Trubiano, J. A., Beekmann, S. E., Worth, L. J., Polgreen, P. M., Thursky, K. A., Slavin, M. A., et al. (2016). Improving antimicrobial stewardship by antibiotic allergy delabeling: evaluation of knowledge, attitude, and practices throughout the emerging infections network. *Open Forum Infect. Dis.* 3 (3), ofw153–4. doi:10.1093/ofid/ofw153

Trubiano, J. A., Franklin Adkinson, N., and Phillips, E. J. (2017a). Penicillin allergy is not necessarily forever. *JAMA - J. Am. Med. Assoc.* 318 (1), 82–83. doi:10.1001/jama.2017.6510

Trubiano, J. A., Thursky, K. A., Stewardson, A. J., Urbancic, K., Worth, L. J., Jackson, C., et al. (2017b). Impact of an integrated antibiotic allergy testing program on antimicrobial stewardship: a multicenter evaluation. *Clin. Infect. Dis.* 65 (1), 166–174. doi:10.1093/cid/cix244

Wijnakker, R., van Maaren, M. S., Bode, L. G. M., Bulatovic, M., Hendriks, B. J. C., Loogman, M. C. M., et al. (2023). The Dutch Working Party on Antibiotic Policy (SWAB) guideline for the approach to suspected antibiotic allergy. *Clin. Microbiol. Infect.* 29 (7), 863–875. doi:10.1016/j.cmi.2023.04.008

Wong, A., Seger, D. L., Lai, K. H., Goss, F. R., Blumenthal, K. G., and Zhou, L. (2019). Drug hypersensitivity reactions documented in electronic health records within a large health system. *J. Allergy Clin. Immunol. Pract.* 7 (4), 1253–1260. doi:10.1016/j.jaip.2018.11.023

frontiers | Frontiers in Pharmacology

TYPE Original Research
PUBLISHED 29 November 2023
DOI 10.3389/fphar.2023.1325227

OPEN ACCESS

EDITED BY
Zul Kamal,
Shaheed Benazir Bhutto University, Pakistan

REVIEWED BY
Javeed Mahmood,
King Abdullah University of Science and Technology, Saudi Arabia
Ajmir Khan,
Michigan State University, United States

*CORRESPONDENCE
Mohibullah Shah,
mohib@bzu.edu.pk,
mohibusb@gmail.com
Ke Chen,
chen_ke@swmu.edu.cn

†These authors have contributed equally to this work

RECEIVED 20 October 2023
ACCEPTED 20 November 2023
PUBLISHED 29 November 2023

CITATION
Shah M, Khan F, Ahmad I, Deng C-L, Perveen A, Iqbal A, Nishan U, Zaman A, Ullah R, Ali EA and Chen K (2023), Computer-aided identification of *Mycobacterium tuberculosis* resuscitation-promoting factor B (RpfB) inhibitors from *Gymnema sylvestre* natural products.
Front. Pharmacol. 14:1325227.
doi: 10.3389/fphar.2023.1325227

Computer-aided identification of *Mycobacterium tuberculosis* resuscitation-promoting factor B (RpfB) inhibitors from *Gymnema sylvestre* natural products

Mohibullah Shah[1*†], Fatiha Khan[1†], Iqra Ahmad[1], Cun-Liang Deng[2], Asia Perveen[1], Anwar Iqbal[3], Umar Nishan[4], Aqal Zaman[5], Riaz Ullah[6], Essam A. Ali[7] and Ke Chen[2*]

[1]Department of Biochemistry, Bahauddin Zakariya University, Multan, Pakistan, [2]Department of Infectious Diseases, The Affiliated Hospital of Southwest Medical University, Luzhou, China, [3]Department of Chemical Sciences, University of Lakki Marwat, Lakki Marwat, Pakistan, [4]Department of Chemistry, Kohat University of Science and Technology, Kohat, Pakistan, [5]Department of Microbiology and Molecular Genetics, Bahauddin Zakariya University, Multan, Pakistan, [6]Department of Pharmacognosy, College of Pharmacy, King Saud University, Riyadh, Saudi Arabia, [7]Department of Pharmaceutical Chemistry, College of Pharmacy, King Saud University, Riyadh, Saudi Arabia

Tuberculosis (TB), an infectious disease caused by multi-drug resistant *Mycobacterium tuberculosis* (Mtb), has been a global health concern. Mtb affects over a third of the world's population, causing two million deaths annually due to its dormancy and propensity to spread infection during this period. Resuscitation-promoting factor B (RpfB) plays a pivotal role in the growth of Mtb during dormant periods, making it a critical target for eliminating Mtb and curing TB. Gymnema sylvestre is a famous medicinal plant with several medicinal properties, including antimicrobial activity; however, the therapeutic potential of the various reported metabolites of this plant against Mtb has not yet been explored. The aim of this study was to explore the reported natural products of *G. sylvestre* against the RpfB of the Mtb. A total of 131 reported secondary metabolites of this plant were collected and virtually screened against the RpfB. We particularly targeted the Glu292 residue of RpfB as it is crucial for the catalysis of this protein. From our *in-house* library, 114 compounds showed a binding affinity higher than the standard drug. The binding stability of the top three lead compounds was further confirmed through MD simulation analysis. Drug likeness analyses indicated that the ten hits had zero violations of the Lipinski rule of five. In addition, analyses of pharmacokinetics, toxicity, and target prediction revealed that the top compounds are devoid of toxicity and do not affect human proteins. Additionally, they reflect multifaceted approach as anti-TB agents. Our selected hits not only exhibit molecular properties favoring physiological compatibility but also exhibit properties enhancing their potential efficacy as therapeutic candidates. The compounds investigated here are worthy of experimental validation for the discovery of novel treatments against TB. Further, this study also provides a promising avenue for research on the pharmacological potential of *G. sylvestre*.

KEYWORDS

multi-drug resistance, tuberculosis, RpfB, dormancy, *Gymnema sylvestre*, *in-silico*

Introduction

Mycobacterium tuberculosis (Mtb) is the causative agent of one of the most prevalent infectious diseases, tuberculosis (TB). This pathogen mostly affects the lungs, but it can spread to other body parts such as the brain and spine (Chouhan et al., 2023). An important factor leading to its ineffective treatment is incorrect prescription guidance, causing Mtb to develop multi-drug resistance and increased activity in the infection process (Amorim et al., 2022). Mtb uses an effective survival strategy that alternates between active replication and latent non-replication. It goes into reversible low metabolic dormancy, allowing it to survive for a longer period of time without dividing (Kell and Young, 2000). Mtb is compromising the host's immune defense mechanism due to its latent infections, resulting in immune system weakening (Rabaan et al., 2023), and lack of symptoms. According to a WHO study (2018) on the latent TB infection, Mtb affects over a third of the world's population (WHO, 2021a), causing two million deaths annually (Corbett et al., 2003), mainly due to its dormancy and propensity to spread infection during this period (WHO, 2021a).

The increasing multi-drug resistance due to latent infections poses a life-threatening challenge, as current treatments such as isoniazid, rifampicin, ethambutol, and pyrazinamide are effective only for drug-susceptible TB (WHO, 2021b) and are inadequate for its multidrug-resistant, extensively drug-resistant, and totally drug-resistant strains (CDC, 2020; Rabaan et al., 2023). Hence, there exists an urgent necessity to comprehensively grasp the mechanisms underlying the dormancy period of Mtb. This understanding is pivotal to targeting its various metabolic pathways and restricting its strategy to enter low metabolic dormancy. Among the targets considered vital for bacterial growth, especially in the dormant period, is–resuscitation-promoting factor B (RpfB) (Chouhan et al., 2023). Resuscitation-promoting factors have five gene homologues, RpfA, RpfB, RpfC, RpfD, and RpfE, which help Mtb grow in the stationary phase. RpfB is the enzyme that is present in the cell wall of the bacteria and helps in dormancy. RpfB shows the highest complexity in its structure among the five homologs due to the presence of three DUF348 protein domains and one G5 domain, which is made up of two beta-sheets connected to a small triple helix motif (Ruggiero et al., 2016). Targeting the RftB protein is an effective strategy to treat TB as it interacts with peptidoglycan-hydrolyzing endopeptidase, controlling its activity and being responsible for the reactivation of Mtb in chronic cases (Hett et al., 2008).

Natural products extracted from plants have been used for the treatment of different diseases for a long time and are currently becoming more popular due to their low side effects (Aiman et al., 2018; Muhammad et al., 2021). Plants are rich in several antimicrobial secondary metabolites and may be a rich source of potent drugs with a variety of chemical moieties that could target different mechanisms in bacteria (Keita et al., 2022). Compounds like tomatidine showing promise as antibiotic potentiators, enhancing the effectiveness of antibiotics such as gentamicin, cefepime, and ciprofloxacin (Khameneh et al., 2019). Additionally, plant-based phytochemicals are being explored as alternatives to traditional antibiotics, offering new solutions to combat antimicrobial resistance (AlSheikh et al., 2020).

Traditionally used medicinal plants for treating TB includes the leaves of *Cercica papaya*, the seeds of *Combretum hereroense,* and roots of *Zanthoxylum capense.* Among the potential medicinal plants, *Gymnema sylvestre,* which belongs to the family of Apocynaceae, is traditionally used for the treatment of different disorders such as cardiovascular disorders, obesity, osteoporosis, asthma, and infectious disorders (Christopoulos et al., 2010; Tiwari et al., 2014). This plant possesses different medicinal activities, including antioxidant, antibiotic, anti-inflammatory, antiviral, gastroprotective, hepatoprotective, anticancer, and lipid-lowering properties (Khan et al., 2019). Despite the identification of different bioactive compounds from this plant, their possible role in the treatment of TB has not yet been explored. In this context, the aim of this study was to investigate the interacting ability of the reported secondary metabolites of *G. sylvestre* with the RpfB through molecular docking and molecular dynamic simulation studies. The druggability analysis of the lead inhibitors of RpfB opened a new avenue for the experimental validation of these compounds for the possible treatment of TB.

Materials and methods

Target protein selection and preparation

Resuscitation-promoting factor B (RftB), which revives dormant bacterial cells, is pivotal in TB research (Chouhan et al., 2023). The crystal structure of RpfB (PDB ID: 4EMN) was obtained from the Protein Data Bank (PDB). The selection of the 4EMN is justified by its direct relevance to MTb. Also, it depicts the RpfB catalytic domain in complex with benzamidine, obtained through X-ray diffraction. Its singular protein chain and high resolution of 1.17Å will provide a clear basis for precise docking simulations. This target protein was prepared using the Molecular Operating Environment (MOE) by removing water molecules and attached ligands to avoid any hurdles during protein-ligand interactions. It was energy minimized and protonated by using default parameters, and then saved as a MOE molecule file (Muhammad et al., 2020; Jaan et al., 2021).

Active site preparation

The active sites of the RpfB were defined using the MOE Site finder tool. This tool predicted the pockets which are accessible for ligands to make interactions with target proteins. The best binding pocket was selected based on the position of the co-crystallized benzamidine and which is further supported by the reported active sites of RpfB (Chouhan et al., 2023). Dummy atoms were created to make the binding pockets approachable for the ligand atoms.

Ligand selection and preparation

All the reported phytochemicals of *G. sylvestre* were selected as an in-house library for virtual screening against RpfB. The reported compounds were retrieved from the literature (Supplementary Table

S1), drawn in ChemDraw 12.0 software, and saved in mol format. A ligand database was generated in the MOE using default parameters. Energy minimization of the ligand database was performed to keep the structures in an energetically favorable and stable conformation during docking. Benzamidine was used as a reference inhibitor in this study.

Validation of the docking protocol

The validation step involves validating conformation by determining the RMSD value of the reference ligand conformation. Our docked RpfB-Benzamidine complex of the modeled structure and the crystallographically determined X-ray structure of RpfB (PDB ID: 4EMN) with co-crystalized benzamidine (PDB ID: BEN) were compared using the latter as a reference (Alananzeh et al., 2023). The docked protein-ligand complex was superimposed on the co-crystallized protein structure in PyMOL, and the output was set to calculate the RMSD of the docked ligands with the reference. RMSD value (≤2.0 A) was considered a successful docking protocol.

Drug-likeness and physicochemical analysis

Further analysis of the compounds was performed by SwissADME (Daina et al., 2017). This web tool computes the drug-likeness, physicochemical, pharmacokinetic, and ADME properties. It also helps to predict the drugs-like nature and medicinal chemistry of compounds to support drug discovery. Different physicochemical properties of the compounds, i.e., molecular weight 150 g/mol < mw > 500 g/mol, H bond acceptors <10, H bond donors <5, polarity: 20 $Å^2$ < and topological surface area (TPSA) < 160 $Å^2$ were determined.

Pharmacokinetic analysis

The pharmacokinetic features of the synthesized drugs were carefully examined in order to comprehensively evaluate their potential therapeutic value (Daina et al., 2017). The studied pharmacokinetics properties of the top compounds included blood-brain barrier permeation (BBB), human gastrointestinal absorption (GI), skin permeability parameters, plasma P-glycoprotein binding (P-gp), and interaction of the synthesized compounds with five important enzymes of the human cytochromes (P450), i.e., CYP1A2, CYP2D6, CYP2C19, CYP3A4, and CYP2C9. This thorough pharmacokinetic analysis provided essential details regarding how the compounds interact with biological systems, influencing their potential for future research and therapeutic use.

Toxicity prediction

The cytotoxicity, hepatotoxicity, and LD50 values of the top compounds were Pevaluated using the ProTox-2 server (Banerjee et al., 2018).

Target fishing analysis

Target-fishing analyses of the most promising compounds were performed to evaluate their interaction ability with human targets. For this purpose, the Swiss Target Prediction Server was used (Daina et al., 2019). The SMILES codes of the top compounds were generated and used as input files. The results were presented as scores ranging from 0 to 1, where the value 1 corresponds to the most likely target of the query molecule (Kamsri et al., 2019).

PASS prediction

The top hits were subjected to PASS (Prediction of Activity Spectra for Substances) analysis (Filimonov et al., 2014) to find potential biological activities in addition to their predicted antibacterial potential for TB. The PASS server forecast the pharmacological effects, action mechanisms, and biological functions of molecules, based on the structure-activity relationships of established chemical compounds. It represents its predictions as probabilities, reflecting the chances of a compound exhibiting a certain biological activity (Pa). In this study, our attention was focused on properties with a Pa value exceeding 0.7, indicating a strong likelihood that our hits would demonstrate such activities. Given the abundance of the predicted properties, we specifically analyzed those common among the identified hits.

Molecular docking, MD simulations and free energy calculation

In computational biology, molecular docking is an important technique for structure-based drug design to screen potential targets, allowing the calculation of the binding energy of the drug-target complexes and monitoring their reliable interactions at the atomic level (Shah et al., 2021). Molecular docking of RpfB against the energy-minimizing ligand database was done by computing the DOCK command in MOE. The induced fit behavior of the receptor was employed to evaluate the flexible docking of the receptor molecule. Dummy atoms were selected from the sites module; they participated as protein active site during the molecular docking process. Five conformational poses were generated in the output results, and the highest-scored pose of each ligand based on the "S" score and binding energy was considered. The scores of ligands were compared with those of benzamidine as the reference inhibitor. Ligands with a higher docking score than the reference compound were shortlisted for further investigations.

The top three ranked compounds after preliminary analysis were subjected to MD simulation for detailed analysis. The protein was used as receptors, and the top-ranked compounds were prepared as ligands as per the standard protocol of GROMACS (Aslam et al., 2021; Sarfraz et al., 2023). After nvt and npt analysis, the constructed complex was subjected to a production run of 200 ns, and results were analyzed using vmd and in-house scripts (Van Der Spoel et al., 2005).

Moreover, Alchemical free energy simulations have been used for the prediction of free energy changes to explain the binding and

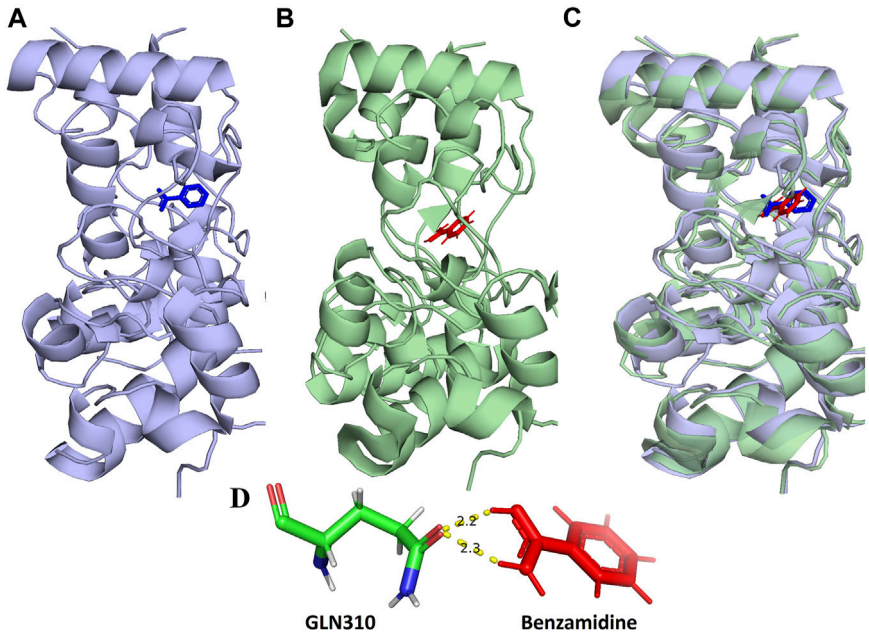

FIGURE 1
(A) Show the location of the binding of benzamidine (blue) in the 3D structure of RpfB (4EMN). **(B)** Binding location of the re-docked benzamidine (red) in RpfB **(C)** Superimposition of A and B complexes shows binding of benzamidine at the same location. **(D)** Molecular interaction of benzamidine in the re-docked benzamidine-RpfB complex.

unbinding mechanism of the three top hits. The binding free energy ($dG_{binding}$) was determined using standard protocol of NAMD (Kim et al., 2020; Phillips et al., 2020). The initial files and simulations step up was established using online server *Free Energy Calculator* (http://www.charmm-gui.org/input/fec). The chemical free energy perturbation for absolute ligand binder was chosen for molecular dynamic simulations (Oshima et al., 2020).

$$\Delta G_{binding} = \Delta G_{Ligand} - \Delta G_{complex}$$

Results and discussion

Validations of docking methodology

The validation of docking methodology was carried out between the co-crystallized Benzamidine-RpfB complex (PDB ID: 4EMN) and the re-docked Benzamidine-RpfB complex. This procedure involved the comparison of 322 residues from both structures. During this alignment, we were able to achieve a match align score of 1780.000, indicating a high level of congruence between the two structures. Notably, in the rigorous refinement process, we observed the exclusion of a small subset of atoms to achieve a more accurate alignment. Specifically, 10 atoms were rejected in the first cycle, followed by the rejection of 3 atoms in the second cycle. Ultimately, the final alignment resulted in the low RMSD value of 0.967 Å, calculated across 309 atoms. This value not only reflects the high quality of our alignment but also serves as a validation of our docking protocol, underscoring its reliability and accuracy in structural comparisons. The superimposition of these structures showed that they share similar binding pockets, suggesting that the ligands engage in analogous molecular interactions across these targets (Figures 1A–C).

Molecular docking results

Molecular docking was accomplished with 129 secondary metabolites of the therapeutic herb *G. sylvestre* and the RpfB protein of Mtb. Binding energies were calculated for all the compounds and ranked accordingly to select the top hits (Supplementary Table S1). The reference ligand showed a docking score of −4.1 kcal/mol. Here, it was found that 110 compounds had a higher docking score than the reference. The docking scores of the top 60 compounds were in the range of −8.25 kcal/mol to −5.1 kcal/mol (Supplementary Table S1), while those of the top ten in the range of −6.2 to −5.1 kcal/mol (Supplementary Table S2). From the results of molecular docking, it was observed that ten compounds, namely, Hop −22 (29)-en-3β-ol, Dimethy 2-methoxy hexane, Benzazirene Carboxylic Acid, Calcium Oxalate, Gymnestrogenin, Lupeol, Gymnemoside C, Gymnemoside D, Gymnemic Acid VII, and Gymnemanol, were inactive and did not show any kind of interactions with the RpfB of Mtb (Supplementary Table S1), This might be due to the structural complexity or flexibility of these compounds, which can hinder the generation of a suitable conformation for docking. Additionally, these compounds may not have been compatible with the chosen binding site, resulting in unsuccessful docking. It is clear that these ten compounds are ineffective as potential inhibitors for RpfB since they are unable to successfully interact with the target protein. This

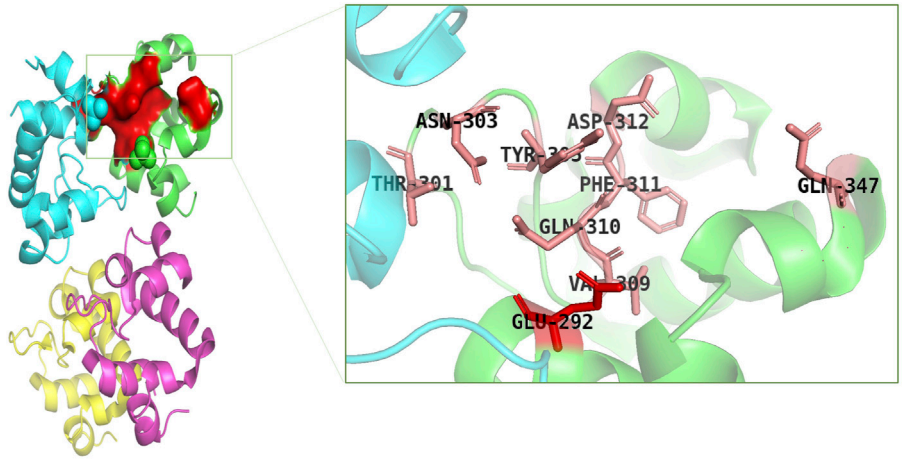

FIGURE 2
Catalytic pocket of RpfB (4EMN); catalytically significant residues are highlighted in pink, and the central residue is highlighted in red.

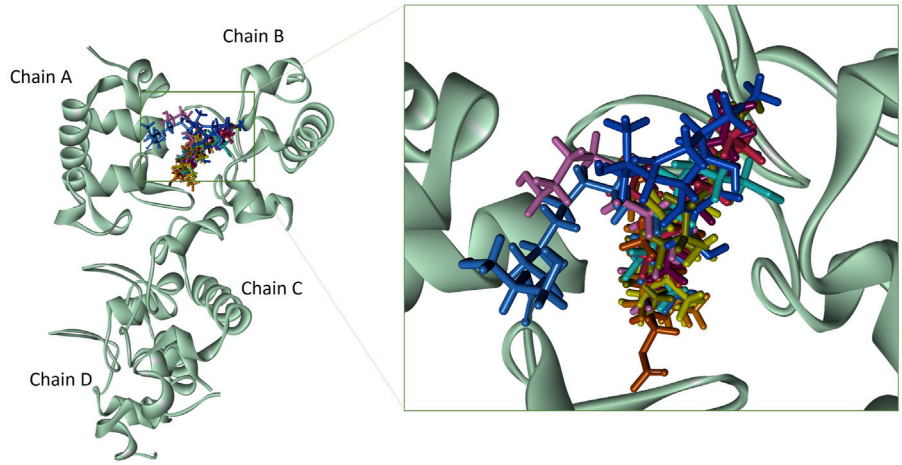

FIGURE 3
Binding of top compounds in the catalytic pocket of RpfB The catalytic pocket resides between chains A and B: nerolidol (yellow), dodecanol (orange), benz(e)azulene-3, 8-dione (zinc-blue), 2-pentadecanone (dark pink), 2-palmitoglycerol (blue), tetradecanoic acid (army green), 6-Octen-1-ol, 3,7-dimethylformate (brown), 8-dodecenol (cyan), methyl tetra decanoate (purple), and tetradecenol (light pink).

implies that additional structural modification of these particular compounds may be necessary to increase their binding affinity.

Protein-ligands interactions

Catalytically significant residues of Rpfb, i. e., Glu292, Tyr305, Val309, Gln310, Phe311, Asp312, Thr301, Gln347 and along with the hydrophobically interacting residues, i. e., CYS291, ILE299, ASN300, THR301, GLY304, TYR305, TYR306, GLY307, GLN310, GLY350, ALA350, PRO354 and CYS355were considered in the active site (Figure 2). It has been observed that residues, particularly Glu292, play an essential role in the hydrogen bond interactions, thereby stabilizing the inhibitors in the catalytic pocket. Moreover, Glu292 is the only amino acid residue that is crucial and indispensable in the catalytic activity and is responsible for the RpfB functions (Squeglia et al., 2013). Interaction with Gln310 is also significant in inhibition, as benzamidine binds to only this residue to inhibit RpfB (Rabaan et al., 2023), and this study also supported these results (Figure 1D).

Based on the drug-likeness criterion, ten ligands were selected for interactions analysis with the receptor. These compounds include 2-Palmitoglycerol, Benz(e)azulene-3,8-dione, Nerolidol, 1-Dodecanol, Tetradecanoic acid, 6-Octen-1-ol-3,7-dimethylformate, 8-Dodecenol, Tetradecanol, Methyl tetra decanoate, and 2-Pentadecanone (Supplementary Table S2). All of the top hits bound to the same region in the catalytic pocket between chains A and B (Figure 3). This position of the hits is similar to the binding location of benzamidine (Figures 1A,B). We observed the hydrogen bond interactions of the ten hits mainly with Glu292 and Gln310

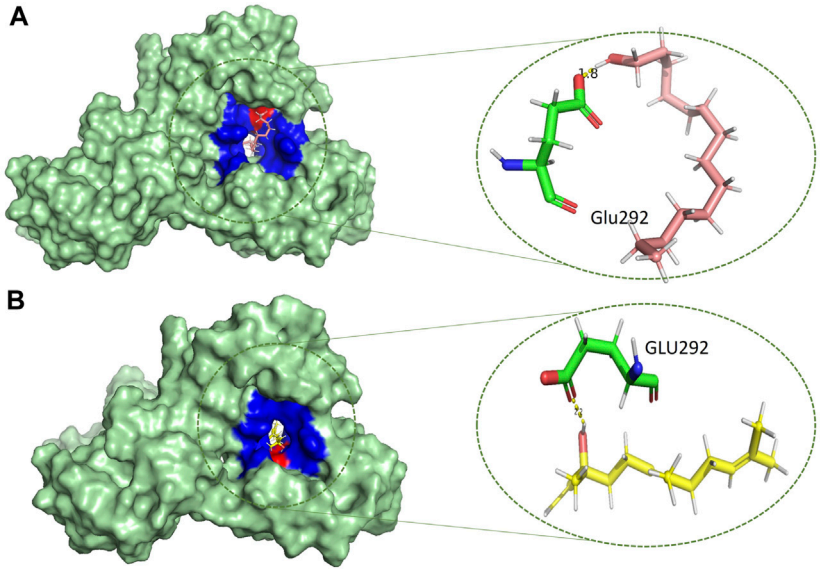

FIGURE 4
Molecular interactions (light green) of **(A)** tetradecanol (light pink) and **(B)** nerolidol (yellow) with RpfB (green), with distinct representations of hydrophilic (red) and hydrophobic (blue) interactions.

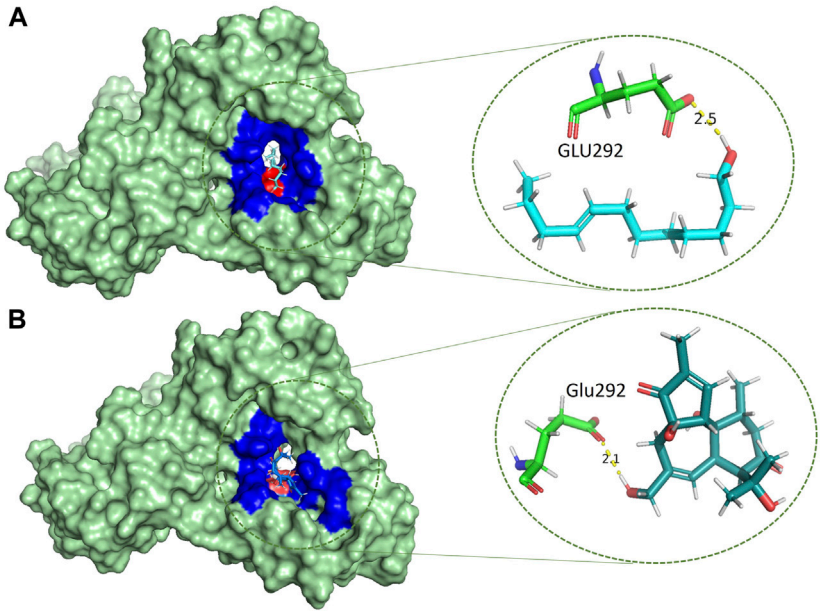

FIGURE 5
Molecular interactions (light green) of **(A)** 8-Dodecenol (cyan) and **(B)** Benz(e)azulene-3,8-dione (zinc-blue) with RpfB (green) with distinct representations of hydrophilic (red) and hydrophobic (blue) interactions.

(Supplementary Table S2). The limited interaction with other residues in the active site suggests a highly targeted mechanism. This focused interaction pattern emphasizes the importance of these residues in the binding affinity and specificity of the compounds. The N-acetyl glucosamine moiety of the Mtb cell wall shows similar interactions with Glu292 and Gln310 of RpfB. This interaction (between RpfB and Mtb cell walls) is involved in the processes that support growth, division, and the maintenance of cell wall integrity (Squeglia et al., 2013). Thereby, targeting these crucial residues significantly suppresses RpfB activity. Some compounds interact with the RpfB protein with shorter bond lengths which indicate stronger bond formation between the protein and the ligands. One of the hits, Tetra-decanol, exhibited hydrogen bonding to the Glu292, with the bond length of 1.8Å

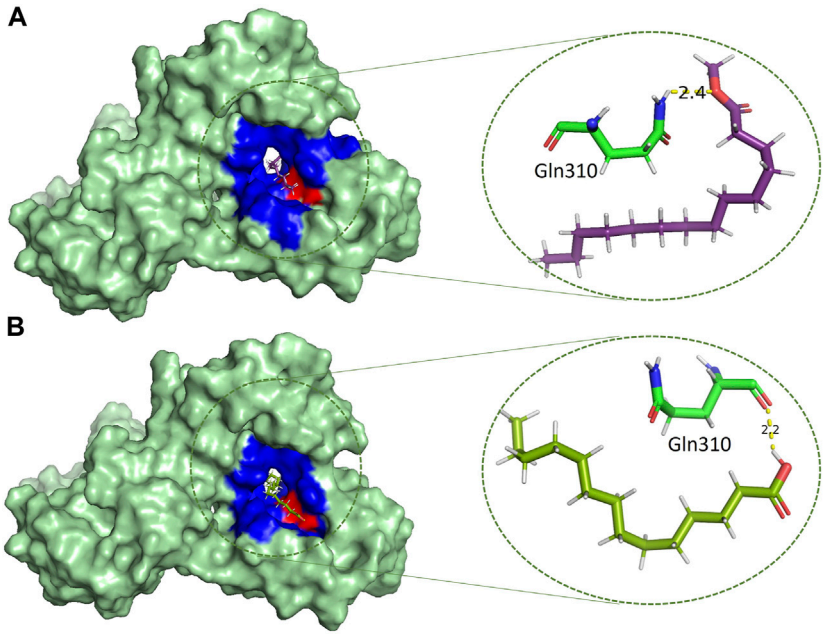

FIGURE 6
Molecular interactions (light green) of **(A)** methyltetradecanoate (purple) and **(B)** tetradecanoic acid (army-green) with RpfB (green), with distinct representations of hydrophilic (red) and hydrophobic (blue) interactions.

(Figure 4A), suggesting biologically significant binding in the inhibition of RpfB. Tetradecanol has been reported previously as an antimicrobial agent (Dherbomez et al., 2006). Other hits showing molecular interaction with RpfB by forming one hydrogen bond with the functional residue, Glu292, are Nerolidol (Figure 4B), 8-Dodecanol (Figure 5A) and Benz(e)-azulene-3,8-dione (Figure 5B) with 2.2Å, 2.5Å and 2.1Å, respectively. Among these compounds, Nerolidol has previously been reported for its antimicrobial, pesticidal, and anti-acne properties (Srinivasan and Kumaravel, 2016).

Methyl tetra decanoate (Figure 6A) and Tetradecanoic acid (Figure 6B) formed a single hydrogen bond with the GGln310, similar to the reference compound Benzamidine with a bond length of 2.4 Å and 2.2 Å, respectively. Tetradecanoic acid has been reported to have antioxidant, anticancer and hypercholesterolemic activities (Srinivasan and Kumaravel, 2016). 2-Pentadecanone showed interactions with the Asn303 of the protein with a bond length of 2.3 Å (Supplementary Figure S1A). 2-pentadecanone has been reported to have wound healing and the antibacterial activity (Mag et al., 2019). 2-Palmitoglycerol, one of the hits, forms a hydrogen bond with Asp312 of the catalytic site of Rpfb (Supplementary Figure S1B). Asp312 is responsible for a more negatively charged electrostatic potential in the substrate binding cleft of RpfB, and it may be associated higher enzymatic activity, but Asp312 is not conversed in all Mtb homologues (Squeglia et al., 2013). Binding between 2-Palmitoglycerol and RpfB could be significant in suppressing RpfB activity. 2-Palmitoglycerol has previously been reported as an antibacterial agent (Adnan et al., 2019). 6-Octen-1-ol-3,7-dimethylformate (Supplementary Figure S2B) formed a hydrogen bond with a minimum bond length of 1.9Å with the Thr301.6-Octen-1-ol-3,7-dimethyl-formate has previously shown monoterpenoid-antiallergenic antimicrobial, and pesticide activity (Srinivasan and Kumaravel, 2016). 1-Dodecanol is the only compound that makes four hydrogen bonds with the RpfB protein with different amino acid residues such as Asn303, Gly302, Thr301 and Tyr305, with different bond lengths (Supplementary Figure S2B). 1-Dodecanol has antibacterial potential and is an insecticide permitted as a food additive in both the U.S. and EU (Togashi et al., 2007; Kazek et al., 2021).

The residues involved in hydrophobic interaction with ligands were mostly common and CYS291, ILE299, ASN300, THR301, GLY304, TYR305, TYR306, GLY307, GLN310, GLY350, ALA350, PRO354, and CYS355. Interestingly, the hydrophobic pocket of RpfB made by these residues is well conserved in the other resuscitation-promoting factors. The preservation of this pocket in all resuscitation-promoting factor types, i.e., A-E, suggests that a hydrophobic environment for Glu292 is important for the catalytic mechanism of these enzymes. Similar to lysozymes and lytic transglycosylases, this hydrophobic environment likely increases the pKa of Glu292, thus allowing this residue to engage a hydrogen-bonding interaction with the glycosidic oxygen of the scissile bond (Inoue et al., 1992). All the significant hydrophobic interactions were observed with the ten hits except for PRO354 (Supplementary Table S2). The maximum number of interactions with the hydrophobically significant residues were observed with Tetradecanoic acid and 2-pentadecanone (Supplementary Table S2). All the lead hits were found to be engaged in hydrophobic interactions in the RpfB binding site (Figures 4–6, Supplementary Figures S1, S2); while they formed 1 to 3 hydrogen bonds, the hydrophobically interacting residues were 8–13. This phenomenon arises from the essential hydrophobic function performed by the active site residues of RpfB. These hydrophobic interactions are

TABLE 1 Drug likeness and physicochemical analysis of the compounds showing higher docking score than benzamidine.

Sr. No.	Compound	Molecular formula	Molecular weight (g/mol)	HA	HBA	HBD	Log P	Log S	MR	TPSA 99 (A^2)	GI absorption	Lipnski rule
1	Vitamin E	$C_{29}H_{50}O_2$	430.71	31	2	1	5.92	−8.60	139.27	29.46	Low	Yes; 1violation
2	Nerolidol	$C_{15}H_{26}O$	222.37	16	1	1	3.64	−3.80	74.00	20.23	High	Yes
3	Oleic acid	$C_{18}H_{34}O_2$	282.46	20	2	1	4.01	−5.41	89.94	37.30	High	Yes; 1 violation
4	Ergosterol	$C_{28}H_{44}O$	396.65	29	1	1	4.01	−6.72	127.47	20.23	Low	Yes; 1violation
5	Cholestan 3 one	$C_{27}H_{46}O$	386.65	28	1	0	4.07	−7.55	123.13	17.07	Low	Yes; 1 violation
6	Dodecanol	$C_{12}H_{26}O$	186.33	13	1	1	3.37	−3.57	60.96	20.23	High	Yes
7	2-pentadecanone	$C_{15}H_{30}O$	226.40	16	1	0	4.01	−4.40	74.42	17.07	High	Yes
8	Hexahydrofarnesyl	$C_{18}H_{36}O$	268.48	19	1	0	4.39	−5.09	88.84	17.07	High	Yes; 1 violation
9	Ethyl palmitate	$C_{18}H_{36}O2$	284.48	20	2	0	4.65	−5.51	89.92	26.30	High	Yes; 1 violation
10	9,12,15-octadecatrienal	$C_{18}H_{30}O$	262.43	19	1	0	4.06	−4.64	87.42	17.07	High	Yes; 1 violation
11	Cholane-5,20 (22)-diene-3b-phenoxy	$C_{30}H_{42}O$	418.65	31	1	0	5.15	−8.03	133.57	9.23	Low	Yes; 1violation
12	1-pentadecanol	$C_{15}H_{32}O$	228.41	16	1	1	4.22	−4.54	75.38	20.23	High	Yes; 1 violation
13	Hopeaphenol	$C_{56}H_{42}O_{12}$	906.93	68	12	10	2.69	−11.40	252.52	220.76	Low	No; 3 violations
14	2-palmitoglycerol	$C_{19}H_{38}O_4$	330.50	23	4	2	4.50	−4.57	97.06	66.76	High	Yes
19	Tetratriacontane	$C_{34}H_{70}$	478.92	34	0	0	8.92	−12.12	165.55	0.00	Low	Yes; 1 violation
20	Triacontane	$C_{30}H_{62}$	422.81	30	0	0	7.86	−10.68	146.32	0.00	Low	Yes; 1 violation
21	Alpha tocopherol acetate	$C_{31}H_{52}O_3$	472.74	34	3	0	6.28	−8.78	148.75	35.53	Low	Yes; 1 violation
22	Diheptan-3-yl Benzene 1,2 Dicarboxylate	$C_{22}H_{34}O_4$	362.50	26	4	0	4.80	−5.58	106.69	52.60	High	Yes; 1 violation
23	Hexacosane	$C_{26}H_{54}$	366.71	26	0	0	7.08	−9.23	127.10	0.00	Low	Yes; 1 violation
24	Gamma tocopherol	$C_{28}H_{48}O_2$	416.68	30	2	1	5.16	−8.29	134.31	29.46	Low	Yes; 1 violation
25	Phytyl acetate	$C_{22}H_{42}O_2$	338.57	24	2	0	5.13	−6.47	108.68	26.30	Low	Yes; 1 violation
27	Isophytol	$C_{20}H_{40}O$	296.53	21	1	1	4.88	−5.75	98.98	20.23	Low	Yes; 1 violation
29	Pentacosane	$C_{25}H_{52}$	352.68	25	0	0	6.81	−8.87	122.29	0.00	Low	Yes; 1 violation
30	Ethyl Octadec-9-enoate	$C_{20}H_{38}O_2$	310.51	22	2	0	5.03	−5.70	99.06	26.30	Low	Yes; 1 violation
31	Eicosane	$C_{20}H_{42}$	282.55	20	0	0	5.64	−7.05	98.25	0.00	Low	Yes; 1 violation

(Continued on following page)

TABLE 1 (*Continued*) **Drug likeness and physicochemical analysis of the compounds showing higher docking score than benzamidine.**

Sr. No.	Compound	Molecular formula	Molecular weight (g/mol)	HA	HBA	HBD	Log P	Log S	MR	TPSA 99 (A^2)	GI absorption	Lipnski rule
32	A-Norcholestan-3-one, 5-ethenyl	$C_{28}H_{46}O$	398.66	29	1	0	4.89	−7.69	127.20	17.07	Low	Yes; 1 violation
34	Methyl palmitate	$C_{17}H_{34}O_2$	270.45	19	2	0	4.41	−5.18	85.12	26.30	High	Yes; 1 violation
35	Bicyclo [2.2.1] heptane, 1,3,3-trimethyl	$C_{22}H_{32}N_2O_4S$	420.57	29	5	1	3.52	−4.46	117.53	84.09	High	Yes
36	Stigmasterol	$C_{29}H_{48}O$	412.69	30	1	1	5.08	−7.46	132.75	20.23	Low	Yes; 1 violation
50	Methyl tetra decanoate	$C_{15}H_{30}O_2$	242.40	17	2	0	75.06	3.88	−4.52	26.30	High	Yes
51	1- pentadecanol	$C_{15}H_{32}O$	228.41	16	1	1	75.38	4.22	−4.54	20.23	High	Yes; 1 violation
53	Tetradecanoic acid	$C_{14}H_{28}O_2$	228.37	16	2	1	71.18	3.32	−4.31	37.30	High	Yes
54	8-dodecanol	$C_{12}H_{24}O$	184.32	13	1	1	60.49	3.45	−3.02	20.23	High	Yes
55	Taxasterol	$C_{50}H_{30}O$	426.42	31	1	1	135.14	4.68	−8.02	20.23	Low	Yes; 1 violation
56	Beta elemene	$C_{15}H_{24}$	204.35	15	0	0	70.42	3.37	−4.76	0.00	Low	Yes; 1 violation
57	6-Octen-1-ol, 3,7-dimethyl-, formate	$C_{11}H_{20}O_2$	184.28	13	2	0	36.19	2.84	−3.36	56.19	High	Yes
58	Tetradecenol	$C_{14}H_{300}$	214.39	15	1	1	70.57	3.90	−4.18	20.23	High	Yes
59	Benz(e)azulene-3,8-dione	$C_{20}H_{28}O_6$	364.43	26	6	4	96.13	0.41	−1.68	115.06	High	Yes

crucial for RpfB to bind to its substrates and perform its enzymatic activities; also, hydrophobic interactions support hydrogen bonds with the catalytically significant residues of RpfB (Inoue et al., 1992).

Drug-likeness and physicochemical analysis

Based on their binding energies, the top sixty compounds were subjected to drug-likeness and physiochemical analysis through Swiss ADME (Daina et al., 2017). It was observed that twenty two compounds did not follow any drug-like property due to their excessive molecular weight (>700 $gmol^{-1}$). Ten compounds were narrowed down from the pool of remaining thirty-eight compounds for thorough examination (as described in the context of molecular interaction analysis), namely, 2-Palmitoglycerol, Benz(e)azulene-3,8-dione, Nerolidol, 1-Dodecanol, Tetradecanoic acid, 6-Octen-1-ol-3,7-dimethylformate, 8-Dodecenol, Tetradecanol, Methyl tetra decanoate, and 2-pentadecanone. These compounds were selected due to their druggability potential and following the Lipinski criterion with no violations, suggesting a promising possibility of having desirable drug-like properties (Lipinski et al., 1997). The compounds meeting this requirement showed adherence to characteristics, including molecular weight (MW), count of hydrogen bond acceptors and donors, logarithm of the partition coefficient (Log P), logarithm of solubility (Log S), molar refractivity (MR), topological polar surface area (TPSA), and potential for gastrointestinal absorption (Table 1). This suggests a favorable balance between hydrophilicity and lipophilicity, ensuring adequate absorption and distribution within the body. The MW, hydrogen bonding capacity and Log P collectively inform on the compound's ability to penetrate cell membranes, while Log S, MR and TPSA are indicative of solubility and overall molecular interaction potential (Ferreira and Andricopulo, 2019).

It is noteworthy that, we opted for the strict adherence to Lipinski's Rule of Five to ensure the selection of compounds with optimal drug-like properties. While it is acknowledged that certain antibiotics in the market may not strictly adhere to these criteria, our choice was guided by the desire to prioritize compounds with favorable pharmacokinetic profiles. Nevertheless, the efficacy of antibiotics can be multifaceted, and deviations from these rules in real-world scenarios underline the complexity of antibiotic drug design. This meticulous process guarantees that the selected compounds not only exhibit molecular properties favoring physiological compatibility but also exhibit properties enhancing their potential efficacy as therapeutic candidates. By combining these multifaceted parameters, the ten compounds emerge as prime candidates warranting in-depth evaluation for their therapeutic potential (Table 1).

TABLE 2 Pharmacokinetic analysis of top compounds performed with the Swiss ADME server.

Sr. No.	Compound name	GI absorption	BBB permeation	P-gp substrate	CYP142 inhibitor	CYP2C19 inhibitor	CYP2C9 inhibitor	CYP2D6 inhibitor	CYP3A4 inhibitor
1	Nerolidol	High	Yes	No	Yes	No	Yes	No	No
2	Dodecanol	High	Yes	No	Yes	No	No	No	No
3	2-Pentadecanone	High	Yes	No	Yes	No	No	No	No
4	2-Palmitoglycerol	High	Yes	No	No	No	No	Yes	No
5	Tetradecanoic acid	High	Yes	No	Yes	No	No	No	No
6	6-Octen-1-ol-3,7-dimethyl-formate	High	Yes	No	No	No	Yes	No	No
7	8-Dodecenol	High	Yes	No	Yes	No	No	No	No
8	Methyltetradecanoate	High	Yes	No	Yes	No	No	No	No
9	Tetradecanol	High	Yes	No	Yes	No	No	No	No
10	Benz(e)-azulene-3,8-dione	High	No	Yes	No	No	No	No	No
Standard	Benzamidine	High	Yes	No	No	No	No	No	No

10.3389/fphar.2023.1325227

TABLE 3 Target fishing analysis of top compounds by swiss target prediction tool.

Sr. No.	Predicted targets	Probability
1	2-Palmitoglycerol	
	Protein kinase C alpha	0.12
	Peptidyl-glycine alphaamidating Monooxygenase	0.10
	NAD-dependent deacetylase sirtuin 2	0.10
	Protein-tyrosine phosphatase 1B	0.10
	Protein kinase C gamma	0.10
2	Methyl tetra decanoate	
	Carbonic anhydrase II	0.2
	Carbonic anhydrase I	0.2
	Estradiol 17-betadehydrogenase 3	0.05
	Fatty acid binding protein adipocyte	0.04
	Peroxisome proliferator activated receptor alpha	0.04
3	Tetra-decenol	
	Transient receptor potential cation channel subfamily M member 8	0.12
	Carbonic anhydrase II	0.09
	Carbonic anhydrase I	0.09
	Carbonic anhydrase IV	0.09
	Androgen Receptor	0.08
4	6-Octen-1-ol-3,7-dimethylformate	
	Transient receptor potential cation channel subfamily A member 1	0.07
	Cholesterol esterase	0.07
	Serotonin 2b (5-HT2b) receptor	0.07
	Alpha-2a adrenergic receptor	0.07
	Serotonin 2c (5-HT2c) receptor	0.07
5	2-pentadecanone	
	Carbonic anhydrase I	0.12
	Carbonic anhydrase II	0.12
	Acyl coenzyme A: cholesterol acyltransferase	0.10
	Carboxylesterase 2	0.10
	Nuclear receptor subfamily 1 group I member 3 (by homology)	0.09
6	8-Dodecenol	
	Nuclear receptor subfamily 1 group I member 3 (by homology)	0.16
	Cytochrome P450 2C19	0.14
	Androgen Receptor	0.12
	Norepinephrine Transporter	0.09
	Protein-tyrosine phosphatase 1B	0.09
7	Tetradecanoic acid	
	Peroxisome proliferator activated Receptor alpha	0.85

(Continued on following page)

TABLE 3 (*Continued*) Target fishing analysis of top compounds by swiss target prediction tool.

Sr. No.	Predicted targets	Probability
	Fatty acid binding protein muscle	0.55
	Free fatty acid receptor 1	0.55
	Peroxisome proliferator activated receptor delta	0.54
	Fatty acid binding protein adipocyte	0.51
8	Dodecanol	
	Transient receptor potential cation channel subfamily M member 8	0.16
	Testis specific androgen-binding protein	0.13
	Dual specificity phosphatase Cdc25B	0.13
	Dual specificity phosphatase Cdc25A	0.12
	Androgen Receptor	0.12
9	Nerolidol	
	Squalene monooxygenase	0.11
	Indoleamine 2,3- dioxygenase	0.06
	Period circadian protein homolog 2	0.06
	Beta-secretase 1	0.06
	Glucagon receptor	0.06

Pharmacokinetic analysis

Pharmacokinetic analysis such as ADME plays a central role in drug design before the clinical trial and decreases the chances of drug failure in the clinical trial (Pires et al., 2015). A compound that has GI absorption >30% shows better absorbance in the body. All hits were predicted to possess high GI absorptions, and they were predicted to not be P-gp (glycoprotein) substrates except Benz(e)-azulene-3,8-dione, providing their favorable intestinal absorption (Table 2). The P-gp is known for efflux of a wide range of molecules, including drug substances, as this can lead to reduced bioavailability or increased resistance (Dahlgren and Lennernäs, 2019). All hits along the reference compound demonstrated the noteworthy ability to permeate the blood-brain barrier (BBB). To mitigate potential neurotoxicity risks of the hits capable of crossing the BBB, we propose structural modifications to reduce BBB permeability and early-stage predictive toxicity screenings. Targeted drug delivery systems can also be employed to limit CNS exposure.

Benz(e)-azulene-3,8-dione and the reference compound benzamidine showed no cytochrome inhibitory potential. These enzymes are responsible for 90% of drug metabolism as well as interfering with the metabolism of a variety of endogenous substances (Kamsri et al., 2019). This suggests that these compounds would not have restrictions due to the inhibition of these cytochromes and would not be metabolized in the body. According to the predictions, CYP142 inhibitors included Nerolidol, 1-Dodecanol, 2-Pentadecanone, Tetra-decanoic acid, 8-Dodecenol, Methyl tetra decanoate and Tetra-decenol. Nerolidol and 6-Octen-1-ol-3,7-dimethylformate can inhibit CYP2C9 cytochromes. CYP2C19 and CYP3A4 were not predicted to be inhibited by any of the hits. This suggests that all ten hits have low affinity for the active sites of two major cytochromes, i.e., CYP2C19 and CYP3A4. Therefore, these compounds will mostly be exposed to CYP2C9, CYP142, and CYP2D6 during absorption, distribution, metabolism, and excretion, and there will be minimal exposure to CYP2C19 and CYP3A4 enzymes during these processes. This might be achieved through rapid clearance or specific tissue targeting.

Cytotoxicity, hepatotoxicity and LD50 value analysis

The prediction of the toxicity of the top ten hits was performed by a ProTox II server (Banerjee et al., 2018). All the hits were predicted to be non-cytotoxic; they show more than a 74% probability of not being cytotoxic agents (Supplementary Table S3). Hepatotoxicity analyses revealed that Tetradecanoic acid has a 52% probability of not being a hepatotoxic agent. LD50 values showed that all the compounds lie in the non-toxic classes except Benz(e)-azulene-3,8-dione which has a LD50 value of 50 kg/mol, and may be toxic to some extent if swallowed (Supplementary Table S3). The non-toxic nature of top hits ensures patient safety and the quality of their lives by minimizing the risk of adverse reactions and harmful effects in the body. Moreover, our hits are more likely to progress efficiently through preclinical studies and clinical efficiently trials, reducing development costs and failures.

Target fishing analysis

Target fishing analyses were performed to identify possible human targets for the selected hits, with a probability value

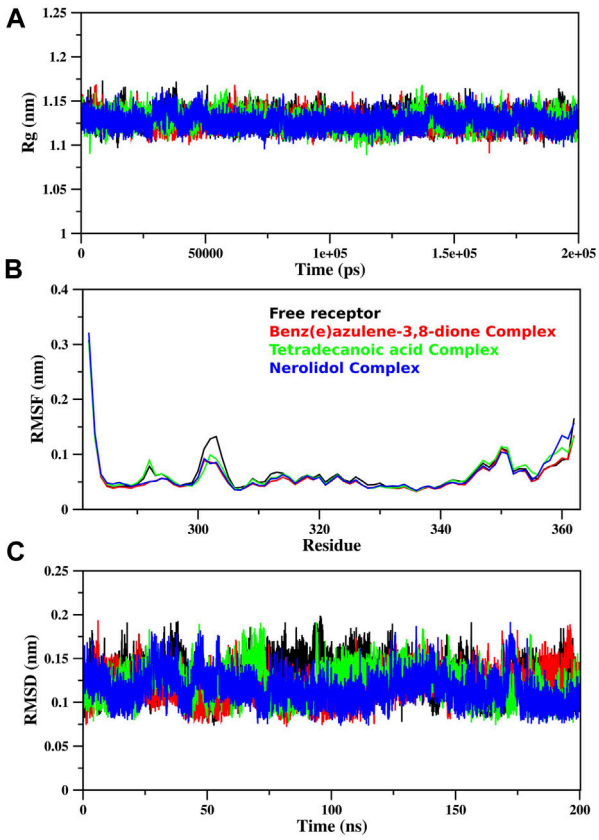

FIGURE 7
MD simulation of RpfB: The simulation of free RpfB and complexes with three lead molecules after docking analysis using MOE The radius of gyration **(A)**, RMSF **(B)**, and RMSD **(C)** were plotted in the figure. Gromacs scripts were used for the extraction of raw data and plotted using Grace Software.

ranging from 0 to 1 (Galati et al., 2021). This step is crucial in assessing the comprehensive pharmacodynamics profile of the hits, particularly for treating Mtb. We aimed to predict both beneficial and harmful interactions within the body. Understanding these interactions helps in evaluating the drug's efficacy and safety, as they can influence both the disease pathology and the drug's therapeutic potential.

The top leads were analyzed by SWISS target prediction to determine if they might inhibit any human protein (Table 3). Among our top hits only one compounds, i.e., Tetradecanoic acid show a high probability (85%) of interacting with human targets, including peroxisome proliferator-activated receptors and fatty acid binding proteins. These targets are involved in lipid metabolism and regulation, thereby suggesting the role of Tetradecanoic acid in such processes (Table 3). Other than Tetradecanoic acid, all other hits showed a very low probability interacting with the human targets. This is significant in terms of the safety and specificity of these compounds. It greatly reduces the risk of adverse effects on human cells and minimizes the potential for drug-drug interactions when used in combination with other medications. 2-Palmitoglycerol, Tetradecenol, 8-Dodecenol and 1-Dodecanol were predicted to interact with various receptors and enzymes, but with very low probabilities (8%–16%). Most of these receptors and enzymes are related to signal transduction and metabolism. Notable targets include protein kinase C alpha, transient receptor potential channels, and CYP2C19. Methyltetradecanoate and 2-pentadecanone were predictively linked to carbonic anhydrase I and II but with very low probabilities of 0.2 and 1.2, respectively, suggesting a limited role in modulating carbon dioxide transport and pH regulation with very low probabilities. 6-Octen-1-ol-3,7-dimethylformate predicted interactions with receptors like serotonin and adrenergic receptors indicating limited involvement in neurotransmission and hormonal signaling. The least possible interactions of Nerolidol with Squalene monooxygenase and Indoleamine 2,3-dioxygenase point toward its non-existent roles in cholesterol synthesis and immune regulation. There were no human targets predicted for Benz(e)-azulene-3,8-dione (Table 3). This suggests that Benz(e)-azulene-3,8-dione will not interact with any human target when taken as an antibiotic drug. This suggests the high degree of the specificity of Benz(e)-azulene-3,8-dione towards the RpfB of the MTb, potentially reducing the likelihood of off-target effects and adverse reactions in the human body. Such specificity could translate into favorable safety profile, making Benz(e)-azulene-3,8-dione a promising candidate for further development. These results demonstrated that our hits can be used across a broader spectrum of patients, regardless of individual variations in human targets, making them versatile and valuable in the treatment of infectious diseases.

Prediction of Activity Spectra

We employed the PASS prediction analysis based on a stringent selection criteria, ensuring that only those properties were considered that showed more than 0.7% probability. Despite the multitude of properties, we strategically focused on commonly shared among the hits. Such analysis is crucial in highlighting alternative therapeutic attributes beyond their primary antibiotic action, possible uncovering multifaceted roles in TB management.

Most of the properties were shown by Tetradecanoic acid and 8-Dodecenol (Supplementary Table S4). The anti-inflammatory property predicted for the hits, is crucial given the inflammatory response often seen in TB infections, which can exacerbate patient suffering and disease progression (Piergallini and Turner, 2018). The anti-hypoxic property is another key finding, given the ability of MTb to survive in hypoxic conditions within the host (Jakkala and Ajitkumar, 2019). Also, as hypoxic Mtb cells have been found to be resistant to anti-tuberculosis drugs, compounds exhibiting this property could play a crucial role in targeting the bacteria in these challenging environments, potentially enhancing the efficacy of TB treatments.

The anti-eczematic and anti-seborrheic properties of most of the hits, while not directly related to TB, indicated a broader spectrum of dermatological benefits, potentially reducing side effects or co-morbid conditions in TB patients (Siewchaisakul et al., 2021). This aspect is particularly relevant given the prolonged treatment regimens required for TB, which often result in patient non-compliance due to adverse effects.

2-Palmitoglycerol was also predicted to have anti-infective and antitoxic property with high probability. Its anti-infective activity

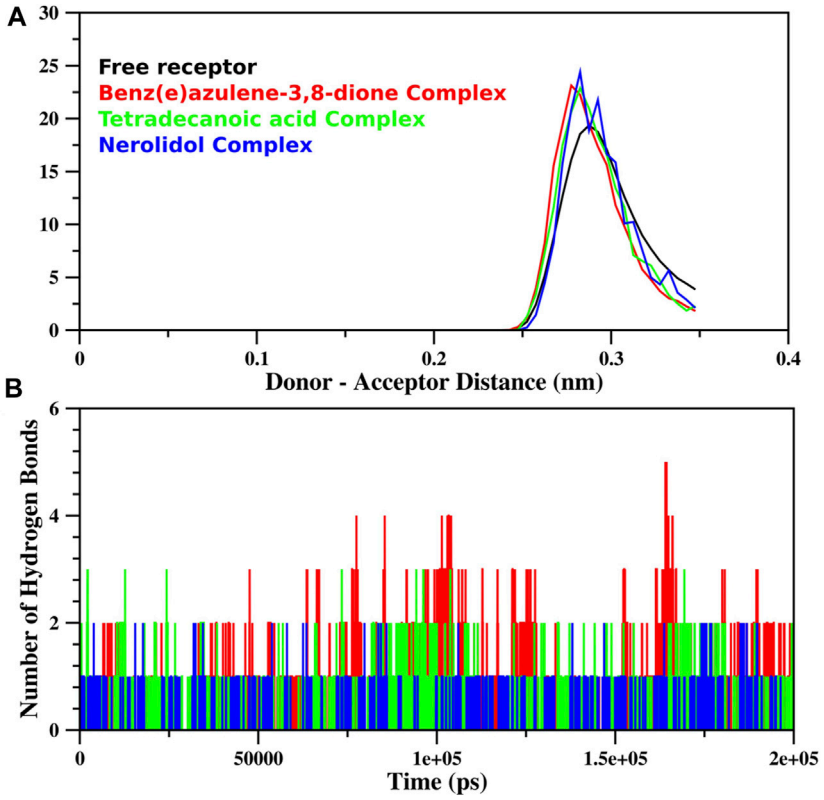

FIGURE 8
Hydrogen bond analysis of the trajectory obtained during MD simulation of RpfB is shown as a function of distance between **(A)** donor and acceptor (nm) and **(B)** simulation time (ps). The total number of hydrogen bonds between receptors and ligands was specified during gromacs command execution. The color profile represents the respective ligands as indicated in the above plot.

suggests its potential in preventing or reducing infections, a critical aspect in TB treatment where secondary infections can complicate patient recovery (Moule and Cirillo, 2020). While the antitoxic capability of 2-Palmitoglycerol indicates its role in neutralizing toxins or reducing their harmful effects. In TB, where the bacterial toxin can contribute to disease severity, this property could provide a dual approach to treatment, targeting both the bacteria and the toxins produced (Pajuelo et al., 2021). Moreover, Benz(e)azulene-3,8-dione due to its unique structure among hits revealed a spectrum of bioactive properties that could be instrumental in developing comprehensive treatment strategies. These properties included its anti-parasitic and anti-helmintic activity. The combined properties of these compounds highlight their potential as multi-target agents in the treatment of TB and associated conditions.

In conclusion, the PASS predictions have provided valuable knowledge about the potential of our hits as anti-TB agents and additional beneficial properties. Further experimental validation of these predictions is necessary to confirm their efficacy and safety.

MD simulation trajectories

The MD simulation of free proteins as receptors and then complexes with the three best-ranked ligands was subjected to 200 ns to ensure the full set of discrete conformational changes and target-bound and target-unbound conformational states. The radius of gyration (Rg), RMSF, and RMSD analyses as functions of time (ns) and residues, respectively, were analyzed (Figure 7). It is important to mention that monomer assembly was used for simulation. Figure 7A represents the degree of compactness; the free RpfB complexed with Nerolidol, Benz(e)azulene-3,8-dione and Tetradecanoic acid was plotted as a function of simulation time. The formation of complexes slightly increases the compactness of the system, but overall, the same and stable profile was observed during the course of simulation. A similar pattern was also observed for RMSD (Figure 7C), and no significant variations were seen during the entire course of simulation, indicating stable interactions of the ligands with the bacterial protein. Hydrogen bonds play an important role in the binding interaction between the ligand and protein. Hydrogen bonds between the three ligands and the receptor were analyzed and plotted as a function of simulation time (Figure 8). We have observed a prominent change in the H-bond donors and acceptors of the free and complexed protein. All the three selected lead compounds increased the number of H bonds acceptor and donors after binding with the receptor proteins. It can be seen from Figure 8 that Benz(e)azulene-3,8-dione form a high number of H bonds in comparison to the other two ligands. However, it is also pertinent to note that the consistency in H bonds with the simulation time was higher in the case of Nerolidol (Figure 8). The number of H bonds and their behavior during the

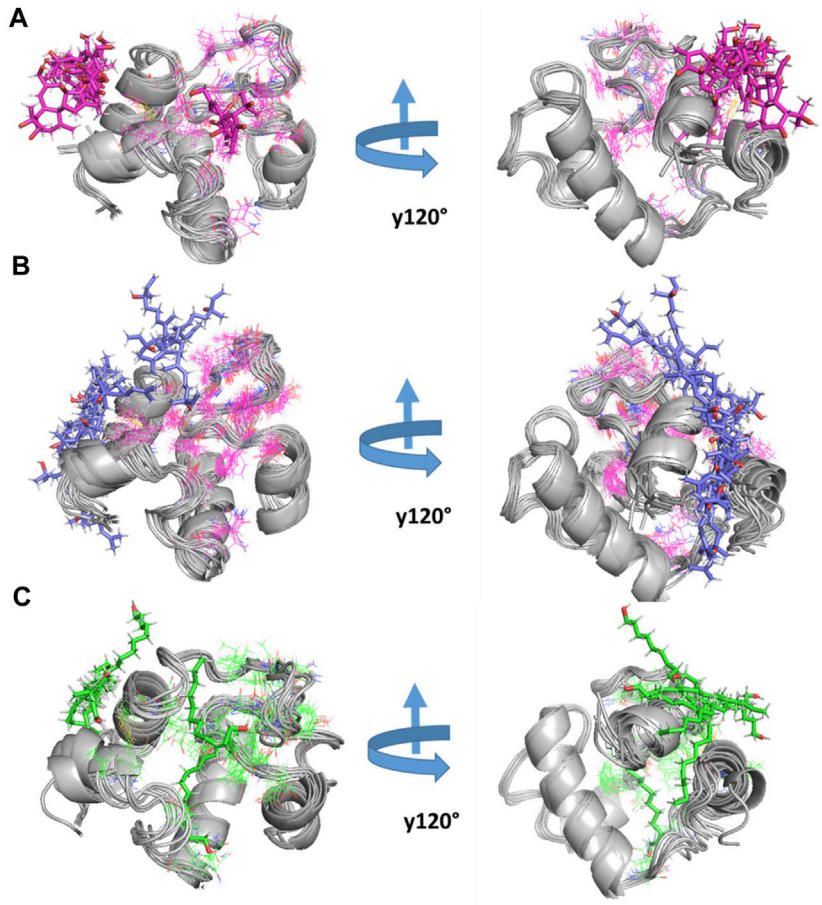

FIGURE 9
MD simulation of RpfB: The three top-ranked ligands were simulated with RpfB using crystal structures (4EMN) as receptors. The complex was constructed using MOE software. After simulation for 200 ns using Gromacs, snap shots at different time intervals (ns) were presented in the figure. **(A)** Represents Benz, **(B)** Nerolidol, and **(C)** represents Tetradecanoic Acid in complex with the receptor.

TABLE 4 The binding free energies of the top three compounds and receptor complexes.

Sr. No.	Compound name	ΔG (kcal/mol)
1	Nerolidol	−14.93 ± 0.34
2	Tetradecanoic acid	−13.86 ± 0.41
3	Benz(e)azulene-3,8-dione	−15.96 ± 0.63

simulation time further indicated the stability of the ligand's protein complexes.

The RMSF analysis of the free RpfB and after complexation with ligands shows variation in different regions (Figure 7B). The degree of perturbation decreases for residues E292-N296, W298-G308, and Q313-W316. The region W298-G308 is the binding pocket as defined by literature and docking experiments (Chouhan et al., 2023). However, the other perturbations in the other two regions were difficult to interpret. To have detailed insight and a plausible explanation, the MD trajectory was transformed into an ensemble analysis. All the structures of the ensembles were analyzed after a 10 ns interval. The ensemble analysis of complexes is important for the recognition of target active sites and ligand stability as a function of time. Figure 8 represents data obtained from the MD simulation of RpfB complexed with all other ligands. Figure 9A represents Benz(e)azulene-3,8-dione, (B) Nerolidol and (C) Tetradecanoicacid in complex with the receptor. In the beginning of the stimulation, the ligand stayed bound to the initial site as defined by docking experiments. For example, in Tetradecanoic acid the initial position of the ligand was maintained for 10 ns, and after 20 ns the ligand shifted towards the binding site constituted by C291, I288, Ala287, I284, R358 and A359 and stayed there for the next 60 ns. The ligand Tetradecanoic acid stayed unbound for 80 ns moved around the receptors, and showed transient interaction for a very short period of time with N-terminal residues. The ligand Tetradecanoic acid shifted towards the active site of the C terminal helix at a time interval of 150 ns and stayed bound for the next 10 ns. A similar pattern was found for Benzo and Nerolidol. The ensemble analysis showed that the ligands changing their position between the defined active site and these: C291, I288, Ala287, I284, R358, and A359. These observations may need further analysis to decode the movement of the ligands between these two different sites.

The binding free energies as obtained from alchemical free methods shows preferentially affinity of ligands towards binding

site (Table 4). The Nerolidol and Benz(e)azulene-3,8-dione shows comparatively greater free energies then tetradecanoic acid as shown by table. These results shows agreement with the hydrogen bonds tendencies as obtained from MD simulations and comparable scaffold of compounds.

Conclusion

It is of utmost importance to comprehend the pathogenesis of TB, which necessitates the revival of Mtb. This is because latent TB affects a staggering one-third of the global population. The resuscitation of Mtb from dormancy is primarily caused by resuscitation-promoting factor (RpfB), making it an attractive target for developing TB drugs in light of latent TB effects. Glu292 of RpfB plays a central role in catalytic activity, and targeting it effectively inhibits RpfB activity, which stops the growth of bacteria in dormancy. This study investigated the phytochemicals from *G. sylvestre* against the RpfB for the discovery of putative novel therapeutic agents for TB. Our results demonstrated that of the reported secondary metabolites from *G. sylvestre*, at least ten compounds showed strong affinity to inhibit RpfB by interacting with the crucial Glu292 residue of the active site. The stability of the ligands with the receptor was further confirmed by the MD simulation at 200 ns, which indicated that the ligands and receptor are highly stable. The top leads were found to follow all the required druggability criteria and possess the least toxicity towards the host. In addition to their direct anti-TB potential, the hits exhibited expanded biological spectra that might further assist in TB treatment. The compounds explored in this study are worthy enough to be subjected to experimental validation. This study also provides a promising for the research on the pharmacological potential of *G. sylvestre*.

Data availability statement

The original contributions presented in the study are included in the article/Supplementary Material, further inquiries can be directed to the corresponding authors.

Author contributions

MS: Conceptualization, Project administration, Resources, Supervision, Writing–review and editing. FK: Formal Analysis, Investigation, Writing–original draft. IA: Formal Analysis, Investigation, Writing–original draft. C-LD: Formal Analysis, Investigation, Methodology, Visualization, Writing–review and editing. AP: Formal Analysis, Investigation, Writing–original draft. AI: Formal Analysis, Investigation, Methodology, Visualization, Writing–review and editing. UN: Data curation, Investigation, Methodology, Visualization, Writing–review and editing. AZ: Investigation, Methodology, Software, Validation, Visualization, Writing–review and editing. RU: Methodology, Software, Validation, Visualization, Writing–review and editing. EA: Conceptualization, Project administration, Visualization, Writing–review and editing. KC: Methodology, Resources, Software, Validation, Writing–review and editing.

Funding

The author(s) declare financial support was received for the research, authorship, and/or publication of this article. This research work was supported by the Doctoral Research Fund awarded to KC. The research work was also supported by the researchers supporting Project number (RSP-2023R45) at King Saud University, Riyadh, Saudi Arabia.

Acknowledgments

The authors wish to thank Researchers Supporting Project Number (RSP-2023R45) at King Saud University Riyadh Saudi Arabia. The authors are also thankful to the Bahauddin Zakariya University, Multan, Pakistan, for providing the necessary infrastructure to perform this research. KC acknowledges the doctoral research fund of the Affiliated Hospital of Southwest Medical University, Luzhou 646000, China.

Conflict of interest

The authors declare that the research was conducted in the absence of any commercial or financial relationships that could be construed as a potential conflict of interest.

Publisher's note

Supplementary material

The Supplementary Material for this article can be found online at: https://www.frontiersin.org/articles/10.3389/fphar.2023.1325227/full#supplementary-material

References

Adnan, Md., Nazim Uddin Chy, Md., Mostafa Kamal, A. T. M., Azad, M., Paul, A., Uddin, S., et al. (2019). Investigation of the biological activities and characterization of bioactive constituents of *Ophiorrhiza rugosa* var. *prostrata* (D.don) & mondal leaves through *in vivo*, *in vitro*, and *in silico* approaches. *Molecules* 24, 1367. doi:10.3390/molecules24071367

Aiman, S., Shehroz, M., Munir, M., Gul, S., Shah, M., and Khan, A. (2018). Species-wide genome mining of Pseudomonas putida for potential secondary metabolites and drug-like natural products characterization. *J. Proteomics Bioinform* 11. doi:10.4172/jpb.1000460

Alananzeh, W. A., Al, M. N., Ayipo, Y. O., and Mordi, M. N. (2023). N - substituted tetrahydro - beta - carboline as mu - opioid receptors ligands: *in silico* study; molecular docking, ADMET and molecular dynamics approach. *Mol. Divers*. doi:10.1007/s11030-023-10655-1

AlSheikh, H. M.Al, Sultan, I., Kumar, V., Rather, I. A., Al-Sheikh, H., Tasleem Jan, A., et al. (2020). Plant-based phytochemicals as possible alternative to antibiotics in combating bacterial drug resistance. *Antibiotics* 9, 480. doi:10.3390/antibiotics9080480

Amorim, J. C., Cabrera Bermeo, A. E., Vásquez Urgilés, V. E., Martínez León, M. R., and Carpio Arévalo, J. M. (2022). An in-silico evaluation of anthraquinones as potential inhibitors of DNA gyrase B of *Mycobacterium tuberculosis*. *Microorganisms* 10, 2434. doi:10.3390/microorganisms10122434

Aslam, M., Shehroz, M., Ali, F., Zia, A., Pervaiz, S., Shah, M., et al. (2021). *Chlamydia trachomatis* core genome data mining for promising novel drug targets and chimeric vaccine candidates identification. *Comput. Biol. Med.* 136, 104701. doi:10.1016/j.compbiomed.2021.104701

Banerjee, P., Eckert, A. O., Schrey, A. K., and Preissner, R. (2018). ProTox-II: a webserver for the prediction of toxicity of chemicals. *Nucleic Acids Res.* 46, W257-W263–W263. doi:10.1093/nar/gky318

CDC (2020). Treatment REgimens for latent TB infection [WWW document]. Centres for Disease Control and Prevention. URL Available at: https://www.google.com/search?q=Treatment+Regimens+for+Latent+TB+Infection&oq=Treatment+Regimens+for+Latent+TB+Infection&gs_lcrp=EgZjaHJvbWUyBggAEEUYOTIGCAEQRRg80gEHMjIxajBqN6gCALACAA&sourceid=chrome&ie=UTF-8 (Accessed August 25, 2023).

Chouhan, M., Tiwari, P. K., Moustafa, M., Chaubey, K., Gupta, A., Kumar, R., et al. (2023). Inhibition of *Mycobacterium tuberculosis* resuscitation-promoting factor B (RpfB) by microbially derived natural compounds: a computational study. *J. Biomol. Struct. Dyn.* 0, 1–12. doi:10.1080/07391102.2023.2208214

Christopoulos, M. V., Rouskas, D., Tsantili, E., and Bebeli, P. J. (2010). Germplasm diversity and genetic relationships among walnut (Juglans regia L.) cultivars and Greek local selections revealed by Inter-Simple Sequence Repeat (ISSR) markers. *Sci. Hortic.* 125, 584–592. doi:10.1016/J.SCIENTA.2010.05.006

Corbett, E. L., Watt, C. J., Walker, N., Maher, D., Williams, B. G., Raviglione, M. C., et al. (2003). The growing burden of tuberculosis: global trends and interactions with the HIV epidemic. *Arch. Intern Med.* 163, 1009–1021. doi:10.1001/archinte.163.9.1009

Dahlgren, D., and Lennernäs, H. (2019). Intestinal permeability and drug absorption: predictive experimental, computational and *in vivo* approaches. *Pharmaceutics* 11, 411. doi:10.3390/PHARMACEUTICS11080411

Daina, A., Michielin, O., and Zoete, V. (2017). SwissADME: a free web tool to evaluate pharmacokinetics, drug-likeness and medicinal chemistry friendliness of small molecules. *Sci. Rep.* 7, 42717–42813. doi:10.1038/srep42717

Daina, A., Michielin, O., and Zoete, V. (2019). SwissTargetPrediction: updated data and new features for efficient prediction of protein targets of small molecules. *Nucleic Acids Res.* 47, W357-W364–W3664. doi:10.1093/nar/gkz382

Dherbomez, M., Viano, J., Jann-Para, G., and Bessière, J. M. (2006). Composition and antimicrobial activity of the essential oil of Hypericum hyssopifolium ssp. hyssopifolium from southeast France. *J. Essent. Oil Res.* 18, 469–471. doi:10.1080/10412905.2006.9699143

Ferreira, L. L. G., and Andricopulo, A. D. (2019). ADMET modeling approaches in drug discovery. *Drug Discov. Today* 24, 1157–1165. doi:10.1016/j.drudis.2019.03.015

Filimonov, D. A., Lagunin, A. A., Gloriozova, T. A., Rudik, A. V., Druzhilovskii, D. S., Pogodin, P. V., et al. (2014). Prediction of the biological activity spectra of organic compounds using the pass online web resource. *Chem. Heterocycl. Compd. (N Y)* 50, 444–457. doi:10.1007/s10593-014-1496-1

Galati, S., Di Stefano, M., Martinelli, E., Poli, G., and Tuccinardi, T. (2021). Recent advances in *in silico* target fishing. *Molecules* 26, 5124. doi:10.3390/molecules26175124

Hett, E. C., Chao, M. C., Deng, L. L., and Rubin, E. J. (2008). A mycobacterial enzyme essential for cell division synergizes with resuscitation-promoting factor. *PLoS Pathog.* 4, e1000001. doi:10.1371/journal.ppat.1000001

Inoue, M., Yasukochi, T., Kuroki, R., Miki, T., Horiuchi, T., Imoto, T., et al. (1992). Multiple role of hydrophobicity of tryptophan-108 in chicken lysozyme:structural stability, saccharide binding ability, and abnormal pKa of glutamic acid-35. *Biochemistry* 31, 5545–5553. doi:10.1021/bi00139a017

Jaan, S., Waheed, S., Bashir, S., Sameem Javed, M., Amjad, A., Nishan, U., et al. (2021). Virtual screening and molecular docking of FDA approved antiviral drugs for the identification of potential inhibitors of SARS-CoV-2 RNA-MTase protein. *Int. J. Adv. Biol. Biomed. Res.* 9, 105–118. doi:10.22034/ijabbr.2021.46320

Jakkala, K., and Ajitkumar, P. (2019). Hypoxic non-replicating persistent *Mycobacterium tuberculosis* develops thickened outer layer that helps in restricting rifampicin entry. *Front. Microbiol.* 10, 2339. doi:10.3389/fmicb.2019.02339

Kamsri, P., Punkvang, A., Hannongbua, S., Suttisintong, K., Kittakoop, P., Spencer, J., et al. (2019). *In silico* study directed towards identification of the key structural features of GyrB inhibitors targeting MTB DNA gyrase: HQSAR, CoMSIA and molecular dynamics simulations. *Sar. QSAR Environ. Res.* 30, 775–800. doi:10.1080/1062936X.2019.1658218

Kazek, M., Kaczmarek, A., Wrońska, A. K., and Boguś, M. I. (2021). Dodecanol, metabolite of entomopathogenic fungus Conidiobolus coronatus, affects fatty acid composition and cellular immunity of Galleria mellonella and Calliphora vicina. *Sci. Rep.* 11, 15963–16016. doi:10.1038/s41598-021-95440-6

Keita, K., Darkoh, C., and Okafor, F. (2022). Secondary plant metabolites as potent drug candidates against antimicrobial-resistant pathogens. *SN Appl. Sci.* 4, 209. doi:10.1007/s42452-022-05084-y

Kell, D. B., and Young, M. (2000). Bacterial dormancy and culturability: the role of autocrine growth factors. *Curr. Opin. Microbiol.* 3, 238–243. doi:10.1016/S1369-5274(00)00082-5

Khameneh, B., Iranshahy, M., Soheili, V., and Fazly Bazzaz, B. S. (2019). Review on plant antimicrobials: a mechanistic viewpoint. *Antimicrob. Resist Infect. Control* 8, 118. doi:10.1186/s13756-019-0559-6

Khan, F., Sarker, M. R., Ming, L. C., Mohamed, I. N., Zhao, C., Sheikh, B. Y., et al. (2019). Comprehensive review on phytochemicals, pharmacological and clinical potentials of Gymnema sylvestre. *Pharmacol. Clin. Potentials Gymnema sylvestre* 10, 1–19. doi:10.3389/fphar.2019.01223

Kim, S., Oshima, H., Zhang, H., Kern, N. R., Re, S., Lee, J., et al. (2020). CHARMM-GUI free energy calculator for absolute and relative ligand solvation and binding free energy simulations. *J. Chem. Theory Comput.* 16, 7207–7218. doi:10.1021/acs.jctc.0c00884

Lipinski, C. A., Discovery, M., Lombardo, F., Lipinski, C. A., Dominy, B. W., and Feeney, P. J. (1997). *Experimental and computational approaches to estimate solubility and permeability in drug discovery and development settings*, 23. Elsevier, 3–25.

Mag, P., Siyumbwa, S. N., Ekeuku, S. O., Amini, F., Emerald, N. M., Sharma, D., et al. (2019). Wound healing and antibacterial activities of 2 - pentadecanone in streptozotocin - induced type 2 diabetic rats. *Pharmacogn. Mag.* 15 (62), 71–78. doi:10.4103/pm.pm_444_18

Moule, M. G., and Cirillo, J. D. (2020). *Mycobacterium tuberculosis* dissemination plays a critical role in pathogenesis. *Front. Cell Infect. Microbiol.* 10, 65. doi:10.3389/fcimb.2020.00065

Muhammad, I., Rahman, N., Gul-E-nayab, Nishan, U., and Shah, M. (2021). Antidiabetic activities of alkaloids isolated from medicinal plants. *Braz. J. Pharm. Sci.* 57, 1–14. doi:10.1590/s2175-97902020000419130

Muhammad, I., Rahman, N., Nayab, G. E., Niaz, S., Shah, M., Afridi, S. G., et al. (2020). The molecular docking of flavonoids isolated from *Daucus carota* as a dual inhibitor of MDM2 and MDMX. *Recent Pat. Anticancer Drug Discov.* 15, 154–164. doi:10.2174/1574892815666200226112506

Oshima, H., Re, S., and Sugita, Y. (2020). Prediction of protein–ligand binding pose and affinity using the gREST+FEP method. *J. Chem. Inf. Model* 60, 5382–5394. doi:10.1021/acs.jcim.0c00338

Pajuelo, D., Tak, U., Zhang, L., Danilchanka, O., Tischler, A. D., and Niederweis, M. (2021). Toxin secretion and trafficking by *Mycobacterium tuberculosis*. *Nat. Commun.* 12, 6592. doi:10.1038/s41467-021-26925-1

Phillips, J. C., Hardy, D. J., Maia, J. D. C., Stone, J. E., Ribeiro, J. V., Bernardi, R. C., et al. (2020). Scalable molecular dynamics on CPU and GPU architectures with NAMD. *J. Chem. Phys.* 153, 044130. doi:10.1063/5.0014475

Piergallini, T. J., and Turner, J. (2018). Tuberculosis in the elderly: why inflammation matters. *Exp. Gerontol.* 105, 32–39. doi:10.1016/j.exger.2017.12.021

Pires, D. E. V., Blundell, T. L., and Ascher, D. B. (2015). pkCSM: predicting small-molecule pharmacokinetic and toxicity properties using graph-based signatures. *J. Med. Chem.* 58, 4066–4072. doi:10.1021/acs.jmedchem.5b00104

Rabaan, A. A., Garout, M., Aljeldah, M., Al, B. R., Abdulsalam, S., Alshengeti, A., et al. (2023). Anti - tubercular activity evaluation of natural compounds by targeting *Mycobacterium tuberculosis* resuscitation promoting factor B inhibition: an *in silico* study. *Mol. Divers*. doi:10.1007/s11030-023-10632-8

Ruggiero, A., Squeglia, F., Romano, M., Vitagliano, L., Simone, A.De, and Berisio, R. (2016). The structure of Resuscitation promoting factor B from *M. tuberculosis* reveals unexpected ubiquitin-like domains. *BBA - General Subj.* 1860, 445–451. doi:10.1016/j.bbagen.2015.11.001

Sarfraz, A., Wara, U. T., Ansari, S. H., Zaman, A., Nishan, U., Iqbal, A., et al. (2023). Structural informatics approach for designing an epitope-based vaccine against the brain-eating naegleria fowleri. *Front. Immunol.* 14, 1284621. doi:10.3389/fimmu.2023.1284621

Shah, M., Bashir, S., Jaan, S., Nawaz, H., Nishan, U., Abbasi, S. W., et al. (2021). Computational analysis of plant-derived terpenes as α -glucosidase inhibitors for the discovery of therapeutic agents against type 2 diabetes mellitus. *South Afr. J. Bot.* 143, 462–473. doi:10.1016/j.sajb.2021.09.030

Siewchaisakul, P., Nanthanangkul, S., Santong, C., Suwanrungruang, K., and Vatanasapt, P. (2021). Survival of cancer patients with Co-morbid tuberculosis in Thailand. *Asian Pac. J. Cancer Prev.* 22, 2701–2708. doi:10.31557/APJCP.2021.22.8.2701

Squeglia, F., Romano, M., Ruggiero, A., Vitagliano, L., De Simone, A., and Berisio, R. (2013). Carbohydrate recognition by RpfB from mycobacterium tuberculosis unveiled by crystallographic and molecular dynamics analyses. *Biophys. J.* 104, 2530–2539. doi:10.1016/j.bpj.2013.04.040

Srinivasan, K., and Kumaravel, S. (2016). Unraveling the potential phytochemical compounds of Gymnema sylvestrethrough GC-MS study. *Int. J. Pharm. Pharm. Sci.* 8, 449–453.

Tiwari, P., Mishra, B. N., and Sangwan, N. S. (2014). Phytochemical and pharmacological properties of Gymnema sylvestre: an important medicinal plant. *Biomed. Res. Int.* 2014, 830285. doi:10.1155/2014/830285

Togashi, N., Shiraishi, A., Nishizaka, M., Matsuoka, K., Endo, K., Hamashima, H., et al. (2007). Antibacterial activity of long-chain fatty alcohols against *Staphylococcus aureus*. *Molecules* 12, 139–148. doi:10.3390/12020139

Van Der Spoel, D., Lindahl, E., Hess, B., Groenhof, G., Mark, A. E., and Berendsen, H. J. C. (2005). GROMACS: fast, flexible, and free. *J. Comput. Chem.* 26, 1701–1718. doi:10.1002/JCC.20291

WHO (2021a). *Latent tuberculosis infection: updated and consolidated guidelines for programmatic management*. Geneva: WHO; 2018. World Health Organization.

WHO (2021b). *Treatment of drug-susceptible tuberculosis: rapid communication*, 5. World Health Organization.

frontiers | Frontiers in Pharmacology

TYPE Review
PUBLISHED 12 January 2024
DOI 10.3389/fphar.2023.1305294

OPEN ACCESS

EDITED BY
Zul Kamal,
Shaheed Benazir Bhutto University, Pakistan

REVIEWED BY
Manigandan Venkatesan,
The University of Texas Health Science Center at San Antonio, United States
Hans Gersbach,
ETH Zurich, Switzerland

*CORRESPONDENCE
Esraa M. Halawa,
esraahalawa@gstd.sci.cu.edu.eg
Rada Olga,
olga_rada@usvt.ro
Ahmed Abdeen,
ahmed.abdeen@fvtm.bu.edu.eg

RECEIVED 01 October 2023
ACCEPTED 18 December 2023
PUBLISHED 12 January 2024

CITATION
Halawa EM, Fadel M, Al-Rabia MW, Behairy A, Nouh NA, Abdo M, Olga R, Fericean L, Atwa AM, El-Nablaway M and Abdeen A (2024), Antibiotic action and resistance: updated review of mechanisms, spread, influencing factors, and alternative approaches for combating resistance.
Front. Pharmacol. 14:1305294.
doi: 10.3389/fphar.2023.1305294

Antibiotic action and resistance: updated review of mechanisms, spread, influencing factors, and alternative approaches for combating resistance

Esraa M. Halawa[1]*, Mohamed Fadel[2], Mohammed W. Al-Rabia[3,4], Ali Behairy[5], Nehal A. Nouh[6,7], Mohamed Abdo[8,9], Rada Olga[10]*, Liana Fericean[10], Ahmed M. Atwa[11], Mohammad El-Nablaway[12,13] and Ahmed Abdeen[14]*

[1]Department of Botany and Microbiology, Faculty of Science, Cairo University, Giza, Egypt, [2]Department of Microbial Chemistry, Biotechnology Research Institute, National Research Centre, Dokki, Cairo, Egypt, [3]Department of Clinical Microbiology and Immunology, Faculty of Medicine, King Abdulaziz University, Jeddah, Saudi Arabia, [4]Department of Clinical Laboratories-Diagnostic Immunology Division, King Abdulaziz University Hospital, Jeddah, Saudi Arabia, [5]Department of Pharmacology, Faculty of Medicine, Benha University, Benha, Egypt, [6]Department of Microbiology, Medicine Program, Batterjee Medical College, Jeddah, Saudi Arabia, [7]Inpatient Pharmacy, Mansoura University Hospitals, Mansoura, Egypt, [8]Department of Animal Histology and Anatomy, School of Veterinary Medicine, Badr University in Cairo (BUC), Badr City, Egypt, [9]Department of Anatomy and Embryology, Faculty of Veterinary Medicine, University of Sadat City, Sadat City, Egypt, [10]Department of Biology and Plant Protection, Faculty of Agriculture, University of Life Sciences "King Michael I" from Timişoara, Timişoara, Romania, [11]Department of Pharmacology and Toxicology, Faculty of Pharmacy, Egyptian Russian University, Cairo, Egypt, [12]Department of Medical Biochemistry, Faculty of Medicine, Mansoura University, Mansoura, Egypt, [13]Department of Basic Medical Sciences, College of Medicine, AlMaarefa University, Riyadh, Saudi Arabia, [14]Department of Forensic Medicine and Toxicology, Faculty of Veterinary Medicine, Benha University, Toukh, Egypt

Antibiotics represent a frequently employed therapeutic modality for the management of bacterial infections across diverse domains, including human health, agriculture, livestock breeding, and fish farming. The efficacy of antibiotics relies on four distinct mechanisms of action, which are discussed in detail in this review, along with accompanying diagrammatic illustrations. Despite their effectiveness, antibiotic resistance has emerged as a significant challenge to treating bacterial infections. Bacteria have developed defense mechanisms against antibiotics, rendering them ineffective. This review delves into the specific mechanisms that bacteria have developed to resist antibiotics, with the help of diagrammatic illustrations. Antibiotic resistance can spread among bacteria through various routes, resulting in previously susceptible bacteria becoming antibiotic-resistant. Multiple factors contribute to the worsening crisis of antibiotic resistance, including human misuse of antibiotics. This review also emphasizes alternative solutions proposed to mitigate the exacerbation of antibiotic resistance.

KEYWORDS

antibiotics, antimicrobial, bacteria, antibiotic resistance, disease spreading

1 Introduction

Microbiology originated the term "antibiotic" from the French words "antibiose" and "antibiotique," as defined by Vuillemin in the late 19th century to delineate substances that exert detrimental effects on living organisms, particularly microorganisms (Laskin, Bennett, and Gadd, 2002). Subsequently, in 1947, Selman A. Waksman provided an all-encompassing definition of antibiotics as chemical compounds produced by microorganisms that possess the capacity to impede the growth and induce the demise of bacteria and other microorganisms (Waksman, 1947; Kaur Sodhi and Singh, 2022). Antibiotics have found widespread application across various sectors, encompassing human health, agriculture, livestock breeding, and fish farms (Okocha, Olatoye, and Adedeji, 2018; Kaur Sodhi and Singh, 2022). The mechanisms underlying the efficacy of antibiotics involve four distinct modes of action (Kaur Sodhi and Singh, 2022), including inhibition of DNA replication (Fàbrega et al., 2009), protein biosynthesis (Tenson, Lovmar, and Ehrenberg, 2003), cell wall biosynthesis (Cho, Uehara, and Bernhardt, 2014), and folic acid metabolism (Saverus 2019). However, the emergence of antibiotic resistance has escalated into a critical global issue (Sarkar et al., 2021; Shree et al., 2023).

This review article comprehensively discusses the multifaceted factors contributing to the propagation of antibiotic resistance, alongside providing potential strategies for mitigating this problem. Furthermore, innovative solutions to combat antibiotic resistance have been uncovered by scientists, such as the utilization of nanoantibiotics, and antibiotic adjuvants, the discovery of novel antibiotics, and the exploration of alternatives to antibiotics, including bacteriophages and botanicals. In addition to exploring the aforementioned topics, this review article delves into the utilization of antibiotics in diverse sectors, the controversies encircling their use, the mechanisms by which antibiotics act, the emergence of antibiotic resistance, the mechanisms governing antibiotic resistance in bacteria, the dissemination of resistance among bacterial populations, and the pivotal factors that contribute to the escalation of resistance. Moreover, this article highlights the accomplishments achieved thus far and presents solutions that scientists have uncovered to combat the global crisis of antibiotic resistance.

2 Antibiotics use

Antibiotics are utilized in a variety of sectors, including agriculture, aquaculture, animal husbandry, and human health (Okocha et al., 2018; Kaur Sodhi and Singh, 2022) (Table 1). These substances are used to treat bacterial infections in humans, animals, and crops, thereby preventing crop loss from bacterial diseases (Svircev, Roach, and Castle, 2018; Kaur Sodhi and Singh, 2022). Additionally, antibiotics are widely used as growth-promoting agents in animal husbandry (Sriram et al., 2021; Kaur Sodhi and Singh, 2022). The utilization of antibiotics in livestock is classified into three categories by scientists (Gonzalez Ronquillo and Angeles Hernandez, 2017): therapeutic agents, prophylactic agents, and growth promoters. Therapeutic agents are administered in high doses to infected animals to treat illnesses (Schwarz, Kehrenberg, and Walsh, 2001), while prophylactic agents are given in sub-therapeutic doses through feed or drinking water to prevent disease when there are no evident symptoms of infection. Antibiotics are periodically administered to animals throughout their life cycle (Greene and Pisano 2012). Growth promoters are used to improve an animal's growth rate and production, and a tiny quantity of antibiotics is regularly administered through its feed (Wierup, 2001). In aquaculture, antimicrobial substances are used to treat fish infections. Fish are given antibiotics by incorporating them into specially formulated feed, and they mostly excrete them into the environment (Dawood, Koshio, and Esteban, 2018). It is worth noting that approximately 75% of the antibiotics provided to fish are excreted into the water (Benbrook, 2002).

TABLE 1 Antibiotic class use in different sectors.

Sector	Antibiotic use
Human health	- Treatment of bacterial infections.
Animal husbandry	- Treatment of bacterial infections.
	- Growth promoting agents.
Agricultural activities	- Prevention of crop loss from bacterial diseases.
Aquaculture	- Treatment of fish diseases.

3 Mechanisms of action of antibiotics

Not all antibiotics have the exact mechanism of action; thus, scientists classify antibiotics according to their mechanism of action and chemical structure (Kaur Sodhi and Singh, 2022) into four mechanisms described as follows:

3.1 Antibiotics inhibit DNA replication

Binary fission is a type of cell division used by bacteria that produces two daughter cells (Bhattacharyya, 2012). Before that can happen, however, bacteria must create exact duplicates of their circular DNA. DNA replication is the procedure used to duplicate DNA (Gilbert, 2001). A DNA double helix strand is split into two single strands by the enzyme DNA helicase to begin this process. The enzyme DNA polymerase then produces new DNA Strands that are complementary to the old ones (Li and Araki, 2013). Positive DNA helical twists build up as a result of DNA helicase and DNA polymerase activity. If not eliminated, these positive helical twists stop DNA replication from continuing. The removal of the positive superhelical twists is carried out by the enzyme DNA gyrase, also known as topoisomerase II, allowing DNA replication to continue (Bush, Evans-roberts, and Maxwell, 2015). A crucial bacterial enzyme called DNA gyrase is made up of 2A and 2B subunits. This enzyme also plays a crucial role in the transcription of several genes and the start of DNA replication. Once the new two daughter DNA molecules have been created, they eventually connect and are interlinked. In order to divide the bacterial cell into two new daughter bacterial cells, the enzyme topoisomerase IV (related to

DNA gyrase) enables the separation of the two connected DNA molecules (Nagaraja et al., 2017) (Figure 1).

3.2 Fluoroquinolones antibiotics

By inhibiting the activity of DNA gyrase and topoisomerase IV, fluoroquinolone antibiotics prevent the synthesis of bacterial DNA (Fàbrega et al., 2009; Shree et al., 2023). These antibiotics have a particular affinity for binding to the complex formed by DNA gyrase and DNA (Pham, Ziora, and Blaskovich, 2019). Such binding destabilizes the enzyme-DNA complex, causing DNA cleavage and ultimately leading to bacterial cell death (Malik, Zhao, and Drlica, 2006) (Figure 1). Fluoroquinolones primarily target DNA gyrase, which is the reason for their effectiveness against most gram-negative bacteria (Blondeau, 2004).

In contrast, in most gram-positive bacteria, fluoroquinolones target topoisomerase IV as their primary mechanism (Blondeau, 2004). However, they also act as a secondary target for DNA gyrase. This results in the binding of fluoroquinolones to DNA and the complex formed by topoisomerase IV, which causes disruption of the separation of the two daughter DNA molecules and eventually leads to DNA breakage (Malik et al., 2006).

3.3 Antibiotics inhibit protein biosynthesis

Like all other living things, bacteria have DNA, which contains the genetic information for every protein they need to survive. This includes the protein needed for metabolism regulation, growth, repair, and reproduction (Wu, 2009). Additionally, it encodes for mRNA, rRNA, and tRNA, three types of RNA that are essential for carrying out protein synthesis (Wu, 2009).

The unwinding and separation of the DNA molecule at a region that codes for the necessary protein to be produced is the first step in the process of protein biosynthesis. The transcription, the process of making mRNA, uses only one strand of DNA as a scaffold. When the mRNA strand is finished, it separates from the DNA template and then is connected to a ribosome. The 50 s and 30 s ribosomal subunits make up the bacterial ribosome. Following the joining of these two subunits along the mRNA strand, the synthesis of the polypeptide chain starts. Up until it encounters the signal along the mRNA to stop, the ribosome keeps adding amino acids to the lengthening polypeptide chain. The full polypeptide chain is generated at this point (Johansson, Lovmar, and Ehrenberg, 2008) (Figure 2). Therefore, targeting the ribosomal 30 or 50 subunits is necessary for antibiotics to inhibit protein synthesis (Scott Champney, 2008).

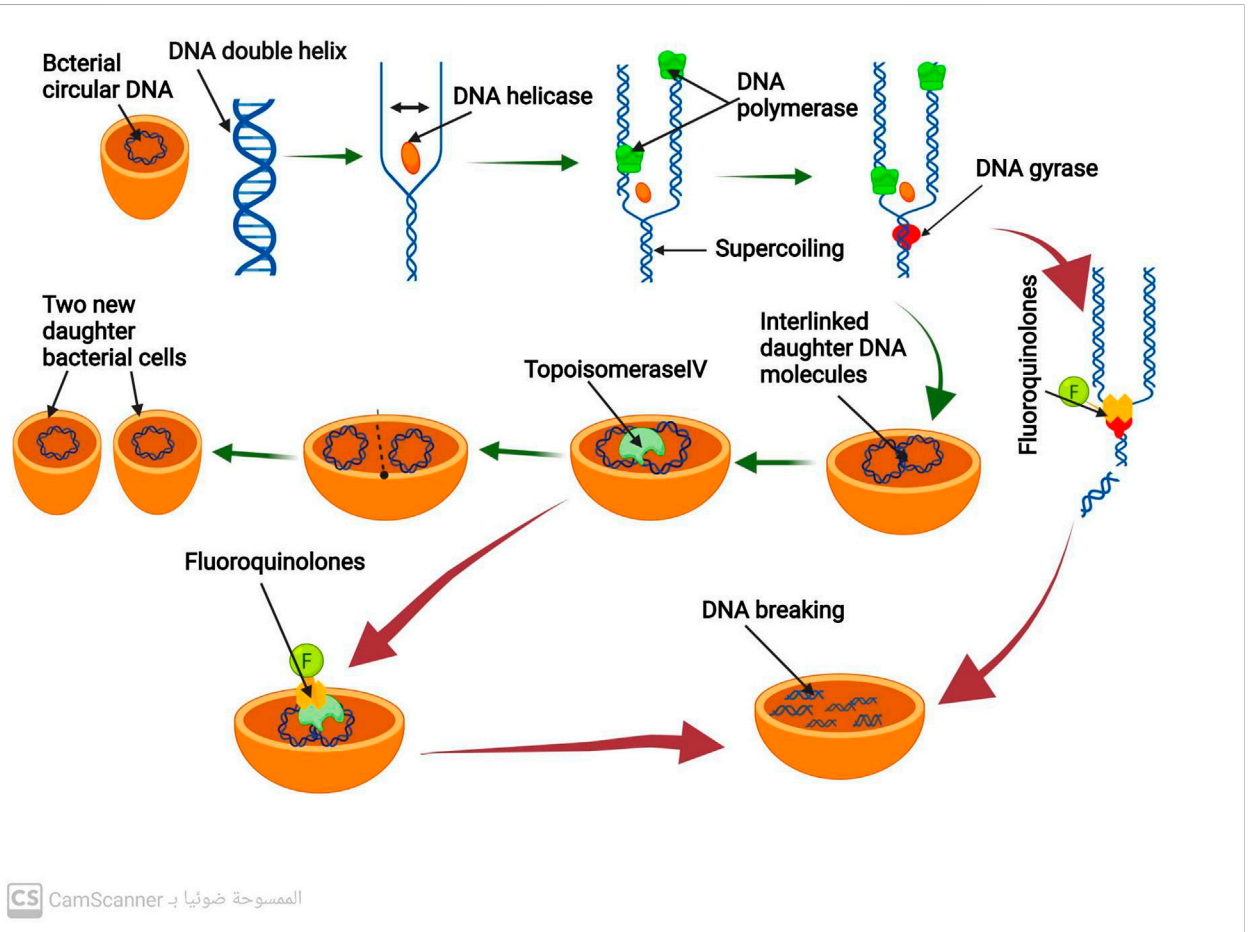

FIGURE 1
Mechanism of DNA replication process and mechanism of action of antibiotics that inhibit DNA replication.

3.3.1 Antibiotics inhibit protein biosynthesis by targeting the ribosomal 305 subunits

3.3.1.1 Aminoglycosides antibiotics

Antibiotics known as aminoglycosides function through a specific mechanism. These antibiotics are positively charged, which attracts the negatively charged outer membrane of bacteria, causing the membrane to develop large pores (Delcour, 2009). The aminoglycosides are then able to enter the bacterial cell through these pores. Additionally, aminoglycosides are able to pass through the bacterial cytoplasmic membrane by utilizing the energy of active bacterial transport (Jana and Deb, 2006). The target of aminoglycosides is the 16s rRNA of the 30s, which they bind to via hydrogen bonds. This binding inhibits protein biosynthesis before it can be completed (Vicens and Westhof, 2003).

Although aminoglycosides are effective against many types of bacteria, they have low efficacy against anaerobic bacteria, as these bacteria require oxygen for active transport pathways to function (Kohanski, Dwyer, and Collins, 2010). However, when combined with an antibiotic that inhibits cell wall synthesis, aminoglycosides have been found to have a greater ability to penetrate bacterial cells at low doses (Wang et al., 2022) (Figure 2).

3.3.1.2 Tetracycline antibiotics

This class of antibiotics targets the highly conserved sequence of the 16S rRNA present in the ribosomal 30S subunit. Tetracycline, for instance, functions by hindering the binding of tRNA to the A-site of the ribosome, which ultimately impedes the process of protein synthesis (Brodersen et al., 2000).

3.3.2 Antibiotics inhibit protein biosynthesis by targeting the ribosomal 50s subunit

3.3.2.1 Macrolides antibiotics

Macrolide antibiotics bind to the 50S subunit of the ribosome, thereby preventing the synthesis of polypeptide chains and inhibiting protein production (Tenson et al., 2003) (Figure 2).

3.3.2.2 Chloramphenicol antibiotics

Chloramphenicol antibiotics inhibit peptidyl transferase, an enzyme located on the 50S ribosomal subunit that is necessary for protein synthesis. This inhibition prevents t-RNA from connecting to the ribosomal A site, leading to the inhibition of protein synthesis (Syroegin et al., 2022) (Figure 2).

3.3.2.3 Oxazolidinone antibiotics

Oxazolidinone antibiotics prevent the synthesis of the initiation complex by binding to the 50S subunit of the ribosome, thereby preventing the production of proteins (Foti et al., 2021) (Figure 2).

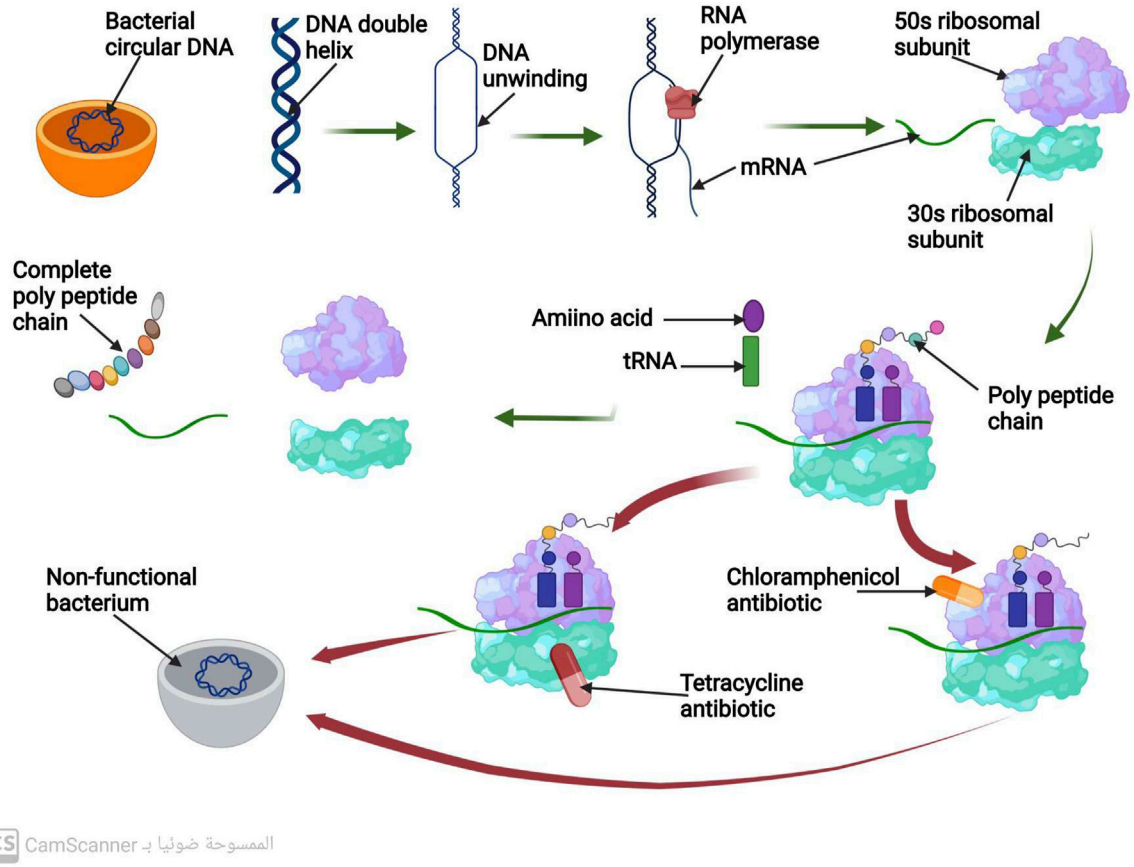

FIGURE 2
Mechanism of protein biosynthesis process and mechanism of action of antibiotics that inhibit protein biosynthesis.

3.4 Antibiotics inhibit cell wall synthesis

Most bacteria are composed of a cell membrane enclosed in a cell wall, while some bacteria also have an extra outer layer. The bacterial cell wall serves two purposes: to keep the bacteria in their distinctive shape and to stop them from bursting when osmosis is used to introduce fluid into the cell (Gupta and Gupta, 2021). The peptidoglycan is the most significant part of the cell wall. N-acetyl muramic acid (NAM) alternates with N-acetyl Glucosamine (NAG), and the two are connected by chains of amino acids to form the polymer known as peptidoglycan (Meroueh et al., 2006). There are several steps in the peptidoglycan synthesis process, which ultimately results in bacterial cell wall formation. A precursor to peptidoglycan is created by combining N-acetyl glucosamine (NAG) with N-acetyl muramic acid. The cell wall acceptors in the periplasm receive this peptidoglycan precursor after it has been delivered across the membrane. The peptidoglycan precursors attach to cell wall receptors in the periplasm and go through a lot of cross-linking (Liu and Breukink, 2016). Trans peptidase and carboxy peptidase enzymes are the two main enzymes in cross-linking. A cell wall eventually develops from many peptidoglycan layers that are all cross-linked (Liu and Breukink, 2016). Gram-positive bacteria may have a thicker cell wall than gram-negative bacteria because they may contain more layers of peptidoglycan (Figure 3) (Pasquina-Lemonche et al., 2020).

The peptidoglycan is the most significant part of the bacterial cell wall. Transpeptidase and carboxypeptidase are the two primary enzymes in cross-linking during cell wall biosynthesis (Liu and Breukink, 2016) (Figure 3).

3.4.1 Betalactams antibiotics

All penicillins and cephalosporins with the beta-lactam ring chemical structure are included in this group (Fernandes, Amador, and Prudêncio, 2013). This distinctive structure allows them to attach to peptidoglycan cross-linking enzymes, such as transpeptidase and carboxypeptidase, ultimately inhibiting bacterial cell wall synthesis and preventing cross-linking (Cho et al., 2014). This inhibition of cell wall manufacturing leads to the destruction of the bacterial cell, as shown in Figure 3 (Cho et al., 2014).

3.4.2 Glycopeptides antibiotics

These antibiotics form non-covalent bonds with the terminal carbohydrates, which prevents the cross-linking of peptidoglycan precursors. This process ultimately leads to the degradation of bacterial cell walls, resulting in the destruction and elimination of bacterial cells (Kang and Park, 2015).

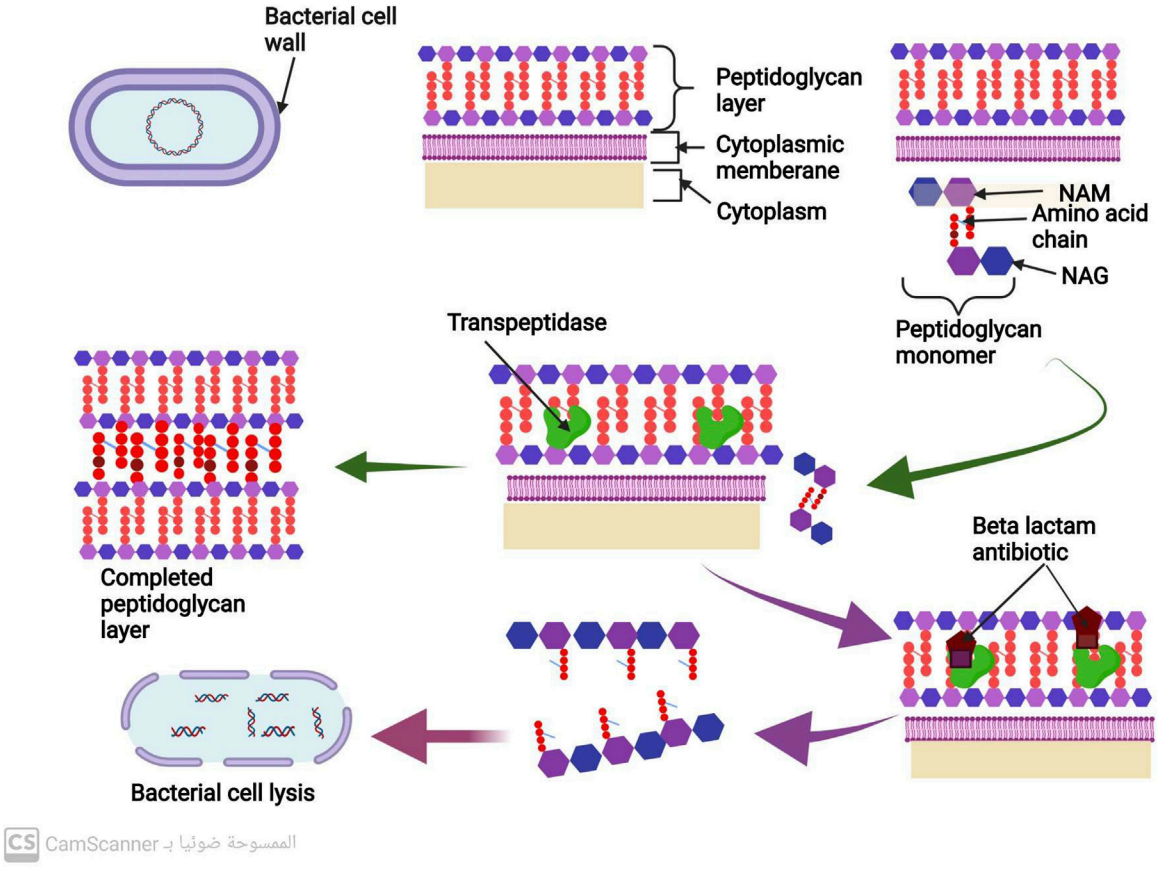

FIGURE 3
Mechanism of cell wall synthesis and Mechanism of action of antibiotics that inhibit cell wall synthesis.

3.5 Antibiotics inhibit folic acid metabolism

These antibiotics are designed to selectively inhibit a key enzyme involved in the pathway for folic acid metabolism. Sulfonamide antibiotics target dihydropteroate synthase, an enzyme in the metabolic pathway. On the other hand, trimethoprim antibiotics target dihydrofolate reductase, another enzyme in the same pathway (Capasso and Supuran, 2014) (Figure 4).

4 Emergence of antibiotic resistance

Dr. Tedros Adhanom Ghebreyesus, CEO of the World Health Organization (WHO), has warned that the global epidemic of antibiotic resistance poses a significant threat to a century of progress in healthcare and the achievement of sustainable development goals (Sarkar et al., 2021). According to current predictions, it is expected that in a quarter of a century, almost 100% of bacteria will be resistant to most antibiotics used in medicine (Kaur Sodhi and Singh, 2022; Murray et al., 2022). Experts also predict that the number of deaths due to antimicrobial resistance may rise to 10 million by the middle of the twenty-first century, up from the current figure of over 700,000 per year (Romandini et al., 2021).

In response to this alarming situation, the WHO proposed the ranking of bacteria with the highest trend in resistance in 2017. This list includes *Acinobacter baumannii*, *Pseudomonas aeruginosa, Enterobacteriaceae, Enterococcus faecium, Helicobacter pylori, Salmonella species, Campylobacter species, Staphylococcus aureus,* and *Nisseria gonorrhoeae*. These microbe species are highly resistant to multiple classes of antibiotic treatments, making them less susceptible to antibiotic therapy (Biondo, 2023).

5 Mechanisms of antibiotic resistance

Bacteria employ three primary mechanisms to counteract the effects of antibiotics (Zhou et al., 2015). These mechanisms are outlined below:

5.1 Bacteria prevent antibiotic accumulation in their cells

5.1.1 Through limiting the entrance of drugs into bacterial cells

Gram-negative bacteria have porin channels in their outer membrane (Kang and Park, 2015). These channels act as gatekeepers,

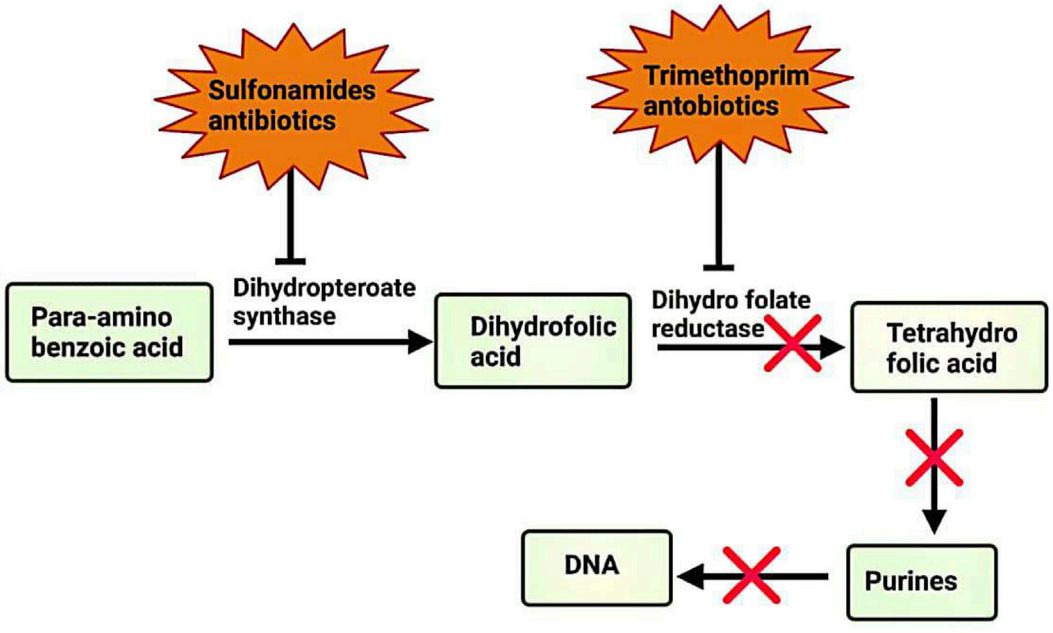

FIGURE 4
Mechanism of action of antibiotics that inhibit folic acid metabolism.

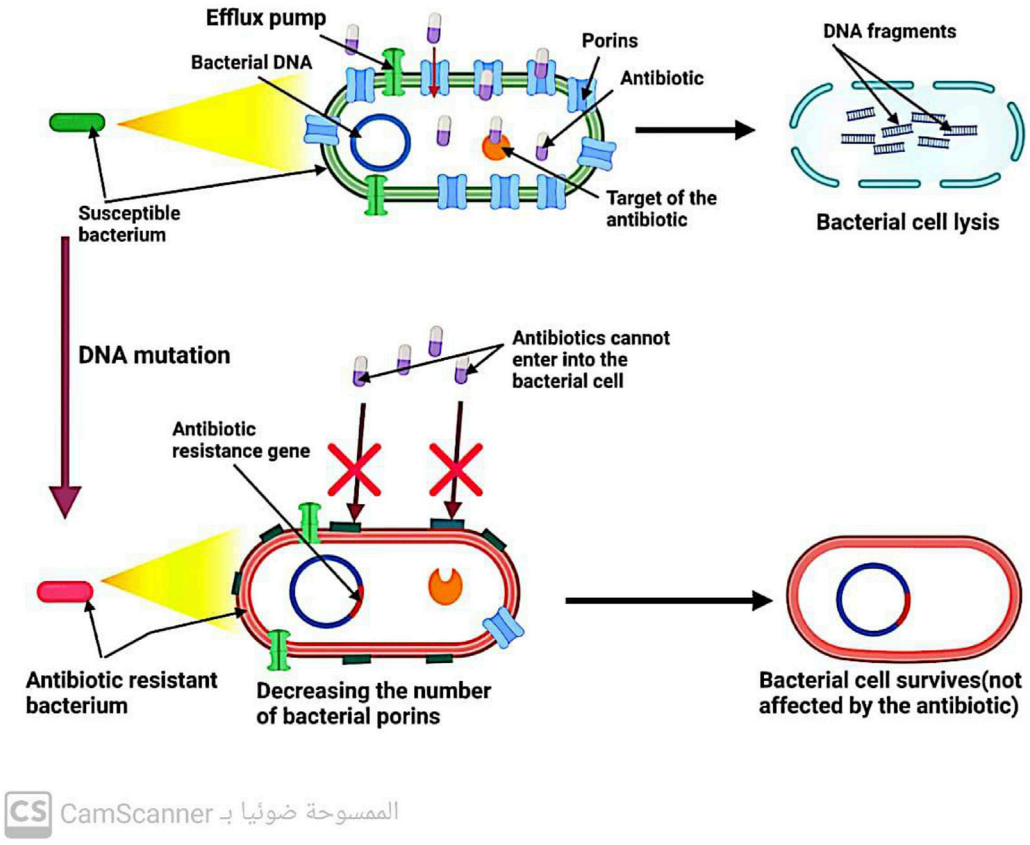

FIGURE 5
Mechanism of antibiotic resistance by decreasing antibiotic entry into the bacterial cell.

allowing only certain antibiotics like B-lactams and quinolones to enter the bacterial cell. Therefore, the reduced number of bacterial porins can hinder the entry of these antibiotics into the cell, leading to increased resistance to these drugs (Darby et al., 2023) (Figure 5).

5.1.2 Increasing the rate at which antibiotics leave bacterial cells

Efflux pumps, located in the cytoplasmic membrane of bacteria, play a crucial role in maintaining the balance of solutes within bacterial cells. However, these pumps also contribute to antibiotic resistance by removing drugs from bacterial cells before they can reach their intended targets (Džidić, Šušković, and Kos, 2008) (Figure 6). Notably, efflux systems have been found to confer resistance (Kaur Sodhi and Singh, 2022; Shree et al., 2023; Sodhi et al., 2023). to all antibiotic classes except for polymyxin (Fernández-Billón et al., 2023). Increasing our understanding of the mechanisms underlying efflux systems may provide new strategies for combating antibiotic resistance.

5.2 Bacteria modify the target molecule of antibiotics

Antibiotics are designed to target specific molecules, but even the slightest alteration can prevent their binding, leading to the emergence of antibiotic resistance (Kang and Park, 2015; Shree et al., 2023).

5.2.1 Modifications to the ribosomal 30s or 50s subunits

One-way bacteria can develop resistance to drugs that affect protein production is by modifying their ribosomal 30S or 50S subunits (Kaur Sodhi and Singh, 2022; Sodhi et al., 2023) (Figure 7). This type of resistance is observed with antibiotics such as aminoglycosides, tetracycline, macrolides, chloramphenicol, lincosamides, and streptogramin (Tenover, 2006; Fernández-Billón et al., 2023).

5.2.2 Changes in penicillin-binding protein (PBP)

Penicillin-binding proteins (PBPs) are enzymes known as transpeptidases, which play a vital role in cross-linking peptidoglycan precursors during the biosynthesis of bacterial cell walls. As these enzymes are the primary targets of β-lactam antibiotics, any changes in their structure or function can lead to bacterial resistance to these drugs (Kaur Sodhi and Singh, 2022; Sodhi et al., 2023) (Figure 8).

5.2.3 Changes in DNA gyrase and topoisomerase enzymes

DNA replication involves the enzymes DNA gyrase and topoisomerase (Hirsch and Klostermeier, 2021). Quinolone antibiotics specifically target these two enzymes, which is why modifications in their structure can lead to bacterial resistance against quinolones (Fàbrega et al., 2009) (Figure 9).

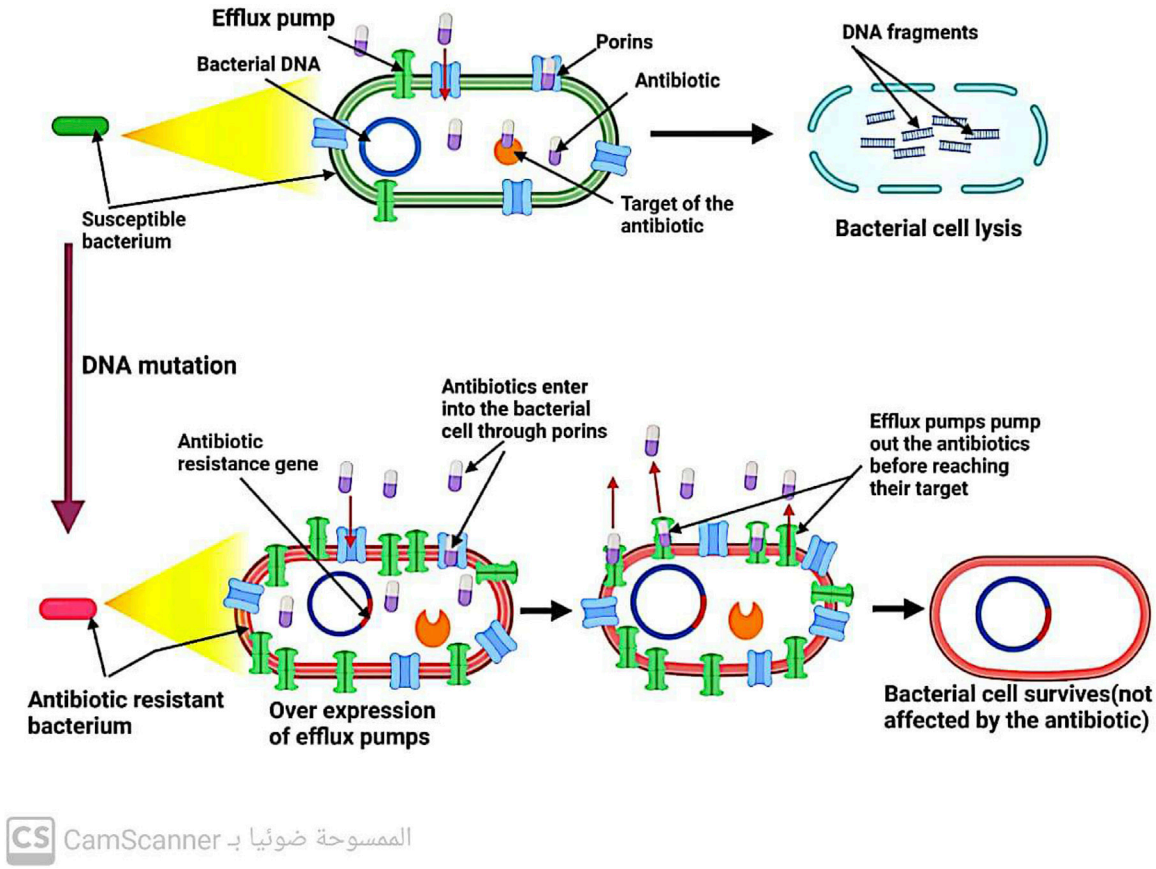

FIGURE 6
Mechanism of antibiotic resistance by increasing antibiotic exit from the bacterial cell.

5.2.4 Changes in D-alanyl-D-alanine

The peptidoglycan precursors contain a dipeptide residue known as D-alanyl-D-alanine, which plays a crucial role in cell wall formation (Peschel et al., 2000). Alterations to this D-alanyl-D-alanine residue can lead to bacterial resistance to antibiotics that target it (Džidić et al., 2008).

5.2.5 Protection of ribosome

Tetracycline antibiotics are known to target the ribosomal 30S subunit, but the ribosome has defense mechanisms that can resist their action (Kang and Park, 2015).

5.2.6 Alteration in RNA polymerase enzyme importing resistance to rifampicin antibiotics

Rifampicin is an antibiotic commonly used to treat bacterial infections. It works by inhibiting the RNA synthesis process in bacteria, specifically by binding to the beta-subunit of the DNA-dependent RNA polymerase enzyme (Hasan et al., 2021). This binding prevents the enzyme from effectively transcribing DNA into RNA, leading to the inhibition of bacterial growth and ultimately causing cell death.

However, bacteria can develop resistance to rifampicin through alterations in the RNA polymerase enzyme. Mutations in the rpoB gene, which encodes the beta-subunit of RNA polymerase, can confer resistance to rifampicin (Patel et al., 2023). These mutations can affect the binding affinity between rifampicin and the RNA polymerase enzyme, reducing the ability of the antibiotic to inhibit RNA synthesis.

The alterations in the RNA polymerase enzyme that result in rifampicin resistance can have several consequences. One of the effects is the alteration of the levels of peptidoglycan precursors, which are essential components of the bacterial cell wall. Changes in the levels of these precursors can impact the integrity and stability of the cell wall, potentially affecting the susceptibility of bacteria to other antibiotics, such as beta-lactams (Patel et al., 2023).

It is important to note that rifampicin resistance can arise through various mechanisms, and alterations in the RNA polymerase enzyme are just one of them. Other mechanisms include the acquisition of resistance genes through horizontal gene transfer and the overexpression of efflux pumps that can actively remove rifampicin from the bacterial cell (Hasan et al., 2021).

5.3 Bacteria inactivate the antibiotic by enzymes

Three key enzymes are responsible for antibiotic inactivation (Figure 10). These enzymes include the following:

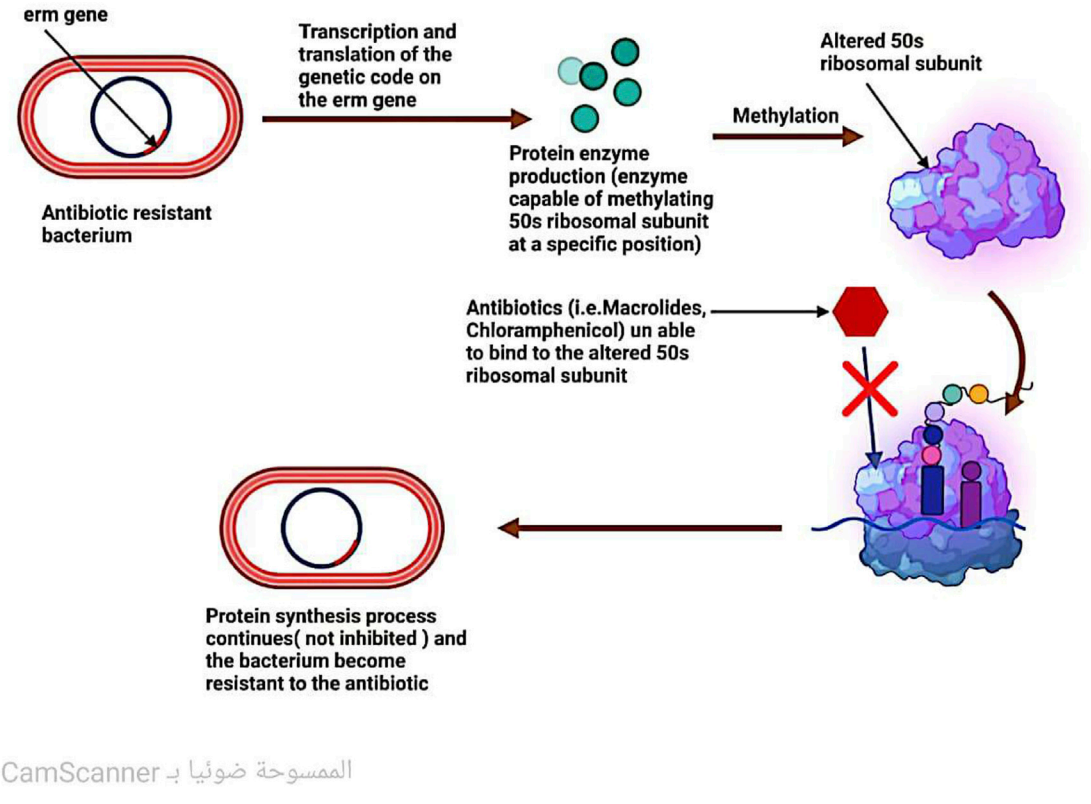

FIGURE 7
Mechanism of antibiotic resistance by alteration in 50 s ribosomal subunit.

5.3.1 Beta-lactamases enzymes

These enzymes produced by bacteria have the ability to break down all B-lactam antibiotics that are bonded with ester and amide. This leads to the development of resistance in bacteria that can produce beta-lactamase enzymes toward beta-lactam antibiotics (Fernández-Billón et al., 2023).

5.3.2 Aminoglycoside modifying enzymes (AGES)

Enzymes are known to play a crucial role in antibiotic resistance. Specifically, enzymes such as aminoglycoside-modifying enzymes (AMEs) have been found to prevent the attachment of aminoglycoside antibiotics to their ribosomal target (Strateva and Yordanov 2009). These enzymes are present in various bacterial strains, including *E. faecalis*, *S. aureus*, and *S. pneumoniae*. In addition to their role in preventing antibiotic attachment, these enzymes also aid in conferring resistance to aminoglycosides and fluoroquinolones (Kang and Park, 2015). Thus, the presence of AMEs in bacterial strains is a major concern in the field of antibiotic resistance, as it poses a significant challenge to the effectiveness of these antibiotics in treating bacterial infections.

5.3.3 Chloramphenicol-acetyl-transferases enzymes

Enzymes known as chloramphenicol-acetyltransferases modify the antibiotic chloramphenicol by acetylating its hydroxyl group, resulting in an altered form of the antibiotic that is unable to bind to its ribosomal target. Consequently, bacteria possessing the chloramphenicol-acetyltransferase enzyme are resistant to chloramphenicol antibiotics, rendering them ineffective (Varela et al., 2021).

6 Spread of antibiotic resistance among bacteria

When a microorganism is able to survive or grow in an antibiotic concentration that would normally inhibit or kill other organisms of the same species, it is considered resistant (Kester and Fortune, 2014; Kaur Sodhi and Singh, 2022). In clinical practice, the terms “susceptible” and “resistant” are often used to describe the likelihood of successful treatment with antibiotics (Sabtu, Enoch, and Brown, 2015). Resistance is more likely to occur when a patient is unable to attain the concentration of antibiotic necessary to inhibit or kill the bacteria (Ordway et al., 2003). Microorganisms can either inherently possess resistance to an antibiotic or acquire it after exposure (Premlatha, 2019). The development of resistance can occur through gene mutations or direct transfer of resistance genes (Sodhi et al., 2023), which can be carried on plasmids (mobile genetic elements) (Kaur Sodhi and Singh, 2022) and transmitted through conjugation (Shree et al., 2023), or through the direct transfer of naked DNA through transformation (Shree et al., 2023) (Figure 11) or the transfer of similar DNA through bacteriophages (Kaur Sodhi and Singh, 2022; Shree et al., 2023), a process known as transduction. Even among bacteria of different species, genetic material, including antibiotic-resistance genes, can

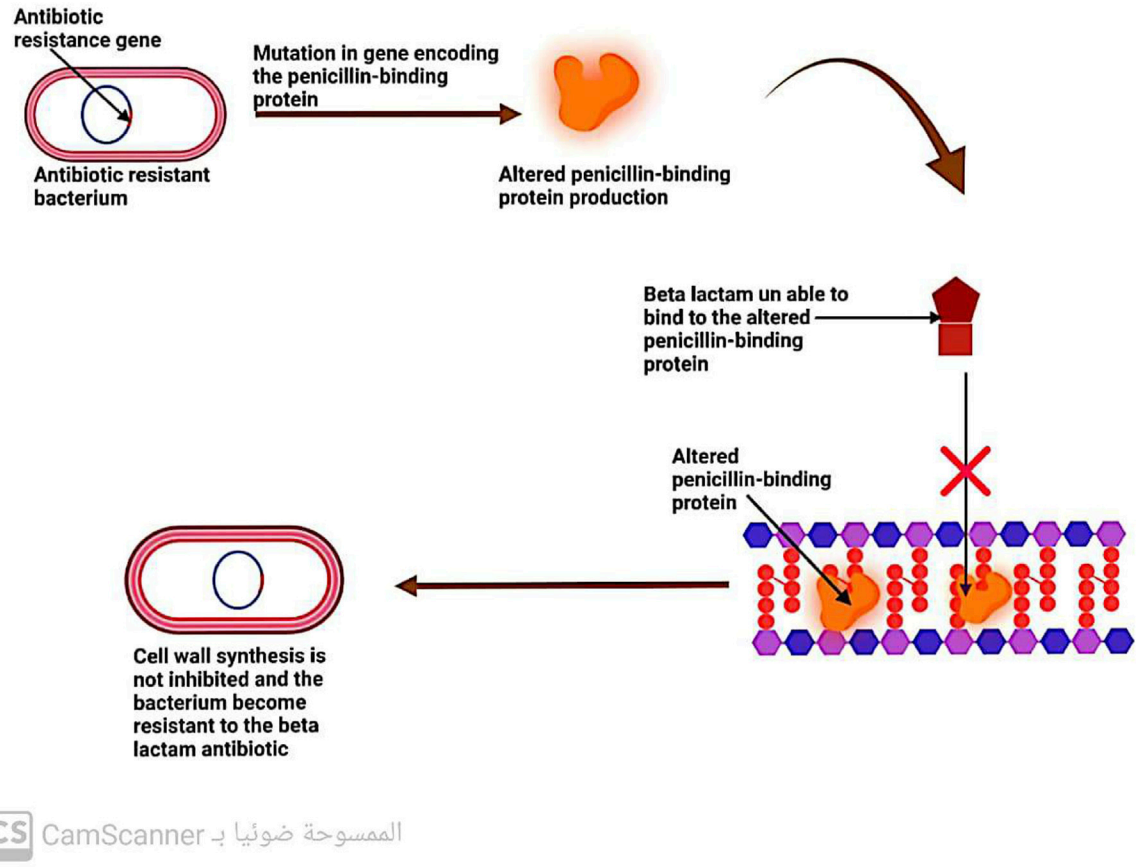

FIGURE 8
Mechanism of antibiotic resistance by alteration in penicillin-binding protein.

spread rapidly (Džidić et al., 2008). It was reported that heavy metals (Sodhi et al., 2023) and biofilm formation (Shree et al., 2023) increase the spread of antibiotic resistance among bacteria.

Different resistant bacteria can travel through various means, allowing them to spread and potentially cause infections in different settings. While the specific mechanisms of travel may vary depending on the bacteria and the environment, there are several common routes through which resistant bacteria can spread. For example:

1. Person-to-person transmission: Resistant bacteria can be transmitted directly from one person to another through close contact. This can occur through physical contact, such as touching or shaking hands with an infected person, or through respiratory droplets when an infected person coughs or sneezes (Ohmagari, 2014).
2. Contaminated surfaces: Resistant bacteria can survive on surfaces for extended periods. When a person touches a contaminated surface, such as doorknobs, countertops, or medical equipment, they can transfer the bacteria to their hands. If they then touch their face or mouth, the bacteria can enter their body and potentially cause an infection (Ohmagari, 2014).
3. Healthcare settings: Hospitals and healthcare facilities can be hotspots for the spread of resistant bacteria. Factors such as poor hygiene practices, inadequate infection control measures, and the close proximity of patients can contribute to the transmission of bacteria. Healthcare workers can inadvertently spread resistant bacteria from one patient to another if proper hand hygiene and infection control protocols are not followed (Clements et al., 2008; Tacconelli et al., 2014).
4. Animal-to-human transmission: Resistant bacteria can also be transmitted from animals to humans. This can occur through direct contact with infected animals or through the consumption of contaminated food products, such as meat or dairy products. Farm animals, in particular, can harbor resistant bacteria due to the use of antibiotics in agriculture (Garcia-Graells et al., 2012).
5. Travel and international spread: Resistant bacteria can be carried across borders through international travel. People who are infected or colonized with resistant bacteria can unknowingly spread them to other countries. This can contribute to the global dissemination of resistant strains and make it more challenging to control their spread (Ohmagari, 2014).

It is important to note that the specific mechanisms of travel and transmission can vary depending on the bacteria and the setting. Additionally, the spread of resistant bacteria can be influenced by factors such as poor hygiene, inadequate sanitation, and suboptimal infection control practices (Tacconelli et al., 2014).

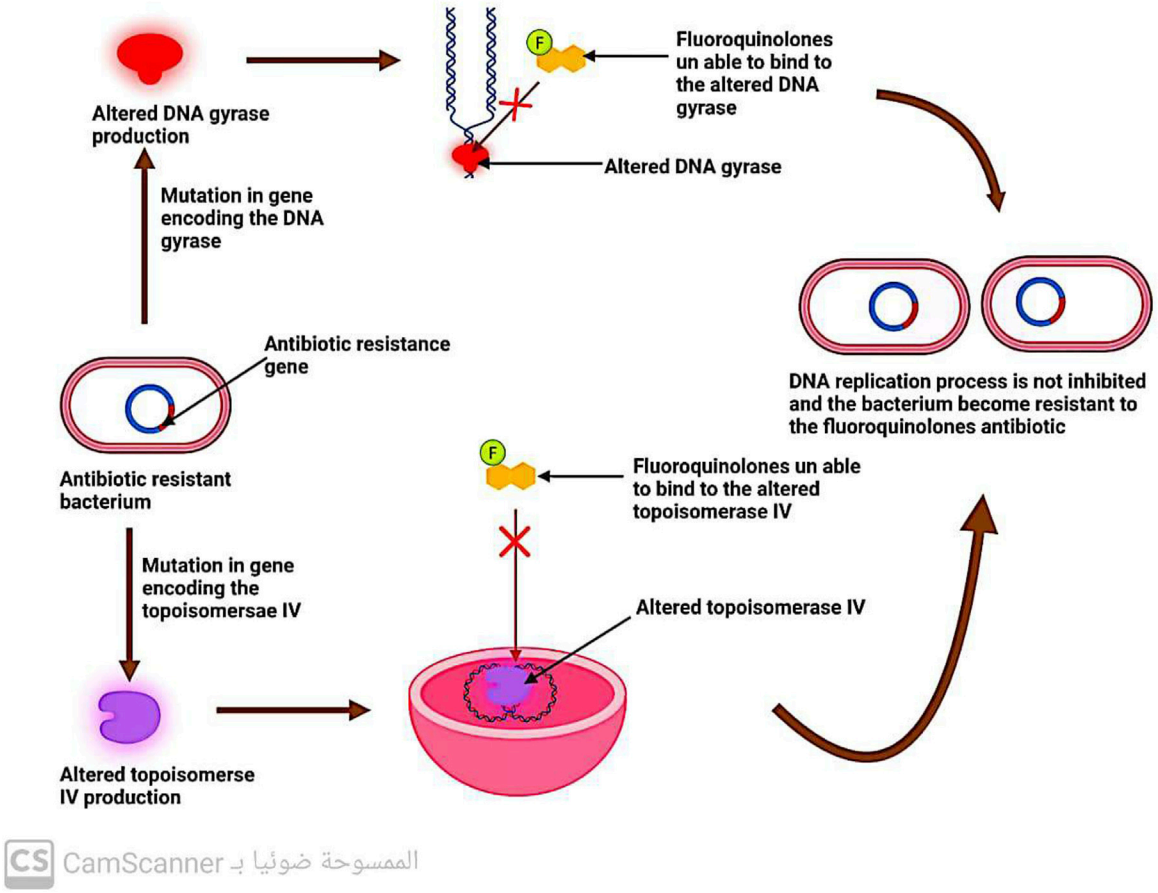

FIGURE 9
Mechanism of antibiotic resistance by alteration in DNA gyrase and topoisomerase IV.

7 Factors affecting the resistance of antibiotics

The emergence of antibiotic resistance is accelerated by the under, over, or improper use of antibiotics (Anwar, Iqbal, and Saleem, 2020; Kaur Sodhi and Singh, 2022; Shree et al., 2023; Sodhi et al., 2023). The indiscriminate use of antibiotics, which promotes antibiotic resistance, is caused by a variety of factors, including patients' noncompliance with prescribed treatment and demand, irrational use of antibiotics by prescribers in human medicine, drug advertising, dispensing doctors, antibiotic use in agriculture, poor antibiotic quality, inadequate surveillance, and susceptibility testing. Despite their knowledge of a patient's diagnosis, doctors and prescribers can be heavily influenced by patient demand, which can contribute to antimicrobial and antibiotic resistance (Acharya and Wilson, 2019).

Patients may discontinue their treatment once they begin to feel better, forget to take their prescriptions, or only purchase a portion of the medication. In such cases, increased physician-patient interaction is often necessary to ensure proper compliance with treatment (Carlet et al., 2012). Additionally, antibiotics are readily available in pharmacies without a prescription, which further contributes to their misuse by patients (Darj, Newaz, and Zaman, 2019; Machowska and Lundborg, 2019).

The pharmaceutical industry also plays a role in promoting antibiotic misuse through advertising. For example, some advertisements claim that certain antibiotics, such as Ciprofloxacin, are the best option for at-risk patients. In the past, advertisements in the Philippines encouraged the use of lincomycin for pharyngitis/tonsillitis and clindamycin for upper respiratory tract infections, despite the fact that these conditions are often caused by viral infections that do not require antibiotics (Ladd, 2005; Tanday, 2016). Overall, inappropriate antibiotic use is a multifaceted issue that requires cooperation between healthcare providers, patients, and the pharmaceutical industry to address.

Medical professionals have a significant impact on the development of antibiotic resistance in bacteria. It is common for doctors to prescribe broad-spectrum antibiotics when narrow-spectrum ones would be more appropriate (Mincey and Parkulo, 2001; Om et al., 2016). The prescribing patterns of doctors can vary, and studies have shown that 30%–60% of patients receive more antibiotics than necessary. Additionally, incorrect prescriptions and recommendations from untrained medical professionals pose a significant risk. A related study found that private practitioners often prescribe unnecessary medications (Thakolkaran et al., 2017).

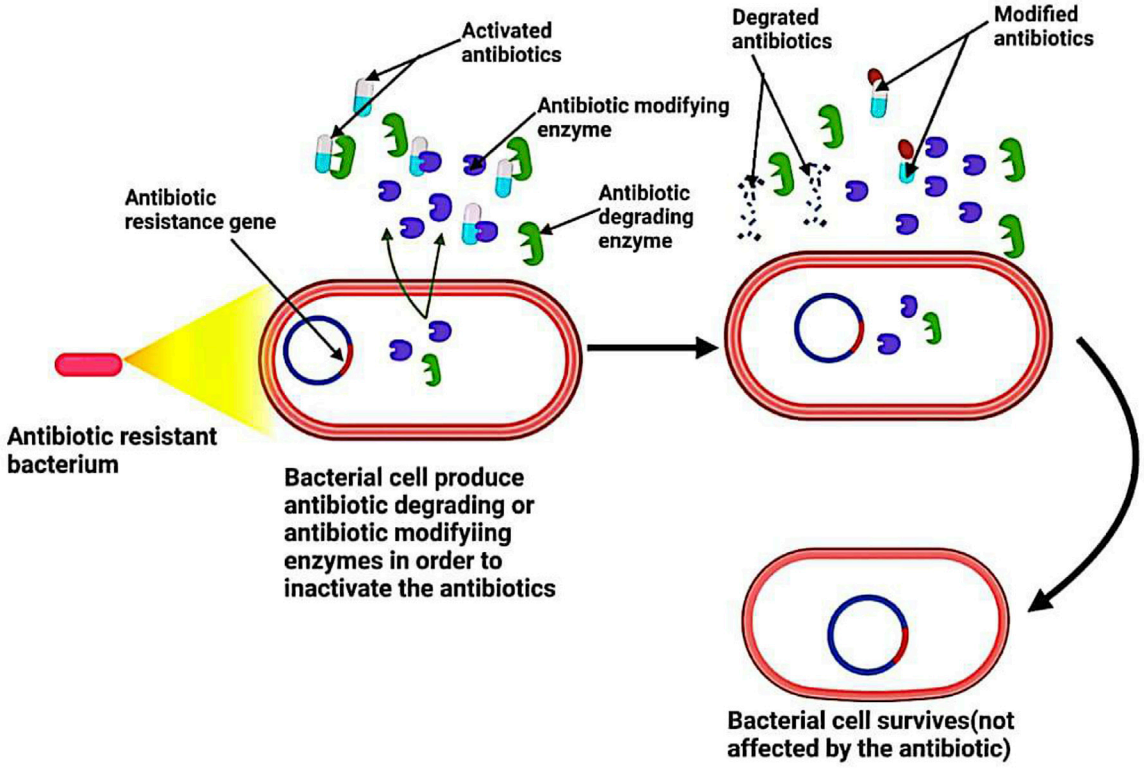

FIGURE 10
Mechanism of antibiotic resistance by inactivation of the antibiotic.

Hospitals and clinics are significant contributors to the development of microbial resistance to antibiotics (Shree et al., 2023). Inadequate infection control protocols, such as failure to wash hands or change gloves regularly, have been identified as factors contributing to this problem (Weinstein, 2001). Another issue is the use of poor-quality antibiotics. This problem persists due to the lack of quality compliance and monitoring, leading to the use of expired and counterfeit antibiotics (Ayukekbong, Ntemgwa, and Atabe, 2017). Inappropriate use of antibiotics in animals is also a concern. Some antibiotics are administered to animals to boost their growth and prevent sickness (Manishimwe, Nishimwe, and Ojok, 2017). However, the surveillance and susceptibility testing of antibiotics are insufficient (Tebano et al., 2020) (Table 2).

8 Alternative approaches to combat antibiotic resistance

We are now in grave danger because of the global antibiotic resistance crisis, which is constantly increasing. Therefore, we should focus on finding solutions to fight this resistance crisis. There are several approaches to fight this crisis which we discuss in this review article as follows:

8.1 Discovery of new antibiotics

In 2015, researchers discovered a new antibiotic called teixobactin, which demonstrated bactericidal activity against *S. aureus*, *Clostridium difficile*, and *Bacillus anthracis* (Piddock, 2015). On 20 February 2020, researchers published an article in Cell titled "A Deep Learning Approach to Antibiotic Discovery." Using artificial intelligence, they discovered a new antibiotic called halicin, which showed bactericidal activity against a broad spectrum of pathogenic and resistant bacteria (Stokes et al., 2020).

On 26 September 2022, researchers published an article in Nature Microbiology titled "Computational identification of a systemic antibiotic for Gram-negative Bacteria." Using computational screening, they discovered a new antibiotic called dynobactin, which demonstrated potent bactericidal activity against dangerous Gram-negative bacteria resistant to other antibiotics (Miller et al., 2022).

The dysfunctional R&D market for detecting new antibiotics refers to the challenges and limitations faced in the research and development of new antibiotics. These challenges include economic, regulatory, and scientific barriers that hinder the discovery and development of effective antibiotics to combat bacterial infections. Some of the key issues in the dysfunctional R&D market for detecting new antibiotics include:

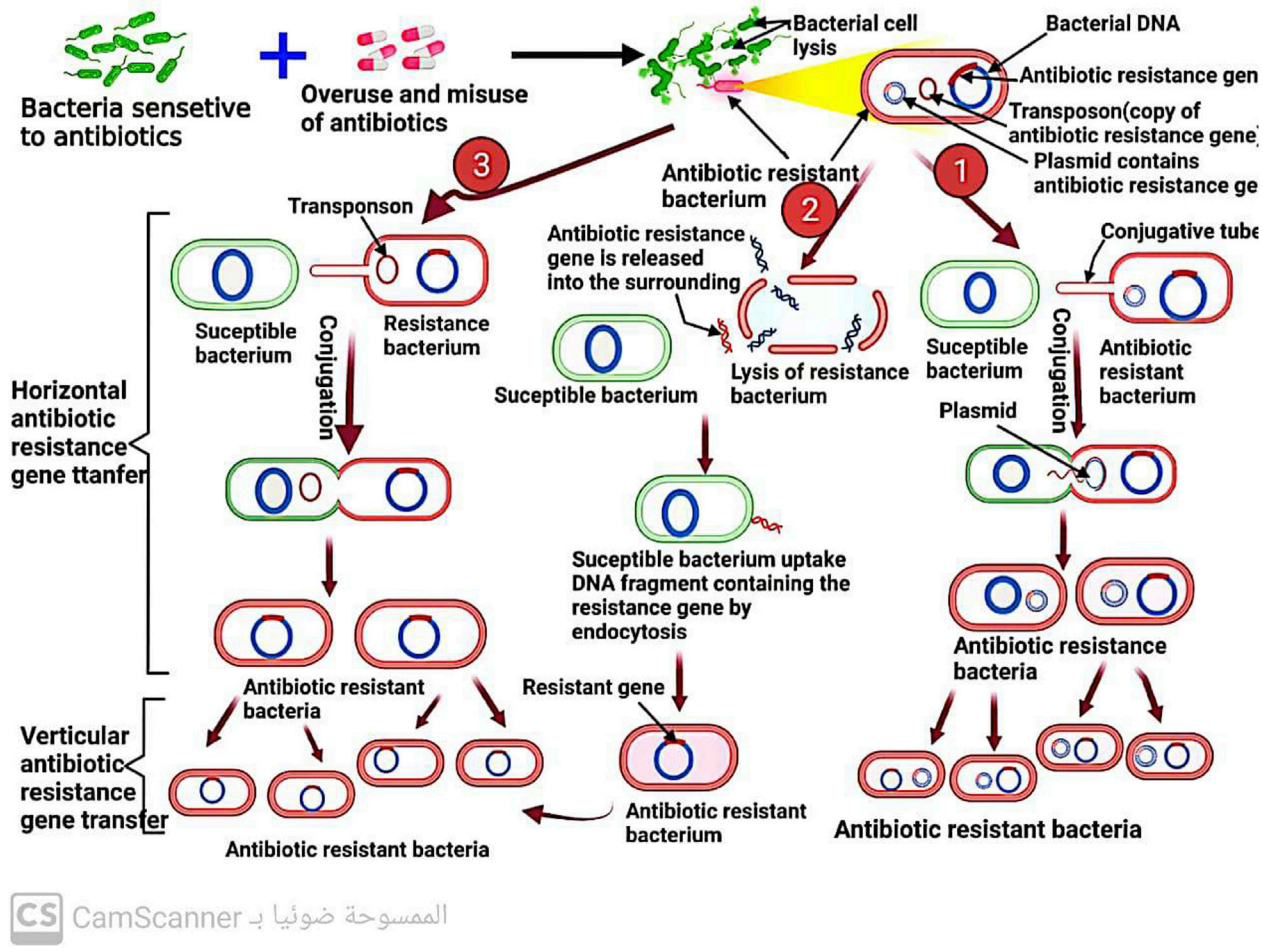

FIGURE 11
Mechanism of antibiotic resistance spread among bacteria by conjugation and transformation.

8.1.1 A-economic challenges

Limited financial incentives: The high cost and low profitability of developing new antibiotics have led to a lack of investment from pharmaceutical companies (Clardy, Fischbach, and Walsh, 2006).

Long development timelines: The lengthy and expensive process of developing new antibiotics makes it less attractive for companies to invest in this area (Clardy et al., 2006).

8.1.2 B-regulatory challenges

Stringent regulatory requirements: The regulatory approval process for new antibiotics is complex and time-consuming, leading to delays in bringing new drugs to market (McDevitt and Rosenberg, 2001).

Limited guidance on clinical trial design: There is a lack of clear guidelines for conducting clinical trials for antibiotics, which can further hinder the development process (McDevitt and Rosenberg, 2001).

8.1.3 C-scientific challenges

Antibiotic resistance: The rise of antibiotic-resistant bacteria poses a significant challenge in the development of new antibiotics (McDevitt and Rosenberg, 2001).

Limited understanding of bacterial biology: Despite advances in genomics and other technologies, there is still much to learn about the biology of bacteria and their mechanisms of resistance (McDevitt and Rosenberg, 2001).

8.2 Antibiotic adjuvants

Antibiotic adjuvants are compounds that do not directly kill bacteria but instead enhance an antibiotic's effectiveness by inhibiting resistance mechanisms. For example, beta-lactamase inhibitors are small-molecule antibiotic adjuvants. Beta-lactamase inhibitors, when combined with beta-lactam antibiotics, have been used successfully for over 30 years to treat Gram-positive and Gram-negative infections. Their use has been extensively documented (Melander and Melander, 2017).

8.3 Nano antibiotics

Nanoscale antibiotics, which consist of pure antibiotic molecules between 1 and 100 nm in size or antibiotic

TABLE 2 Factors causing antibiotic resistance in different sectors and some proposed solutions to overcome these factors.

Sector	Causes of antibiotic resistance	Proposed solutions
Human Health	➢ Prescription and use of antibiotics for viral infections, including Influenza, upper respiratory tract infections, pharyngitis, tonsillitis, and the common cold (Ladd, 2005; Tanday, 2016).	➢ Physicians should not prescribe antibiotics for viral infections.
	➢ Patients are not taking the entire course of antibiotics and interrupting their treatment when they feel better (Carlet et al., 2012).	➢ Patients should take their entire course of antibiotics even if they feel better.
	➢ Self-medication and misuse of antibiotics by patients because it is readily available in the pharmacy, and they can buy them without having a prescription (Darj et al., 2019; Machowska and Cecilia Stålsby, 2019).	➢ Banning the sale of antibiotics in pharmacies without a prescription.
	➢ Overprescription of un- necessary antibiotics, especially broad-spectrum antibiotics, by physicians (Mincey and Parkulo, 2001; Om et al., 2016).	➢ Physicians should only prescribe the necessary antibiotics for the disease without prescribing the unnecessary ones.
	➢ Poor infection control practices in hospitals and clinics, like hand washing and changing gloves (Weinstein, 2001).	➢ Attention should be paid to developing infection control practices in hospitals and clinics.
	➢ Lack of quality compliance and monitoring in hospitals and clinics results in expired and counterfeit antibiotics being used (Ayukekbong et al., 2017).	➢ Attention should be paid to quality compliance in hospitals and clinics to prevent the use of expired and counterfeit antibiotics.
Animal husbandry	➢ Overusing antibiotics in animal feeds for growth and disease control (Anwar et al., 2020; Kaur Sodhi and Singh, 2022; Shree et al., 2023; Sodhi et al., 2023).	➢ Establishing guidelines for prudent usage.
Agriculture	➢ Overusing antibiotics as pesticides for disease control in plants (Anwar et al., 2020; Kaur Sodhi and Singh, 2022; Shree et al., 2023; Sodhi et al., 2023).	➢ Establishing guidelines for prudent usage.
Aquaculture	➢ Overusing antibiotics in fish farming (Anwar et al., 2020; Kaur Sodhi and Singh, 2022; Shree et al., 2023; Sodhi et al., 2023).	➢ Establishing guidelines for prudent usage.

molecules physically attached to nanoparticles, represent one beneficial use of nanotechnology (Soares et al., 2018; Singh and Sodhi, 2023). By reengineering antibiotics at the nanoscale, this new antimicrobial approach revives the arsenal of available medications by making them effective against various clinically important microorganisms. Unlike their bulk chemical counterparts, nanoantibiotics have different physicochemical properties and increased potency (Mamun et al., 2021). Because nanoscale drug delivery systems can transport and bind to intracellular targets, reducing bacterial growth and metabolism and ultimately causing cell death, a medication delivered via or incorporated into nanoparticles at the same dose has significantly greater inhibitory effects on bacterial growth (Jijie et al., 2017; Singh and Sodhi, 2023).

8.4 Botanicals

Plants produce secondary metabolites, including alkaloids, flavonoids, phenolics, quinones, tannins, coumarins, terpenes, lectins, and saponins. These secondary metabolites exhibit antimicrobial activity against various microorganisms (Gupta and Birdi, 2017).

8.5 Bacteriophages

According to the National Institute of Health (NIH, 2014), bacteriophages are innovative elements that could combat microbial resistance (Shree et al., 2023; NIAID's Antibacterial Resistance Program, 2014). Numerous studies applied bacteriophages on humans and animals to treat various bacterial diseases and showed positive, effective results. These bacterial pathogens include *Shigella dysenteriae* (Chanishvili, 2012), *Vibrio cholera* (Chanishvili, 2012), *P. aeruginosa* (Watanabe et al., 2007), *C. difficile* (Meader et al., 2013), Vancomycin-resistant *E. faecium* (Biswas et al., 2002), β-lactamase-producing *E. coli* (Wang et al., 2006), imipenem resistant *P. aeruginosa* (Wang et al., 2006), *Acinetobacter baumannii* (Yuan et al., 2019), *E. coli* (Pouillot et al., 2012), MDR-*S. aureus* (Fish et al., 2016), unclassified bacterial dysentery (Chanishvili and Sharp, 2008), *S. typhi* (Kutateladze and Adamia, 2008), and antibiotic-resistant *P. aeruginosa* (Wright et al., 2009).

9 Conclusion

This review article has discussed various aspects related to antibiotics, their mechanisms of action, the problem of antibiotic resistance, and potential solutions to combat resistance. Antibiotics have diverse applications in different fields but their use remains controversial owing to resistance issues. Antibiotics act through four primary mechanisms to kill or inhibit the growth of bacteria. However, bacteria have evolved mechanisms to become resistant to antibiotics, diminishing the effectiveness of these drugs. Given the limited capabilities of traditional antibiotics due to resistance, we discussed several promising alternative approaches, including the discovery of new antibiotics, the use of antibiotic adjuvants and nanoparticle-based antibiotics, botanicals, and bacteriophages. Although developing new antibiotics is challenging, a combination of complementary strategies such as nanoantibiotics, adjuvants, botanicals, and phage therapy could help address the resistance crisis.

Author contributions

EH: Conceptualization, Data curation, Formal Analysis, Investigation, Project administration, Resources, Validation, Visualization, Writing–original draft, Writing–review and editing. MF: Conceptualization, Data curation, Methodology, Software, Validation, Writing–original draft. MA-R: Data curation, Formal Analysis, Investigation, Software, Validation, Visualization, Writing–original draft. AB: Data curation, Formal Analysis, Software, Validation, Visualization, Writing–original draft. NN: Data curation, Formal Analysis, Methodology, Software, Validation, Writing–original draft. MA: Data curation, Formal Analysis, Investigation, Methodology, Software, Validation, Writing–original draft. RO: Data curation, Formal Analysis, Funding acquisition, Methodology, Software, Validation, Writing–original draft, Writing–review and editing. LF: Data curation, Formal Analysis, Methodology, Resources, Software, Validation, Writing–original draft, Writing–review and editing. AAt: Data curation, Formal Analysis, Methodology, Software, Validation, Writing–original draft. ME-N: Data curation, Formal Analysis, Investigation, Methodology, Software, Validation, Writing–original draft. AAb: Conceptualization, Software, Supervision, Validation, Visualization, Writing–original draft, Writing–review and editing.

Funding

The author(s) declare financial support was received for the research, authorship, and/or publication of this article. This paper was supported from the project 6PFE of the University of Life Sciences "King Mihai I" from Timisoara and Research Institute for Biosecurity and Bioengineering from Timisoara.

Conflict of interest

The authors declare that the research was conducted in the absence of any commercial or financial relationships that could be construed as a potential conflict of interest.

Publisher's note

References

Acharya, K. P., and Trevor Wilson, R. (2019). Antimicrobial resistance in Nepal. *Front. Med.* 6, 105–109. May. doi:10.3389/fmed.2019.00105

Anwar, M., Iqbal, Q., and Saleem, F. (2020). Improper disposal of unused antibiotics: an often overlooked driver of antimicrobial resistance. *Expert Rev. Anti-Infective Ther.* 18 (8), 697–699. doi:10.1080/14787210.2020.1754797

Ayukekbong, J. A., Ntemgwa, M., and Atabe, A. N. (2017). The threat of antimicrobial resistance in developing countries: causes and control strategies. *Antimicrob. Resist. Infect. Control* 6 (1), 47–48. doi:10.1186/s13756-017-0208-x

Benbrook, C. M. (2002). *Antibiotic drug use in US aquaculture*. United States: Institute for Agriculture and Trade Policy Report February, 1–18.

Bhattacharyya, S. (2012). Do bacteria age? *Resonance* 17 (4), 347–364. doi:10.1007/s12045-012-0037-4

Biondo, C. (2023). Bacterial antibiotic resistance: the most critical pathogens. *Pathogens* 12 (1), 116–214. doi:10.3390/pathogens12010116

Biswas, B., Sankar, A., Paul, W., Paul, B., Trostel, A. N., Powell, B., et al. (2002). Erratum: bacteriophage therapy rescues mice bacteremic from a clinical isolate of vancomycin-resistant Enterococcus faecium (infection and immunity (2002) 70:1 (204-210)). *Infect. Immun.* 70 (3), 1664. doi:10.1128/iai.70.3.1664-1664.2002

Blondeau, J. M. (2004). Fluoroquinolones: mechanism of action, classification, and development of resistance. *Surv. Ophthalmol.* 49, S73–S78. 2 SUPPL. 2. doi:10.1016/j.survophthal.2004.01.005

Brodersen, D. E., Clemons, W. M., Carter, A. P., Morgan-Warren, R. J., Wimberly, B. T., and Ramakrishnan, V. (2000). The structural basis for the action of the antibiotics tetracycline, pactamycin, and hygromycin B, on the 30S ribosomal subunit. *Cell* 103 (7), 1143–1154. doi:10.1016/S0092-8674(00)00216-6

Bush, N. G., Evans-roberts, K., and Anthony, M. (2015). DNA topoisomerases. *EcoSal Plus* 6 (2), 1–34. doi:10.1128/ecosalplus.ESP-0010-2014

Capasso, C., and Supuran, C. T. (2014). Sulfa and trimethoprim-like drugs-antimetabolites acting as carbonic anhydrase, dihydropteroate synthase and dihydrofolate reductase inhibitors. *J. Enzyme Inhibition Med. Chem.* 29 (3), 379–387. doi:10.3109/14756366.2013.787422

Carlet, J., Jarlier, V., Harbarth, S., Voss, A., Goossens, H., and Pittet, D. (2012). Ready for a World without antibiotics? The pensières antibiotic resistance call to action. *Antimicrob. Resist. Infect. Control* 1, 11–13. doi:10.1186/2047-2994-1-11

Chanishvili, N. (2012). *Phage therapy-history from twort and d'Herelle through soviet experience to current approaches. Vol. 83*. 1. Amsterdam, Netherlands: Elsevier Inc.

Chanishvili, N., and Sharp, R. (2008). Bacteriophage therapy: experience from the eliava Institute, Georgia. *Microbiol. Aust.* 29 (2), 96. doi:10.1071/ma08096

Cho, H., Uehara, T., and Bernhardt, T. G. (2014). Beta-lactam antibiotics induce a lethal malfunctioning of the bacterial cell wall synthesis machinery. *Cell* 159 (6), 1300–1311. doi:10.1016/j.cell.2014.11.017

Clardy, J., Fischbach, M. A., and Walsh, C. T. (2006). New antibiotics from bacterial natural products. *Nat. Biotechnol.* 24 (12), 1541–1550. doi:10.1038/nbt1266

Clements, A., Halton, K., Graves, N., Pettitt, A., Morton, A., Looke, D., et al. (2008). Overcrowding and understaffing in modern health-care systems: key determinants in meticillin-resistant Staphylococcus aureus transmission. *Lancet Infect. Dis.* 8 (7), 427–434. doi:10.1016/S1473-3099(08)70151-8

Darby, E. M., Trampari, E., Siasat, P., Solsona Gaya, M., Alav, I., Webber, M. A., et al. (2023). Molecular mechanisms of antibiotic resistance revisited. *Nat. Rev. Microbiol.* 21 (5), 280–295. doi:10.1038/s41579-022-00820-y

Darj, E., Md Shah, N., and Zaman, M. H. (2019). Pharmacists' perception of their challenges at work, focusing on antimicrobial resistance: a qualitative study from Bangladesh. *Glob. Health Action* 12, 1735126. sup1. doi:10.1080/16549716.2020.1735126

Dawood, M. A. O., Koshio, S., and Ángeles Esteban., M. (2018). Beneficial roles of feed additives as immunostimulants in aquaculture: a review. *Rev. Aquac.* 10 (4), 950–974. doi:10.1111/raq.12209

Delcour, A. H. (2009). Outer membrane permeability and antibiotic resistance. *Biochimica Biophysica Acta - Proteins Proteomics* 1794 (5), 808–816. doi:10.1016/j.bbapap.2008.11.005

Džidić, S., Šušković, J., and Kos, B. (2008). Antibiotic resistance mechanisms in bacteria: biochemical and genetic aspects. *Food Technol. Biotechnol.* 46 (1), 11–21.

Fàbrega, A., Madurga, S., Giralt, E., and Vila, J. (2009). Mechanism of action of and resistance to quinolones. *Microb. Biotechnol.* 2 (1), 40–61. doi:10.1111/j.1751-7915.2008.00063.x

Fernandes, R., Amador, P., and Prudêncio, C. (2013). β-Lactams: chemical structure, mode of action and mechanisms of resistance. *Rev. Res. Med. Microbiol.* 24 (1), 7–17. doi:10.1097/MRM.0b013e3283587727

Fernandez, B., María, A. E., Llambías, C., Jordana-Lluch, E., Oliver, A., and Macià, M. D. (2023). Mechanisms of antibiotic resistance in Pseudomonas aeruginosa biofilms. *Biofilm* 5, 100129. Figure 1. doi:10.1016/j.bioflm.2023.100129

Fish, R., Kutter, E., Wheat, G., Blasdel, B., Kutateladze, M., and Kuhl, S. (2016). *Saint peter, hospital family, and medicine residency*. England: Fish2016.

Foti, C., Piperno, A., Scala, A., and Giuffrè, O. (2021). Oxazolidinone antibiotics: chemical, biological and analytical aspects. *Molecules* 26 (14), 4280. doi:10.3390/molecules26144280

Garcia-Graells, C., Antoine, J., Larsen, J., Catry, B., Skov, R., and Denis, O. (2012). Livestock veterinarians at high risk of acquiring methicillin-resistant Staphylococcus aureus ST398. *Epidemiol. Infect.* 140 (3), 383–389. doi:10.1017/S0950268811002263

Gilbert, D. M. (2001). Making sense of eukaryotic DNA replication origins. *Science* 294 (5540), 96–100. doi:10.1126/science.1061724

Gonzalez Ronquillo, M., and Juan Carlos Angeles, H. (2017). Antibiotic and synthetic growth promoters in animal diets: review of impact and analytical methods. *Food control.* 72, 255–267. doi:10.1016/j.foodcont.2016.03.001

Gupta, P. D., and Birdi, T. J. (2017). Development of botanicals to combat antibiotic resistance. *J. Ayurveda Integr. Med.* 8 (4), 266–275. doi:10.1016/j.jaim.2017.05.004

Gupta, R., and Gupta, N. (2021). *Fundamentals of bacterial physiology and metabolism*. Singapore: Springer.

Hasan, C. M., Dutta, D., and Nguyen, A. N. T. (2021). Revisiting antibiotic resistance: mechanistic foundations to evolutionary outlook *Antibiotics* 11, 40. doi:10.3390/antibiotics11010040

Hirsch, J., and Klostermeier, D. (2021). What makes a type IIA topoisomerase a gyrase or a topo IV? *Nucleic Acids Res.* 49 (11), 6027–6042. doi:10.1093/nar/gkab270

Jana, S., and Deb, J. K. (2006). Molecular understanding of aminoglycoside action and resistance. *Appl. Microbiol. Biotechnol.* 70 (2), 140–150. doi:10.1007/s00253-005-0279-0

Jijie, R., Barras, A., Teodorescu, F., Boukherroub, R., and Szunerits, S. (2017). Advancements on the molecular design of nanoantibiotics: current level of development and future challenges. *Mol. Syst. Des. Eng.* 2 (4), 349–369. doi:10.1039/c7me00048k

Johansson, M., Lovmar, M., and Ehrenberg, M. (2008). Rate and accuracy of bacterial protein synthesis revisited. *Curr. Opin. Microbiol.* 11 (2), 141–147. doi:10.1016/j.mib.2008.02.015

Kang, H. K., and Park, Y. (2015). Glycopeptide antibiotics: structure and mechanisms of action. *J. Bacteriol. Virology* 45 (2), 67–78. doi:10.4167/jbv.2015.45.2.67

Kaur Sodhi, K., and Singh, C. K. (2022). Recent development in the sustainable remediation of antibiotics: a review. *Total Environ. Res. Themes* 3–4, 100008. May. doi:10.1016/j.totert.2022.100008

Kester, J. C., and Fortune, S. M. (2014). Persisters and beyond: mechanisms of phenotypic drug resistance and drug tolerance in bacteria. *Crit. Rev. Biochem. Mol. Biol.* 49 (2), 91–101. doi:10.3109/10409238.2013.869543

Kohanski, M. A., Dwyer, D. J., and Collins, J. J. (2010). How antibiotics kill bacteria: from targets to networks. *Nat. Rev. Microbiol.* 8 (6), 423–435. doi:10.1038/nrmicro2333

Kutateladze, M., and Adamia, R. (2008). Phage therapy experience at the eliava Institute. *Med. Maladies Infect.* 38 (8), 426–430. doi:10.1016/j.medmal.2008.06.023

Ladd, E. (2005). The use of antibiotics for viral upper respiratory tract infections: an Analysis of nurse practitioner and physician prescribing practices in ambulatory care, 1997-2001. *J. Am. Acad. Nurse Pract.* 17 (10), 416–424. doi:10.1111/j.1745-7599.2005.00072.x

Laskin, A. I., Bennett, J. W., and Gadd, G. M. (2002). *Adv. Appl. Microbiol.* 51.

Li, Y., and Araki, H. (2013). Loading and activation of DNA replicative helicases: the key step of initiation of DNA replication. *Genes Cells* 18 (4), 266–277. doi:10.1111/gtc.12040

Liu, Y., and Breukink, E. (2016). The membrane steps of bacterial cell wall synthesis as antibiotic targets. *Antibiotics* 5 (3), 28. doi:10.3390/antibiotics5030028

Machowska, A., and Cecilia Stålsby, L. (2019). Drivers of irrational use of antibiotics in europe. *Int. J. Environ. Res. Public Health* 16 (1), 27. doi:10.3390/ijerph16010027

Malik, M., Zhao, X., and Drlica, K. (2006). Lethal fragmentation of bacterial chromosomes mediated by DNA gyrase and quinolones. *Mol. Microbiol.* 61 (3), 810–825. doi:10.1111/j.1365-2958.2006.05275.x

Mamun, M. M., Sorinolu, A. J., Munir, M., and Eric, P. V. (2021). Nanoantibiotics: functions and properties at the nanoscale to combat antibiotic resistance. *Front. Chem.* 9, 687660–687723. May. doi:10.3389/fchem.2021.687660

Manishimwe, R., Nishimwe, K., and Lonzy, O. (2017). Assessment of antibiotic use in farm animals in Rwanda. *Trop. Animal Health Prod.* 49 (6), 1101–1106. doi:10.1007/s11250-017-1290-z

McDevitt, D., and Rosenberg, M. (2001). Exploiting genomics to discover new antibiotics. *Trends Microbiol.* 9 (12), 611–617. doi:10.1016/S0966-842X(01)02235-1

Meader, E., Mayer, M. J., Steverding, D., Carding, S. R., and Narbad, A. (2013). Evaluation of bacteriophage therapy to control Clostridium difficile and toxin production in an invitro human colon model system. *Anaerobe* 22, 25–30. doi:10.1016/j.anaerobe.2013.05.001

Melander, R. J., and Melander., C. (2017). The challenge of overcoming antibiotic resistance: an adjuvant approach? *ACS Infect. Dis.* 3 (8), 559–563. doi:10.1021/acsinfecdis.7b00071

Meroueh, S. O., Bencze, K. Z., Hesek, D., Lee, M., Jed, F. F., Timothy, L. S., et al. (2006). Three-dimensional structure of the bacterial cell wall peptidoglycan. *Proc. Natl. Acad. Sci. U. S. A.* 103 (12), 4404–4409. doi:10.1073/pnas.0510182103

Miller, R. D., Iinishi, A., Curtis, T. D., Lariviere, P. J., Liang, L., Son, S., et al. (2022). Computational identification of a systemic antibiotic for gram-negative bacteria. *Nat. Microbiol.* 7 (10), 1661–1672. doi:10.1038/s41564-022-01227-4

Mincey, B. A., and Parkulo, M. A. (2001). Antibiotic prescribing practices in a TeachingClinic: comparison of resident and staff physicians. *South. Med. J.* 94 (4), 365–369. doi:10.1097/00007611-200194040-00001

Murray, C. J. L., Kevin, S. I., Sharara, F., Swetschinski, L., Aguilar, G. R., Gray, A., et al. (2022). Global burden of bacterial antimicrobial resistance in 2019: a systematic Analysis. *Lancet* 399 (10325), 629–655. doi:10.1016/S0140-6736(21)02724-0

Nagaraja, V., Godbole, A. A., Henderson, S. R., and Anthony, M. (2017). DNA topoisomerase I and DNA gyrase as targets for TB therapy. *Drug Discov. Today* 22 (3), 510–518. doi:10.1016/j.drudis.2016.11.006

NIAID's Antibacterial Resistance Program (2014). *NIAID's antibacterial resistance Program: current status and future directions*. 13.

Ohmagari, N. (2014). Antimicrobial resistant bacteria. *Respir. Circulation* 62 (3), 279–283.

Okocha, R. C., Isaac, O. O., and Olufemi, B. A. (2018). Food safety impacts of antimicrobial use and their residues in aquaculture. *Public Health Rev.* 39 (1), 1–22. doi:10.1186/s40985-018-0099-2

Om, C., Frances Daily, Vlieghe, E., McLaughlin, J. C., and McLaws, M. L. (2016). 'If it's a broad spectrum, it can shoot better': inappropriate antibiotic prescribing in Cambodia. *Antimicrob. Resist. Infect. Control* 5 (1), 58–8. doi:10.1186/s13756-016-0159-7

Ordway, D., Viveiros, M., Leandro, C., Bettencourt, R., Almeida, J., Martins, M., et al. (2003). Clinical concentrations of thioridazine kill intracellular multidrug-resistant Mycobacterium tuberculosis. *Antimicrob. Agents Chemother.* 47 (3), 917–922. doi:10.1128/AAC.47.3.917-922.2003

Pasquina-Lemonche, L., Burns, J., Turner, R. D., Kumar, S., Tank, R., Mullin, N., et al. (2020). The architecture of the gram-positive bacterial cell wall. *Nature* 582 (7811), 294–297. doi:10.1038/s41586-020-2236-6

Peschel, A., Vuong, C., Otto, M., and Gotz, F. (2000). The D-alanine residues of Staphylococcus aureus teichoic acids alter the susceptibility to Vancomycin and the activity of autolytic enzymes. *Antimicrob. Agents Chemother.* 44 (10), 2845–2847. doi:10.1128/AAC.44.10.2845-2847.2000

Patel, Y., Soni, V., Rhee, K. Y., and Helmann, J. D. (2023). Mutations in rpoB that confer rifampicin resistance can alter levels of peptidoglycan precursors and affect β-lactam susceptibility. *Mbio* 14 (2), e03168–22.

Pham, T. D. M., Ziora, Z. M., and Blaskovich, M. A. T. (2019). Quinolone antibiotics. *MedChemComm* 10 (10), 1719–1739. doi:10.1039/c9md00120d

Piddock, L. J. V. (2015). Teixobactin, the first of a new class of antibiotics discovered by ichip technology? *J. Antimicrob. Chemother.* 70 (10), 2679–2680. doi:10.1093/jac/dkv175

Pouillot, F., Chomton, M., Blois, H., Courroux, C., Julien, N., Bidet, P., et al. (2012). Efficacy of bacteriophage therapy in experimental sepsis and meningitis caused by a clone O25b: H4-st131 Escherichia coli strain producing CTX-M-15. *Antimicrob. Agents Chemother.* 56 (7), 3568–3575. doi:10.1128/AAC.06330-11

Premlatha, M. (2019). Microbial resistance to antibiotics. *Bact. Adapt. Co-Resistance* 4, 61–80. December. doi:10.1007/978-981-13-8503-2_4

Romandini, A., Pani, A., Andrea Schenardi, P., De Giacomo, C., Scaglione, F., and Scaglione, F. (2021). Antibiotic resistance in pediatric infections: global emerging threats, predicting the near future. *Antibiotics* 10 (4), 393–412. doi:10.3390/antibiotics10040393

Sabtu, N., Enoch, D. A., and Brown, N. M. (2015). Antibiotic resistance: what, why, where, when and how? *Br. Med. Bull.* 116 (1), 105–113. doi:10.1093/bmb/ldv041

Sala, F. (1972). Structure and function of bacterial flagella. *Bolletino Di Zool.* 39 (2), 111–118. doi:10.1080/11250007209430052

Sarkar, R., Kaushik, P. B., Champak, D., Palash, J. S., and Dutta, S. (2021). Bacteriophage therapy to combat antibiotic resistance: a brief review. ~ *389* ~ *Pharma Innovation J.* 10 (5), 389–394.

Schwarz, S., Kehrenberg, C., and Walsh, T. R. (2001). Use of antimicrobial agents in veterinary medicine and food animal production. *Int. J. Antimicrob. Agents* 17 (6), 431–437. doi:10.1016/S0924-8579(01)00297-7

Scott Champney, W. (2008). The other target for ribosomal antibiotics: inhibition of bacterial ribosomal subunit formation. *Infect. Disord. - Drug Targets* 6 (4), 377–390. doi:10.2174/187152606779025842

Shree, P., Singh, C. K., Kaur Sodhi, K., Surya, J. N., and Singh, D. K. (2023). Biofilms: understanding the structure and contribution towards bacterial resistance in antibiotics. *Med. Microecology* 16, 100084. October 2022. doi:10.1016/j.medmic.2023.100084

Singh, C. K., and Kaur Sodhi, K. (2023). The emerging significance of nanomedicine-based approaches to fighting COVID-19 variants of concern: a perspective on the nanotechnology's role in COVID-19 diagnosis and treatment. *Front. Nanotechnol.* 4, 1–13. January. doi:10.3389/fnano.2022.1084033

Soares, S., Sousa, J., Pais, A., and Vitorino, C. (2018). Nanomedicine: principles, properties, and regulatory issues. *Front. Chem.* 6, 360–415. AUG. doi:10.3389/fchem.2018.00360

Sodhi, K. K., Singh, C. K., Kumar, M., and Singh, D. K. (2023). Whole-genome sequencing of alcaligenes sp. Strain MMA: insight into the antibiotic and heavy metal resistant genes. *Front. Pharmacol.* 14, 1144561–1144611. May. doi:10.3389/fphar.2023.1144561

Sriram, A., Kalanxhi, E., Kapoor, G., Craig, J., Balasubramanian, R., Sehr Brar, , et al. (2021). *State World ' s Antibiotics* 8 (2), 30–34.

Stokes, J. M., Yang, K., Swanson, K., Jin, W., Cubillos-Ruiz, A., Donghia, N. M., et al. (2020). A Deep learning approach to antibiotic discovery. *Cell* 180 (4), 688–702. doi:10.1016/j.cell.2020.01.021

Strateva, T., and Yordanov, D. (2009). Pseudomonas aeruginosa - a phenomenon of bacterial resistance. *J. Med. Microbiol.* 58 (9), 1133–1148. doi:10.1099/jmm.0.009142-0

Svircev, A., Roach, D., and Castle, A. (2018). Framing the future with bacteriophages in agriculture. *Viruses* 10 (5), 218–313. doi:10.3390/v10050218

Syroegin, E. A., Flemmich, L., Klepacki, D., Vazquez-Laslop, N., Micura, R., and Polikanov, Y. S. (2022). Structural basis for the context-specific action of the classic peptidyl transferase inhibitor chloramphenicol. *Nat. Struct. Mol. Biol.* 29 (2), 152–161. doi:10.1038/s41594-022-00720-y

Tacconelli, E., Cataldo, M. A., Dancer, S. J., De Angelis, G., Falcone, M., Frank, U., et al. (2014). ESCMID guidelines for the management of the infection control measures to reduce transmission of multidrug-resistant gram-negative bacteria in hospitalized patients. *Clin. Microbiol. Infect.* 20, 1–55. doi:10.1111/1469-0691.12427

Tanday, S. (2016). Resisting the use of antibiotics for viral infections. *Lancet. Respir. Med.* 4 (3), 179. doi:10.1016/S2213-2600(16)00060-6

Tebano, G., Mouelhi, Y., Zanichelli, V., Charmillon, A., Fougnot, S., Lozniewski, A., et al. (2020). Selective reporting of antibiotic susceptibility testing results: a promising antibiotic stewardship tool. *Expert Rev. Anti-Infective Ther.* 18 (3), 251–262. doi:10.1080/14787210.2020.1715795

Tenover, F. C. (2006). Mechanisms of antimicrobial resistance in bacteria. *Am. J. Med.* 119, S3–S10. 6 SUPPL. 1. doi:10.1016/j.amjmed.2006.03.011

Tenson, T., Lovmar, M., and Ehrenberg, M. (2003). The mechanism of action of macrolides, lincosamides and streptogramin B reveals the nascent peptide exit path in the ribosome. *J. Mol. Biol.* 330 (5), 1005–1014. doi:10.1016/S0022-2836(03)00662-4

Thakolkaran, N., Shetty, A. V., D′Souza, N. D. R., and Shetty, A. K. (2017). Antibiotic prescribing knowledge, attitudes, and practice among physicians in teaching Hospitals in south India. *J. Fam. Med. Prim. Care* 6 (3), 526–532. doi:10.4103/2249-4863.222057

Varela, M. F., Stephen, J., Lekshmi, M., Ojha, M., Wenzel, N., Sanford, L. M., et al. (2021). Bacterial resistance to antimicrobial agents. *Antibiotics* 10, 593. doi:10.3390/antibiotics10050593

Vicens, Q., and Westhof, E. (2003). RNA as a drug target: the case of aminoglycosides. *ChemBioChem* 4 (10), 1018–1023. doi:10.1002/cbic.200300684

Waksman, S. A. (1947). What is an antibiotic or an antibiotic substance? *Mycologia* 39 (5), 565–569. doi:10.1080/00275514.1947.12017635

Wang, J., Hu, B., Xu, M., Yan, Q., Liu, S., Zhu, X., et al. (2006). Use of bacteriophage in the treatment of experimental animal bacteremia from imipenem-resistant Pseudomonas aeruginosa. *Int. J. Mol. Med.* 17 (2), 309–317. doi:10.3892/ijmm.17.2.309

Wang, N., Luo, J., Deng, F., Huang, Y., and Zhou, H. (2022). Antibiotic combination therapy: a strategy to overcome bacterial resistance to aminoglycoside antibiotics. *Front. Pharmacol.* 13, 839808–839815. February. doi:10.3389/fphar.2022.839808

Watanabe, R., Matsumoto, T., Go, S., Ishii, Y., Tateda, K., Sumiyama, Y., et al. (2007). Efficacy of bacteriophage therapy against gut-derived sepsis caused by Pseudomonas aeruginosa in mice. *Antimicrob. Agents Chemother.* 51 (2), 446–452. doi:10.1128/AAC.00635-06

Weinstein, R. A. (2001). Controlling antimicrobial resistance in Hospitals: infection control and use of antibiotics. *Emerg. Infect. Dis.* 7 (2), 188–192. doi:10.3201/eid0702.010206

Wierup, M. (2001). The Swedish experience of the 1986 Year ban of antimicrobial growth promoters, with special reference to animal health, disease prevention, productivity, and usage of antimicrobials. *Microb. Drug Resist.* 7 (2), 183–190. doi:10.1089/10766290152045066

Wright, A., Hawkins, C. H., Änggård, E. E., and Harper, D. R. (2009). A controlled clinical trial of a therapeutic bacteriophage preparation in chronic otitis due to antibiotic-resistant Pseudomonas aeruginosa; A preliminary report of efficacy. *Clin. Otolaryngol.* 34 (4), 349–357. doi:10.1111/j.1749-4486.2009.01973.x

Wu, G. (2009). Amino acids: metabolism, functions, and nutrition. *Amino Acids* 37 (1), 1–17. doi:10.1007/s00726-009-0269-0

Yuan, Y., Wang, L., Li, X., Tan, D., Cong, C., and Xu, Y. (2019). Efficacy of a phage cocktail in controlling phage resistance development in multidrug resistant acinetobacter baumannii. *Virus Res.* 272 (June), 197734. doi:10.1016/j.virusres.2019.197734

Zhou, G., Shi, Q. S., Huang, X.Mo, and Xiao, B. X. (2015). The three bacterial lines of defense against antimicrobial agents. *Int. J. Mol. Sci.* 16 (9), 21711–21733. doi:10.3390/ijms160921711

frontiers | Frontiers in Pharmacology

TYPE Original Research
PUBLISHED 26 February 2024
DOI 10.3389/fphar.2024.1347832

OPEN ACCESS

EDITED BY
Mingkai Li,
Air Force Medical University, China

REVIEWED BY
Dana Carmen Zaha,
University of Oradea, Romania
Gabriela Cristina Fernandez,
National Scientific and Technical Research Council (CONICET), Argentina

*CORRESPONDENCE
Khalid S. Ibrahim,
khalid.ibrahim@uoz.edu.krd
Delveen R. Ibrahim,
delveen.ibrahim@uod.ac

RECEIVED 01 December 2023
ACCEPTED 29 January 2024
PUBLISHED 26 February 2024

CITATION
Ibrahim DR, Saadi AT, Yahya NB, Ibrahim MS, Saeed AY, Abdulaziz SS, Hasqyal RY, Alarsalani BK and Ibrahim KS (2024), Retrospective analysis of pediatric sepsis and the burden of antimicrobial resistance in Duhok, Kurdistan Region of Iraq.
Front. Pharmacol. 15:1347832.
doi: 10.3389/fphar.2024.1347832

Retrospective analysis of pediatric sepsis and the burden of antimicrobial resistance in Duhok, Kurdistan Region of Iraq

Delveen R. Ibrahim[1]*, Abdulrhaman T. Saadi[2,3], Nizar B. Yahya[3,4], Marwa S. Ibrahim[5], Ali Y. Saeed[1], Sawsan S. Abdulaziz[3], Revan Y. Hasqyal[3], Berivan K. Alarsalani[3] and Khalid S. Ibrahim[6]*

[1]Department of Biology, Collage of Science, University of Duhok, Duhok, Kurdistan Region, Iraq, [2]Medical Microbiology Department, College of Medicine, University of Duhok, Duhok, Kurdistan Region, Iraq, [3]Heevi Pediatrics Teaching Hospital, Duhok Health Directorate, Duhok, Kurdistan Region, Iraq, [4]Pediatrics Department, College of Medicine, University of Duhok, Duhok, Kurdistan Region, Iraq, [5]Department of Medical Laboratory Technology, College of Health and Medical Techniques-Shekhan, Duhok Polytechnic University, Duhok, Kurdistan Region, Iraq, [6]Department of Biology, College of Sciences, University of Zakho, Zakho, Kurdistan Region, Iraq

Introduction: Sepsis is a life-threatening complication in pediatric patients. This study primarily aimed to investigate sepsis-causing bacteria and their antimicrobial resistance profile and check the change in the antimicrobial resistance trend for some selected bacteria. In addition, we evaluated the incidence of sepsis, the related mortality rate, and the effectiveness and outcome of the treatment regimes in sepsis pediatric patients.

Methods: A retrospective analysis was conducted on 4-year data (2018–2021) collected from three intensive care units at the Hevi Pediatric Teaching Hospital. Sepsis screening involved clinical detection and confirmation by blood culture.

Results: A total of 520 out of 1,098 (47.35%) blood samples showed positive microbial growth. A decrease in sepsis rate was observed during the COVID-19 pandemic. Coagulase-negative Staphylococci (CoNS) and *Klebsiella pneumonia* were the most commonly isolated bacteria. A notable variation in the antimicrobial resistance trend was observed among sepsis-causing bacteria. The empirical sepsis treatment recommended by the WHO was ineffective, as certain bacteria exhibited 100% resistance to every antibiotic tested. The mortality rate significantly increased from 1.3% in 2018 to 16.5% in 2021.

Discussion: The antimicrobial resistance profile of sepsis causing bacteria is of concerns, indicating a potentially serious situation. Thus, to avoid treatment failure, the monitoring of antimicrobial resistance in pediatric patients is essential.

KEYWORDS

sepsis, pediatric, retrospective, antimicrobial resistance, Duhok-Iraq

1 Introduction

Sepsis represents the systemic condition that arises from microbial infections associated with clinical findings and hemodynamic changes. It is a state of immune imbalance and an immune response to microbial invasion that results in organ injury that is sometimes associated with severe morbidity and mortality (Hotchkiss et al., 2016;

Odabasi and Bulbul, 2020). In 2017, an estimated 48.9 million cases of sepsis were recorded worldwide and 11.0 million sepsis-related deaths were reported (Rudd et al., 2020). Sepsis remains a major health problem for critically ill adults and children. Additionally, it is one of the leading causes of death in infants and children (Jiang et al., 2020; Hermon et al., 2021). Neonatal sepsis is classified as early-onset (<72 h) and late-onset (4–30 days) according to the time of onset (WHO, 2022).

The excessive and improper use of antibiotics, particularly broad-spectrum antibiotics, plays a major role in the emergence of drug-resistant strains, as observed in several studies (Doern et al., 2014; Tessema et al., 2021; Hasan and Ibrahim, 2022; Hami and Ibrahim, 2023; Ibrahim, 2023). Neonatal sepsis caused by antimicrobial-resistant (AMR) bacteria is a multifactorial issue of global concern due to the increased illness, death, and hospital expenses associated with it. Recent research revealed that the antibiotic resistance patterns of the bacterial pathogens responsible for newborn sepsis vary between hospital settings and time periods, which might be due to the different treatment regimens used in neonatal care (Tessema et al., 2021).

The current study aimed to evaluate the prevalence and susceptibility of the predominant sepsis-causing bacteria among pediatric patients in the Hevi Pediatric Teaching Hospital, Kurdistan region of Iraq. This will provide an epidemiological analysis of sepsis data among patients. In addition, the correlation between the gender and age of patients and the rates of mortality within the studied population was analyzed. Accordingly, suggestions are made regarding sepsis identification and patient treatment regimens.

2 Materials and methods

2.1 Samples and data collection

The current study used data collected from the intensive care unit at the Hevi Pediatric Teaching Hospital in Duhok Governorate, Iraq. Four-year data were obtained from between 1 January 2018, and 31 December 2021. During the study period, 1,098 blood samples were collected from both genders from 3,865 patients. The samples were collected from suspected sepsis patients who were referred by pediatric consultants; the ages of the patient ranged from 1 day to 15 years, with 771 males and 327 females. The samples were processed in the microbiology laboratory at the same hospital. The 5-age pediatric patient subgroup's demographic data were designated based on a previous study (Hermon et al., 2021) (Supplementary Table S1).

2.2 Inclusion and exclusion criteria

All clinically suspected cases of sepsis (newborns and children) from the age of 1 day–15 years admitted to the pediatric intensive care unit (PICU), neonatal intensive care unit (NICU), and semi intensive care unit (ICU) were included in the study. The criteria for clinically suspected sepsis were based on signs of infections. This involved fever, elevated heart rate, rapid breathing, or signs of a localized infection, such as a skin or urinary tract infection. Furthermore, some cases showed clinical deterioration as the child may exhibit signs of systemic illness, such as lethargy, irritability, poor feeding, or decreased responsiveness. In addition, abnormal vital signs were recorded, including abnormal body temperature (either fever or hypothermia), tachycardia, or tachypnoea. For all suspected sepsis patients, detailed laboratory tests were performed, e.g., complete blood picture (CBP), C-reactive protein (CRP), and blood cultures.

The exclusion criteria were based on two main factors: the age of the patient and sepsis symptoms. Any child cases that were over 15 years old or did not exhibit sepsis symptoms were not included in this research.

2.3 Ethics

The approval for conducting this study was provided by the Ethical Committee for Medical and General Health Research Ethics from the Duhok Directorate General of Health (14012018-0001).

2.4 Culture

The blood samples were immediately transferred to BACT/ALERT®PF PLUS pediatric culture bottles and placed in a BACT/ALERT 3D instrument for 2–5 days (De La Rica et al., 2016). A small amount of culture was inoculated on blood agar (BA), chocolate agar (CHOC), and MacConkey (MAC) (Neogen, UK) and incubated overnight up to 24 h in case bacterial growth was observed. Isolates were identified using classical methods (Mahon et al., 2014) and an automated system (Vitek2, BioMerieux, France).

2.5 Antibiotics susceptibility test

Various antibiotic discs (Bioanalyses, Turkey) were used for antimicrobial susceptibility tests (Supplementary Tables S4, S5). The tests were performed manually (CLSI, 2017) from 1 January 2018, to 19 May 2019. Mueller–Hinton agar (MHA) (Neogen, UK) was used for the disc diffusion test. The diameters of the inhibition zones around each disc were measured and compared with the standard inhibition zone, as recommended by the Clinical Laboratory Standard Institution (CLSI, 2017). The results were interpreted as sensitive or resistant; intermediate resistance was also considered as resistance. On the other hand, from 20 May 2019, onward, the antimicrobial susceptibility test was carried out using an automated system with a Vitek®2 AST-P640 card for Gram-positive bacteria (G+) and AST-N327 cards for Gram-negative bacteria (G–) (BioMerieux, France).

2.6 Statistical analysis

GraphPad Prism 8.1 software and Excel were used for statistical analysis. The Chi-square test and two-way ANOVA were used to compare significant differences between data. $p < 0.05$ was considered statistically significant.

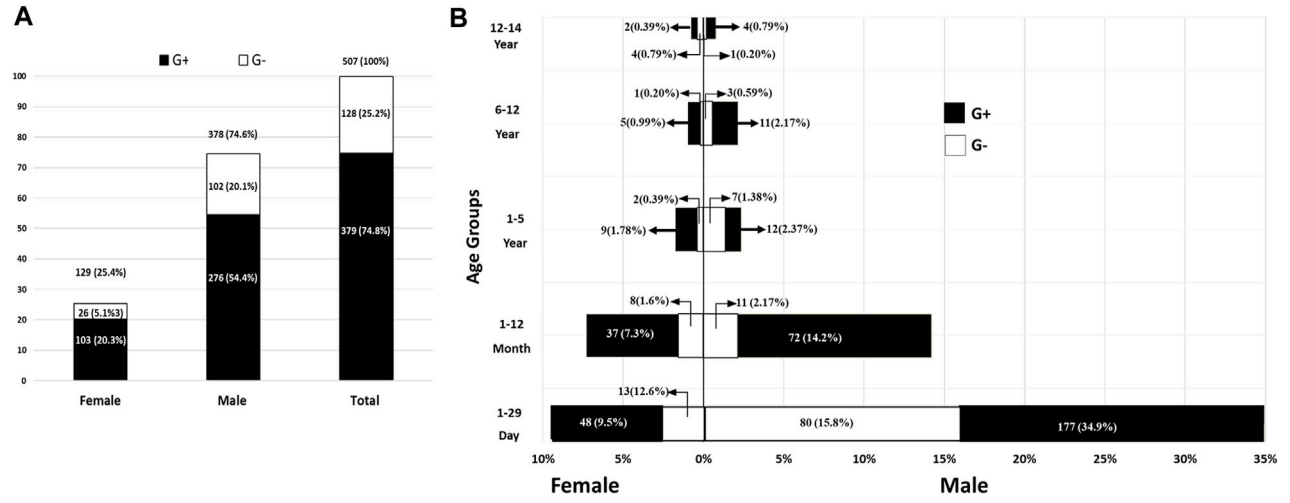

FIGURE 1
The overall count and rates of pediatric bacterial sepsis in both genders **(A)** and different age groups **(B)**. G+, Gram-positive bacteria; G-, Gram-negative bacteria.

3 Results

3.1 The prevalence of sepsis

In the current study, a total of 1,098 out- and in-patient children (<15 years) were recruited from between 1 January 2018, to 31 December 2021. Overall, 520 (47.35%) sepsis cases were found in 1,098 patients; 507 (97.5%) were caused by bacteria and 13 (2.5%) were caused by *Candida* (Supplementary Table S2), whereas no growth was observed in 578 (52.64%) of the 1,098 samples. The infection rate in males was 378 (74.6%), which was three-fold higher than that in females (129, 25.4%; Figure 1A). Moreover, the rate of Gram-positive bacterial infection was three-fold higher than Gram-negative bacterial infection (379 [74.75%] and 128 [25.25%], respectively). Most remarkably, for both sexes, the 1–29 days age group had the greatest prevalence of sepsis (28.96%), followed by the group up to 1 year (11.66%); the rates then gradually decreased until the age of 15 years (Figure 1B; Supplementary Table S2). Statistically, there was a significant difference between age group and the number of sepsis cases ($p < 0.0001$).

3.1.1 Trends of bacterial infection

Overall, based on the monthly distribution of sepsis rates, the trend of sepsis reached a peak in February and decreased in the following months, with some fluctuation. However, in July 2021, the trend increased again (Figure 2A). Generally, a statistically significant difference ($p < 0.0001$) was observed between incidence rates based on monthly distribution using a chi-square test (Supplementary Table S3).

3.1.2 Sepsis rate during the COVID-19 pandemic

As the main part of the study was conducted during the COVID-19 pandemic, a statistical analysis was conducted to compare the rates of sepsis during and before the pandemic. It had been noticed that the rate of sepsis was lower during the COVID-19 pandemic in 2020 and 2021 (since Kurdistan officially registered its first COVID-19 case in March 2020) than during the pre-pandemic period of 2018 and 2019, and according to a chi-square test the rates were significantly reduced ($p < 0.0001$; Figure 2B; Supplementary Table S3).

3.2 Bacterial causes of pediatric sepsis

The total number and percentages of various bacteria isolated from pediatric sepsis are shown in Table 1. Bacterial infection was higher in males than in females. Of the 507 strains cultured from children, 379 (74.75) were Gram positive and CoNS and methicillin-resistant *Staphylococcus aureus* (MRSA) were found in 264 (52.07%) and 45 (8.88%) cases, respectively. By contrast, *Klebsiella* spp. (55 cases, 10.85%) was the most common Gram-negative bacteria followed by non-lactose fermenter bacteria (42 cases, 8.28%) and *Escherichia coli* (29 cases, 5.72%) (Table 1). The main non-lactose fermenting bacteria identified were *Pseudomonas aeruginosa*, *Sphingomonas paucimobilis*, *Acinetobacter baumannii*, *Serratia* spp., and *Stenotrophomonas maltophilia*.

3.3 Bacterial antibiotic resistance profile

The antibiotic resistance profiles of the isolated bacteria were varied according to the time of the study and the type of bacteria. The World Health Organization (WHO) has recommended guidelines for the treatment of sepsis in neonates and children (WHO, 2022) (Supplementary Table S4). The WHO recommends two categories for treatment: access antibiotics (first choice) and watch antibiotics (second choice). Figure 3 illustrates the efficiency of the suggested antibiotics together with the resistance rate trends for G+ bacteria represented by *Staphylococcus aureus*, including MRSA, and G-bacteria represented by *Klebsiella pneumoniae* and *E. coli*. Supplementary Tables S5, S6 provide specifics about antibiotic resistance for these microorganisms.

In general, during the whole period of the study (Supplementary Table S5), all MRSA were resistant to AK, AMC, AMP, P, and OXI,

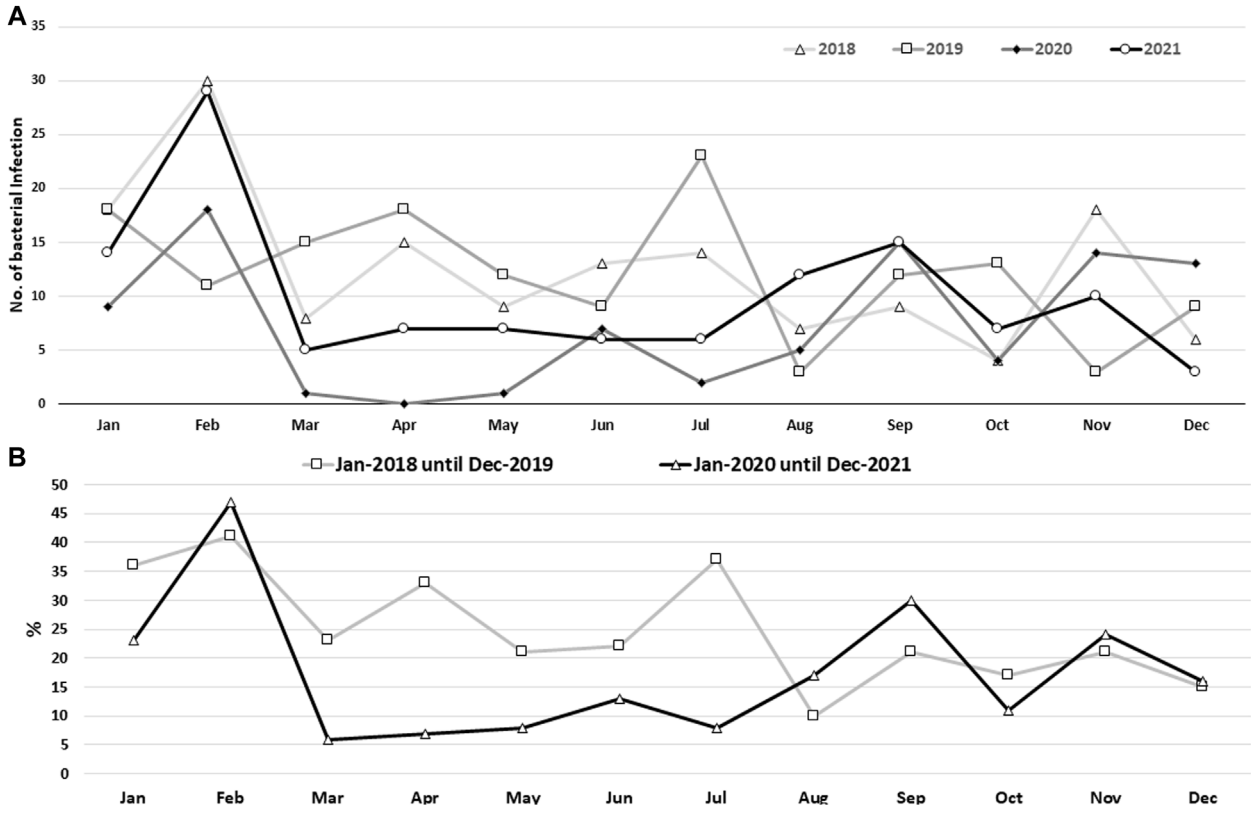

FIGURE 2
Bacterial sepsis rate based on monthly records **(A)** and the monthly record for phase I (pre-COVID-19 pandemic) and phase II (during the COVID-19 pandemic) **(B)** for the four-year data, 2018–2021. Using the Chi-square test, a statistically significant difference ($p < 0.0001$) was found between the various monthly data sets.

while the resistance trend of these bacteria to GM was reduced from 75% (13/16) in 2018 to 64.3% and 27.8% in 2019 and 2020, respectively, and then increased again to 70% in 2021. Furthermore, the resistance values to vancomycin (VA) fluctuated across the 4-year study period, as the resistance rates were 0%, 21%, 0%, and 9%, respectively. In addition, all *Klebsiella* spp. isolates exhibited complete resistance to AMP, CTX, and CRO, while there was a variation in their resistant to AK, GM, and TZP. The resistant trends for AK and TZP were increased from above 50%–100% in 2021, whereas the trends against GM were almost resistant in the first 3 years and then decreased to 50% in 2021. In addition, all *E. coli* isolates were completely resistant to AMP and CRO, whereas their resistant rates to AK, GM, CTX, and TZP varied. The resistant trends increased from 50% to 75% for AK and from 75% to 100% for CTX and TZP, whereas the trend decreased from 100% resistance to 50% for GM in 2021.

In this investigation, MDR bacteria were prevalent. Some of the G+ and G-bacteria exhibited complete resistance to every class of antibiotic that was tested. Certain strains of *S. aureus* isolates, including MRSA, were also identified as MDR bacteria, showing sensitivity to only one antibiotic (vancomycin) within the tested antibiotics group. Some of the G-isolates were also 100% resistant to all the tested antibiotics, such as non-lactose fermenters, *Klebsiella* spp., and *E. coli*, while many other isolates demonstrated susceptibility to only one or two of the tested antibiotics, such as sulphamethaxazol/trimethoprim and imipenem.

3.4 Morbidity and mortality rates among pediatric sepsis patients

In terms of mortality rate, 47 (9.7%) out of 507 sepsis patients died. The mortality rate of pediatric sepsis caused by G+ bacteria was significantly higher than that caused by G- bacteria. The most common bacteria related to death in sepsis cases were CoNS (25 cases) and G-none-lactose fermenters (8 cases). Furthermore, sepsis brought on by MRSA (7 cases), *S. aureus* (3 cases), *E. coli* (2 cases), and *Klebsiella pneumoniae* (2 cases) resulted in an additional 14 deaths. It is noteworthy that all the deceased patients received local empirical treatment.

4 Discussion

In the current study, 46.17% of children suffered from sepsis because of bacterial infection; the incidence rate among males was three times greater than that of females. This finding contrasted with studies carried out in Austria by Hermon et al. (2021) and Libya by Benamer et al. (2015) that found that the rates of bacterial sepsis were comparable in both genders. In addition, a global study on the prevalence of sepsis showed that the rate of sepsis using age-standardized values is higher in females than in males (Rudd et al., 2020). The higher incidence of pediatric bacterial sepsis in

TABLE 1 Sepsis-causing bacteria according to their phenotypic characteristics and based on the gender of patients.

Microorganism	Total No. (%)	Sex		*p*-value
		Female No. (%)	Male No. (%)	
G+ Bacteria	379 (74.75)	103 (20.32)	276 (54.44)	$p = 0.0217$
Bacillus spp.	7 (1.38)	—	7 (1.38)	
Diphtheroids	2 (0.39)	1 (0.2)	1 (0.2)	
Enterococci	27 (5.33)	11 (2.17)	16 (3.16)	
Kocuria spp.	4 (0.79)	1 (0.20)	3 (0.59)	
Listeria monocytogenes	1 (0.20)	—	1 (0.20)	
Micrococcus luteus	7 (1.38)	3 (0.59)	4 (0.79)	
Methicillin-resistant Staphylococcus aureus	45 (8.88)	13 (2.56)	32 (6.31)	
Coagulase-negative Staphylococci (CoNS)	264 (52.07)	68 (13.41)	196 (38.66)	
Staphylococcus aureus	18 (3.55)	6 (1.18)	12 (2.37)	
Streptococci spp.	4 (0.79)	—	4 (0.79)	
G- Bacteria	128 (25.25)	26 (5.13)	102 (20.12)	$p = 0.2404$
Escherichia coli	29 (5.72)	7 (1.38)	22 (4.34)	
Klebsiella pneumonia[a]	55 (10.85)	8 (1.58)	47 (9.27)	
Moraxella spp.	1 (0.2)	1 (0.2)	—	
Neisseria spp.	1 (0.2)	—	1 (0.2)	
Non-lactose fermenter[b]	42 (8.28)	10 (1.8)	32 (6.31)	

[a]*Only 1 species K. oxytoca.*

[b]Include all non-lactose fermenter bacteria such as *Pseudomonas aeruginosa, Sphingomonas paucimobilis, Acinetobacter baumannii, Serratia* spp., *and Stenotrophomonas maltophilia.*

males compared with females is likely due to a complex interplay of biological and environmental factors, proper hygiene, and immunization. Numerous studies have demonstrated sex-specific differences in sepsis and others infectious diseases. It has been found that females are protected under such conditions. However, a number of factors, such as a diminished cell-mediated immune response, cardiovascular functions, and some biological differences, especially the weight of X-linked variability and the role of sex hormones, can make males more vulnerable to such infection (De La Rica et al., 2016). However, it has been noted that despite reports of a higher prevalence of sepsis in males than in females, the exact mechanism underlying sepsis is still unknown (Xu et al., 2019).

The current study showed that the frequency of bacterial sepsis was more commonly observed in a subgroup of 1–29 days of age, followed by 1–12 months. It is thought that the maternal obstetric factors are the main cause of early-onset infections and sepsis in infants (Flannery et al., 2022). In fact, this might be due to the transfer of pathogenic bacteria to the fetus not only by crossing the placenta but also perinatally through the birth canal during delivery. Indeed, late-onset neonatal sepsis is caused by environmental factors, such as hospital and invasive procedures as well as the prolonged use of antibiotics (Rannikko et al., 2017; Herbozo et al., 2021).

Intriguingly, in the current study, the rate of sepsis was significantly different and decreased from 2018 to 2021. This finding was consistent with the global trend of sepsis, as the incidence of age-standardized sepsis decreased by 37·0% (95% uncertainty interval (UI)) from 1990 to 2017, which varied substantially across regions, with the highest burden in sub-Saharan Africa, Oceania, south Asia, east Asia, and southeast Asia (Rudd et al., 2020). By contrast, an epidemiological trends study of sepsis in western countries stated that the incidence of sepsis had increased over recent years (De La Rica et al., 2016). The increase in sepsis over time might be due to the aging population, an increase in comorbidities, and potential overuse of sepsis coding for less severe cases (Danai and Martin, 2005).

In contrast to the rate of sepsis reduction during the current study period, the rate of mortality increased significantly during the same period, Figure 4. This was in line with the increasing rate of antibiotic resistance and the emergence of MDR bacteria within the causative agents of sepsis. The rate of mortality was higher in males than in females, which was expected as the rate of sepsis was higher in males than in females. This finding was consistent with another study that found a higher mortality rate in males (70%) than in females, which was related to the variation in the respiratory tract infection rate and IL-6 plasma levels between males and females (Nasir et al., 2015).

According to the monthly recorded data of the entire study period, the highest incidence of sepsis was recorded in February, except in 2019, when the highest incidence was in July. This finding was not surprising as previous studies recorded seasonal variation in sepsis rates, especially during winter (Benamer et al., 2015; Abdel Mawla et al., 2021). The incidence and death rate of sepsis were highest during winter, particularly for respiratory sepsis (respiratory tract infection), in which respiratory viral infection in sepsis patients played an important role in the progression of the infection (Aykac et al., 2019).

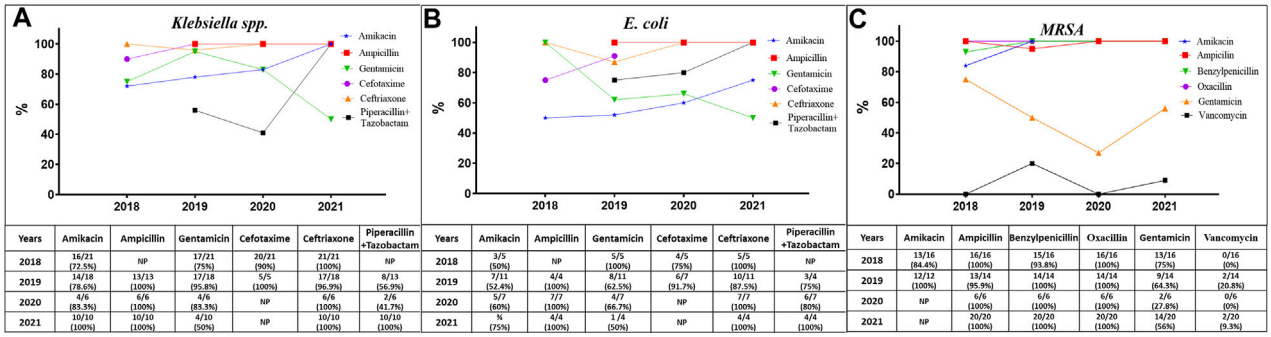

Years	Amikacin	Ampicillin	Gentamicin	Cefotaxime	Ceftriaxone	Piperacillin +Tazobactam
2018	16/21 (72.5%)	NP	17/21 (75%)	20/21 (90%)	21/21 (100%)	NP
2019	14/18 (78.6%)	13/13 (100%)	17/18 (95.8%)	5/5 (100%)	17/18 (96.9%)	8/13 (56.9%)
2020	4/6 (83.3%)	6/6 (100%)	4/6 (83.3%)	NP	6/6 (100%)	2/6 (41.7%)
2021	10/10 (100%)	10/10 (100%)	4/10 (50%)	NP	10/10 (100%)	10/10 (100%)

Years	Amikacin	Ampicillin	Gentamicin	Cefotaxime	Ceftriaxone	Piperacillin +Tazobactam
2018	3/5 (50%)	NP	5/5 (100%)	4/5 (75%)	5/5 (100%)	NP
2019	7/11 (52.4%)	4/4 (100%)	8/11 (62.5%)	6/7 (91.7%)	10/11 (87.5%)	3/4 (75%)
2020	5/7 (60%)	7/7 (100%)	4/7 (66.7%)	NP	7/7 (100%)	6/7 (80%)
2021	¾ (75%)	4/4 (100%)	1/4 (50%)	NP	4/4 (100%)	4/4 (100%)

Years	Amikacin	Ampicillin	Benzylpenicillin	Oxacillin	Gentamicin	Vancomycin
2018	13/16 (84.4%)	16/16 (100%)	15/16 (93.8%)	16/16 (100%)	13/16 (75%)	0/16 (0%)
2019	12/12 (100%)	13/14 (95.9%)	14/14 (100%)	14/14 (100%)	9/14 (64.3%)	2/14 (20.8%)
2020	NP	6/6 (100%)	6/6 (100%)	6/6 (100%)	2/6 (27.8%)	0/6 (0%)
2021	NP	20/20 (100%)	20/20 (100%)	20/20 (100%)	14/20 (56%)	2/20 (9.3%)

FIGURE 3
The trends of resistance of *Klebsiella* spp. **(A)**, *E. coli* **(B)**, and MRSA **(C)** to the antibiotics recommended by the World Health Organization for the treatment of pediatric sepsis. NP, not performed.

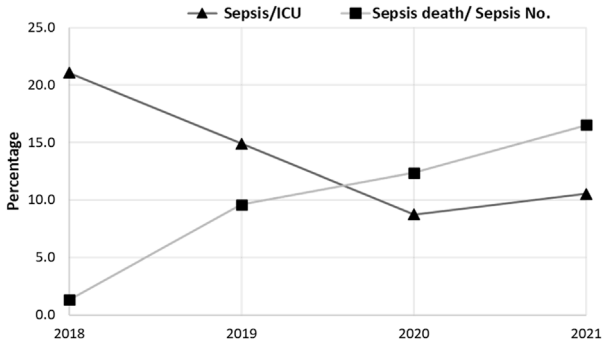

FIGURE 4
The rate of morbidity and mortality within sepsis cases in the intensive care unit (ICU) for the 4-year study (2018–2021). The prevalence of morbidity sepsis decreased from 154, 146, and 89 cases in 2018, 2019, and 2020, respectively, and then increased (121 cases) in 2021. The prevalence of mortality significantly increased from 1.3% (2/154 cases), 9.6% (14/46 cases), 12.4% (11/89 cases), and 16.5% (20/121 cases) in 2018, 2019, 2020, and 2021, respectively. The Chi-square test was used to evaluate the data, and significant differences ($p < 0.0001$) were observed.

Compared with previous years, the COVID-19 pandemic had the lowest rate of sepsis. This could be because people sought care at outpatient clinics during the pandemic instead of staying in hospitals. Additionally, it might be due to reduced elective surgeries, changes in hospital admissions during the pandemic, such as for chronic conditions, and heightened infection control measures. It has been reported that one of the main reasons for the increased mortality due to sepsis during the COVID-19 pandemic was the reluctance of patients to seek medical attention or present themselves at a hospital (Unterberg et al., 2022).

With regard to the prevalence of sepsis-causing bacteria in the current study, CoNS and *Klebsiella pneumoniae* were the most predominate bacteria among G+ and G-bacteria, respectively. This was in line with a previous study conducted in a neonatal intensive care unit in Arab states in the Gulf region (Hammoud et al., 2017). By contrast, several previous studies reported that G-bacteria were the most common pathogens that led to sepsis (Danai and Martin, 2005; Hafsa et al., 2011; Flannery et al., 2022).

G+ and G-bacteria showed increasing resistance to antibiotics and the trend rates were characterized by fluctuations over time. This was due to several factors and mainly the normal evolutionary process of microorganisms, which is accelerated by the overuse and misuse of antibiotics, poor infection control, a lack of access to quality medicines, a lack of awareness and knowledge, and a lack of enforcement of legislation (Tessema et al., 2021).

Various studies observed that bacteria isolated from blood displayed a high level of resistance, not only to commonly used antibiotics but also to broad-spectrum antibiotics (Saleem et al., 2013; Ibrahim et al., 2023). To effectively control infections, the prolonged use of broad-spectrum antibiotics can lead to a resurgence of multidrug-resistant organisms; therefore, they should be used sparingly. Instead, specific short-term use of antibiotics is recommended, and the rotation of antibiotic regimens may also be a solution (Hammoud et al., 2017).

Furthermore, there is no universally accepted method for identifying and diagnosing sepsis and that delays in doing so can result in a significant increase in both morbidity and mortality (Rannikko et al., 2017; Oruganti et al., 2022).

This study has some limitations, including the manual methods employed for bacterial identification prior to the adoption of the VITEK system, which does not identify some bacteria at the species level, such as non-lactose fermenter bacteria. Additionally, it was unclear whether the infections were hospital-acquired or community-acquired, whether the patients had other infections, and whether they were taking medication prior to the sepsis infection. Furthermore, the survival status of patients after receiving antibiotics was unclear; the rate of deaths was stated according to the data reordered but there may have been additional occurrences if the patients were released from the hospital and then developed a new complication.

5 Conclusion

Our study evaluated the rate of sepsis in newborns and children in one hospital over the course of 4 years, from 2018 to 2021. The study period divided into 2 intervals: before and after the COVID-19 pandemic. In addition, the death rate and antibiotic resistance rate for the sepsis etiological agent were assessed in the study cases. Sepsis should be recognized quickly and managed promptly, otherwise it can lead to septic shock, multiple organ failure, and

death. It is most frequently a serious complication of infection. In our study, many sepsis cases were identified and treated but then died, which might be due to treatment failure or organ failure but has not been properly investigated until now. Consequently, continuous efforts should be provided to reduce the burden of sepsis by improving public and healthcare worker awareness, especially to avoid delays in diagnosis and treatment. Furthermore, rapid treatment using appropriate antibiotics should be followed along with monitoring of the effectiveness of the treatment throughout the treatment period, especially with the increasing emergence of MDR bacteria within the isolated bacteria.

Data availability statement

The original contributions presented in the study are included in the article/Supplementary Material, further inquiries can be directed to the corresponding author.

Ethics statement

The studies involving humans were approved by the Ethical Committee for Medical and General Health Research Ethics from Duhok Directorate General of Health (14012018-0001). The studies were conducted in accordance with the local legislation and institutional requirements. The human samples used in this study were acquired from a by- product of routine care or industry. Written informed consent for participation was not required from the participants or the participants' legal guardians/next of kin in accordance with the national legislation and institutional requirements.

Author contributions

DI: Conceptualization, Data curation, Formal Analysis, Visualization, Writing–original draft, Writing–review and editing, Methodology, Supervision, Validation, Investigation, Resources. ATS: Conceptualization, Methodology, Writing–review and editing, Investigation, Resources. NY: Investigation, Writing–review and editing, Conceptualization, Project administration, Supervision, Resources. MI: Writing–review and editing, Investigation, Methodology, Writing–original draft, Data curation, Formal Analysis, Resources, Visualization. AYS: Writing–review and editing. SA: Investigation, Methodology, Writing–review and editing, Data curation. RH: Investigation, Methodology, Writing–review and editing, Data curation. BA: Writing–review and editing. KI: Conceptualization, Data curation, Formal Analysis, Software, Visualization, Writing–original draft, Writing–review and editing, Investigation, Resources, Validation.

Funding

The author(s) declare that no financial support was received for the research, authorship, and/or publication of this article.

Conflict of interest

The authors declare that the research was conducted in the absence of any commercial or financial relationships that could be construed as a potential conflict of interest.

Publisher's note

Supplementary material

The Supplementary Material for this article can be found online at: https://www.frontiersin.org/articles/10.3389/fphar.2024.1347832/full#supplementary-material

References

Abdel Mawla, M. A., Mostafa, E. A., Hasanin, R. M., and Salah, M. M. (2021). Assessment of seasonal variation on neonatal sepsis. *Bull. Natl. Res. Centre* 45, 29–36. doi:10.1186/s42269-021-00490-5

Aykac, K., Karadag-Oncel, E., Tanır Basaranoglu, S., Alp, A., Cengiz, A. B., Ceyhan, M., et al. (2019). Respiratory viral infections in infants with possible sepsis. *J. Med. Virology* 91, 171–178. doi:10.1002/jmv.25309

Benamer, H. M., Alsaiti, A. A., Bofarraj, M., Abud, H., and Tip, R. (2015). Diagnosis, management and outcome of sepsis at benghazi children hospital (1 Year review). *Pediatr. Ther.* 05, 1–5. doi:10.4172/2161-0665.1000267

CLSI (2017). *Performance standards for antimicrobial susceptibility testing*. Clinical and Laboratory Standards Institute: Wayne, United States, 106–112.

Danai, P., and Martin, G. S. (2005). Epidemiology of sepsis: recent advances. *Curr. Infect. Dis. Rep.* 7, 329–334. doi:10.1007/s11908-005-0005-1

De La Rica, A. S., Gilsanz, F., and Maseda, E. (2016). Epidemiologic trends of sepsis in western countries. *Ann. Transl. Med.* 4, 325–329. doi:10.21037/atm.2016.08.59

Doern, C. D., Mirrett, S., Halstead, D., Abid, J., Okada, P., and Reller, L. B. (2014). Controlled clinical comparison of new pediatric medium with adsorbent polymeric beads (PF Plus) versus charcoal-containing PF medium in the bact/alert blood culture system. *J. Clin. Microbiol.* 52, 1898–1900. doi:10.1128/JCM.00175-14

Flannery, D. D., Mukhopadhyay, S., Morales, K. H., Dhudasia, M. B., Passarella, M., Gerber, J. S., et al. (2022). Delivery characteristics and the risk of early-onset neonatal sepsis. *Pediatrics* 149, e2021052900. doi:10.1542/peds.2021-052900

Hafsa, A., Fakruddin, M., Hakim, M. A., and Sharma, J. D. (2011). Neonatal bacteremia in a neonatal intensive care unit: analysis of causative organisms and antimicrobial susceptibility. *Bangladesh J. Med. Sci.* 10, 187–194. doi:10.3329/bjms.v10i3.8363

Hami, I. A., and Ibrahim, K. S. (2023). Incidence of methicillin-resistant Staphylococcus aureus (MRSA) recovered from patients with urinary tract infections in zakho city/kurdistan-Iraq. *Sci. J. Univ. Zakho* 11, 91–97. doi:10.25271/sjuoz.2023.11.1.1041

Hammoud, M. S., Al-Taiar, A., Al-Abdi, S. Y., Bozaid, H., Khan, A., AlMuhairi, L. M., et al. (2017). Late-onset neonatal sepsis in Arab states in the Gulf region: two-year prospective study. *Int. J. Infect. Dis.* 55, 125–130. doi:10.1016/j.ijid.2017.01.006

Hasan, S. M., and Ibrahim, K. S. (2022). Molecular characterization of extended spectrum β-lactamase (ESBL) and virulence gene-factors in uropathogenic *Escherichia coli* (UPEC) in children in Duhok City, Kurdistan Region, Iraq. *Antibiotics* 11, 1246. doi:10.3390/antibiotics11091246

Herbozo, C., Julca, I., Flores, F., Hernandez, R., and Zegarra, J. (2021). Incidence and microbiological characteristics of neonatal late onset sepsis in a neonatal intensive care unit in Peru. *Int. J. Infect. Dis.* 108, 171–175. doi:10.1016/j.ijid.2021.05.012

Hermon, M. M., Etmayr, T., Brandt, J. B., Sadeghi, K., Burda, G., and Golej, J. (2021). Pediatric infection and sepsis in five age subgroups: single-center registry. *Wien. Med. Wochenschr.* 171, 29–35. doi:10.1007/s10354-020-00787-6

Hotchkiss, R. S., Moldawer, L. L., Opal, S. M., Reinhart, K., Turnbull, I. R., and Vincent, J.-L. (2016). Sepsis and septic shock. *Nat. Rev. Dis. Prim.* 2, 16045–16121. doi:10.1038/nrdp.2016.45

Ibrahim, D. R. (2023). PREVALENCE OF PLASMID MEDIATED QNRA, QNRB AND QNRS AMONG CLINICAL ESCHERICHIA COLI ISOLATED FROM URINARY TRACT INFECTIONS IN DUHOK, KURDISTAN REGION OF IRAQ. *Sci. J. Univ. zakho* 11, 523–531. doi:10.25271/sjuoz.2023.11.4.1196

Ibrahim, D. R., Dodd, C. E. R., Stekel, D. J., Meshioye, R. T., Diggle, M., Lister, M., et al. (2023). Multidrug-resistant ESBL-producing *E. coli* in clinical samples from the UK. *Antibiotics* 12, 169. doi:10.3390/antibiotics12010169

Jiang, S., Yang, C., Yang, C., Yan, W., Shah, V., Shah, P. S., et al. (2020). Epidemiology and microbiology of late-onset sepsis among preterm infants in China, 2015–2018: a cohort study. *Int. J. Infect. Dis.* 96, 1–9. doi:10.1016/j.ijid.2020.03.034

Mahon, C. R., Lehman, D. C., and Manuselis, G. (2014). *Textbook of diagnostic microbiology*. 5th ed. New York: Saunders.

Nasir, N., Jamil, B., Siddiqui, S., Talat, N., Khan, F. A., and Hussain, R. (2015). Mortality in sepsis and its relationship with gender. *Pak. J. Med. Sci.* 31, 1201–1206. doi:10.12669/pjms.315.6925

Odabasi, I. O., and Bulbul, A. (2020). Neonatal sepsis. *Şişli Etfal Hast. Tip. Bülteni* 54, 142–158. doi:10.14744/SEMB.2020.00236

Oruganti, S., Evans, J., Cromarty, T., Javaid, A., and Roland, D. (2022). Identification of sepsis in paediatric emergency departments: a scoping review. *Acta Paediatr. Int. J. Paediatr.* 111, 2262–2277. doi:10.1111/apa.16536

Rannikko, J., Syrjänen, J., Seiskari, T., Aittoniemi, J., and Huttunen, R. (2017). Sepsis-related mortality in 497 cases with blood culture-positive sepsis in an emergency department. *Int. J. Infect. Dis.* 58, 52–57. doi:10.1016/j.ijid.2017.03.005

Rudd, K. E., Johnson, S. C., Agesa, K. M., Shackelford, K. A., Tsoi, D., Kievlan, D. R., et al. (2020). Global, regional, and national sepsis incidence and mortality, 1990–2017: analysis for the Global Burden of Disease Study. *Lancet* 395, 200–211. doi:10.1016/S0140-6736(19)32989-7

Saleem, A. F., Qamar, F. N., Shahzad, H., Qadir, M., and Zaidi, A. K. M. (2013). Trends in antibiotic susceptibility and incidence of late-onset *Klebsiella pneumoniae* neonatal sepsis over a six-year period in a neonatal intensive care unit in Karachi, Pakistan. *Int. J. Infect. Dis.* 17, e961–e965. doi:10.1016/j.ijid.2013.04.007

Tessema, B., Lippmann, N., Knüpfer, M., Sack, U., and König, B. (2021). Antibiotic resistance patterns of bacterial isolates from neonatal sepsis patients at university hospital of Leipzig, Germany. *Antibiotics* 10, 323–412. doi:10.3390/antibiotics10030323

Unterberg, M., Rahmel, T., Rump, K., Wolf, A., Haberl, H., von Busch, A., et al. (2022). The impact of the COVID-19 pandemic on non-COVID induced sepsis survival. *BMC Anesthesiol.* 22, 12–18. doi:10.1186/s12871-021-01547-8

WHO (2022). The WHO AWaRe (access, watch, reserve) antibiotic book. Available at: https://www.who.int/publications/i/item/9789240062382.

Xu, J., Tong, L., Yao, J., Guo, Z., Lui, K. Y., Hu, X., et al. (2019). Association of sex with clinical outcome in critically ill sepsis patients: a retrospective analysis of the large clinical database MIMIC-III. *Shock (Augusta, Ga.)* 52, 146–151. doi:10.1097/SHK.0000000000001253

frontiers | Frontiers in Pharmacology

TYPE Original Research
PUBLISHED 28 February 2024
DOI 10.3389/fphar.2024.1293458

OPEN ACCESS

EDITED BY
Rizwan Shahid,
Alberta Health Services, Canada

REVIEWED BY
Dafne Bongiorno,
University of Catania, Italy
Haroon Rashid,
Federal University of Pelotas, Brazil
Ikram Ullah,
Hazara University, Pakistan

*CORRESPONDENCE
Momin Khan,
mominkhan.ibms@kmu.edu.pk
Muhammad Ali,
muhammad.ali@qau.edu.pk

RECEIVED 13 September 2023
ACCEPTED 25 January 2024
PUBLISHED 28 February 2024

CITATION
Khan AA, Khan M, Khan SW, Siddique N, Abid R, Zulfiqar S, Rahman S and Ali M (2024), Chiral phthalimides against penicillin-binding protein 2a of methicillin-resistant *Staphylococcus aureus*: molecular docking and *in vitro* analysis. *Front. Pharmacol.* 15:1293458.
doi: 10.3389/fphar.2024.1293458

Chiral phthalimides against penicillin-binding protein 2a of methicillin-resistant *Staphylococcus aureus*: molecular docking and *in vitro* analysis

Aamina Azam Khan[1], Momin Khan[2]*, Sher Wali Khan[3], Nayyer Siddique[4], Rimsha Abid[1], Shandana Zulfiqar[1], Sidra Rahman[5] and Muhammad Ali[5]*

[1]Institute of Pathology and Diagnostic Medicine, Khyber Medical University (KMU), Peshawar, Pakistan, [2]Department of Microbiology, Khyber Medical University (KMU), Peshawar, Pakistan, [3]Department of Chemistry, Rawalpindi Women University, Rawalpindi, Pakistan, [4]Institute of Basic Medical Science, Khyber Medical University (KMU), Peshawar, Pakistan, [5]Department of Biotechnology, Quaid-i-Azam University Islamabad, Isalmabad, Pakistan

Staphylococcus aureus (*S. aureus*) is a commensal bacterium and an opportunistic pathogen causing a wide variety of infections ranging from localized skin and soft tissue infections to life-threatening severe bacteremia, osteomyelitis, endocarditis, atopic dermatitis, prosthetic joint infection, staphylococcal food poisoning, medical device-related infections, and pneumonia. It is attributed to an acquired resistant gene, *mecA*, encoding penicillin-binding protein 2a (PBP2a). PBP2a is an essential protein responsible for the resistivity of methicillin-resistant *S. aureus* (MRSA) to various beta-lactam antibiotics. The antimicrobial treatment alternatives for MRSA are increasingly limited. Therefore, developing alternative therapeutic options for its treatment is the need of the day. Phthalimides and their N-substituted derivatives are of biological importance as they possess extensive biological and pharmaceutical properties and can serve as an excellent therapeutic option for MRSA. This study uses three chiral phthalimides (FIA, FIB, and FIC) to check their *in silico* and *in vitro* inhibitory effects. Molecular docking of these chiral phthalimides against PBP2a of MRSA was performed initially. After promising results, these novel compounds were screened through the agar-well diffusion method and micro-broth dilution assay to investigate their *in vitro* inhibitory activities with FIB being the strongest anti-staphylococcal agent yielding a 21 mm zone of inhibition and a minimum inhibitory concentration (MIC) of 0.022 ug, respectively. The zones of inhibition obtained through the *in vitro* activity showed that these chiral phthalimides possess substantial anti-MRSA activities and have the potential to be considered as alternative chemotherapeutics to treat the infections caused by MRSA after the confirmation of their cytotoxic and pharmacokinetic studies.

KEYWORDS

methicillin-resistant gene, penicillin-binding protein2a, methicillin-resistant *Staphylococcus aureus*, chiral phthalimides, molecular docking, cytotoxicity

Introduction

Genus *Staphylococcus* contains gram-positive, bacitracin-resistant, catalase-positive, non-spore-forming coccus bacteria (Cheung et al., 2021). It is a coagulase-positive bacterium, which is the common colonizer of the human body. It is a highly virulent pathogen of "Risk Group Level 2" because of its ability to invade, persist, replicate, and infect human tissues (Wang et al., 2016). It is an opportunistic pathogen responsible for several human infections, from localized skin and soft tissue infections to life-threatening severe bacteremia (Matuszewska et al., 2020), endocarditis, osteomyelitis, atopic dermatitis, staphylococcal food poisoning, staphylococcal toxic shock syndrome (TSS) (Turner et al., 2019), prosthetic joint infections, medical device-related infections, and pneumonia (Senobar Tahaei et al., 2021). Due to its toxin-producing abilities (i.e., staphylococcal enterotoxin), it is a significant cause of staphylococcal foodborne disease (Fri et al., 2020). *S. aureus* can also cause infections in livestock, like mastitis (in ruminants) and bumblefoot (in poultry), as well as diseases in domestic animals (dogs and cats), resulting in substantial morbidity rates in animals and a significant economic loss to the farmers.

Methicillin-resistant *S. aureus* (MRSA) was first isolated in 1961 in a hospital in the UK (Ullah et al., 2016). MRSA is resistant to almost all β-lactams (Craft et al., 2019), including penicillin, trimethoprim, erythromycin, clindamycin, and tetracyclines (Turner et al., 2019), hence minimizing the safe and effective treatment options for MRSA. These strains also resist other antibiotic groups, e.g., fluoroquinolones, macrolides, and aminoglycosides, and are, therefore, known as "Superbug" (Senobar Tahaei et al., 2021). The success of this pathogen is related to the presence of its extensive virulence factors such as enzymes (hyaluronic acid, lipases, proteases, coagulase, and staphylokinase), toxins (hemolysins and leukocidins), antigens, and evasive immune factors (protein A and capsule) coupled with its remarkable ability to quickly acquire resistance to different antibiotics used in clinical practice over the years (Fri et al., 2020).

Methicillin resistance is associated with the modifications in penicillin-binding proteins (PBP2a/2c/2′), due to the presence of *mecA*, *mecB*, or *mecC* genes in *S. aureus*. In addition to PBP1-4, MRSA strains encode a high-molecular-weight fifth penicillin-binding protein, called penicillin-binding protein 2a (PBP2a), responsible for their resistance (Fergestad et al., 2020). PBP2a is encoded by the *mecA* gene, which is present inside a mobile genetic element known as the *Staphylococcal* cassette chromosome mec (SCC*mec*) (Miragaia, 2018; Craft et al., 2019). PBP2a enables the synthesis of the bacterial cell wall in the presence of antibiotics, as it has a low affinity for all beta-lactam antibiotics, thus allowing cross-linking to proceed (Craft et al., 2019; Fergestad et al., 2020). Like other PBPs, the active site of PBP2a contains the active site serine (Ser403) located at the N-terminus. Still, it lies deep in the pocket and is inaccessible to beta-lactam antibiotics. This closed active site indicates the resistance offered by PBP2a (Bien et al., 2011). Moreover, some additional genes essential for methicillin resistance, such as factors necessary for the expression of methicillin resistance (*fem*) and auxiliary factors (*aux*), have also been identified (Bien et al., 2011).

The common antibiotics used against MRSA currently include daptomycin, gentamicin, vancomycin, linezolid, TMP–SMZ (trimethoprim/sulfamethoxazole), tigecycline, clindamycin, and amikacin, but these antibiotics are losing their efficacy (Okwu et al., 2019). In addition, teicoplanin, daptomycin, and linezolid are expensive (Okwu et al., 2019). As the therapeutic options available at present for the treatment of MRSA infections are limited, there is an urgent need to develop novel drugs effective for treating MRSA infections (Okwu et al., 2019). Cyclic imides and their N-substituted derivatives [-CO-N(R)-CO-] are an important class of organic compounds containing bis-amide linkages. Their neutral structures and hydrophobicity allow them to cross biological membranes easily. The nitrogen and oxygen atoms as donor sites can co-ordinate these molecules with the biological system causing some pharmacological effects (Hassoun et al., 2017). Among the imide-ring-containing heterocyclic compounds, phthalimides and their N-substituted derivatives possess extensive biological and pharmaceutical properties. They have also been used as tumor necrosis factor-alpha (TNF-alpha) inhibitors, which has a crucial role in several physiological immune systems (Kushwaha and Kaushik, 2016). These molecules are reported to possess important biological properties including antifungal, antibacterial, antiviral, anticancer, analgesic, antidepressant, apoptosis induction, anti-inflammatory, androgen receptor antagonist, anxiolytic, anticonvulsant, and muscle relaxant activities (Jafari et al., 2017). The antibacterial properties of different phthalimide derivatives of N-alkyl, N-alkyloxy, N-acyl, butyl, and N-hydroxyl have been reported against both Gram-positive (*Streptococcus pneumoniae*, *Micrococcus luteus*, and *Listeria monocytogenes)* and Gram-negative (*Pseudomonas aeruginosa*, *Salmonella typhimurium*, and *Escherichia coli)* bacterial strains which have shown promising results because of their smaller size and high potency in disease control management (Othman et al., 2019). Similarly, the derivatives of chiral phthalimides with N-alkyloxy and N-alkyl substitution in combination with maleimide have shown antifungal activity against fungi (*Candida albicans* and *Aspergillus fumigatus)* (Imran et al., 2019). One of the reasons for inflammatory diseases is the denaturation of the protein present in tissues that leads to the development of autoantigens. Phthalimide derivatives with the combination of N-aryl or aryl amines in the presence of an L-proline catalyst can prevent this denaturation process and, hence, inhibit the development of inflammatory diseases (Perveen and Orfali, 2018). So, these compounds can serve as an excellent therapeutic approach for treating MRSA infections; therefore, our study used three different chiral phthalimides to check their *in silico* and *in vitro* inhibitory effects. Regardless of the enormous investments and the time consumed in discovering new drugs, its success rate through clinical trials is only 13%, with a relatively high failure rate. These failures have been reported at a later stage in the majority of cases (40%–60%) because of the lack of optimum pharmacokinetic properties (absorption, distribution, metabolism, excretion, and toxicity) of the drugs (Gurung et al., 2021). So, recently, a decrease in the market has been noted in the number of new drugs because they failed in different phases of the clinical trials. Therefore, it is essential to cope with the limitations in the conventional drug discovery methods with a cost-effective, efficient, and broad-spectrum computational drug development process. Such computational techniques will aid the drug discovery and development process by minimizing the costs and final stage failure chances when used by various pharmaceutical companies and

research groups in the preliminary studies (Batool et al., 2019; Gurung et al., 2021).

Molecular docking is a structure-based drug-designing approach (SBDD). It was first developed for predicting the binding action of known active molecules and virtual screening of sizeable digital compound libraries to minimize the cost and speed up drug discovery processes (Torres et al., 2019). It has been widely used as an inexpensive and fast technique in industrial and academic settings. The objective of molecular docking is to get an optimized conformation for both the ligand and the protein and the relative orientation between the ligand and the protein in such a manner that the free energy of the overall system is minimized (Torres et al., 2019). This drug-designing approach is effectively fast and specific for the identification and opsonization of lead molecules, which has helped to understand the molecular level of a disease (Gurung et al., 2021). In the current study, the chiral phthalimides (FIA, FIB, and FIC) used were docked against the PBP2a protein of MRSA before their *in vitro* antibacterial activity. The reason for selecting these chiral phthalimides was their good antibacterial activity against several Gram-positive and Gram-negative bacteria present in the literature.

Materials and methods

Molecular docking analysis

Retrieving the 3D structure of the ligands

All three chiral phthalimides' chemical structures were retrieved from PubChem (https://pubchem.ncbi.nlm.nih.gov/). Their PubChem IDs are FIA (ID = 334207), FIB (ID = 688554), and FIC (ID = 1714209).

Structure retrieval of PBP2a

The sequence of the protein PBP2a was retrieved from the NCBI (Accession No. ALJ 10988.1). This sequence was saved in the FASTA format, which gives information regarding the total number of amino acids present in the sequence and other related information.

Homology modeling and structure evaluation

Since no information was present in the Protein Data Bank (PDB) (www.rcsb.org), the protein was modeled using SWISS-MODEL to deduce the structure of the protein PBP2a. SWISS-MODEL is consistently ranked among the top modeling servers for several crucial modeling aspects, and it deduces the protein structure on the basis of the already available protein structures (homology modeling). The structure obtained through modeling was then evaluated using PROCHECK (Laskowski et al., 1996) for checking the accuracy of stereochemical parameters (e.g., bond length, G factor, conformational angles, and bond angles). The relationship of the sequence with the 3D structure was verified utilizing VERIFY3D (Eisenberg et al., 1997). The ERRAT scheme plot was also performed to verify protein structure validity on the basis of crystallography, and structure structures generally produce values around 95% or higher, considered suitable high-resolution structures. The Ramachandran plot was generated to predict the structural stereochemical property (i.e., structures that score more than 85% will be considered valid). The assessment and validity of the structure was also carried out again once the minimization of the structure was carried out. This step-by-step procedure validated the protein structure of PBP2a, and a high-quality model was generated at the end.

Energy minimization

Once the structure modeling is performed, a crucial step, i.e., energy minimization, must be performed, removing all the torsions within a molecule and bringing it to the lowest possible energy state to ensure a good structure. To accomplish energy minimization of the structure, ModRefiner adjusted the root mean square deviation (RMSD) value for the refined structure by changing the bond angles of the unrefined structure of PBP2a.

Binding pocket determination

For determining the active sites of the PBP2a protein of MRSA, CASTp (Binkowski et al., 2003; Raffo et al., 2022) and ProteinsPlus (Schöning-Stierand et al., 2020) (https://proteins.plus/) were used by uploading the file of the protein structure in the .pdb format. The residues in the pocket were then noted.

Molecular docking

For docking the chiral phthalimides with the active sites of PBP2a, PatchDock (Duhovny et al., 2002) was used. At one time, .pdb formats of the targeted protein and only one ligand were uploaded for docking. The BIOVIA Discovery Studio (DS Visualizer) 2021 Client was finally used for analyzing the results of the docked molecules obtained.

In vitro study analysis

Sample collection and processing

It is an experimental study for which ten MRSA samples were collected from the microbiology laboratory of Hayatabad Medical Complex. The samples were collected from different sites such as wound, pus, and high vaginal swabs. Those samples were further processed in the microbiology laboratory of IPDM, KMU, according to the laboratory-optimized protocol. The confirmed strains of MRSA were stored in the KMU repository with strain numbers from AAK001IPDM to AAK010IPDM.

Inoculation on different growth media and the identification of *S. aureus*

All the samples obtained were inoculated on MSA (Mannitol salt agar) and blood agar plates. The identification of *S. aureus* was made

10.3389/fphar.2024.1293458

TABLE 1 Ligands and their 3D structures.

Name of the ligand	3D picture
Compound 1: FIA [2-(1, 3-dioxoisoindolin-2-yl)-3-phenylpropanoic acid]	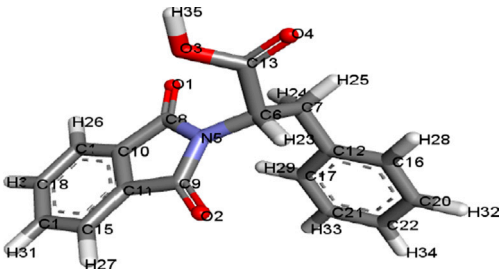
Compound 2: FIB [2-(1, 3-dioxoisoindolin-2-yl)-4-methylpentanoic acid]	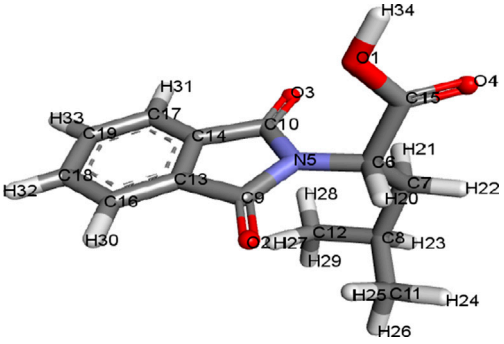
Compound 3: FIC [2-(1, 3-dioxoisoindolin-2-yl)-4-(methylthio) butanoic acid]	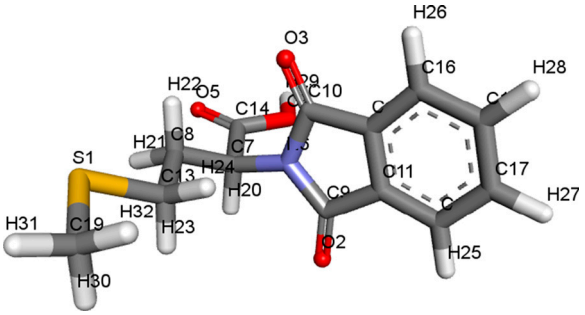

based on morphological features and biochemical tests such as Gram staining, catalase, and coagulase tests.

Antibiotic susceptibility testing

The standardized method, i.e., the Kirby–Bauer disc agar diffusion method, was performed using different antibiotic discs on Mueller–Hinton agar (MHA) to differentiate MRSA from MSSA samples. The Clinical and Laboratory Standard Institution Guidelines (CLSI) 2022 established the susceptibility pattern. Different antibiotic discs, including cefoxitin (FOX- 30 µg), ciprofloxacin (CIP- 5 µg), penicillin (P- 10 ug), vancomycin (V- 30 µg), gentamicin (CN- 10 µg), erythromycin (E– 15 ug), amikacin (AK- 30 ug), cefepime (CPM- 30 ug), clindamycin (DA- 2 µg), and linezolid (LZD- 30 µg), were used.

Antibacterial activity of chiral phthalimides

The antimicrobial activity of the chiral phthalimides was checked against *S. aureus* (MRSA) through the agar-well diffusion method using Muller–Hinton agar, which is commonly used for checking the antibacterial activities of novel compounds. Following the standard protocol, 5000 ug (5 mg) of each of the compounds were dissolved in 1000 uL (1 mL) of DMSO, and a final volume of approximately −250–300 uL was added to the wells (−4 mm diameter) made on agar plates. 100% DMSO was used as a control for this assay.

Chiral phthalimides used in the current study

i) Compound 1 (FIA): [2-(1, 3-Dioxoisoindolin-2-yl)-3-phenylpropanoic acid]
ii) Compound 2 (FIB): [2-(1, 3-Dioxoisoindolin-2-yl)-4-methylpentanoic acid]
iii) Compound 3 (FIC): [2-(1, 3-Dioxoisoindolin-2-yl)-4-(methylthio) butanoic acid]

Determining the minimum inhibitory concentration

The 96-well plate assay was used to determine the minimum inhibitory concentration (MIC) of the compounds. It is a well-known worldwide method for determining the minimum inhibitory concentrations of the test compounds, that is, the minimum concentration of test compounds required to inhibit the visible growth of bacteria. This technique used a sterilized 96-well plate with proper positive (McFarland standard) and negative (nutrient broth) controls. Each well has a total capacity of holding 200 ul of the solution.

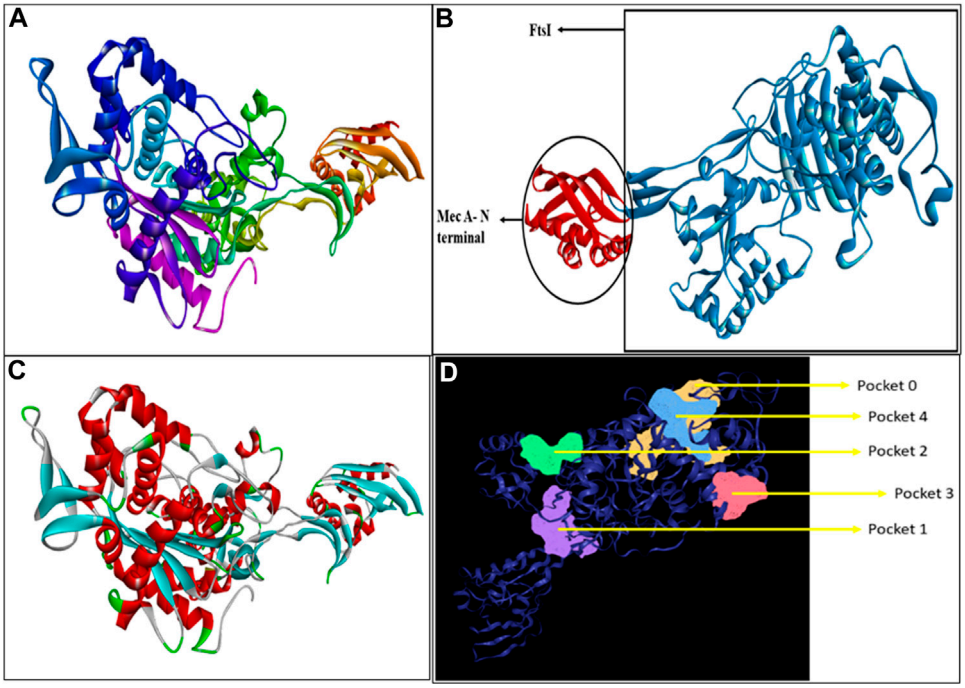

FIGURE 1
(A) Modeled 3D structure of chain A of PBP2a. **(B)** Labeled 3D structure of PBP2a showing two different regions; red color indicates the N-terminal of mecA (amino acids 25–140), and blue color indicates the conserved protein domain FtsI (amino acids 136–667). **(C)** Energy-minimized refined model of PBP2a. **(D)** Structure of PBP2a with its five active pockets.

Determining the minimum bactericidal concentration

For identifying the minimum bactericidal concentration (MBC), a visual plate assay was performed on the MHA and blood agar plates.

Results

Molecular docking analysis

3D structures of the ligands obtained

The structures of ligands retrieved via PubChem are given in Table 1.

Homology modeling and structure evaluation

Penicillin-binding protein 2a contains a single amino acid chain (chain A) totaling 668 amino acids. The 3D structure of PBP2a was obtained through SWISS-MODEL Figure 1A. Figure 1B shows the labeled 3D structure of PBP2a in which the red color indicates the N-terminal of mecA (comprising amino acids 25–140), whereas the blue color indicates the conserved protein domain FtsI (containing amino acids 136–667).

The modeled protein structure was further verified through VERIFY3D, as shown in Figure 2A. The blue line indicates the average score of the actual 3D protein model. In contrast, the green dots mark the raw scores for our protein model generated. The VERIFY3D score showed that 92.37% of the residues had scored >=0.1 and are compatible with the average score, so our protein model is acceptable. This further validates the 2D–3D construction (compatibility of the 2D sequence to the 3D structure). The general criteria for the structures to be considered as PASS in VERIFY3D is that at least 80% of the amino acids should score >=0.1 in the 3D/1D profile. Since our structure fulfilled this criterion, it was considered as PASS. The ERRAT scheme plot further validated the structure and showed a good high-resolution structure with a value score of 97.47%, more than 95%, as shown in Figure 2B.

The evaluation of the modeled structure through PROCHECK produced a Ramachandran plot, as shown in Figure 2C. The results from the Ramachandran plot indicated that 92.8% of the residues reside in the most favored region (red), hence indicating the suitable stereochemical parameters for the structure of PBP2a, whereas 6.4% of the residues reside in the additional allowed region (dark yellow), 0.3% residues reside in the generously allowed region (light yellow), and 0.5% residues reside in the disallowed region (white).

Energy minimization

Energy minimization through ModRefiner adjusted the RMSD (root mean square deviation) value for the refined structure to 0.440, as shown in Figure 1C, which was further used for docking.

Binding pocket determination

A total of five active pockets in PBP2a were determined using ProteinsPlus, as shown in Figure 1D by different colors. The properties of those pockets are summarized in Table 2 (Supplementary Table S1 for the amino acids in the binding pockets is attached in Supplementary Material).

Molecular docking

The results from PatchDock showed that compound 1 (FIA) formed one hydrogen bond (ARG-151), compound 2 (FIB) formed

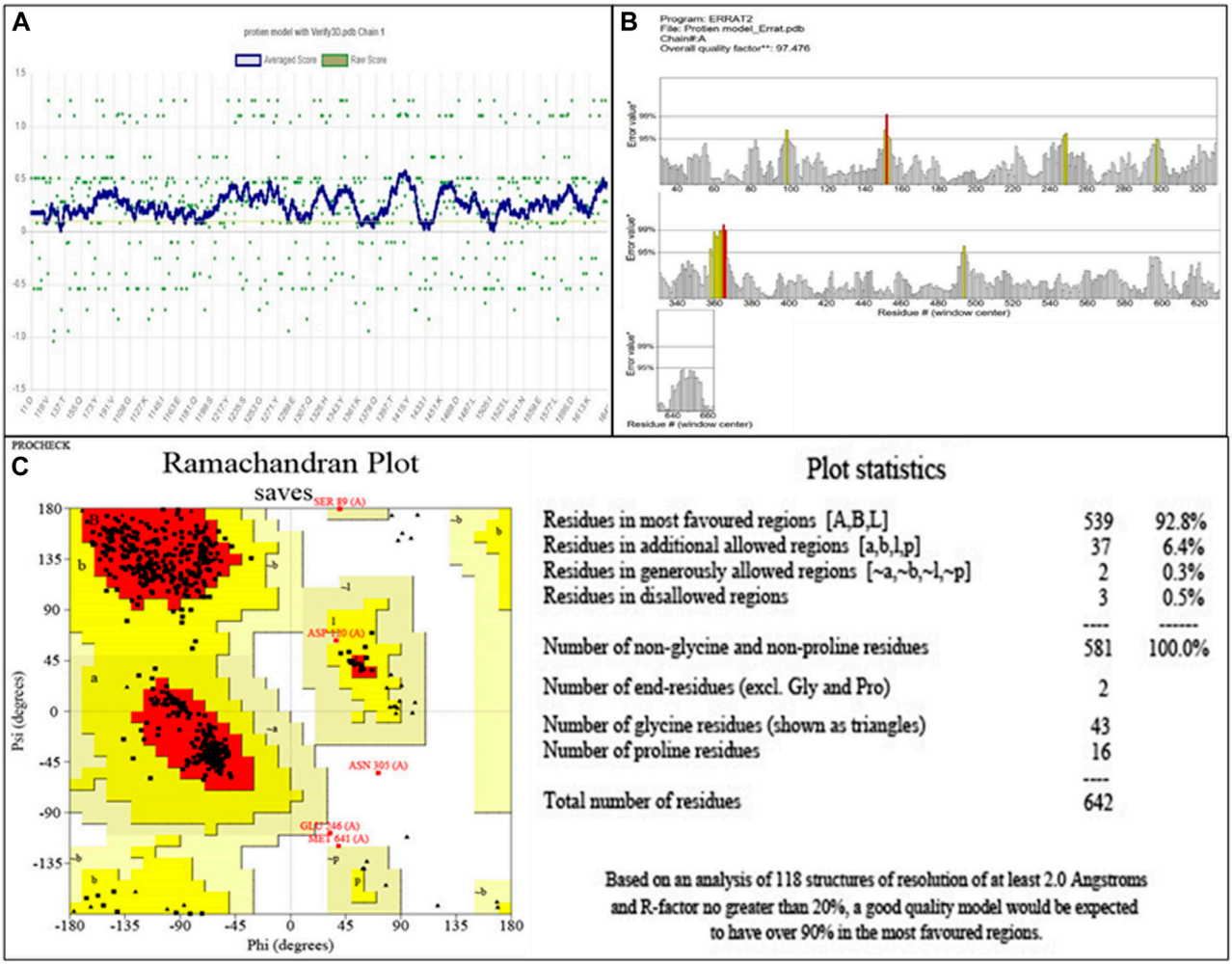

FIGURE 2
(A) Validation of 2D–3D construction via VERIFY3D. Blue color indicates the average residue score, while green dots represent the raw residue score. **(B)** The ERRAT scheme plot shows the overall quality of the protein model with 97.47%, which is higher than 95%, indicating the good high-resolution structure. *On the error axis, two lines are drawn to represent the confidence with which regions exceeding the error value can be rejected. **, expressed as the proportion of proteins for which the estimated error value falls below the 95% rejection threshold. Good high-resolution structures typically produce values of at least 95 percent. For lower resolutions (2.5–3A), the average quality factor is approximately 91%. **(C)** The Ramachandran plot showing amino acid residues in different regions for the evaluation of PBP2a. Red color indicates the most favored region that is 95.0%. Dark yellow color indicates the additional allowed region that is 4.1%, while light yellow and white colors indicate the generously allowed region and disallowed region that are 0.3% and 0.5%, respectively.

TABLE 2 Properties of the active pocket of PBP2a.

S. no.	Active pocket	Volume A^3	Surface A^2	Drug score
1	Pocket 3	441.26	791.51	0.84
2	Pocket 0	1412.11	1647.33	0.8
3	Pocket 4	365.22	373.88	0.77
4	Pocket 1	932.15	1145.63	0.76
5	Pocket 2	553.97	727.26	0.71

two hydrogen bonds (THR 216, LYS 218), and compound 3 (FIC) also formed one hydrogen bond (THR 216) with the PBP2a (Figure 3). The basis of the selection of the compounds was the number of hydrogen bonds it formed with the PBP2a. The more the number of hydrogen bonds, the strongest is the compound. In addition, those compounds which interacted with the PBP2a protein through a covalent bond were rejected because of the chances of their off-site toxicity in the host. Both the 2D and 3D confirmations of the ligand and protein along with the hydrogen bonds involved are shown. Table 3 summarizes docking parameters for the selected chiral phthalimides with PBP2a.

10.3389/fphar.2024.1293458

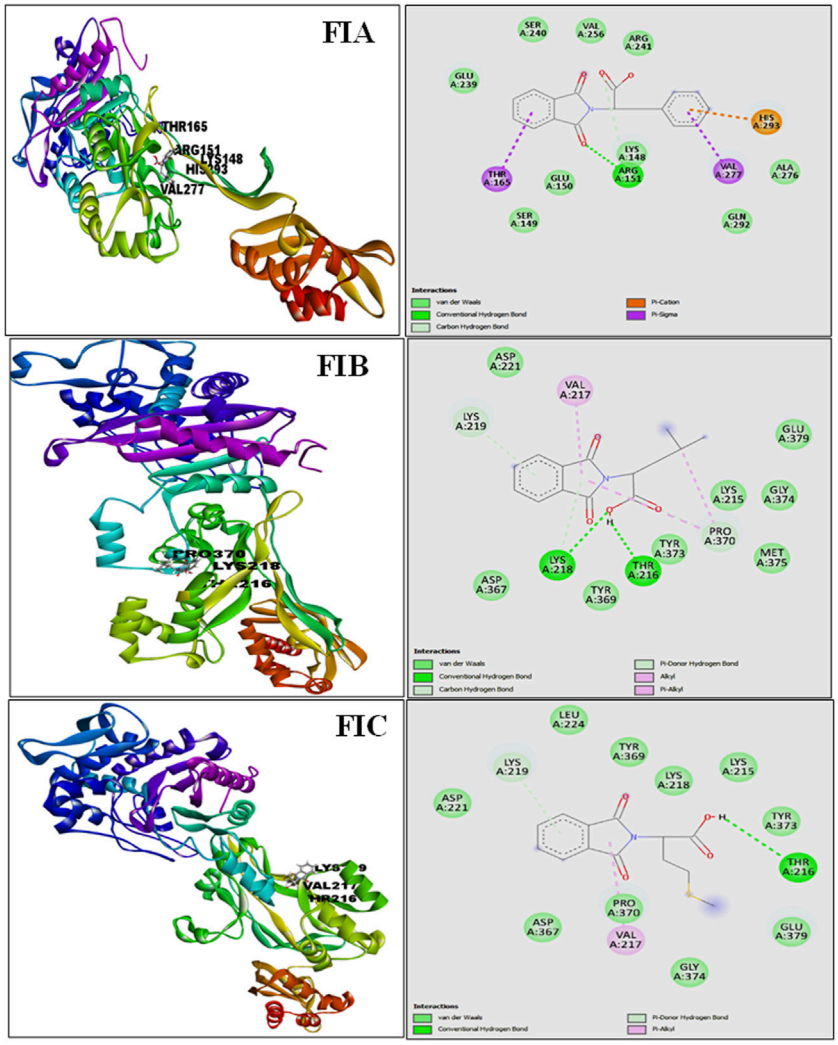

FIGURE 3
Complete 3D structure of FIA, FIB, and FIC docked with PBP2a (left) and their respective 2D diagram showing hydrogen bonding and the specific amino acids involved (right). It is shown that compound 1 (FIA) formed one hydrogen bond (ARG-151), compound 2 (FIB) formed two hydrogen bonds (THR 216, LYS 218), and compound 3 (FIC) also formed one hydrogen bond (THR 216) with the PBP2a.

TABLE 3 Docking parameters.

Ligand name	Score	Area	ACE	Number of hydrogen bonds	Number of covalent bonds
Compound 1 (FIA)	3594	451.70	−101.27	1	0
Compound 2 (FIB)	3468	372.90	−110.25	2	0
Compound 3 (FIC)	3592	378.60	−132.78	1	0

In vitro study analysis

Inoculation on different growth media

All samples of *Staphylococcus aureus* produced small yellow colonies with yellow zones on MSA because of the fermentation of mannitol present in the medium, which produces an acidic byproduct that turns the color of phenol red indicator dye of MSA to yellow (Figure 4A). In contrast, on blood agar, it had β-hemolytic colonies surrounded by a clear zone due to complete lysis of red blood cells. The complete lysis occurred because of the production of hemolysins by *S. aureus* (Figure 4B).

Biochemical testing for identification (Gram staining, catalase test, and coagulase test)

All samples of *S. aureus* appeared as purple cocci (Gram-positive) occurring as clusters like the bunches of grapes under the compound microscope after Gram staining (Figure 4C). When the catalase test was performed for *S. aureus*, bubble

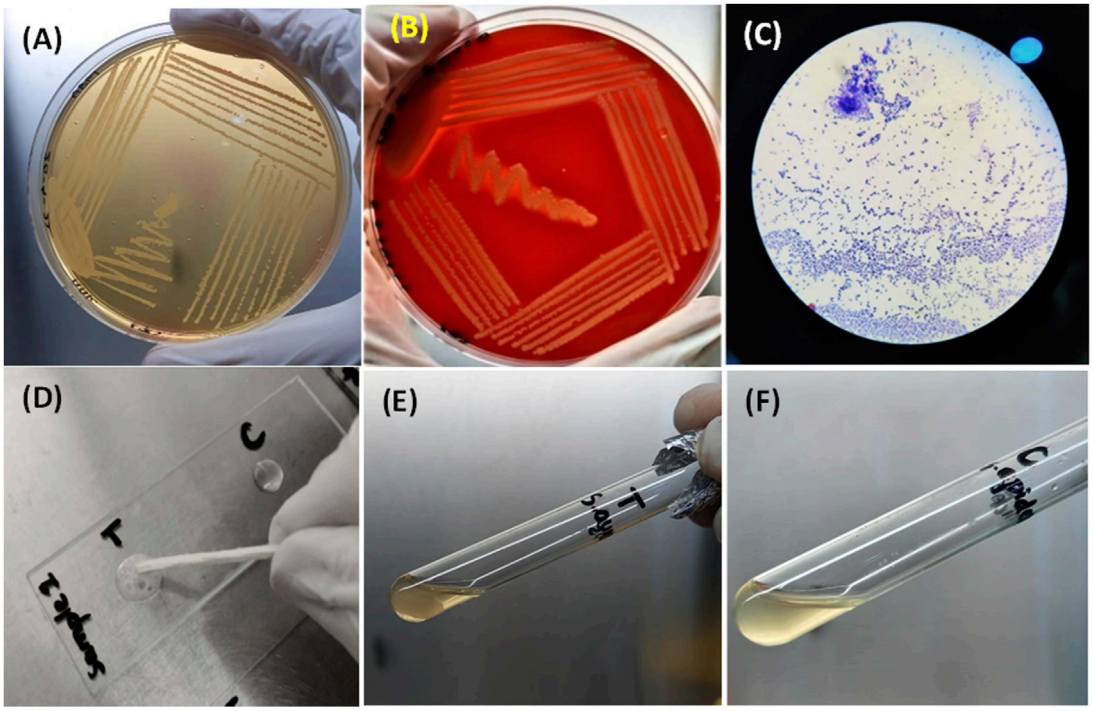

FIGURE 4
(A) Growth of *S. aureus* on MSA showing mannitol fermentation by turning the media yellow. **(B)** Beta-hemolytic colonies of *S. aureus* on blood indicated by a clear zone of hemolysis. **(C)** *S. aureus* as Gram-positive (purple color) cocci under the microscope. **(D)** Bubble production by the catalase-positive *S. aureus* (left) and no bubble production in the control (right) **(E)** and **(F)** clot formation by *S. aureus* and no clot formation by *S. epidermidis* (control).

production was observed because of the production of the catalase enzyme, whereas for the control, no bubble production was observed (Figure 4D). A clot was produced in the test tube after a coagulase test for *S. aureus*, indicating the coagulase enzyme production by *S. aureus*. In comparison, no clot formation occurred in the test tube containing *S. epidermidis* (Figures 4E, F).

Antibiotic susceptibility testing

The zones obtained for different antibiotics through the Kirby–Bauer disc agar diffusion method, after incubation for 18–24 h, are summarized in Table 4. While measuring the zones of inhibition produced by *S. aureus* (MRSA), the cefoxitin disc needs to be in the resistant range (</ = 21 mm) as it serves as the basis of identification for MRSA. All the samples obtained were resistant to four antibiotics (FOX, P, VA, and CIP) and sensitive to three antibiotics (CN, AK, and LZD), whereas for the antibiotic erythromycin, half of the samples were susceptible, whereas the other half were resistant, which, in turn, resisted clindamycin because of the phenomenon of D-test (Figure 5A). For AST, all the experiments have been performed on all 10 samples of MRSA.

Antibacterial activity of chiral phthalimides

The antibacterial activity of chiral phthalimides was evaluated through the agar-well diffusion method. The average zones of inhibition for FIA, FIB, and FIC (conc. 5 mg/ml) were ≤15 mm, ≤21 mm, and ≤12 mm, respectively, and no zone was observed in control (100% DMSO), as shown in Figure 5B. For checking the antibacterial activity of chiral phthalimides, all the experiments were performed in triplicate, and their average is mentioned in the results.

MIC through the micro-broth dilution method

The results obtained for MIC are interpreted in Table 5. In the table, the "–" sign indicates no growth (clear well), and the "+" sign indicates growth (turbid well). The encircled regions in the table indicate the MICs. The minimum inhibitory concentration of a particular compound is one dilution lesser than the dilution at which visible growth has occurred. So, for FIA, FIB, and FIC, the concentrations 0.73 ug, 0.022 ug, and 93 ug per mL of DMSO, respectively, are the MICs. Initially, 10 dilutions were made from the stock solution, but when results were visualized, the MIC for compound 3 (FIC) was obtained only. The last dilution was then diluted 10 times to get the minimum inhibitory concentrations for FIA and FIB. These results were further verified through MBC.

Determining the minimum bactericidal concentration

The results for MBC on the overnight incubated MHA and blood agar are shown in Supplementary Figure S1, confirming the MBC. The specific concentrations of the chiral phthalimide compounds FIA, FIB, and FIC for MIC and MBC were 0.73 ug, 0.022 ug, and 93 ug/mL of DMSO, respectively. It can be interpreted from the above results that the chiral phthalimides used in this project were bactericidal, killed MRSA, and yielded the same values for MIC and MBC. Furthermore, the results indicate that FIA has the most potent antibacterial activity among all the three chiral phthalimides used.

TABLE 4 Table for the interpretation of AST.

S. no.	Antibiotic disc	Standard resistant range (CLSI 2022) (mm)	Zone obtained via AST (mm)	Interpretation
1	Cefoxitin (FOX-30 ug)	≤21	9	RESISTANT (indicating the presence of MRSA)
2	Penicillin (P- 10 ug)	≤28	9	RESISTANT
3	Vancomycin (VA-30 ug)	≤17	16	RESISTANT
4	Ciprofloxacin (CIP- 5 ug)	≤15	12	RESISTANT
5	Cefepime (CPM-30 ug)	≤23	10	RESISTANT
5	Gentamicin (CN-10 ug)	≤12	20	SUSCEPTIBLE
6	Erythromycin (E-15 ug)	≤13	13	Half of the samples were RESISTANT, whereas half were SUSCEPTIBLE
7	Clindamycin (DA- 2 ug)	≤14	19	SUSCEPTIBLE (but reported as resistant where the spp. was resistant to erythromycin because of the D-test)
8	Amikacin (AK-30 ug)	≤17	22	SUSCEPTIBLE
9	Linezolid (LZD-30 ug)	≤20	30	SUSCEPTIBLE

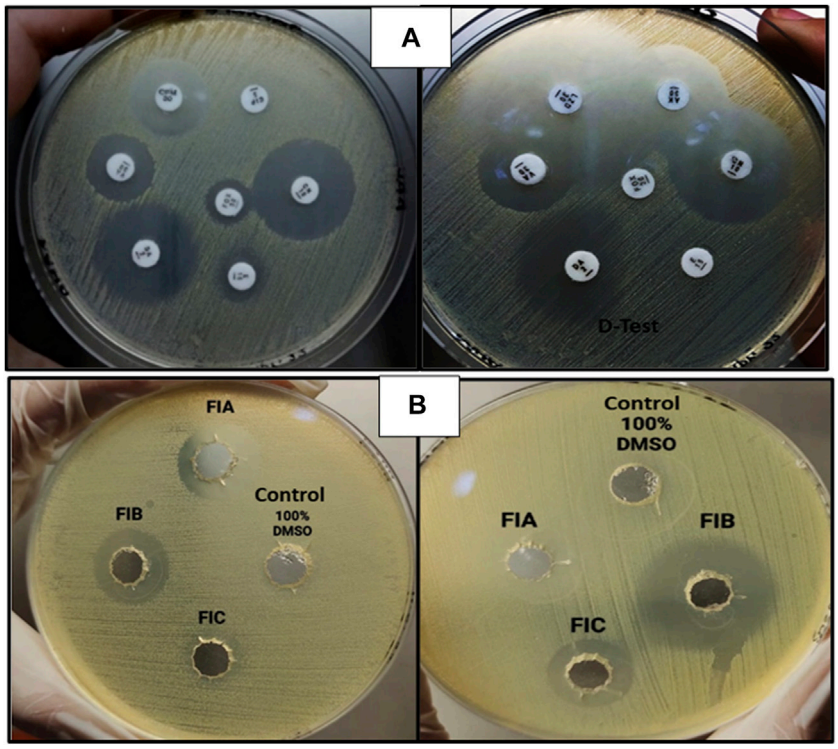

FIGURE 5
(A) AST for MRSA showing clear zones of inhibition (left) and D-test [inducible clindamycin resistance in the presence of erythromycin (right)]. **(B)** Zones of inhibition obtained as a result of agar-well diffusion assay for chiral phthalimides.

TABLE 5 Table for the result interpretation of MIC from the 96-well plate.

Initial concentration (3000 ug/mL)												
Dilutions 1 to 20												
Well dilution	+ve C	1	2	3	4	5	6	7	8	9	10	-ve C
Conc. of compounds in the well (ug/mL)	200ul MF	3000	1500	750	370	180	93	46	23	11	5.8	200ul NB
FIA	+	–	–	–	–	–	–	–	–	–	–	–
FIB	+	–	–	–	–	–	–	–	–	–	–	–
FIC	+	–	–	–	–	–	– MIC	+	+	+	+	–
Dilutions 11 to 20												
Well dilution	**+ve C**	**11**	**12**	**13**	**14**	**15**	**16**	**17**	**18**	**19**	**20**	**-ve C**
Concentration of compounds in well (ug/ml)	**200ul MF**	**2.9**	**1.4**	**0.73**	**0.36**	**0.18**	**0.09**	**0.045**	**0.022**	**0.011**	**0.0055**	**200ul NB**
FIA	+	–	–	– MIC	+	+	+	+	+	+	+	-
FIB	+	–	–	–	–	–	–	–	– MIC	+	+	–
FIC	+	+	+	+	+	+	+	+	+	+	+	-

In the table above, MF indicates McFarland Standard; NB indicates nutrient broth; MIC, Minimum Inhibitory Concentration. The "–" sign indicates no growth (clear well), and the "+" sign indicates growth. Number range 1–20, indicates the wells of the 96-well plate. Values in (ul), indicates the diluted compound in each well.

Discussion

Antibiotic resistance has been declared a "Global Public Health Concern" by the Centers for Disease Control and Prevention (CDC), WHO, the World Economic Forum, and the Infectious Diseases Society of America. In the past 2 decades, the acquired MDR infections have increased because of the production of beta-lactamase enzymes (including extended-spectrum β-lactamases (ESBLs), carbapenemases, and metallo-β-lactamases), which leads to 3rd-generation cephalosporin and carbapenem resistance (Aslam et al., 2018; Vestergaard et al., 2019). Currently, a group of MDR pathogens collectively known as "ESKAPE" bacteria also includes MRSA, which is considered the most important pathogen due to its resistance, mortality, and clinical importance. So, being a member of a highly pathogenic group of microorganisms, *S. aureus* was selected for this project (Senobar Tahaei et al., 2021). Considering the resistance story of *S. aureus*, it rapidly became MDR over several decades, starting with the production of penicillinase and penicillin resistance early in the 1940s, followed by the macrolide and tetracycline resistance in the 1950s and, finally, the emergence of MRSA (methicillin resistance) in the early 1960s (Morehead and Scarbrough, 2018), showing resistance to β-lactam antibiotics such as methicillin, oxacillin, nafcillin, cloxacillin, and dicloxacillin. This increased resistance rate was attributed to the presence of a "mecA"-resistant gene encoding a "penicillin-binding protein 2a" (PBP2a), which made the MRSA strains more resistant to methicillin (Liu et al., 2016). This is because the active site of PBP2a contains the active site serine (Ser403) located at the N-terminus which lies deep in the pocket and is inaccessible to beta-lactam antibiotics. This closed active site indicates the resistance offered by PBP2a (Bien et al., 2011). Although this multidrug resistance was developed subsequently, it has become a worldwide issue; therefore, the CDC has labeled it a severe threat to the healthcare system (Morehead and Scarbrough, 2018; Senobar Tahaei et al., 2021). Hence, due to the vital role of PBP2a protein in the resistance of MRSA, it was used as a target protein for checking the anti-MRSA activities of the novel chiral phthalimides in the current project.

Considering these susceptibility reports for MRSA (Fri et al., 2020; Senobar Tahaei et al., 2021) mentioned in the literature, we conducted AST using the CLSI guidelines 2022 in our project, and it was examined that all the MRSA isolates showed complete resistance to the antibiotics: cefoxitin (30 ug), penicillin (10 ug), ciprofloxacin (5 ug), vancomycin (30 ug), and cefepime (30 ug), and the highest level of susceptibility to the antibiotics was shown by gentamicin (10 ug), amikacin (30 ug), and linezolid (30 ug), whereas some isolates showed variable degree of resistance to two of the antibiotics, erythromycin (15 ug) and clindamycin (2 ug), because of the phenomenon of the D-test. The results of AST obtained followed the previous studies and indicated a high threat. Therefore, current-day researchers need to use alternative treatment options for microbial resistance. In this regard, an interdisciplinary approach to dealing with the resistance issue is gaining interest in the scientific community. So, our project used methods such as bioinformatics, synthetic chemistry, and microbiology. The emphasis on an interdisciplinary approach, involving bioinformatics for compound selection, synthetic chemistry for compounds synthesis and characterization, and microbiology for their antibacterial actions, ensures a comprehensive investigation. This collaboration

increases the study's depth and validity by highlighting the distinct contributions of each discipline to the overall findings. This research project was focused on using the novel compound "chiral phthalimides" by checking its antibacterial activities under *in silico* and *in vitro* environments against the PBP2a protein of MRSA. This will provide safe preventive and treatment approaches against *S. aureus* infections, contributing to the efficient management of infections and reducing the spread of antimicrobial resistance. The *in silico* part (molecular docking) strengthens the importance of this research project, which was carried out before reporting the *in vitro* activity of chiral phthalimides. The chiral phthalimides were initially docked against the PBP2a protein of MRSA to report their *in silico* antibacterial activity. For this purpose, online computational databases such as NCBI and PubChem were used for retrieving the sequences of the target protein and the compounds, respectively. Once the active sites of PBP2a protein were determined using CASTp, docking of all the three chiral phthalimides was performed using PatchDock. Results generated through molecular docking reported that these compounds gave the best results by interacting with the active site of PBP2a through hydrogen bonds. Compound 1 (FIA) interacted with the amino acid ARG-151, compound 2 (FIB) interacted with the amino acid THR 216, and compound 3 (FIC) interacted with the amino acid THR 216 within the active site of PBP2a through hydrogen bonds. FIB also interacted with PBP2a through a 2nd hydrogen bond (LYS 218) which resides outside the active pocket of the target protein. A similar molecular coupling study was conducted in 2019 in the active pocket of the PBP2a protein of MRSA with the monomeric units of "Eudragit E-100 chloride" (EuCl) and "the sodium salt of poly(maleic acid-alt-octadecene)" (PAM18Na) polymers in both neutral and ionized forms as well as with antibiotic ampicillin. Results suggested that the monomeric forms of both the EuCl and PAM18Na polymers, as well as ampicillin antibiotic, showed interactions of different types and intensities [i.e., hydrophobic interactions (HIs), hydrogen bonds (HBs), and electrostatic interactions (EIs)] with the amino acids in the active site of PBP2a which, in turn, suggested antibacterial activities against the resistant strains of *S. aureus* (Liscano et al., 2021). Another docking study was conducted in 2016 for the synergistic effects of metronidazole–triazole hybrids with oxacillin against PBP2a of MRSA. The results of the docking studies and docking confirmations for these MTZ–triazole hybrids gave the best scores in the active pocket of PBP2a by interaction through hydrogen bonds as well as π–π interactions in the predicted binding pockets (Negi et al., 2016).

After getting the results for molecular docking, the *in vitro* antibacterial activity of the selected chiral phthalimides was checked against MRSA using standard protocols. Different zones of inhibition were obtained for FIA, FIB, and FIC, indicating positive outcomes for their antibacterial activity. A related study carried out in Egypt by Lamie et al. has reported the antibacterial and antifungal activities of the novel phthalimide derivative against the fungus (*C. albicans*), as well as Gram-positive and Gram-negative bacteria, i.e., *Bacillus subtilis* and *P. aeruginosa*, respectively, by performing the agar-well diffusion assay. Similarly, those compounds were characterized to be non-cytotoxic after completing the cytotoxicity assay in cancer and normal human cell lines (Lamie et al., 2015). From this study, it may be assumed that our synthesized chiral phthalimides (FIA, FIB, and FIC) may be non-toxic in normal therapeutic concentration ranges. Still, the cytotoxicity of these chiral phthalimides is recommended for further confirmation.

To further evaluate the antibacterial activity of these compounds, we performed the micro-broth dilution method (96-well plate method) and visual plate assay to identify the minimum inhibitory and minimum bactericidal concentrations of these chiral phthalimides. All the compounds showed excellent anti-MRSA activities, with FIB being the strongest anti-staphylococcal agent having an MIC of 0.022 ug (probably because of the structural differences in FIB and two covalent bonds formed with the PBP2a of MRSA in contrast to only one covalent bond in case of FIA and FIC) compared to FIA and FIC, which have MICs of 0.73 ug and 93 ug/mL of DMSO, respectively. In our study, the MIC and MBC values obtained for these chiral phthalimides were the same, meaning our compounds were bactericidal at the lowest concentration. This strengthens our research because bactericidal compounds are usually preferred over bacteriostatic compounds due to the complete elimination of the pathogenic agent from a particular site rather than just inhibiting its growth. A related study conducted in Bangladesh by Nayab et al. (2015) reported the antibacterial, antioxidant, and DNA-binding activities of the novel phthalimide derivatives, where significant antibacterial activity was shown by the novel N-substituted phthalimides against *E. coli* and *S. mutans*. Similarly, the chiral phthalimides used in our project along with some additional derivatives, i.e., FIB and FIC, as well as FIF: 2-(1,3-dioxoisoindolin-2yl)-3 mercaptopropionic acid, FIH: 2-(1,3-dioxoisoindolin-2yl)-3 (4-hydroxyphenyl prophanic acid, and FII: 3-(1,3-dioxoisoindolin-2yl) prophanic acid, have been reported to have good antibacterial activities against the MDR hypervirulent strain of *Klebsiella pneumonia* (hvKp) when the agar-well diffusion method and micro-broth dilution assay were performed in a similar study conducted at IPDM, Khyber Medical University. Similarly, these chiral phthalimides were reported to have no cytotoxic effects (non-cytotoxic) when their cytotoxicity assay was performed against human red blood cells (RBCs) (Khan et al., 2022).

As the results obtained during our research project align with the findings of similar studies conducted in the past, it confirms that, yes, the chiral phthalimides used against MRSA possess good antibacterial activities and could be a possible treatment option for the drug-resistant staphylococcal infections in future. Moreover, to our understanding, this is a novel study because no such studies have been explicitly conducted against *S. aureus* previously. These findings provide useful insights within the defined area of the investigation, despite the fact that the current study has a limited sample size of ten MRSA due to resource limitations. The findings of this study add to the existing body of information and have the potential to serve as a basis for additional research.

In conclusion, the chiral phthalimides exhibited antibacterial activities against multidrug-resistant MRSA and have the potential to be considered as alternative chemotherapeutics to treat the infections caused by MRSA after the confirmation of their cytotoxic and pharmacokinetic studies. The observed activities highlight their importance in the fight against antibiotic-resistant strains. Recognizing the need for a comprehensive assessment, future research will concentrate on cytotoxicity and pharmacokinetics. Confirming these aspects will help us better understand the safety and efficacy profiles of chiral phthalimides, positioning them as

potential candidates for treating MRSA infections. This study lays the groundwork for further investigation into the full therapeutic potential of these compounds, providing a potential solution to the problems caused by MRSA infections.

Data availability statement

The datasets presented in this study can be found in online repositories. The names of the repository/repositories and accession number(s) can be found in the article/Supplementary Material.

Author contributions

AK: writing–review and editing, conceptualization, investigation, and writing–original draft. MK: conceptualization, writing–original draft, resources, supervision, and writing–review and editing. SK: writing–review and editing, investigation, software, and validation. NS: investigation, software, methodology, and writing–original draft. RA: investigation, methodology, formal analysis, and writing–original draft. SZ: formal analysis, software, validation, and writing–review and editing. SR: formal analysis, software, validation, writing–review and editing, and methodology. MA: validation and writing–review and editing, Resources.

Funding

The authors declare that no financial support was received for the research, authorship, and/or publication of this article.

Acknowledgments

The authors thank the Department of Microbiology, Hayatabad Medical Complex (HMC), Peshawar, for providing the MRSA samples and the Department of Pathology and Diagnostic Medicine (IPDM), Khyber Medical University, Peshawar, for supporting and facilitating this research project.

Conflict of interest

The authors declare that the research was conducted in the absence of any commercial or financial relationships that could be construed as a potential conflict of interest.

Publisher's note

All claims expressed in this article are solely those of the authors and do not necessarily represent those of their affiliated organizations, or those of the publisher, the editors, and the reviewers. Any product that may be evaluated in this article, or claim that may be made by its manufacturer, is not guaranteed or endorsed by the publisher.

Supplementary material

The Supplementary Material for this article can be found online at: https://www.frontiersin.org/articles/10.3389/fphar.2024.1293458/full#supplementary-material

References

Aslam, B., Wang, W., Arshad, M. I., Khurshid, M., Muzammil, S., Rasool, M. H., et al. (2018). Antibiotic resistance: a rundown of a global crisis. *Infect. drug Resist.* 11, 1645–1658. doi:10.2147/IDR.S173867

Batool, M., Ahmad, B., and Choi, S. (2019). A structure-based drug discovery paradigm. *Int. J. Mol. Sci.* 20, 2783. doi:10.3390/ijms20112783

Bien, J., Sokolova, O., and Bozko, P. (2011). Characterization of virulence factors of *Staphylococcus aureus*: novel function of known virulence factors that are implicated in activation of airway epithelial proinflammatory response. *J. pathogens* 2011, 601905. doi:10.4061/2011/601905

Binkowski, T. A., Naghibzadeh, S., and Liang, J. (2003). CASTp: computed atlas of surface topography of proteins. *Nucleic acids Res.* 31, 3352–3355. doi:10.1093/nar/gkg512

Cheung, G. Y., Bae, J. S., and Otto, M. (2021). Pathogenicity and virulence of *Staphylococcus aureus*. *Virulence* 12, 547–569. doi:10.1080/21505594.2021.1878688

Craft, K. M., Nguyen, J. M., Berg, L. J., and Townsend, S. D. (2019). Methicillin-resistant *Staphylococcus aureus* (MRSA): antibiotic-resistance and the biofilm phenotype. *MedChemComm* 10, 1231–1241. doi:10.1039/c9md00044e

Duhovny, D., Nussinov, R., and Wolfson, H. J. (2022). "Efficient unbound docking of rigid molecules," in Algorithms in Bioinformatics: Second International Workshop, WABI 2002, Rome, Italy, September 17-21, 2002 (Springer), 185–200.

Eisenberg, D., Lüthy, R., and Bowie, J. U. (1997). "VERIFY3D: assessment of protein models with three-dimensional profiles," in *Methods in enzymology* (Amsterdam, Netherlands: Elsevier).

Fergestad, M. E., Stamsås, G. A., Morales Angeles, D., Salehian, Z., Wasteson, Y., and Kjos, M. (2020). Penicillin-binding protein PBP2a provides variable levels of protection toward different β-lactams in *Staphylococcus aureus* RN4220. *Microbiologyopen* 9, e1057. doi:10.1002/mbo3.1057

Fri, J., Njom, H. A., Ateba, C. N., and Ndip, R. N. (2020). Antibiotic resistance and virulence gene characteristics of methicillin-resistant *Staphylococcus aureus* (MRSA) isolated from healthy Edible Marine Fish. *Int. J. Microbiol.* 2020, 9803903. doi:10.1155/2020/9803903

Gurung, A. B., Ali, M. A., Lee, J., Farah, M. A., and Al-Anazi, K. M. (2021). An updated review of computer-aided drug design and its application to COVID-19. *BioMed Res. Int.* 2021, 8853056. doi:10.1155/2021/8853056

Hassoun, A., Linden, P. K., and Friedman, B. (2017). Incidence, prevalence, and management of MRSA bacteremia across patient populations—a review of recent developments in MRSA management and treatment. *Crit. care* 21, 211. doi:10.1186/s13054-017-1801-3

Imran, M., Bisht, A., and Asif, M. (2019). A review on biological and chemical potential of phthalimide and maleimide derivatives. *Acta Sci. Pharma Sci.* 3, 51–67.

Jafari, E., Jahanian-Najafabadi, A., Poorirani, S., Hassanzadeh, F., and Sadeghian-Rizi, S. (2017). Synthesis and evaluation of antimicrobial activity of cyclic imides derived from phthalic and succinic anhydrides. *Res. Pharm. Sci.* 12, 526–534. doi:10.4103/1735-5362.217433

Khan, I. A., Ahmad, S., Ullah, F., Niaz, F., Iqbal, S., Khan, E. A., et al. (2022). Chiral phthalimides demonstrated bactericidal effect against multi drug resistant hyper virulent Klebsiella pneumonia. *Pak. J. Med. Health Sci.* 16, 810–813. doi:10.53350/pjmhs22166810

Kushwaha, N., and Kaushik, D. (2016). Recent advances and future prospects of phthalimide derivatives. *J. Appl. Pharm. Sci.* 6, 159–171. doi:10.7324/japs.2016.60330

Lamie, F., Phillopes, P. N., El-Gendy, O., Rarova, L., and Gruz, J. (2015). Design, synthesis and evaluation of novel phthalimide derivatives as *in vitro* anti-microbial, anti-oxidant and anti-inflammatory agents. *Molecules* 20, 16620–16642. doi:10.3390/molecules200916620

Laskowski, R. A., Rullmann, J. a. C., Macarthur, M. W., Kaptein, R., and Thornton, J. M. (1996). AQUA and PROCHECK-NMR: programs for checking the quality of protein structures solved by NMR. *J. Biomol. NMR* 8, 477–486. doi:10.1007/BF00228148

Liscano, Y., Amú, A., González, A., Oñate-Garzón, J., and Salamanca, C. H. (2021). *In silico* characterization of the interaction between the PBP2a "decoy" protein of resistant *Staphylococcus aureus* and the monomeric units of eudragit E-100 and poly (maleic acid-alt-octadecene) polymers. *Polymers* 13, 2320. doi:10.3390/polym13142320

Liu, J., Chen, D., Peters, B. M., Li, L., Li, B., Xu, Z., et al. (2016). Staphylococcal chromosomal cassettes mec (SCCmec): a mobile genetic element in methicillin-resistant *Staphylococcus aureus*. *Microb. Pathog.* 101, 56–67. doi:10.1016/j.micpath.2016.10.028

Matuszewska, M., Murray, G. G., Harrison, E. M., Holmes, M. A., and Weinert, L. A. (2020). The evolutionary genomics of host specificity in *Staphylococcus aureus*. *Trends Microbiol.* 28, 465–477. doi:10.1016/j.tim.2019.12.007

Miragaia, M. (2018). Factors contributing to the evolution of mecA-mediated β-lactam resistance in staphylococci: update and new insights from whole genome sequencing (WGS). *Front. Microbiol.* 9, 2723. doi:10.3389/fmicb.2018.02723

Morehead, M. S., and Scarbrough, C. (2018). Emergence of global antibiotic resistance. *Prim. care Clin. office Pract.* 45, 467–484. doi:10.1016/j.pop.2018.05.006

Nayab, P. S., Pulaganti, M., Chitta, S. K., and Oves, M., (2015). Synthesis, spectroscopic studies of novel N-substituted phthalimides and evaluation of their antibacterial, antioxidant, DNA binding and molecular docking studies. *Bangladesh J. Pharmacol.* 10, 703–713. doi:10.3329/bjp.v10i3.23637

Negi, B., Kumar, D., Kumbukgolla, W., Jayaweera, S., Ponnan, P., Singh, R., et al. (2016). Anti-methicillin resistant *Staphylococcus aureus* activity, synergism with oxacillin and molecular docking studies of metronidazole-triazole hybrids. *Eur. J. Med. Chem.* 115, 426–437. doi:10.1016/j.ejmech.2016.03.041

Okwu, M. U., Olley, M., Akpoka, A. O., and Izevbuwa, O. E. (2019). Methicillin-resistant *Staphylococcus aureus* (MRSA) and anti-MRSA activities of extracts of some medicinal plants: a brief review. *AIMS Microbiol.* 5, 117–137. doi:10.3934/microbiol.2019.2.117

Othman, I. M., Gad-Elkareem, M. A., El-Naggar, M., Nossier, E. S., and Amr, A. E.-G. E. (2019). Novel phthalimide based analogues: design, synthesis, biological evaluation, and molecular docking studies. *J. enzyme inhibition Med. Chem.* 34, 1259–1270. doi:10.1080/14756366.2019.1637861

Perveen, S., and Orfali, R. (2018). L-proline-catalyzed synthesis of phthalimide derivatives and evaluation of their antioxidant, anti-inflammatory, and lipoxygenase inhibition activities. *J. Chem.* 2018, 1–6. doi:10.1155/2018/5198325

Raffo, A., Gagliardi, L., Fugacci, U., Sagresti, L., Grandinetti, S., Brancato, G., et al. (2022). Chanalyzer: a computational geometry approach for the analysis of protein channel shape and dynamics. *Front. Mol. Biosci.* 9, 933924. doi:10.3389/fmolb.2022.933924

Schöning-Stierand, K., Diedrich, K., Fährrolfes, R., Flachsenberg, F., Meyder, A., Nittinger, E., et al. (2020). Proteins Plus: interactive analysis of protein–ligand binding interfaces. *Nucleic acids Res.* 48, W48–W53. doi:10.1093/nar/gkaa235

Senobar Tahaei, S. A., Stájer, A., Barrak, I., Ostorházi, E., Szabó, D., and Gajdács, M. (2021). Correlation between biofilm-formation and the antibiotic resistant phenotype in *Staphylococcus aureus* isolates: a laboratory-based study in Hungary and a review of the literature. *Infect. drug Resist.* 14, 1155–1168. doi:10.2147/IDR.S303992

Torres, P. H., Sodero, A. C., Jofily, P., and Silva-, F. P., Jr (2019). Key topics in molecular docking for drug design. *Int. J. Mol. Sci.* 20, 4574. doi:10.3390/ijms20184574

Turner, N. A., Sharma-Kuinkel, B. K., Maskarinec, S. A., Eichenberger, E. M., Shah, P. P., Carugati, M., et al. (2019). Methicillin-resistant *Staphylococcus aureus*: an overview of basic and clinical research. *Nat. Rev. Microbiol.* 17, 203–218. doi:10.1038/s41579-018-0147-4

Ullah, A., Qasim, M., Rahman, H., Khan, J., Haroon, M., Muhammad, N., et al. (2016). High frequency of methicillin-resistant *Staphylococcus aureus* in peshawar region of Pakistan. *Springerplus* 5, 600–606. doi:10.1186/s40064-016-2277-3

Vestergaard, M., Frees, D., and Ingmer, H. (2019). Antibiotic resistance and the MRSA problem. *Microbiol. Spectr.* 7, 2–18. doi:10.1128/microbiolspec.GPP3-0057-2018

Wang, D., Zhang, L., Zhou, X., He, Y., Yong, C., Shen, M., et al. (2016). Antimicrobial susceptibility, virulence genes, and randomly amplified polymorphic DNA analysis of *Staphylococcus aureus* recovered from bovine mastitis in Ningxia, China. *J. Dairy Sci.* 99, 9560–9569. doi:10.3168/jds.2016-11625

frontiers | Frontiers in Pharmacology

TYPE Review
PUBLISHED 02 April 2024
DOI 10.3389/fphar.2024.1350391

OPEN ACCESS

EDITED BY
Rizwan Shahid,
Alberta Health Services, Canada

REVIEWED BY
Carlos R. Pungitore,
National Scientific and Technical Research Council (CONICET), Argentina
Viviane de Cássia Oliveira,
University of São Paulo, Brazil

*CORRESPONDENCE
Aref Shariati,
arefshariati0111@gmail.com
Zahra Chegini,
parisa.chegini72@gmail.com

RECEIVED 05 December 2023
ACCEPTED 19 March 2024
PUBLISHED 02 April 2024

CITATION
Shariati A, Noei M, Askarinia M, Khoshbayan A, Farahani A and Chegini Z (2024), Inhibitory effect of natural compounds on quorum sensing system in *Pseudomonas aeruginosa*: a helpful promise for managing biofilm community.
Front. Pharmacol. 15:1350391.
doi: 10.3389/fphar.2024.1350391

Inhibitory effect of natural compounds on quorum sensing system in *Pseudomonas aeruginosa*: a helpful promise for managing biofilm community

Aref Shariati[1]*, Milad Noei[2], Marzieh Askarinia[3], Amin Khoshbayan[4], Abbas Farahani[5] and Zahra Chegini[3]*

[1]Infectious Diseases Research Center (IDRC), Arak University of Medical Sciences, Arak, Iran, [2]Department of Genetics, Faculty of Advanced Science and Technology, Tehran Medical Sciences, Islamic Azad University, Tehran, Iran, [3]Department of Microbiology, School of Medicine, Hamadan University of Medical Sciences, Hamadan, Iran, [4]Department of Microbiology, School of Medicine, Iran University of Medical Sciences, Tehran, Iran, [5]Molecular and Medicine Research Center, Khomein University of Medical Sciences, Khomein, Iran

Pseudomonas aeruginosa biofilm is a community of bacteria that adhere to live or non-living surfaces and are encapsulated by an extracellular polymeric substance. Unlike individual planktonic cells, biofilms possess a notable inherent resistance to sanitizers and antibiotics. Overcoming this resistance is a substantial barrier in the medical and food industries. Hence, while antibiotics are ineffective in eradicating *P. aeruginosa* biofilm, scientists have explored alternate strategies, including the utilization of natural compounds as a novel treatment option. To this end, curcumin, carvacrol, thymol, eugenol, cinnamaldehyde, coumarin, catechin, terpinene-4-ol, linalool, pinene, linoleic acid, saponin, and geraniol are the major natural compounds extensively utilized for the management of the *P. aeruginosa* biofilm community. Noteworthy, the exact interaction of natural compounds and the biofilm of this bacterium is not elucidated yet; however, the interference with the quorum sensing system and the inhibition of autoinducer production in *P. aeruginosa* are the main possible mechanisms. Noteworthy, the use of different drug platforms can overcome some drawbacks of natural compounds, such as insolubility in water, limited oral bioavailability, fast metabolism, and degradation. Additionally, drug platforms can deliver different antibiofilm agents simultaneously, which enhances the antibiofilm potential of natural compounds. This article explores many facets of utilizing natural compounds to inhibit and eradicate *P. aeruginosa* biofilms. It also examines the techniques and protocols employed to enhance the effectiveness of these compounds.

KEYWORDS

natural compounds, *P. aeruginosa*, quorum sensing, biofilm, curcumin

1 Introduction

Most bacteria in nature, including those that cause hospital-acquired illnesses, exist in the form of biofilms, which are communities of microorganisms attached to surfaces (Persat et al., 2015). Biofilm communities are surrounded by a strong matrix consisting of proteins, extracellular DNA, and polysaccharides. This matrix makes them less vulnerable to antimicrobial drugs and the immune system (Walsh et al., 2019a). The concept of bacterial biofilm was initially introduced in 1987. It refers to a population of microorganisms that can attach to surfaces and produce an exopolysaccharide and extracellular matrix (Chegini et al., 2020). Biofilms readily develop on foreign objects introduced into the body, such as intravascular and urinary catheters, prosthetic valves, intrauterine devices, contact lenses, and other foreign objects, as well as on surfaces within the body (Shariati et al., 2022). Biofilms exhibit significantly higher resistance to antibiotics, ranging from 10 to 1,000 times, compared to individual planktonic cells. This enhanced resistance is mostly attributed to the limited ability of antibiotics to penetrate the intricate polysaccharide matrix, known as glycocalyx, present in biofilms (Spoering and Lewis, 2001).

Pseudomonas aeruginosa is a Gram-negative and rod-shaped bacterium with a pronounced tendency to form biofilms. It is also an opportunistic pathogen that exhibits multi-drug resistance (MDR) (Walsh et al., 2019a). Infection with this bacterium results in diseases characterized by a significant death rate in individuals suffering from cystic fibrosis, cancer, severe burns, and immunocompromised patients (Bahramian et al., 2019). This bacterium exhibits the ability to persist on water, various surfaces, and medical devices through the utilization of its potent adhesive elements, including flagella, pili, and biofilms. *P. aeruginosa* is highly prevalent in both natural and man-made settings, including lakes, hospitals, and domestic sink drains (Remold et al., 2011). The rising prevalence of this bacteria in generating diverse diseases and its contribution to the rise of antibiotic resistance has led to a significant global issue of treatment failure. *P. aeruginosa* exhibits substantial inherent resistance to many antibiotics, such as beta-lactams, fluoroquinolones, and aminoglycosides, leading to notable rates of morbidity and mortality (Breidenstein et al., 2011).

Therefore, the presence of biofilms and the intrinsic and acquired antibiotic resistance mechanisms of *P. aeruginosa* have led to a rise in the occurrence of MDR strains in recent years, with very few medications that are completely effective in halting the growth of this bacterium. Moreover, numerous antibacterial medications are now linked to constraints such as heightened resistance, limited antibacterial range, toxicity, and elevated treatment expenses for patients (Lone and Ahmad, 2020). To this end, scientists are seeking novel methods to impede the growth of *P. aeruginosa* biofilms (Lou et al., 2015). The utilization of natural compounds as novel and efficacious medicines has acquired a prominent position in clinical therapies (Al-khazraji et al., 2022; Alarkwazi et al., 2022; Hossain et al., 2022; Salman, 2022). Research has demonstrated that plant-derived substances, such as essential oils (EOs), extracts, and pure chemicals, have notable impacts on bacteria that are resistant to treatment and capable of producing biofilms (Ahmad et al., 2015).

The natural compounds derived from various plant components, including roots, leaves, and fruits, provide therapeutic attributes that exhibit distinct medicinal effects upon modification (Rangel et al., 2018). Plant extracts have been examined for their inherent antioxidant, antibacterial, anti-inflammatory, and antiseptic properties, as well as their role as precursors in the production of medicinal compounds (Radulović et al., 2013). In this regard, this review article will examine various aspects of the interaction between natural compounds with the quorum sensing (QS) system and the biofilm community of *P. aeruginosa*. Additionally, it will explore different drug delivery platforms that can enhance the therapeutic effectiveness of natural compounds and promote their extensive utilization in clinical practice.

2 Quorum sensing in *P. aeruginosa*

QS is a bacterial communication system that is dependent on cell density. It allows *P. aeruginosa* to coordinate with different determinants of virulence factors, which helps the bacteria colonize the host and develop resistance to antibiotics. QS is a system that operates on the principle of signal-response. In this system, the levels of secreted signal molecules, known as autoinducers (AIs), rise as the population density increases. These AIs are then recognized by transcriptional regulators that control specific genes (Davies et al., 1998). *P. aeruginosa* mainly possesses two QS systems: *lasI*/*lasR* and *rhlI*/*rhlR*. In these systems, *lasI* and *rhlI* (signal synthase genes) synthesize AIs like N-(3-oxododecanoyl)- L-homoserine lactone (OdDHL) and N-butyryl-L-Homoserine lactone (BHL), respectively. These AIs are then specifically recognized by intracellular receptors, LasR and RhlR. *P. aeruginosa* possesses an additional QS system known as *Pqs*, which specifically detects the *Pseudomonas* quinolone signal (PQS, 2-heptyl-3-hydroxy-4(1H)-quinolone). This system interacts with the transcriptional regulator PqsR (MvfR). Upon stimulation by their endogenous signals, these receptors will form homodimers and function as transcription factors to control the expression of the specified gene(s). Under normal circumstances, the *las* system is commonly considered the primary controller of the QS systems in *P. aeruginosa* and triggers the activation of both the *Rhl* and *Pqs* circuits (Lee and Zhang, 2015).

The DNA-binding transcription regulator LasR activates the production of the *rhl* and *pqs*, QS circuits, as well as virulence factors including *lasA* (staphylolytic), *lasB* (elastase), *toxA* (exotoxin A), *aprA* (alkaline protease), and *hcnABC* (hydrogen cyanide synthase). Therefore, under normal circumstances, the *las* system has traditionally been considered the primary controller of the QS systems *in P. aeruginosa*. Within this bacterium, the second QS pathway, known as the Rhl system, triggers the activation of the *rhlI* gene (responsible for signal synthesis), resulting in the production of BHL, which is recognized by the RhlR receptor. The BHL-RhlR complex serves as the transcriptional activator for various genes, including rpoS (a sigma factor associated with stationary phase), pqs, rhlAB (genes involved in rhamnolipid synthesis), lecA (a type I lectin), and lecB (a type II lectin) (Kim et al., 2015; Rathinam et al., 2017).

P. aeruginosa employs N-acyl homoserine lactone (AHL) and non-AHL-mediated cell density-dependent complicated QS

signaling to control its virulence. To achieve this objective, AHL-driven QS consists of two hierarchical subsystems known as LasI/R and RhlI/R (Gambello and Iglewski, 1991; Pearson et al., 1995). The LasI/R and RhlI/R systems employ 3-oxo-C12-HSL and C4-HSL, respectively, to control the expression of approximately 10% of the genes in the *P. aeruginosa* genome. These genes control important virulence factors, including elastase, protease, hydrogen cyanide, pyocyanin, lipase, pyoverdin, rhamnolipid, swarming, and biofilm formation (Schuster et al., 2003; Wagner et al., 2003). Furthermore, *P. aeruginosa* employs two intercellular signal molecules, namely, 2-heptyl-3-hydroxy-4-quinolone (PQS) and 2-(2-hydroxyphenyl)-thiazole-4-carbaldehyde (IQS), which are not AHL-based, to control its fundamental pathogenicity (Tang et al., 1996; Pesci et al., 1999; Smith and Iglewski, 2003; Lee et al., 2013; Sethupathy et al., 2016).

Therefore, as mentioned, given the substantial role of the QS mechanism in microbial pathogenicity, inhibiting QS serves as an alternate strategy for managing nosocomial infections associated with biofilms. Anti-QS drugs, both synthetic and natural, have demonstrated efficacy in combating *P. aeruginosa* infections by reducing the thickness of biofilms and diminishing pathogenicity (Kumar et al., 2009). It is noteworthy to mention that QS suppression primarily happens through two methods: signal degradation and signal mimicking. These mechanisms lead to the inhibition of genetic control systems and the disruption of downstream virulence and biofilm genes (Ni et al., 2009; Rathinam et al., 2017). QS/biofilm inhibitors have been observed to impose limited or no selection pressure on infections to develop resistance. This is because they specifically target the production of virulence factors and the creation of biofilms without significantly affecting the growth of the pathogens. Therefore, it is crucial to identify and assess novel non-toxic substances that can effectively combat biofilm infections by inhibiting bacterial communication and biofilm formation. Various natural compounds have a considerable impact on different aspects of QS in *P. aeruginosa*. In the following part, we will explore the interactions between natural compounds and the QS system in this bacterium.

3 Curcumin

Curcumin is a curcuminoid compound that is present in *Curcuma longa*, a medicinal plant from the ginger family. Curcumin is widely regarded as a remarkable phytochemical due to its anti-Alzheimer, anticancer, apoptotic, anti-inflammatory, and antioxidant activities. In addition, curcumin is renowned for its antibacterial and antifungal characteristics, making it a popular ingredient in traditional medicine in India, China, and other Southeast-Asian nations. Numerous reports indicated that this remarkable phytochemical can also function as QS inhibitors, as demonstrated in studies with *Candida albicans* and *Aeromonas hydrophila* (Neyestani et al., 2019; Tanhay Mangoudehi et al., 2020). To this end, scientists are interested in employing this compound for degrading *P. aeruginosa* biofilm.

Sethupathy et al. (2016) found that curcumin reduces the activity of QS and the production of biofilms by disrupting the balance of iron levels and the response to oxidative stress in *P. aeruginosa*. This study found that curcumin modulates proteins responsible for the detoxification of reactive oxygen species (ROS), iron uptake, the tricarboxylic acid cycle, and the synthesis of pyoverdin and pyocyanin. Consequently, the authors propose that curcumin regulates the response to oxidative stress and the acquisition of iron in *P. aeruginosa* PAO1 strain by reducing the activity of antioxidant enzymes such as catalase, superoxide dismutases (SOD), peroxidase, ferroxidase, etc. This inhibition leads to the prevention of biofilm formation and the controlled production of protease, elastase, and pyocyanin through QS. Another study has identified curcumin as a QS-antagonist, which can effectively inhibit the generation of extracellular polymeric substances (EPS), biofilm, pyocyanin, and rhamnolipid, along with improving the susceptibility to antibiotics (Shukla et al., 2021). Therefore, the inhibition of QS by curcumin could inhibit the virulence factor and biofilm formation of *P. aeruginosa*.

To this end, the inhibitory effect of curcumin on QS and inhibition of the *P. aeruginosa* biofilm community were reported in other studies (Rudrappa and Bais, 2008; Packiavathy et al., 2014; Bali et al., 2019; Shukla et al., 2020; Fernandes et al., 2023). For instance, a recently published study reported that curcumin has inhibitory effects on the LuxS/AI-2 and LasI/LasR QS systems, resulting in a reduction of 33%–77% and 21%, respectively. Significantly, curcumin (at a concentration of 200 μg/mL) resulted in a 21% decrease in the generation of 3-oxo-C12-HSL by *P. aeruginosa* PA14 strain (Fernandes et al., 2023). Additionally, Rudrappa and Bais (2008) found that curcumin decreased the overall production of AHLs in PAO1 bacteria, and its supplementation resulted in a decrease in bacterial pathogenicity. Similarly, the introduction of external AHL along with curcumin reversed the harmful effects of the bacteria, resulting in the restoration of greater levels of bacterial populations. These observations suggest that curcumin may affect the QS responses in PAO1 by inhibiting the synthesis of AHL or preventing the reception of QS signals.

Noteworthy, curcumin exhibits a significant structural resemblance to AHLs. Curcumin has aromatic ring structures that consist of phenols and are linked by two α, β-unsaturated carbonyl groups. The phenolic component of curcumin imitates the lactone component of AHL. The ketone moiety present in curcumin is structurally identical to the one observed in AHLs (Packiavathy et al., 2012; Packiavathy et al., 2014). To this end, the results of an *in silico* investigation showed that curcumin can form bonds with both LasR and LuxR through distinct combinations of hydrogen bonding and hydrophobic interactions. These interactions can result in the deactivation of both proteins, enabling this plant-derived organic AHL antagonist to be categorized as a QS inhibitor (Shukla et al., 2020). In line with these results, another *in silico* study also found that the LasR protein has the highest binding affinities for curcumin (Bajire et al., 2023).

Therefore, it could be concluded that the spontaneous interaction between curcumin and AHL receptors can modify their structure, preventing them from activating a group of genes that are responsible for curcumin's role as an inhibitor of QS (Shukla et al., 2021). Recently published study showed that the process of forming biofilms in various species is controlled by QS regulation. As previously stated, curcumin hindered the development of biofilm by disrupting the signal molecule-dependent QS mechanism. Considering the prevalence of signal-mediated QS systems, it has

TABLE 1 The interaction of different natural compounds with *Pseudomonas aeruginosa* biofilm.

Publication year (Reference)	Natural compound	Natural compound origin	Outcome
Bose et al. (2020a)	Terpinen-4-ol	Sigma-Aldrich	Inhibition of QS and downregulated QS genes
Noumi et al. (2018)	Terpinen-4-ol	The tea tree oil	Inhibition of swarming motility
Wira Septama et al. (2023)	Terpinen-4-ol, sabinene, γ-terpinene	*Zingiber cassumunar* EOs	Significant inhibition of biofilm formation and QS system, as well as the reduction in the levels of pyocyanin, pyoverdin, and proteolytic activity
He et al. (2022)	Linalool	Linalool emulsion	The disruption of the cellular membrane structure leads to the release of intracellular substances and effectively eliminates biofilms
Pejčić et al. (2020)	Linalool, anethole α-thujone and camphor	Basil (*Ocimum basilicum*) and sage (*Salvia officinalis*)	Suppression of the growth of biofilms and decrease in the generation of pyocyanin. Both oils had a significant impact on the motility patterns of swimming, swarming, and twitching
Kačániová and Vukovic (2023)	(E)-caryophyllene	*Salvia sclarea* EO	Inhibition of biofilm formation on plastic surfaces and stainless steel
Ghannay et al. (2022b)	Cuminaldehyde, _-pinene terpinene, and p-cymene	*Cuminum cyminum* L. EO	Inhibition of elastase and protease production and flagellar motility
Kim et al. (2021)	Linoleic acid	Sigma-Aldrich	Linoleic acid shares functional and structural similarities with cis-2-decenoic acid, a diffusible signaling component of *P. aeruginosa*. Consequently, linoleic acid works as an agonist molecule in the dispersal of biofilms
Li et al. (2023)	Geraniol	Shanghai Aladdin Bio-Chem Technology	Suppressed the virulence factors by inhibiting the three QS systems
Shafiei et al. (2017)	Saponin	*Cyclamen coum*	The combination of saponin extract and ciprofloxacin resulted in the breakdown of biofilm through different mechanisms, including the reduction of stress protein production, disturbance of cell envelope integrity, promotion of motility, and perturbation of signal transduction
Chipenzi et al. (2020)	Tormentic acid congener	*Callistemon viminalis*	Detachment of the biofilm and reduction of release of capsular polysaccharides and extracellular DNA from biofilms
Gambino and Maione (2022)	Limonene	Sigma Aldrich	Limonene therapy is highly efficacious in cases where the biofilm has been cultivated under shear stress, resulting in substantial and irreversible harm to the biofilm's structure
Luciardi et al. (2020)	D-limonene	*Citrus paradisi*	Inhibition of biofilm production, sessile viability, autoinducer production, and elastase activity
Ghannay et al. (2022a)	Carvone and limonene	Caraway	Reduced production of virulence-related factors regulated by QS systems in Gram-negative bacteria
Husain et al. (2015a)	Menthol	Peppermint oil	Strong interference with AHL regulation of virulence factors and biofilm formation
Niu and Gilbert (2004)	Cinnamaldehyde, citronellol, and eugenol	Citronellol and cinnamaldehyde were acquired from Sigma Aldrich, while eugenol was procured from Acros Organics	Cinnamaldehyde reduced biofilm formation, citronellol increased the specific biofilm formation, and eugenol did not result in a change
Chakraborty et al. (2020)	Caffeine	NR	Caffeine not only hindered the formation of biofilm but also decreased the secretion of virulence factors by *P. aeruginosa*

(Continued on following page)

TABLE 1 (*Continued*) The interaction of different natural compounds with *Pseudomonas aeruginosa* biofilm.

Publication year (Reference)	Natural compound	Natural compound origin	Outcome
Husain et al. (2015b)	Caffeine	*Trigonella foenum-graecum* L. (Fenugreek)	Caffeine showed anti-QS potential and anti-biofilm properties
Khan et al. (2021)	Caffeine	Caffeine-loaded gold nanoparticles	The synthesized nanoparticles exhibited several properties, including the dispersal of mature biofilms, the ability to prevent biofilm formation, and to kill a variety of Gram-negative bacteria
Rosi-Marshall et al. (2013)	Caffeine	NR	Biofilm respiration was significantly suppressed by diphenhydramine, caffeine, cimetidine, and the combination therapy. These drugs, alone or in combination, affect the biofilms in streams
Norizan et al. (2013)	Caffeine	Sigma Aldrich	Caffeine was able to inhibit the production of N-acyl homoserine lactone and the swarming
Ivanov et al. (2022)	Hesperidin, hesperetin, naringenin, naringin, hesperidin, taxifolin, morin, chlorogenic acid, ferulic acid, p-coumaric acid, gallic acid, and rutin	Sigma Aldrich	Treatment with hesperetin, hesperidin, rutin, and ferulic acid resulted in a substantial decrease in biofilm formation. The therapy with naringin and taxifolin did not cause any substantial changes in biofilm formation. Hesperetin and hesperidin showed significant antibiofilm activity. Naringenin, a flavanone, exhibits greater antibiofilm efficacy in comparison to its glycoside form, naringin
Lou et al. (2015)	Tenacissoside I, chlorogenic acid, caffeic acid, p-coumaric acid, quercetin, ursolic acid, rutin, cynarin, luteolin, crocin, and benzoic acid	The burdock leaf	The primary anti-biofilm chemicals that were identified are P-coumaric acid, quercetin, caffeic acid, ursolic acid, and rutin
Danaraj et al. (2020)	4-hydroxybenzoic acid	*Seagrass Halodule pinifolia* (Miki) Hartog	The concentration of 62.5 μg/mL of 4-methoxybenzoic acid decreased the levels of proteins, lipids, and exopolysaccharides in the biofilm matrix of *P. aeruginosa*
Quatrin et al. (2017)	1-8-Cineol	*Eucalyptus Globulus*	The nanoemulsion did not show any antimicrobial activity against *P. aeruginosa*, as only 5% of the oil was present, which is ineffective against this microorganism
Kouki and Polito (2022)	p-cymene	*Eucalyptus* Species	Inhibition of biofilm ranges between 51.21% and 91.65%
O'May et al. (2012)	Epigallocathecin gallate, tannic acid, gallic acid	Sigma Aldrich	Epigallocatechin gallate and tannic acid demonstrated the ability to impede swarming movement and enhance the development of biofilms; however, gallic acid did not exhibit any impact
Ahmed and Syed (2021)	Gallo-tannin	NR	Suppression of growth and biofilm formation of the MDR *P. aeruginosa*
Taganna et al. (2011)	Tannin	*Terminalia catappa*	Inhibition of biofilm maturation
Maisetta et al. (2019)	Tannin	*Cytinus hypocistis* and *Cytinus ruber*	Cytinus extracts did not affect Gram-negative strains
Lakshmanan et al. (2019)	Tannin	*Cinnamomum tamala* leaves	This compound can affect the production of rhamnolipid and flagellin and downregulate the expression of the fliC and *rhlA* genes
Bose et al. (2020b)	α-terpineol	Sigma Aldrich	Suppressed the QS-mediated virulence factors and the production of biofilm
Chadha et al. (2023)	α-Terpineol	NR	Suppression of the biofilm formation and the synthesis of virulence factors
Kumar Bose et al. (2021)	α-terpineol	Nano-lipoidal α-terpineol	Inhibition of biofilm formation

(Continued on following page)

TABLE 1 (*Continued*) The interaction of different natural compounds with *Pseudomonas aeruginosa* biofilm.

Publication year (Reference)	Natural compound	Natural compound origin	Outcome
Das et al. (2023)	Piperine	NR	Suppression of the formation of biofilm and reduction in the expression of the QS gene (*lasI*)
Pejin et al. (2015)	Phytol	NR	Reduced the biofilm formation, twitching flagella motility, and pyocyanin
Ahmad and Ansari (2022)	Fenchone	NR	Reduced the production of biofilm
Li et al. (2018)	Diallyl disulfide	Garlic oil	Inhibition of virulence factors through inactivation of genes involved in different QS systems
Häkkinen and Soković (2021)	Lactucopicrin and costunolide	*Cichorium intybus L*	Lactucopicrin and costunolide inhibited the development of *P. aeruginosa* IBRS P001 biofilms
Jagani et al. (2009)	Polyphenol, polyanacardic acid, polycardanol, ascorbic acid, catechin, epigallocatechin, tannic acid, tocopherol, anticardia acid, cardanol, salicylic acid, ethyl linoleate, and tocopherol	Sigma Aldrich	A significant reduction in biofilm formation by *P. aeruginosa* was observed with all compounds except tocopherol and ethyl linoleate
Kasthuri et al. (2022)	Carvacrol and nerol	Sigma Aldrich	The effective biofilm disruption potential
Bahari et al. (2017)	Curcumin	NR	The generation of biofilms was significantly reduced. The combination of azithromycin and curcumin at 1.4 MIC had the most potent inhibitory effect on biofilm development
Di Salle and Viscusi (2021)	Curcumin	Sigma Aldrich	Decrease in biofilm formation
Ramesh et al. (2022)	Curcumin	Arjuna Natural Extracts	Decrease in biofilm formation
Targhi et al. (2021)	Curcumin	NR	Curcumin in combination with free and encapsulated nanoparticles significantly reduced biofilm formation in strains compared to free forms of curcumin. The *arr* gene, which plays a role in biofilm formation, was significantly suppressed
Gholami et al. (2020)	Curcumin	Merck (Germany)	The presence of curcumin-metal complexes and free curcumin suppressed biofilm formation by 45%–90%, and this inhibitory effect was dependent on the concentration
Khaleghi et al. (2023)	Curcumin	Acros organic (Geel, Belgium)	Curcumin-loaded hydrogel significantly reduced biofilm formation
Prateeksha et al. (2019)	Curcumin	Sigma–Aldrich	Zinc Oxide–Curcumin nanocomposites at a concentration of 2.5 μg/mL were much more efficient in inhibiting biofilm formation by 84.5% than the Nanoparticles-Curcumin (32%) and nanoparticles-zinc oxide (15%)
Roudashti et al. (2017)	Curcumin	NR	Decrease in biofilm formation
Kart et al. (2021b)	Curcumin	Sigma Chemical	Decrease in biofilm formation
Lu et al. (2022b)	Carvacrol and thymol	Sigma–Aldrich	Eradication of *P. aeruginosa* biofilms
Ramasamy et al. (2017b)	Cinnamaldehyde	NR	Cinnamaldehyde-coated gold nanoparticles inhibited biofilm formation by *P. aeruginosa* ~65%
Ramasamy et al. (2017a)	Cinnamaldehyde	Sigma–Aldrich	The growth of *P. aeruginosa* biofilm and cells was entirely suppressed by cinnamaldehyde-conjugated gold nanoparticles at a concentration of 0.025% v/v. The nanoparticles penetrated the EPS matrix and effectively disrupted biofilms, but neither

(Continued on following page)

TABLE 1 (*Continued*) The interaction of different natural compounds with *Pseudomonas aeruginosa* biofilm.

Publication year (Reference)	Natural compound	Natural compound origin	Outcome
			cinnamaldehyde nor silica-coated gold nanoparticles had any effect
S'Thebe N et al. (2023)	Cinnamaldehyde	NR	Cinnamaldehyde showed a 60% inhibitory effect on biofilm formation
Zhang et al. (2018)	Coumarin	Sigma-Aldrich	Wound model and microtiter plates exhibited a substantial decrease in biofilm production
Qais et al. (2021)	Coumarin	Sigma-Aldrich	Coumarin inhibited the growth of the *P. aeruginosa* PAO1 biofilm
Gutiérrez-Barranquero et al. (2015)	Coumarin	Sigma-Aldrich	Biofilm was significantly reduced in *P. aeruginosa*
Liu and Xiao (2020)	Catechin	Shanghai Hanhong Chemical	The nanocoating consisting of catechin and rare-earth ions exhibited remarkable antibacterial and anti-adhesion properties against *P. aeruginosa*, effectively inhibiting the formation of biofilms on the surface of the material

QS, quorum sensing; AHL, acyl homoserine lactone; NR, not reported; MDR, multi-drug resistant; MIC, minimum inhibitory concentration.

been discovered that disrupting the QS system could potentially hinder the generation of signal-mediated biofilms and the resulting biofilm-related illnesses. Therefore, curcumin can be utilized as an anti-pathogenic substance, specifically targeting *P. aeruginosa*, due to its ability to inhibit QS. Nevertheless, curcumin, like other natural chemicals, has restricted applicability in clinical settings due to several disadvantages, including insolubility in water, limited oral bioavailability, fast metabolism, and degradation, as well as inadequate absorption from the gut and low blood plasma levels (Shariati et al., 2019).

In this regard, researchers have been interested in using nano-curcumin and various drug delivery platforms for enhancing curcumin-antibiofilm efficacy. Notably, the higher solubility and longer half-life of nano-curcumin compared to curcumin and its higher resistance to enzymatic hydrolysis have been reported in recently published studies. Nano-curcumin exhibits more tissue reabsorption and a prolonged half-life compared to curcumin. Consequently, this molecule has been extensively studied for its potential impact on biofilm formation. The bioavailability and solubility of nano-curcumin are superior to those of curcumin. This improved water solubility can be attributed to the greater surface area of nano-curcumin, which facilitates dissolution (Shariati et al., 2019; Sharifian et al., 2020; Rahimi et al., 2023). To this end, different methods, such as the wet-milling technique and the ultrasonic homogenizer sonication method, were used for the production of nano-curcumin, and it was reported that the synthesized nanoparticles could significantly inhibit *P. aeruginosa* biofilm (Shariati et al., 2019; Sharifian et al., 2020; Rahimi et al., 2023). Additionally, the combined usage of nano-curcumin and other antibacterial agents, such as natural compounds and other nanoparticles, also showed a synergistic effect against *P. aeruginosa* biofilm (Loo et al., 2016; Rahimi et al., 2023). Xue et al. (2020) also fabricated nano-curcumin using solution-enhanced dispersion by supercritical CO_2, and the results showed better anti-P. aeruginosa activity than the original curcumin. Therefore, nano-curcumin, in comparison to the original curcumin, not only has an improved dissolution rate and bioavailability, but also has improved antibacterial activity against the *P. aeruginosa* biofilm community.

In addition to nano-curcumin, different drug platforms were also used for the enhancement of the antibiofilm activity of curcumin. In one study that was published in 2021, curcumin was loaded onto a bioactive bone substitute (hydroxyapatite, HA) using a single-step precipitation process. The release of curcumin from HA was limited, indicating the presence of robust hydrogen bonding and van der Waals contacts between curcumin molecules and calcium ions of HA, which impeded the release of curcumin. Although the curcumin release was modest, the curcumin-functionalized HA successfully prevented bacterial cell attachment and the subsequent stages of biofilm generation in *P. aeruginosa*. The findings indicated that the quantity of curcumin released from HA was adequate to hinder the formation of biofilm and regulate the count of viable planktonic cells concurrently (Lee et al., 2021). Furthermore, other studies also used curcumin-based drug platforms for inhibition of *P. aeruginosa* biofilm (Table 1). Nanocarriers and drug platforms enhance the solubility and transportation of curcumin in bacterial suspensions, hence intensifying its antibacterial efficacy. Moreover, the utilization of a drug platform can result in a prolonged and controlled release of curcumin, reducing the required dosage of this chemical and improving its therapeutic efficacy.

It should be noted that when we use a drug platform, in addition to curcumin, other compounds can also be used along with curcumin. For instance, Sadeghi Mohammadi et al. (2022) used gentamicin- and curcumin-loaded lipid-polymer hybrid nanoparticles for inhibition of the *P. aeruginosa* biofilm community. The findings demonstrated that synthesized nanoparticles have excellent antibacterial activity compared to pure curcumin at the same concentration, due to the increased solubility of curcumin with nanoparticles. Additionally, simultaneous usage of curcumin and gentamycin enhanced antibacterial activity. The hybrid nanoparticles exhibit a notable increase in both anti-inflammatory and antibacterial effectiveness

when hydrophilic gentamicin and hydrophobic curcumin are used as the drug molecules for loading. Altogether, stimuli-responsive nano-systems can enhance the delivery of drugs to specific targets with spatial and temporal control. This has the potential to be beneficial for treating biofilm-related infections using topical therapy. Curcumin should be regarded as a potential co-delivery system for dual medicines with both hydrophilic and hydrophobic properties. This approach can boost antibacterial activities and effectively cure chronic and persistent illnesses associated with biofilm formation.

Finally, it is noteworthy to mention that curcumin was used in photodynamic therapy (PDT) for the reduction of bacterial biofilm. PDT is an effective method for combating antibiotic-resistant bacteria without the need for intrusive procedures. PDT utilizes non-toxic dyes and innocuous visible light to generate ROS, which specifically induces the death of microbial cells. Curcumin was employed as a photosensitizer in recently conducted research, targeting both the planktonic and biofilm forms of *P. aeruginosa* (Abdulrahman et al., 2020; Mirzahosseinipour et al., 2020; Zangirolami et al., 2020; Ghasemi et al., 2021; Silva et al., 2023). The use of curcumin, then PDT, reduced the number of viable bacteria (Ghasemi et al., 2021). Noteworthy, curcumin, acting as a photosensitizer, can penetrate the bacterial cell. Subsequently, when exposed to light of a specific wavelength, the photosensitizer molecules become activated and transfer their energy to the nearby molecular oxygen, leading to the production of ROS. ROS can interact with crucial molecular constituents of cells, such as DNA, membrane components, lipids, and proteins, resulting in a retardation of growth and ultimately the demise of the cell (Sánchez-López et al., 2020; Ghasemi et al., 2021). Abdulrahman et al. (2020) also reported that curcumin, when exposed to 405 nm laser light, decreased the synthesis of EPS by *P. aeruginosa* biofilm, therefore inhibiting biofilm formation. Furthermore, following curcumin-mediated PDT, it was observed that the genes associated with QS were downregulated. Additionally, a higher intensity of light resulted in a significant decrease in gene expression. On the other hand, Silva et al. (2023) documented that PDT serves as an antibacterial substitute; however, the arrangement of the biofilm poses challenges for photodynamic penetration. In addition, *P. aeruginosa* is a Gram-negative bacterium that impedes the interactions between the cell wall and molecules. In this particular scenario, the application of sonodynamic therapy utilizing ultrasound waves can mechanically break the biofilm. When combined with curcumin as a sonosensitizer, this process results in the generation of ROS. However, it is important to note that the level of ROS produced is insufficient for complete elimination of the microbes. Therefore, the authors reported that sonophotodynamic inactivation, the combination of photodynamic and sonodynamic, using curcumin could be a much more efficient approach for biofilm inactivation. However, this is a preliminary study, and more confirmatory studies are needed in this field.

Collectively, the recently published studies introduce curcumin as a sensitizer that can function as a photo and sonosensitizer, leading to highly effective inactivation of the *P. aeruginosa* biofilm. Curcumin-induced antimicrobial-PDT effectively hinders the production of biofilms by generating ROS. The regulation of biofilm formation may involve the reduction of the QS system in *P. aeruginosa*, leading to the elimination of EPS. Therefore, curcumin-mediated PDT has the potential to be a viable therapeutic method for controlling *P. aeruginosa* biofilm-induced infections. Further research should be conducted to explore the effectiveness of this treatment in managing biofilm communities of drug-resistant bacteria.

4 Cinnamaldehyde

Cinnamaldehyde, a primary constituent of cinnamomum, accounts for approximately 65% of its composition. Its antimicrobial activity may be attributed to the presence of an acrolein group (α, β-unsaturated carbonyl moiety). Despite its potent impact on pathogen infections, cinnamaldehyde is not susceptible to typical antibiotic resistance mechanisms (Bae et al., 1992). Recently, scientists have become interested in utilizing cinnamomum and its derivative components, particularly cinnamaldehyde, not only for their antibacterial properties but also for their ability to hinder microbial biofilm formation. Cinnamaldehyde effectively eradicated *P. aeruginosa* biofilms after exhibiting its antibacterial action through several routes (Firmino et al., 2018; Ferro et al., 2019; Kosari et al., 2020).

The principal mechanism by which cinnamaldehyde inhibits the formation of *P. aeruginosa* biofilm is through the reduction of QS. Recent reviews indicate that the sub-inhibitory concentration of cinnamaldehyde, without having any bactericidal effect, resulted in the suppression of both the *las* and *rhl* systems by inhibiting the activity of the regulatory proteins LasR and RhlR. This effect not only reduced the production of extracellular virulence agents such as elastase, pyocyanin, and protease but also repressed the expression of the rhamnolipid gene and impeded biofilm formation in *P. aeruginosa* PAO1. This study did not identify the precise mechanism by which cinnamaldehyde inhibits QS; however, the authors put forward the hypothesis that this chemical functions as a QS antagonist (Ahmed et al., 2019).

To this end, the synergistic effect of cinnamaldehyde and conventional antibiotics was investigated to eradicate *P. aeruginosa* biofilm by inhibiting QS. A recent study found that cinnamaldehyde suppressed the expression of *lasB*, *rhlA*, and *pqsA*, indicating its ability to inhibit QS. The concurrent application of cinnamaldehyde and tobramycin demonstrated potent inhibitory effects on QS. In addition, the utilization of combination therapy showed an additional impact of cinnamaldehyde when administered in conjunction with tobramycin and colistin, resulting in the inhibition of PAO1 biofilm growth and the dispersion of preexisting biofilm. This effect was more pronounced compared to the use of each treatment individually (Topa et al., 2020). In line with these findings, *Brackman* et al. used a *P. aeruginosa* mutant incapable of QS (due to a disruption of both *rhlI* and *lasI*, this strain cannot produce AHL signaling molecules). In comparison to the wild type, this mutant exhibited a significantly higher susceptibility to tobramycin, thereby confirming the involvement of a functional QS system in resistance. Furthermore, although cinnamaldehyde caused the wild-type strain to become more vulnerable to tobramycin, this effect was not detected in the QS mutant strain. This suggests that the cinnamaldehyde impact is dependent on the presence of a functional QS system. Therefore, these data indicate that the combination of tobramycin and cinnamaldehyde could

enhance the effectiveness of a treatment by improving the ability of tobramycin to combat infections caused by biofilms (Brackman et al., 2011).

Additionally, the combination of cinnamaldehyde and gentamycin demonstrated a synergistic effect and showed potential action against QS. This combination therapy demonstrated the ability to inhibit the generation of AHL and reduce the expression of important QS genes in *P. aeruginosa* PAO1. The molecular docking analysis demonstrated robust binding interactions between the QS receptors and cinnamaldehyde, confirming its significant potential as a QS modulator. This dual treatment effectively eliminated pre-existing biofilms and suppressed the creation of new biofilms by disrupting the production of EPS (Chadha et al., 2022). Noteworthy, the authors suggested that the synergistic interaction between the drugs can be related to their unique mechanisms of action. Cinnamaldehyde causes membrane rupture and oxidative damage, while gentamycin inhibits bacterial protein production. This renders the bacterial cell more vulnerable as the medications can simultaneously target two separate cellular areas. In addition, cinnamaldehyde efficiently inhibits the QS circuits in *P. aeruginosa* by reducing the expression of QS genes and preventing the production of AHL molecules (Shaw and Wuest, 2020; Chadha et al., 2022). The mentioned function of cinnamaldehyde was attributed to its potent interaction with the QS receptors of *P. aeruginosa*. As a result, this reduces the activity of the virulence factors and the creation of biofilms associated with the QS system, consequently decreases the pathogenesis of the bacterium. Furthermore, the addition of gentamycin increases the effectiveness of inhibiting QS and enhances the ability of cinnamaldehyde to reduce virulence (Chadha et al., 2022).

In another study, Kart et al. (2021a) reported that the combined use of cinnamaldehyde and ciprofloxacin demonstrated a greater decrease in the minimum biofilm eradication concentration compared to the use of ciprofloxacin alone. The scientists found that cinnamaldehyde hindered the process of QS and the creation of alginate. As a result, it prevented the formation of biofilms by PAO1 and enhanced the effectiveness of ciprofloxacin in combating biofilms. As a result of these findings, there is a possibility that cinnamaldehyde could enhance the effectiveness of antibiotic treatment in combination therapy by reducing QS and thereby increasing the vulnerability of bacterial biofilms to antibiotics. Nevertheless, this hypothesis has not been experimentally verified. Collectively, cinnamaldehyde is a powerful phytochemical that has been shown to effectively combat the virulence of *P. aeruginosa*. It has the potential to be used alongside conventional antibiotics to develop new intervention methods. However, further comprehensive investigations are necessary to assess its therapeutic effectiveness using *in vivo* models in order to utilize its potential for combating virulent infections in future clinical applications.

Furthermore, a recent study has revealed that cinnamaldehyde not only inhibits QS but also inhibits the activity of Cyclic di-guanosine monophosphate (c-di-GMP) (Topa et al., 2018). C-di-GMP is recognized as a crucial intracellular signal and secondary messenger that regulates virulence, cell cycle progression, movement, and various other activities, including the life cycle of biofilms in multiple bacterial species (Ryan et al., 2006). To this end, Topa et al. (2018) reported that cinnamaldehyde decreased c-di-GMP expression by 66.2% after 5 h in comparison to the untreated control. To this end, cinnamaldehyde interfered with the transmembrane potential, pre-existing biofilms, and swarming motility of PAO1. The authors proposed that the carbon atoms of cinnamaldehyde could potentially form bonds with nitrogen-containing components, such as proteins, in the cytoplasmic membrane. This interaction could lead to changes in the structure of the proteins and result in a loss of membrane integrity. Nevertheless, there is a scarcity of information regarding the connection between cinnamaldehyde and intracellular c-di-GMP levels. Consequently, the precise chemical mechanism via which cinnamaldehyde influences variations in c-di-GMP levels is still unknown. Therefore, although the specific mechanism by which cinnamaldehyde counteracts the QS system is not yet understood, it seems to function as both a QS and c-di-GMP antagonist. Cinnamaldehyde not only eradicates *P. aeruginosa* biofilm but also eliminates the bacterium's virulence factors via blocking QS-related factors and c-di-GMP. This occurrence would enhance the effectiveness of the host's innate immunity and other antibiofilm agents. The administration of cinnamaldehyde to boost antibiofilm agents has promising potential for future research. However, there is limited understanding of the molecular-level effects of such synergy. Therefore, further investigation is necessary to validate the aforementioned discoveries.

5 Carvacrol

Carvacrol, a phenolic monoterpenoid, is a prominent component found in EOs derived from fragrant herbs like pepperwort (*Lepidium flavum*), oregano (*Origanum vulgare*), and thyme (*Thymus vulgaris*). Carvacrol is utilized as a food preservative, additive, and flavoring, as well as a fragrance in cosmetic items. Carvacrol has been found to exhibit several biological properties, such as antioxidant, anticancer, and antibacterial activity, according to recent studies (Sharifi-Rad et al., 2018; Javed et al., 2021). Carvacrol has been demonstrated to disrupt the cytoplasmic membrane by enhancing its fluidity, resulting in the release of ions, a reduction in the pH gradient across the membrane, and the suppression of Adenosine triphosphate (ATP) synthesis in bacteria (Ultee et al., 2002; Sharifi-Rad et al., 2018). Additionally, the results of recently published studies demonstrated that carvacrol could significantly inhibit the biofilm community of *P. aeruginosa* (Ceylan and Ugur, 2015; Walsh et al., 2019b; Pazarci et al., 2019; Tapia-Rodriguez et al., 2019; Walczak et al., 2021). For instance, the findings of a study indicated that carvacrol inhibited the formation of biofilms by up to 74%–88% for *P. aeruginosa* and decreased the enzyme activity of the biofilm by up to 40%–100% (Walczak et al., 2021). A biofilm eradication assay in another study also showed the potential of carvacrol for inhibition of *Staphylococcus epidermidis* and *P. aeruginosa* (Walsh et al., 2019b). In addition, *Pazarci* et al. identified carvacrol as the primary constituent of *Mentha longifolia* EO. This EO showed efficacy against *P. aeruginosa* and fungal biofilms that develop on the surface of steel and titanium implants. Hence, the authors suggested that the use of *M. longifolia* EO could be advantageous in treating infections associated with implant biofilms (Pazarci et al., 2019).

Noteworthy, the precise mechanism of how carvacrol interacts with bacterial biofilm has not been fully understood. However, a docking analysis conducted in a study revealed that this molecule does interact with the QS system in bacteria. The study revealed that when exposed to carvacrol, *P. aeruginosa* exhibited a 60% decrease in the production of AHLs. Importantly, this reduction in AHLs did not have any impact on the viability of the cells, suggesting a decrease in the activity of the LasI synthase enzyme. Carvacrol decreased the expression of the *lasR* gene while leaving the lasI gene unaffected. Furthermore, computational docking analysis revealed that carvacrol interacts with certain amino acids located in the active site pocket of LasI and within the binding pocket of LasR. Carvacrol action led to a decrease in AHLs, perhaps impacting LasI activity, resulting in the suppression of the sequence of signals, pathways, and virulence-related gene expression in *P. aeruginosa* (Tapia-Rodriguez et al., 2019). Therefore, the aforementioned research offers pertinent data regarding the impact of carvacrol on *P. aeruginosa* biofilm by disrupting the QS system. These discoveries can aid in the advancement of natural anti-QS compounds, which can impact the biofilm community and pathogenicity of *P. aeruginosa*.

Noteworthy, researchers also explored the synergistic effects of carvacrol in combination with other antibacterial agents for the management of *P. aeruginosa* biofilm. A study published in 2023 investigated the effectiveness of two proteolytic enzymes, pepsin and trypsin, in breaking down *P. aeruginosa* biofilms. The study also explored the combination of these enzymes with carvacrol. Pepsin and trypsin, both mammalian digestive enzymes, rely on certain amino acids in the polypeptide chain to break down proteins through hydrolysis. The *P. aeruginosa* biofilm population experienced a greater reduction when treated with a combination of pepsin or trypsin along with carvacrol compared to treatment with carvacrol alone. The reduction of biofilms was much greater when sequential enzyme treatments were followed by carvacrol treatment, as opposed to employing a single enzyme followed by carvacrol. The enhanced efficiency is also apparent in the analysis of epifluorescence microscopy. It was observed that the combined treatment involving enzymes, either individually or in sequence, followed by carvacrol, demonstrated a synergistic effect. This effect resulted from the enzymes' ability to disperse biofilms and carvacrol antimicrobial activity. As a result, the biofilms exhibited a greater reduction in terms of both biomass and viability (Mechmechani et al., 2023). It is important to mention that these two enzymes, by potentially interacting with proteins, such as outer membrane proteins in *P. aeruginosa*, can lead to structural defects in the biofilms and weaken their protective properties. This interaction may enhance the entry of carvacrol and decrease the ability of the cells to survive. Therefore, the aforementioned discoveries indicate that proteins can serve as viable targets for elimination, enabling the successful infiltration of antibiofilm agents like carvacrol to deactivate *P. aeruginosa* cells within the biofilm (Mechmechani et al., 2023).

Gobin et al. (2022) also reported that the combination of gallic acid and carvacrol exhibits a potent and synergistic effect in eliminating both mono- and dual-species mature biofilms of *Staphylococcus aureus* and *P. aeruginosa*. The antibiofilm efficacy of gallic acid may be attributed to alterations in the characteristics of the plasma membrane. Indeed, besides modifying bacterial adhesion, these alterations can result in the release of intracellular constituents. Evidence has demonstrated that gallic acid stimulates the outward flow of potassium ions (K^+) from *P. aeruginosa*. The release of intracellular components, such as ions, can ultimately lead to cell death through various mechanisms, including changes in gene expression, disruption of cellular ion balance, and interference with cell signaling. Moreover, gallic acid possesses the ability to form complexes with Ca^{2+} and Fe^{2+}, two crucial metals required for bacterial growth and certain enzyme functions (Borges et al., 2013; Sarjit et al., 2015; Gobin et al., 2022). Therefore, gallic acid has the potential to modify the activity of membrane proteins and bacterial iron uptake mechanisms, such as siderophore. Gallic acid possesses an anti-adherence property that can disrupt biofilm, enhancing the diffusion and effectiveness of carvacrol, which in turn permeabilize the bacterial membrane and causes bacterial demise. Hence, the amalgamation of these molecules not only produces an additive effect but also enhances the activity of active molecules, resulting in the synergistic eradication properties of the combination (Gobin et al., 2022).

Another investigation also revealed that the concurrent use of carvacrol and nerol can effectively dismantle the preexisting biofilm structure and enhance the elimination of bacteria after subsequent water rinsing. Nerol is an acyclic monoterpenoid that is the cis-isomer of geraniol. It possesses a main alcohol functional group and has a more pleasant rose odor compared to geraniol (Kasthuri et al., 2022). The exceptional chemical composition of carvacrol and nerol is responsible for their extensive antibacterial efficacy across a wide range of bacteria. Carvacrol has a secondary alcohol known as phenolic alcohol, which is a–OH functional group in the benzene ring. Acyclic monoterpenoid nerol contains the functional group–OH at an acyclic ring structure called primary alcohol (Elsharif and Buettner, 2018). To this end, efficient broad-spectrum antibacterial action is achieved by combining the bactericidal effect of both carvacrol and nerol, which are monocyclic phenols and acyclic primary alcohols, respectively. Furthermore, there is speculation that the combined action of carvacrol and nerol, namely, their–OH groups, effectively depolarizes the cell membrane by dissipating pH and protons (H^+ and K^+) gradients across it (Kasthuri et al., 2022). Thus, as mentioned, the combined treatment using carvacrol and other antibacterial treatments, including natural products and enzymes, shows potential as a viable strategy for eliminating *P. aeruginosa* biofilm infections. Implementing carvacrol-based combination therapy would additionally decrease the use of chemical agents, energy expenditures, and water usage required for biofilm management.

Finally, it is noteworthy to mention that different drug platforms and techniques were used for the enhancement of carvacrol activity against bacterial biofilm. Mechmechani et al. (2022b) used the spray drying method, one of the most common microencapsulation techniques, to develop microcapsules containing carvacrol.

The results showed that the minimum inhibitory concentration (MIC) of carvacrol against *P. aeruginosa*, when encapsulated, was four times lower compared to carvacrol in its free form. Additionally, encapsulated carvacrol was able to reduce biofilm below the detection limit for this bacterium after 15 min of treatment (Mechmechani et al., 2022b). In line with these results, in another study, spray drying method was also used to produce

novel microencapsulated (ME) proteases, pepsin and trypsin, and carvacrol. The findings of this study revealed that the sequential treatment in the order ME-trypsin, ME-pepsin, and ME-carvacrol resulted in more efficient biofilm removal with a maximum reduction of 5 log CFU/mL for *P. aeruginosa* (Mechmechani et al., 2022a). Notably, the pharmaceutical and food industries have extensively employed ME techniques to regulate the release of active compounds, enhance formulation stability, and conceal odors. Moreover, encapsulation aims to safeguard the active chemicals against external elements like light, water, oxygen, pH, etc., thereby preserving their antibacterial efficacy for an extended duration. This approach can hinder the interactions between antimicrobials and the biofilm EPS matrix, resulting in the rejection or retention of the biocide. This prevents the biocide from interacting with microbial cells, allowing for effective disinfection of the deep layers of the biofilm (Dias et al., 2015; Yan et al., 2022). Therefore, the results have demonstrated a favorable potential for utilizing ME carvacrol as a substitute for traditional sanitization approaches in combating biofilms in medical settings. However, before using these encapsulated products as anti-biofilm agents, they must undergo approval and registration by regulatory agencies.

Furthermore, in other studies, the researchers also loaded carvacrol on different materials, including chitosan polymers, antimicrobial polymers, and carvacrol-loaded polylactic acid (PLA) scaffolds. All of the mentioned platforms showed enhanced antibiofilm activity in comparison to the individual compounds. The increased effectiveness of the described drug platforms in preventing the formation of biofilms can be related to the specific transport of carvacrol to the biofilm. This transport is facilitated by the electrostatic contact between the positively charged delivery vehicles, in the form of polymeric micelles, and the negatively charged bacteria. Moreover, chitosan nanoparticles have the potential to enhance the infiltration of carvacrol into the biofilm population of *P. aeruginosa* (Namivandi-Zangeneh et al., 2020; Bernal-Mercado et al., 2022; Farto-Vaamonde et al., 2022). Therefore, the successful performance of drug platforms in enhancing the antibiofilm activity of carvacrol demonstrates the potential application of these platforms as both therapeutic agents and delivery vehicles for hydrophobic compounds or drugs. These platforms can be used to specifically deliver cargo molecules to the *P. aeruginosa* biofilm.

6 Eugenol

Eugenol, also known as 2-methoxy-4-[2-propenyl] phenol, is a phenolic aromatic compound primarily obtained from EO found in nutmeg, clove, basil, cinnamon, and bay leaf. It belongs to a unique group of microbiocidal phenylpropanoids and has been extensively utilized as a dental analgesic for a considerable duration (Hassan et al., 2018; Wijesinghe et al., 2021a). Eugenol can be created via guaiacol allylation using allyl chloride or produced through a biotransformation process using microorganisms such as *Escherichia coli*, *Corynebacterium* spp., and *Bacillus cereus* (Abrahão et al., 2013). Eugenol has been documented to exhibit several pharmacological activities, including anti-cancer, anti-inflammatory, analgesic, anesthetic, antioxidant, and antibacterial effects (Kozam, 1977; Reddy and Lokesh, 1994; Hassan et al., 2018; Nisar et al., 2021). Noteworthy, eugenol is a lipophilic molecule and has the potential to effectively pass through the phospholipid bilayer of the cell membrane. This causes changes in the membrane's fluidity and permeability, ultimately leading to its disruption. Additionally, published data indicates that eugenol can enhance the protein leakage of cell membranes in both Gram-positive and Gram-negative bacteria. The compromised integrity of the cell walls and subsequent cellular leakages ultimately result in the demise of the microbial cell (Marchese et al., 2017; Wijesinghe et al., 2021b).

In addition, recently published studies reported that eugenol could inhibit the biofilm community of *P. aeruginosa* and the inhibitory effect of eugenol on the QS system of this bacterium is one of the most important possible mechanisms for inhibition of biofilm (Zhou et al., 2013; Rathinam et al., 2017; Rathinam and Viswanathan, 2018; Wijesinghe et al., 2021b; Lahiri et al., 2021; Shariff et al., 2022; Wang et al., 2023). Wang et al. (2023) reported that eugenol can reduce the amount of the QS signaling molecule 3-oxo-C12-homoseine lactone outside of cells by influencing the activity of the efflux pump MexAB-OprM. This indirectly disrupted the bacterial QS mechanism, thereby impeding the production of biofilms. The result of another study also showed that eugenol had a significant impact on the biofilm structure by causing a decrease in the protein and carbohydrate levels of the EPS. In addition, eugenol has the potential to impact the production of QS proteins, specifically LasA and LasB, as well as virulence factors like pyocyanin and rhamnolipid, which significantly impede the formation of biofilm (Lahiri et al., 2021).

In line with these findings, another investigation also reported that eugenol effectively decreased biofilm formation on urinary catheters and inhibited the production of virulence factors such as extracellular polysaccharides, rhamnolipid, elastase, protease, pyoverdin, and pyocyanin. Furthermore, computational docking analysis demonstrated a consistent molecular interaction between eugenol and LasR and RhlR receptors, indicating a strong binding affinity between eugenol and the QS receptors, as compared to the corresponding naturally released signal molecules (autoinducers). An examination of reporter strains has verified that eugenol competitively binds to a QS receptor (LasR), potentially inhibiting QS and resulting in substantial suppression of genes related to QS and virulence factors (Rathinam et al., 2017). Molecular modeling studies published in 2016 also demonstrated that eugenol, the main constituent of clove bud oil, effectively attaches to the QS receptor through hydrophobic interactions and hydrogen bonding with Arg61 and Tyr41, which are important amino acid residues of the LasR receptor (Jayalekshmi et al., 2016). Moreover, it was reported in another experiment that the inhibitory effect of eugenol on QS is likely due to its ability to decrease the ability of LasR transcription factors to detect their specific signal molecules, resulting in a decrease in the expression of quorum-controlled virulence factor genes and signal synthase genes (Rathinam and Viswanathan, 2018).

Finally, Zhou et al. (2013) data showed that eugenol inhibits the *las* system by reducing both the elastase activity of PAO1 and the transcriptional activation of *lasB* in *E. coli*. Moreover, eugenol demonstrated a decrease in both the pyocyanin production of PAO1 and the transcriptional activation of *pqsA* in *E. coli*. This suggests that eugenol acts as an inhibitor of the *pqs* system. By

inhibiting the *las* and *pqs* systems, which control the expression of multiple genes linked to virulence, the use of eugenol would greatly reduce the virulence of *P. aeruginosa*. Altogether, according to the docking study and competitive test, it is hypothesized that the anti-QS actions are initiated by eugenol binding to the LasR receptor due to its demonstrated binding stability. Eugenol's binding to the LasR signal receptor results in the inhibition of its role as a transcriptional activator. Moreover, eugenol most likely inhibited QS by reducing the activity of QS systems such as *las*, *rhl*, and pqs. Eugenol not only reduces the production of virulence components such as proteases, elastase, rhamnolipid, and pyocyanin in the biofilm community of *P. aeruginosa* but also significantly decreases their levels. Thus, it may be inferred that this molecule can impede the operation of various components of QS systems, namely, *las*, *rhl*, and *pqs*, at both the transcriptional and post-translational stages (Wang et al., 2023).

Prior research has indicated that eugenol is susceptible to degradation when exposed to oxygen, light, high temperatures, and humidity. Moreover, this compound exhibits a high degree of volatility, limited solubility in water, and inherent instability. Consequently, the aforementioned drawbacks have the potential to diminish the effectiveness, biological potency, and stability of eugenol (Karmakar et al., 2012; Shao et al., 2018). Therefore, given the drawbacks of eugenol in terms of its solubility, instability, and volatilization, employing various drug delivery methods could serve as a viable solution to address these issues and offer a stable, secure, and efficient antibiofilm agent for clinical application. To achieve this objective, *Rathinam* et al. applied sol-gel thin films containing eugenol onto urinary catheters and assessed the antibiofilm properties of the eugenol-coated portions against *P. aeruginosa*. The application of eugenol-coated silicone segments resulted in a decrease in the number of bacteria associated with the biofilm and effectively prevented bacterial attachment to the surface, even when a conditioning film was present. The study observed a notable decrease in the activity of genes related to virulence and biofilm formation, which confirms that silicone segments coated with eugenol have qualities that can block the expression of these genes and prevent biofilm formation (Rathinam et al., 2021). Noteworthy, silica sol-gels exhibit exceptional drug release characteristics, which may be extensively modified by manipulating the nanostructure network of the sol-gel. This modification results in a desirable therapeutic effect. Sol-gels are synthesized as thin films, coatings, and hydrogels for use in the antimicrobial and catalytic fields. They are also used for encapsulating enzymes, proteins, growth factors, and antibacterial agents (Dehghanghadikolaei et al., 2018; Rathinam et al., 2021). Therefore, sol-gel-coated silicone implants with prolonged release of eugenol could be a promising agent for managing *P. aeruginosa* biofilm; however, more confirmatory results are needed.

Another study also showed that eugenol and its nanoemulsion demonstrated that eugenol and its nanoemulsion exhibited 36% and 63% inhibition, respectively, of biofilm formation by *P. aeruginosa* at a dosage of 0.2 mg/mL. The eugenol nanoemulsion had a notable impact on the production of biofilm by this bacterium, in contrast to pure eugenol. In addition, eugenol and its nanoemulsion demonstrated the ability to decrease the activity of genes responsible for producing 3-oxo-C12-HSL and C4-HSL AHL. The impact was more prominent in the eugenol nanoemulsion compared to the pure eugenol for both synthase genes. Overall, due to its ability to hinder all the QS-mediated virulence factors and biofilm development of *P. aeruginosa*, the eugenol nanoemulsion shows promise as a new antibacterial and antibiofilm agent that targets QS, making it effective in controlling this bacterium (Lou et al., 2019).

Finally, the recently published study assessed the molecular docking of eugenol-conjugated silver nanoparticles (AgNPs) on QS regulator proteins (LasR, LasI, and MvfR). AgNPs coupled with eugenol exhibited significant binding affinities with proteins related to QS. The findings revealed that the synthesized nanoparticle can deactivate the transcriptional regulator LasR and suppress AHL synthesis. Moreover, the synthesized nanoparticle exhibits positive interactions with MvfR, potentially reducing the activity of the QS signaling system in *P. aeruginosa*. In this regard, eugenol-conjugated AgNPs may be regarded as a highly promising option for combating the production of *P. aeruginosa* biofilms (Shah et al., 2019). Therefore, as mentioned, the use of eugenol-based nanoplatforms could not only enhance the eugenol antibiofilm activity, but also suppress the QS system in *P. aeruginosa* (Figure 1). To this end, the use of these drug platforms should be considered in future studies where pure eugenol is not effective against the biofilm community.

7 Catechin

Catechins are bioactive compounds that are classified as polyphenolic phytochemicals. Catechins are present in a diverse range of foods and herbs, such as tea, apples, persimmons, grapes, and berries. There is a growing body of research that links the use of foods high in catechins to the prevention and treatment of chronic diseases in humans. Moreover, catechins have antioxidant properties, the ability to decrease tumor growth, and antibacterial effects (Fan et al., 2017). Noteworthy, irreversible damage to the microbial cytoplasmic membrane has been reported as the antimicrobial mechanism of catechins (Hirasawa et al., 2006). To this end, the antibiofilm activity of these compounds has also been considered by researchers.

Mombeshora et al., 2021 identified catechins as the predominant phytochemical present in *Triumfetta welwitschii*, a traditional African medicinal plant. This chemical effectively decreased both the amount of capsular polysaccharide in biofilms generated by *P. aeruginosa* and the amount of extracellular DNA in these bacterial biofilms. Noteworthy, the exact antibiofilm mechanism of catechin has not been elucidated yet; however, a recently published study indicated that catechin can disrupt QS in *P. aeruginosa*. In this concept, the study's findings demonstrated that catechin effectively decreased the formation of biofilm, elastase, pyocyanin, and rhamnolipid, while having no impact on growth. The *in silico* analysis of this work demonstrated that catechin-7-xyloside can interact with the QS regulator LasR (Zhong et al., 2020). Another study also investigated the inhibitory effect of 19 different natural compounds on the QS system of *P. aeruginosa*. The results showed a high potency of catechin to interfere with LasR; therefore, the authors suggested catechin as a potent QS antagonist (Chaieb et al., 2022). In line with these results, the co-administration of catechin and gallic acid markedly reduced the expression of *lasI* and *lasR* in *P. aeruginosa*. The docking study revealed that catechin was

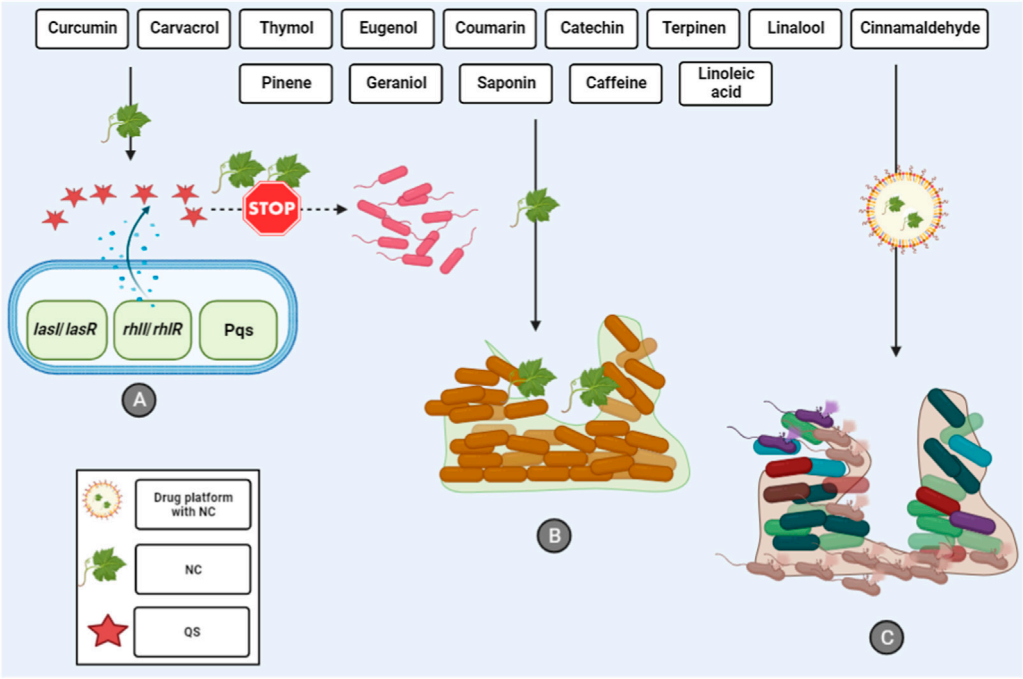

FIGURE 1
Interactions between natural compounds and *P. aeruginosa* biofilm. **(A)** Inhibition of QS system that inhibits the first step of biofilm formation. **(B)** Natural compounds can destroy the biofilm community and **(C)** The usage of different drug platforms can enhance the antibiofilm activity of natural compounds. NC, natural compounds; QS, quorum sensing.

successfully positioned in the ligand-binding domain of LasR. Catechin formed hydrogen bonds with Thr-115 and Ser-129 amino acid residues, which are known to play a role in the interaction with the autoinducer ligand. This supports the notion that the combination of catechin and gallic acid has a strong potential to inhibit the LasR and disrupt both QS and biofilm formation in *P. aeruginosa* (Abdel Bar et al., 2022).

Finally, Vandeputte et al. (2010) found that catechin had a notable inhibitory impact on the synthesis of pyocyanin and elastase, as well as on the formation of biofilm. Additionally, catechin affected the expression of the genes *lasB* and *rhlA*, as well as the important QS regulatory genes *lasI*, *lasR*, *rhlI*, and *rhlR*. Utilizing RhlR and LasR-based biosensors, it was observed that catechin might potentially disrupt the detection of the QS signal N-butanoyl-L-homoserine lactone by RhlR. As a result, this interference leads to a decrease in the production of QS factors. Therefore, as mentioned, the *las* system is the main QS regulator of the biofilm and the interaction of catechin with this system can significantly inhibit the biofilm community of *P. aeruginosa*. To this end, catechin may be proposed as an anti-QS agent, able to reduce the biofilm, virulence, and pathogenicity of *P. aeruginosa*.

8 Thymol

Thymol, also known as 2-isopropyl-5-methyl phenol, is a kind of phenolic monoterpene that has a powerful smell and can dissolve well in alcohol and other organic solvents but does not dissolve well in water (Shariati et al., 2022). Thymol is plentifully present in specific plants and has been utilized in traditional medicine for an extended period due to its diverse pharmacological characteristics (Salehi et al., 2018). Thymol has been proven to possess antibacterial and anti-inflammatory properties against microbes. This compound has been found to possess potent antibacterial activities, which make it effective in treating respiratory infections, oral cavity infections, and intestinal disorders (Jo et al., 2022). Thymol has been observed to display antibacterial properties against both planktonic and biofilm communities of Gram-negative and Gram-positive bacteria such as *E. coli*, *S. aureus*, *Salmonella* spp., and *P. aeruginosa* (Flores et al., 2019).

According to Walczak et al. (2021), when dealing with the biofilm formed on surfaces made of polypropylene, polyvinyl chloride, polyethylene, and stainless steel, commonly used in medical technologies and food production, thymol reduced the amount of *P. aeruginosa* biofilm by 70%–77% after 3 days of exposure. In addition, following a 10-day exposure to thymol, the production of biofilm was significantly decreased by 80%–100%. In another study that was published in 2022, the antibiofilm efficacy of thymol against biofilms generated by ciprofloxacin-resistant *P. aeruginosa* (CRPA) was examined on tympanostomy tubes. Noteworthy, the placement of these devices frequently results in ear infections, with otorrhea being the predominant consequence in youngsters. The authors of this study observed significant reductions in the viability and adhesion of CRPA in response to thymol therapy, which depended on the concentration of thymol. Thymol exposure also hindered the development of CRPA biofilms. In addition, thymol was found to improve the elimination of fully matured biofilms created by CRPA and also contributed to a decrease in the

rates of CRPA breakdown. Moreover, thymol was found to effectively eliminate CRPA biofilms that had developed on the surface of tympanostomy tubes. The data suggest that thymol is a powerful inhibitor of CRPA biofilms, making it a promising therapeutic drug for treating biofilm-related post-tympanostomy tube otorrhea caused by CRPA infection. It is noteworthy to mention that the authors propose that thymol antibiofilm activity may be due to its ability to disrupt the surface adherence of antibiotic-resistant strains and damage the structure of the cell membrane (Walczak et al., 2021).

In line with these results, the recently published study also demonstrated that thymol, with a concentration ranging from 52.33% to 62.46%, was the primary constituent in the thyme EOs. The strongest antibacterial and anti-biofilm activity was shown in thyme oil obtained through distillation of fresh plant material gathered at the onset of the flowering period. This oil demonstrated efficacy against many microorganisms, including *P. aeruginosa* (Bakó et al., 2023). Finally, a further study on the anti-biofilm properties of thymol found that this powerful plant compound is mostly present in log (30.28%) and stationary phase (20.89%) extracts. The log phase extracts exhibited the lowest MIC (25 mg/mL) in comparison to other developmental phases. The extracts obtained from the stationary phase demonstrated the most effective biofilm dispersal activity against *P. aeruginosa*, with a rate of 80%. The log phase extracts exhibited the most potent biofilm inhibitory effect against *P. aeruginosa* (66%). Overall, leaf extracts of *Plectranthus amboinicus* in the log phase demonstrated a multifaceted mechanism of action. They exhibited antibacterial and antibiofilm actions while also lowering the motility and hydrophobicity of *P. aeruginosa*, which are crucial components in the development of this pathogen (Sawant et al., 2022). Therefore, as mentioned, thymol has the potential to inhibit bacterial biofilm. Thymol's antibacterial effectiveness is linked to its ability to disturb both the outer and inner membranes. This disruption has been observed through the following indicators: a decrease in membrane potential and the release of potassium ions, ATP, and carboxyfluorescein (Gómez-Sequeda et al., 2020). In addition, thymol can inhibit extracellular polysaccharides present in the biofilm matrix (Valliammai et al., 2020). Thymol also inhibits *cdrA* which contributes to *P. aeruginosa* biofilm formation and stabilization (Jo et al., 2022). Noteworthy, CdrA serves as the cargo for the two-partner secretion system, which is encoded by the cdrAB operon. Inside the matrix, the bound CdrA-Psl creates strong and resistant bacterial aggregates that strengthen the structure of the biofilm (Cendra and Torrents, 2021). CdrA can bind to unidentified EPS molecules, which aids in the development of biofilms and enhances their stability (Reichhardt et al., 2018). To this end, the interactions of thymol and *cdrA* could inhibit the *P. aeruginosa* biofilm; however, data in this field is limited, and more confirmatory studies are needed.

Finally, the results of recently published study showed that thymol, derived from the root exudates of *Sedum alfredii*, has the ability to hinder the production of protease and elastase in *P. aeruginosa*. This is achieved by reducing the expression of *lasB*, without causing any notable impact on the primary *las* system. Thymol shows promise as a potential natural inhibitor of QS (Zhu et al., 2021). Additionally, thymol showed inhibitory effects against the QS system in other microorganisms; however, data about the interactions of this compound with the *P. aeruginosa* QS system is limited. Thus, the inhibitory effect of thymol on the QS system of *P. aeruginosa* is one possible antibiofilm effect of this natural compound; however, more confirmatory studies are required on this issue (Cáceres et al., 2020; Scandorieiro et al., 2023).

Although thymol has beneficial antimicrobial effects, it is limited by poor solubility in water, easy degradation, inadequate distribution on target sites, and chemical and biological instability caused by its volatile nature. These limitations restrict the applicability of thymol as an antimicrobial agent (Piri-Gharaghie et al., 2022). In this regard, as mentioned earlier, researchers are looking for more effective ways, such as new methods of drug delivery with this compound. To this end, *Velázquez-Carriles* et al. developed a novel nanohybrid structure consisting of zinc-layered hydroxide salt (ZnLHS) and thymol to inhibit bacterial growth. The synthesized pharmacological platform effectively suppressed *P. aeruginosa* biofilm by over 90%. Noteworthy, common disinfectants induce oxidation of the cell membrane before the formation of biofilm; therefore, the authors suggested that the hydroxide salt, owing to its anionic character, can impede the synthesis of this polysaccharide (Köse and Yapar, 2017). Furthermore, scientific evidence has demonstrated that thymol effectively inhibits the expression of genes linked with biofilm development. Consequently, the combined use of these substances may enhance the rate at which biofilm formation is inhibited (Sreelatha et al., 2021). Collectively, the hydroxide salt possesses an anionic character that facilitates oxidation, whereas thymol effectively inhibits the growth of bacterial biofilm. The greater degree of inhibition found with thymol–(ZnLHS) in comparison to thymol alone can be due to the latter's hydrophilic characteristics. The hydrophilic nature of this substance, when it is stabilized in a colloidal dispersion, can enhance its ability to spread across the polysaccharide matrix, which also has a polar nature. Unlike thymol, ZnLHS possesses a hydrophobic property that allows it to specifically engage with the bacterial membrane. Therefore, the nanohybrid improves inhibition by capitalizing on a synergistic effect (Velázquez-Carriles et al., 2022).

Furthermore, one potential approach to addressing the constraints of thymol is to encapsulate it in nanocarriers (Fathi-Achachelouei et al., 2019). Nanocarriers, due to their small size and physicochemical characteristics, enhance the stability of the compound and can transport significant quantities of medicine (Heidari et al., 2018). In this regard, Piri-Gharaghie et al. also fabricated thymol-loaded chitosan nanogels. These nanogels can be used as a drug delivery system due to their low cytotoxicity, biodegradability, and biocompatibility (Pourebrahim et al., 2021). The antibacterial activity test showed that the thymol-loaded chitosan nanogel (thymol -CsNG) decreased the MIC by 4–6 times compared to free thymol. Thus, the authors propose that the increased antibacterial properties of thymol-CsNG can be attributed to the amalgamation of chitosan with the bacterial cell membrane and the specific discharge of thymol into the bacterial cell. Furthermore, thymol-CsNG may have an anti-biofilm effect by decreasing the number of microorganisms, leading to a subsequent

reduction in biofilm development. One of the reasons is that the antibiotic can more effectively enter the biofilm structure because thymol-CsNG binds to the biofilm matrix, resulting in a decrease in viable counts and a reduction in the formation of biofilms. Furthermore, the thymol-CsNG compound effectively suppressed the expression of *ompA* and *pgaB* genes in bacterial strains. This suppression is likely a result of thymol interactions with transcription factors, leading to their inactivation and subsequent inhibition of biofilm gene transcription. Consequently, the expression of biofilm genes is diminished. Based on the findings, it can be inferred that thymol-CsNG has the potential to be a good candidate for improving antibacterial and anti-biofilm properties (Pourebrahim et al., 2021; Piri-Gharaghie et al., 2022).

In addition to the methods mentioned for how to use thymol, multiple research studies have examined the combined impact of thymol and blue light (BL) and how they work together. BL with a wavelength range of 400–495 nm is an emerging antibacterial method, especially effective against skin infections. Recent research has confirmed the effectiveness of BL in eliminating bacteria, regardless of their resistance profiles (Zhang et al., 2014). The precise process by which BL operates remains ambiguous. Nevertheless, there is a widespread consensus that BL triggers the activation of internal protoporphyrin-like derivatives and initiates a cascade of ROS generation. The hazardous ROS interacts with many constituents of bacteria and ultimately causes the cell to rupture. The broad-spectrum and rapid effects of ROS reduce the likelihood of bacterial resistance to different antibiotics such as beta-lactam antibiotics (Zhang et al., 2014). Similarly, Lu et al. (2021) established an antibacterial synergy between BL and thymol. This study investigates a combinatory approach to eliminate MDR *P. aeruginosa*, targeting both planktonic cells and established biofilms. The strategy successfully reduces bacterial populations by up to 7.5 log in less than 30 min. When used in combination, BL and thymol effectively sterilized acute infected or biofilm-associated wounds and successfully inhibited the spread of infection throughout the body in mice. BL and thymol induced oxidative bursts specifically in bacteria due to the presence of proporphyrin-like chemicals that are more numerous in bacteria than in mammalian cells. These compounds convert thymol, which is normally innocuous, into blue-laser sensitizers called thymoquinone and thymohydroquinone. These agents, when exposed to light, increased the generation of ROS and triggered a series of harmful effects in bacteria without causing any harm to the human tissue. The work reveals a hitherto unrecognized characteristic of thymol as a pro-photosensitizer, similar to a prodrug, which is specifically active in bacteria (Lu et al., 2021).

Again, in 2022, the researchers of the previous study investigated another synergistic effect. The study showed that the combination of BL and oregano EO effectively decreased *P. aeruginosa* planktonic cells and mature biofilms by more than $7\log_{10}$. In contrast, the treatment with only BL or oregano EO did not result in a substantial reduction of bacteria. The findings indicate that thymol and carvacrol are the main constituents accountable for the bactericidal properties of oregano EO. The fundamental reason for the bactericidal effect of oregano EO is its ability to enhance the generation of ROS triggered by BL. This activation stimulates the endogenous tetrapyrrole macrocycles in bacteria, leading to their destruction. Importantly, this phototoxic action is limited to the bacteria and does not harm the surrounding tissues. An examination of the ingredients of oregano EO, together with microbiological tests, revealed that carvacrol and its isomer thymol are the primary phytochemicals that work together with BL to achieve synergistic killing. This research provides compelling evidence for the use of carvacrol and thymol as helpful benchmarks in evaluating and establishing the antibacterial effectiveness of different oregano EO products (Lu et al., 2022a). Therefore, as mentioned, in addition to the use of a thymol-based drug platform, the combined use of BL and thymol could be a promising antibiofilm approach for managing *P. aeruginosa* infections; however, more confirmatory studies are needed in this field.

9 Conclusion

The biofilm community of *P. aeruginosa* is one of the most important reasons for antibiotic resistance in this bacterium. As reported by recently published studies, natural compounds can inhibit biofilm formation and enhance the antibiofilm efficacy of conventional antibiotics and other antibacterial agents. The exact interactions between natural compounds and *P. aeruginosa* biofilm have not been elucidated yet; however, inhibition and interference with the QS system are the main possible mechanisms that have been reported until now. Additionally, the use of different nanostructures and drug platforms could overcome the disadvantages of natural compounds such as rapid metabolism and degradation, water insolubility, and low oral bioavailability. Hence, it is vital to contemplate the utilization of drug platforms in forthcoming investigations that prioritize the assessment of the antibiofilm efficacy of natural compounds. It is important to note that there is a lack of animal studies and clinical studies on this subject. Therefore, future research should focus on evaluating the effectiveness of natural compounds in preventing biofilm formation through these types of investigations. Additionally, data about some of the natural compound interactions with the biofilm community is limited. To this end, focusing on these natural compounds can lead to finding new ways to manage the *P. aeruginosa* biofilm community.

Author contributions

AS: Conceptualization, Investigation, Writing–original draft, Writing–review and editing. MN: Investigation, Writing–original draft. MA: Data curation, Investigation, Writing–original draft. AK: Formal Analysis, Methodology, Writing–original draft. AF: Supervision, Writing–original draft. ZC: Conceptualization, Investigation, Writing–original draft, Writing–review and editing.

Acknowledgments

We greatly appreciate the input from the BioRender team (BioRender.com) for their collaboration with us in figure design.

Conflict of interest

The authors declare that the research was conducted in the absence of any commercial or financial relationships that could be construed as a potential conflict of interest.

The authors declared that they were an editorial board member of Frontiers, at the time of submission. This had no impact on the peer review process and the final decision.

Publisher's note

References

Abdel Bar, F. M., Alossaimi, M. A., Elekhnawy, E., Alzeer, M. a.A., Abo Kamer, A., Moglad, E., et al. (2022). Anti-*quorum* sensing and anti-biofilm activity of Pelargonium × hortorum root extract against *Pseudomonas aeruginosa*: combinatorial effect of catechin and gallic acid. *Molecules* 27 (22), 7841. doi:10.3390/molecules27227841

Abdulrahman, H., Misba, L., Ahmad, S., and Khan, A. U. (2020). Curcumin induced photodynamic therapy mediated suppression of *quorum* sensing pathway of *Pseudomonas aeruginosa*: an approach to inhibit biofilm *in vitro*. *Photodiagnosis Photodyn. Ther.* 30, 101645. doi:10.1016/j.pdpdt.2019.101645

Abrahão, M. R., Molina, G., and Pastore, G. M. (2013). Endophytes: recent developments in biotechnology and the potential for flavor production. *Food Res. Int.* 52 (1), 367–372. doi:10.1016/j.foodres.2013.03.007

Ahmad, A., Wani, M. Y., Khan, A., Manzoor, N., and Molepo, J. (2015). Synergistic interactions of eugenol-tosylate and its congeners with fluconazole against Candida albicans. *Plos one* 10 (12), e0145053. doi:10.1371/journal.pone.0145053

Ahmad, W., Ansari, M. A., Yusuf, M., Amir, M., Wahab, S., Alam, P., et al. (2022). Antibacterial, anticandidal, and antibiofilm potential of fenchone: *in vitro*, molecular docking and *in silico*/ADMET study. *Study* 11 (18), 2395. doi:10.3390/plants11182395

Ahmed, B., Syed, A., Ali, K., Elgorban, A. M., Khan, A., Lee, J., et al. (2021). Synthesis of gallotannin capped iron oxide nanoparticles and their broad spectrum biological applications. *RSC Adv.* 11 (17), 9880–9893. doi:10.1039/d1ra00220a

Ahmed, S., Rudden, M., Smyth, T. J., Dooley, J. S. G., Marchant, R., and Banat, I. M. (2019). Natural *quorum* sensing inhibitors effectively downregulate gene expression of *Pseudomonas aeruginosa* virulence factors. *Appl. Microbiol. Biotechnol.* 103 (8), 3521–3535. doi:10.1007/s00253-019-09618-0

Alarkwazi, R. K., Abdulreda, G. R., and Ali, A. S. (2022). Secondary metabolism compounds study of essential oils for the Mentha spicata L. And ocimum basilicum L. *J. Biomed. Biochem.* 1 (1), 27–33. doi:10.57238/jbb.2022.18906

Al-Khazraji, S. M., Hossain, M. H., and Hassoon, A. S. (2022). Estimation of some bioactive substances and antibacterial activity of zingiber officinale (ginger) extract. *J. Biomed. Biochem.* 1 (2), 29–33. doi:10.57238/jbb.2022.5544.1017

Bae, K.-H., Ji, J.-M., and Park, K.-L. (1992). The antibacterial component from Cinnamomi Cortex against a cariogenic bacterium Streptococcus mutans OMZ 176. *Archives Pharmacal Res.* 15 (3), 239–241. doi:10.1007/bf02974062

Bahari, S., Zeighami, H., Mirshahabi, H., Roudashti, S., and Haghi, F. (2017). Inhibition of *Pseudomonas aeruginosa quorum* sensing by subinhibitory concentrations of curcumin with gentamicin and azithromycin. *J. Glob. Antimicrob. Resist* 10, 21–28. doi:10.1016/j.jgar.2017.03.006

Bahramian, A., Khoshnood, S., Shariati, A., Doustdar, F., Chirani, A. S., and Heidary, M. (2019). Molecular characterization of the pilS2 gene and its association with the frequency of *Pseudomonas aeruginosa* plasmid pKLC102 and PAPI-1 pathogenicity island. *Infect. Drug Resist.* 12, 221–227. doi:10.2147/IDR.S188527

Bajire, S. K., Ghate, S. D., Shetty, S., Banerjee, S., Rao, R. S. P., Shetty, V., et al. (2023). Unveiling the role of hub proteins in controlling *quorum* sensing regulated virulence through analogues in *Pseudomonas aeruginosa* PAO1: a functional protein-protein network biology approach. *Biochem. Biophys. Res. Commun.* 660, 13–20. doi:10.1016/j.bbrc.2023.03.079

Bakó, C., Balázs, V. L., Kerekes, E., Kocsis, B., Nagy, D. U., Szabó, P., et al. (2023). Flowering phenophases influence the antibacterial and anti-biofilm effects of Thymus vulgaris L. essential oil. *BMC Complement. Med. Ther.* 23 (1), 168. doi:10.1186/s12906-023-03966-1

Bali, E. B., Türkmen, K. E., Erdönmez, D., and Sağlam, N. (2019). Comparative study of inhibitory potential of dietary phytochemicals against *quorum* sensing activity of and biofilm formation by chromobacterium violaceum 12472, and swimming and swarming behaviour of *Pseudomonas aeruginosa* PAO1. *Food Technol. Biotechnol.* 57 (2), 212–221. doi:10.17113/ftb.57.02.19.5823

Bernal-Mercado, A. T., Juarez, J., Valdez, M. A., Ayala-Zavala, J. F., Del-Toro-Sánchez, C. L., and Encinas-Basurto, D. (2022). Hydrophobic chitosan nanoparticles loaded with carvacrol against *Pseudomonas aeruginosa* biofilms. *Molecules* 27 (3), 699. doi:10.3390/molecules27030699

Borges, A., Ferreira, C., Saavedra, M. J., and Simões, M. (2013). Antibacterial activity and mode of action of ferulic and gallic acids against pathogenic bacteria. *Microb. Drug Resist* 19 (4), 256–265. doi:10.1089/mdr.2012.0244

Bose, S. K., Chauhan, M., Dhingra, N., Chhibber, S., and Harjai, K. (2020a). Terpinen-4-ol attenuates *quorum* sensing regulated virulence factors and biofilm formation in *Pseudomonas aeruginosa*. *Future Microbiol.* 15, 127–142. doi:10.2217/fmb-2019-0204

Bose, S. K., Nirbhavane, P., Batra, M., Chhibber, S., and Harjai, K. (2020b). Nanolipoidal α-terpineol modulates *quorum* sensing regulated virulence and biofilm formation in *Pseudomonas aeruginosa*. *Nanomedicine Lond*, 15(18), 1743–1760. doi:10.2217/nnm-2020-0134

Brackman, G., Cos, P., Maes, L., Nelis, H. J., and Coenye, T. (2011). *Quorum* sensing inhibitors increase the susceptibility of bacterial biofilms to antibiotics *in vitro* and *in vivo*. *Antimicrob. Agents Chemother.* 55 (6), 2655–2661. doi:10.1128/aac.00045-11

Breidenstein, E. B., De La Fuente-Núñez, C., and Hancock, R. E. (2011). *Pseudomonas aeruginosa*: all roads lead to resistance. *Trends Microbiol.* 19 (8), 419–426. doi:10.1016/j.tim.2011.04.005

Cáceres, M., Hidalgo, W., Stashenko, E., Torres, R., and Ortiz, C. (2020). Essential oils of aromatic plants with antibacterial, anti-biofilm and anti-*quorum* sensing activities against pathogenic bacteria. *Antibiot. Basel* 9 (4), 147. doi:10.3390/antibiotics9040147

Cendra, M. D. M., and Torrents, E. (2021). *Pseudomonas aeruginosa* biofilms and their partners in crime. *Biotechnol. Adv.* 49, 107734. doi:10.1016/j.biotechadv.2021.107734

Ceylan, O., and Ugur, A. (2015). Chemical composition and anti-biofilm activity of Thymus sipyleus BOISS. subsp. sipyleus BOISS. var. davisianus RONNIGER essential oil. *Arch. Pharm. Res.* 38 (6), 957–965. doi:10.1007/s12272-014-0516-0

Chadha, J., Singh, J., Chhibber, S., and Harjai, K. (2022). Gentamicin augments the *quorum* quenching potential of cinnamaldehyde *in vitro* and protects *Caenorhabditis elegans* from *Pseudomonas aeruginosa* infection. *Front. Cell Infect. Microbiol.* 12, 899566. doi:10.3389/fcimb.2022.899566

Chadha, J., Singh, J., and Harjai, K. (2023). α-Terpineol synergizes with gentamicin to rescue *Caenorhabditis elegans* from *Pseudomonas aeruginosa* infection by attenuating *quorum* sensing-regulated virulence. *Life Sci.* 313, 121267. doi:10.1016/j.lfs.2022.121267

Chaieb, K., Kouidhi, B., Hosawi, S. B., Baothman, O. a.S., Zamzami, M. A., and Altayeb, H. N. (2022). Computational screening of natural compounds as putative *quorum* sensing inhibitors targeting drug resistance bacteria: molecular docking and molecular dynamics simulations. *Comput. Biol. Med.* 145, 105517. doi:10.1016/j.compbiomed.2022.105517

Chakraborty, P., Dastidar, D. G., Paul, P., Dutta, S., Basu, D., Sharma, S. R., et al. (2020). Inhibition of biofilm formation of *Pseudomonas aeruginosa* by caffeine: a potential approach for sustainable management of biofilm. *Arch. Microbiol.* 202 (3), 623–635. doi:10.1007/s00203-019-01775-0

Chegini, Z., Khoshbayan, A., Taati Moghadam, M., Farahani, I., Jazireian, P., and Shariati, A. (2020). Bacteriophage therapy against *Pseudomonas aeruginosa* biofilms: a review. *Ann. Clin. Microbiol. Antimicrob.* 19, 45–17. doi:10.1186/s12941-020-00389-5

Chipenzi, T., Baloyi, G., Mudondo, T., Sithole, S., Fru Chi, G., and Mukanganyama, S. (2020). An evaluation of the antibacterial properties of tormentic acid congener and extracts from callistemon viminalis on selected ESKAPE pathogens and effects on biofilm formation. *Adv. Pharmacol. Pharm. Sci.* 2020, 8848606. doi:10.1155/2020/8848606

Danaraj, J., Mariasingarayan, Y., Ayyappan, S., and Karuppiah, V. (2020). Seagrass Halodule pinifolia active constituent 4-methoxybenzioic acid (4-MBA) inhibits *quorum* sensing mediated virulence production of *Pseudomonas aeruginosa*. *Microb. Pathog.* 147, 104392. doi:10.1016/j.micpath.2020.104392

Das, S., Paul, P., Dastidar, D. G., Chakraborty, P., Chatterjee, S., Sarkar, S., et al. (2023). Piperine exhibits potential antibiofilm activity against *Pseudomonas aeruginosa* by accumulating reactive oxygen species, affecting cell surface hydrophobicity and *quorum* sensing. *Affect. Cell Surf. Hydrophobicity Quorum Sens.* 195 (5), 3229–3256. doi:10.1007/s12010-022-04280-1

Davies, D. G., Parsek, M. R., Pearson, J. P., Iglewski, B. H., Costerton, J. W., and Greenberg, E. P. (1998). The involvement of cell-to-cell signals in the development of a bacterial biofilm. *Science* 280 (5361), 295–298. doi:10.1126/science.280.5361.295

Dehghanghadikolaei, A., Ansary, J., and Ghoreishi, R. (2018). Sol-gel process applications: a mini-review. *Proc. Nat. Res. Soc.* 2 (1), 02008–02029. doi:10.11605/j.pnrs.201802008

Dias, M. I., Ferreira, I. C., and Barreiro, M. F. (2015). Microencapsulation of bioactives for food applications. *Food Funct.* 6 (4), 1035–1052. doi:10.1039/c4fo01175a

Di Salle, A., Viscusi, G., Di Cristo, F., Valentino, A., Gorrasi, G., Lamberti, E., et al. (2021). Antimicrobial and antibiofilm activity of curcumin-loaded electrospun nanofibers for the prevention of the biofilm-associated infections. *Molecules* 26 (16), 4866. doi:10.3390/molecules26164866

Elsharif, S. A., and Buettner, A. (2018). Structure-odor relationship study on geraniol, nerol, and their synthesized oxygenated derivatives. *J. Agric. Food Chem.* 66 (10), 2324–2333. doi:10.1021/acs.jafc.6b04534

Fan, F. Y., Sang, L. X., and Jiang, M. (2017). Catechins and their therapeutic benefits to inflammatory bowel disease. *Molecules* 22 (3), 484. doi:10.3390/molecules22030484

Farto-Vaamonde, X., Diaz-Gomez, L., Parga, A., Otero, A., Concheiro, A., and Alvarez-Lorenzo, C. (2022). Perimeter and carvacrol-loading regulate angiogenesis and biofilm growth in 3D printed PLA scaffolds. *J. Control Release* 352, 776–792. doi:10.1016/j.jconrel.2022.10.060

Fathi-Achachelouei, M., Knopf-Marques, H., Ribeiro Da Silva, C. E., Barthès, J., Bat, E., Tezcaner, A., et al. (2019). Use of nanoparticles in tissue engineering and regenerative medicine. *Front. Bioeng. Biotechnol.* 7, 113. doi:10.3389/fbioe.2019.00113

Fernandes, S., Borges, A., Gomes, I. B., Sousa, S. F., and Simões, M. (2023). Curcumin and 10-undecenoic acid as natural *quorum* sensing inhibitors of LuxS/AI-2 of Bacillus subtilis and LasI/LasR of *Pseudomonas aeruginosa*. *Food Res. Int.* 165, 112519. doi:10.1016/j.foodres.2023.112519

Ferro, T. a.F., Souza, E. B., Suarez, M. a.M., Rodrigues, J. F. S., Pereira, D. M. S., Mendes, S. J. F., et al. (2019). Topical application of cinnamaldehyde promotes faster healing of skin wounds infected with *Pseudomonas aeruginosa*. *Molecules* 24 (8), 1627. doi:10.3390/molecules24081627

Firmino, D. F., Cavalcante, T. T. A., Gomes, G. A., Firmino, N. C. S., Rosa, L. D., De Carvalho, M. G., et al. (2018). Antibacterial and antibiofilm activities of cinnamomum sp. Essential oil and cinnamaldehyde: antimicrobial activities. *ScientificWorldJournal* 2018, 7405736. doi:10.1155/2018/7405736

Flores, P. I. G., Valenzuela, R. B., Ruiz, L. D., López, C. M., and Cháirez, F. E. (2019). Antibacterial activity of five terpenoid compounds: carvacrol, limonene, linalool, α-terpinene and thymol. *Trop. subtropical Agroecosyst.* 22 (2). doi:10.56369/tsaes.2838

Gambello, M. J., and Iglewski, B. H. (1991). Cloning and characterization of the *Pseudomonas aeruginosa* lasR gene, a transcriptional activator of elastase expression. *J. Bacteriol.* 173 (9), 3000–3009. doi:10.1128/jb.173.9.3000-3009.1991

Gambino, E., Maione, A., Guida, M., Albarano, L., Carraturo, F., Galdiero, E., et al. (2022). Evaluation of the pathogenic-mixed biofilm formation of *Pseudomonas aeruginosa*/*Staphylococcus aureus* and treatment with limonene on three different materials by a dynamic model. *Model* 19 (6), 3741. doi:10.3390/ijerph19063741

Ghannay, S., Aouadi, K., Kadri, A., and Snoussi, M. (2022a). GC-MS profiling, vibriocidal, antioxidant, antibiofilm, and anti-*quorum* sensing properties of *Carum carvi* L. Essential oil: *in vitro* and *in silico* approaches. *Essent. Oil Vitro Silico Approaches* 11 (8), 1072. doi:10.3390/plants11081072

Ghannay, S., Aouadi, K., Kadri, A., and Snoussi, M. (2022b). *In vitro* and *in silico* screening of anti-*Vibrio* spp., antibiofilm, antioxidant and anti-*quorum* sensing activities of *Cuminum cyminum* L. Volatile oil. *Plants Basel* 11 (17), 2236. doi:10.3390/plants11172236

Ghasemi, M., Khorsandi, K., and Kianmehr, Z. (2021). Photodynamic inactivation with curcumin and silver nanoparticles hinders *Pseudomonas aeruginosa* planktonic and biofilm formation: evaluation of glutathione peroxidase activity and ROS production. *World J. Microbiol. Biotechnol.* 37 (9), 149. doi:10.1007/s11274-021-03104-4

Gholami, M., Zeighami, H., Bikas, R., Heidari, A., Rafiee, F., and Haghi, F. (2020). Inhibitory activity of metal-curcumin complexes on *quorum* sensing related virulence factors of *Pseudomonas aeruginosa* PAO1. *Amb. Express* 10 (1), 111. doi:10.1186/s13568-020-01045-z

Gobin, M., Proust, R., Lack, S., Duciel, L., Des Courtils, C., Pauthe, E., et al. (2022). A combination of the natural molecules gallic acid and carvacrol eradicates *P. aeruginosa* and *S. aureus* mature biofilms. *Int. J. Mol. Sci.* 23 (13), 7118. doi:10.3390/ijms23137118

Gómez-Sequeda, N., Cáceres, M., Stashenko, E. E., Hidalgo, W., and Ortiz, C. (2020). Antimicrobial and antibiofilm activities of essential oils against *Escherichia coli* O157:H7 and methicillin-resistant *Staphylococcus aureus* (MRSA). *Antibiot. (Basel)* 9 (11), 730. doi:10.3390/antibiotics9110730

Gutiérrez-Barranquero, J. A., Reen, F. J., Mccarthy, R. R., and O'gara, F. (2015). Deciphering the role of coumarin as a novel *quorum* sensing inhibitor suppressing virulence phenotypes in bacterial pathogens. *Appl. Microbiol. Biotechnol.* 99 (7), 3303–3316. doi:10.1007/s00253-015-6436-1

Häkkinen, S. T., Soković, M., Nohynek, L., Ćirić, A., Ivanov, M., Stojković, D., et al. (2021). Chicory extracts and sesquiterpene lactones show potent activity against bacterial and fungal pathogens. *Pathogens* 14 (9), 941. doi:10.3390/ph14090941

Hassan, H. A., Geniady, M. M., Abdelwahab, S. F., Abd-Elghany, M. I., Sarhan, H. A., Abdelghany, A. A., et al. (2018). Topical eugenol successfully treats experimental Candida albicans-induced keratitis. *Ophthalmic Res.* 60 (2), 69–79. doi:10.1159/000488907

He, R., Zhang, Z., Xu, L., Chen, W., Zhang, M., Zhong, Q., et al. (2022). Antibacterial mechanism of linalool emulsion against *Pseudomonas aeruginosa* and its application to cold fresh beef. *World J. Microbiol. Biotechnol.* 38 (4), 56. doi:10.1007/s11274-022-03233-4

Heidari, Z., Salehzadeh, A., Sadat Shandiz, S. A., and Tajdoost, S. (2018). Anti-cancer and anti-oxidant properties of ethanolic leaf extract of Thymus vulgaris and its bio-functionalized silver nanoparticles. *3 Biotech.* 8 (3), 177. doi:10.1007/s13205-018-1199-x

Hirasawa, M., Takada, K., and Otake, S. (2006). Inhibition of acid production in dental plaque bacteria by green tea catechins. *Caries Res.* 40 (3), 265–270. doi:10.1159/000092236

Hossain, M. H., Al-Khazraji, S. M., and Hassoon, A. S. (2022). Estimation of some Essential oils and study Antibacterial activity of Rosmarinus officinalis Extract. *J. Biomed. Biochem.* 1 (3), 34–38. doi:10.57238/jbb.2022.20108

Husain, F. M., Ahmad, I., Khan, M. S., Ahmad, E., Tahseen, Q., Khan, M. S., et al. (2015a). Sub-MICs of Mentha piperita essential oil and menthol inhibits AHL mediated *quorum* sensing and biofilm of Gram-negative bacteria. *Front. Microbiol.* 6, 420. doi:10.3389/fmicb.2015.00420

Husain, F. M., Ahmad, I., Khan, M. S., and Al-Shabib, N. A. (2015b). Trigonella foenum-graceum (seed) extract interferes with *quorum* sensing regulated traits and biofilm formation in the strains of *Pseudomonas aeruginosa* and Aeromonas hydrophila. *Evid. Based Complement. Altern. Med.* 2015, 879540. doi:10.1155/2015/879540

Ivanov, M., Novović, K., Malešević, M., Dinić, M., Stojković, D., Jovčić, B., et al. (2022). Polyphenols as inhibitors of antibiotic resistant bacteria-mechanisms underlying rutin interference with bacterial virulence. *Pharm. Basel.* 15 (3), 385. doi:10.3390/ph15030385

Jagani, S., Chelikani, R., and Kim, D. S. (2009). Effects of phenol and natural phenolic compounds on biofilm formation by *Pseudomonas aeruginosa*. *Biofouling* 25 (4), 321–324. doi:10.1080/08927010802660854

Javed, H., Meeran, M. F. N., Jha, N. K., and Ojha, S. (2021). Carvacrol, a plant metabolite targeting viral protease (mpro) and ACE2 in host cells can Be a possible candidate for COVID-19. *Front. Plant Sci.* 11, 601335. doi:10.3389/fpls.2020.601335

Jayalekshmi, H., Omanakuttan, A., Pandurangan, N., Vargis, S. V., Maneesh, M., Nair, G. B., et al. (2016). Clove bud oil reduces kynurenine and inhibits pqs A gene expression in *P. aeruginosa*. *Appl. Microbiol. Biotechnol.* 100 (8), 3681–3692. doi:10.1007/s00253-016-7313-2

Jo, E. R., Oh, J., and Cho, S. I. (2022). Inhibitory effect of thymol on tympanostomy tube biofilms of methicillin-resistant *Staphylococcus aureus* and ciprofloxacin-resistant *Pseudomonas aeruginosa*. *Microorganisms* 10 (9), 1867. doi:10.3390/microorganisms10091867

Kačániová, M., Vukovic, N. L., Čmiková, N., Galovičová, L., Schwarzová, M., Šimora, V., et al. (2023). Salvia sclarea essential oil chemical composition and biological activities. *Int. J. Mol. Sci.* 24 (6), 5179. doi:10.3390/ijms24065179

Karmakar, S., Choudhury, M., Das, A. S., Maiti, A., Majumdar, S., and Mitra, C. (2012). Clove (Syzygium aromaticum Linn) extract rich in eugenol and eugenol derivatives shows bone-preserving efficacy. *Nat. Prod. Res.* 26 (6), 500–509. doi:10.1080/14786419.2010.511216

Kart, D., Reçber, T., Nemutlu, E., and Sagiroglu, M. (2021a). Sub-inhibitory concentrations of ciprofloxacin alone and combinations with plant-derived compounds against *P. aeruginosa* biofilms and their effects on the metabolomic profile of *P. aeruginosa* biofilms. *Antibiotics* 10 (4), 414. doi:10.3390/antibiotics10040414

Kart, D., Reçber, T., Nemutlu, E., and Sagiroglu, M. (2021b). Sub-inhibitory concentrations of ciprofloxacin alone and combinations with plant-derived compounds against *P. aeruginosa* biofilms and their effects on the metabolomic profile of *P. aeruginosa* biofilms. *Antibiot. Basel* 10 (4), 414. doi:10.3390/antibiotics10040414

Kasthuri, T., Swetha, T. K., Bhaskar, J. P., and Pandian, S. K. (2022). Rapid-killing efficacy substantiates the antiseptic property of the synergistic combination of carvacrol and nerol against nosocomial pathogens. *Arch. Microbiol.* 204 (9), 590. doi:10.1007/s00203-022-03197-x

Khaleghi, M., Haghi, F., Gholami, M., Hourfar, H., Shahi, F., Mir Mousavi Zekoloujeh, A., et al. (2023). A fabricated hydrogel of hyaluronic acid/curcumin shows super-activity to heal the bacterial infected wound. *Amb. Express* 13 (1), 29. doi:10.1186/s13568-023-01533-y

Khan, F., Park, S. K., Bamunuarachchi, N. I., Oh, D., and Kim, Y. M. (2021). Caffeine-loaded gold nanoparticles: antibiofilm and anti-persister activities against pathogenic bacteria. *Appl. Microbiol. Biotechnol.* 105 (9), 3717–3731. doi:10.1007/s00253-021-11300-3

Kim, H. S., Cha, E., Ham, S. Y., Park, J. H., Nam, S., Kwon, H., et al. (2021). Linoleic acid inhibits *Pseudomonas aeruginosa* biofilm formation by activating diffusible signal factor-mediated *quorum* sensing. *Biotechnol. Bioeng.* 118 (1), 82–93. doi:10.1002/bit.27552

Kim, H. S., Lee, S. H., Byun, Y., and Park, H. D. (2015). 6-Gingerol reduces *Pseudomonas aeruginosa* biofilm formation and virulence via *quorum* sensing inhibition. *Sci. Rep.* 5, 8656. doi:10.1038/srep08656

Kosari, F., Taheri, M., Moradi, A., Alni, R. H., and Alikhani, M. Y. (2020). Evaluation of cinnamon extract effects on clbB gene expression and biofilm formation in *Escherichia coli* strains isolated from colon cancer patients. *BMC cancer* 20 (1), 267–268. doi:10.1186/s12885-020-06736-1

Köse, H., and Yapar, N. (2017). The comparison of various disinfectants? efficacy on *Staphylococcus aureus* and *Pseudomonas aeruginosa* biofilm layers. *Turk J. Med. Sci.* 47 (4), 1287–1294. doi:10.3906/sag-1605-88

Kouki, H., Polito, F., De Martino, L., Mabrouk, Y., Hamrouni, L., Amri, I., et al. (2022). Chemistry and bioactivities of six Tunisian Eucalyptus species. *Pharm. Basel.* 15 (10), 1265. doi:10.3390/ph15101265

Kozam, G. (1977). The effect of eugenol on nerve transmission. *Oral Surg. Oral Med. Oral Pathol.* 44 (5), 799–805. doi:10.1016/0030-4220(77)90390-5

Kumar, R., Chhibber, S., and Harjai, K. (2009). *Quorum* sensing is necessary for the virulence of *Pseudomonas aeruginosa* during urinary tract infection. *Kidney Int.* 76 (3), 286–292. doi:10.1038/ki.2009.183

Kumar Bose, S., Sharma, K., Chhibber, S., and Harjai, K. (2021). Therapeutic potential of nanolipoidal α-terpineol in combating keratitis induced by *Pseudomonas aeruginosa* in the murine model. *Int. J. Pharm.* 594, 120175. doi:10.1016/j.ijpharm.2020.120175

Lahiri, D., Nag, M., Dutta, B., Dey, S., Mukherjee, D., Joshi, S. J., et al. (2021). Antibiofilm and anti-*quorum* sensing activities of eugenol and linalool from Ocimum tenuiflorum against *Pseudomonas aeruginosa* biofilm. *J. Appl. Microbiol.* 131 (6), 2821–2837. doi:10.1111/jam.15171

Lakshmanan, D., Harikrishnan, A., Vishnupriya, S., and Jeevaratnam, K. (2019). Swarming inhibitory potential of cinnamtannin B1 from cinnamomum tamala T. Nees and eberm on *Pseudomonas aeruginosa*. *ACS Omega* 4 (16), 16994–16998. doi:10.1021/acsomega.9b02471

Lee, J., Wu, J., Deng, Y., Wang, J., Wang, C., Wang, J., et al. (2013). A cell-cell communication signal integrates *quorum* sensing and stress response. *Nat. Chem. Biol.* 9 (5), 339–343. doi:10.1038/nchembio.1225

Lee, J., and Zhang, L. (2015). The hierarchy *quorum* sensing network in *Pseudomonas aeruginosa*. *Protein Cell* 6 (1), 26–41. doi:10.1007/s13238-014-0100-x

Lee, W. H., Rohanizadeh, R., and Loo, C. Y. (2021). *In situ* functionalizing calcium phosphate biomaterials with curcumin for the prevention of bacterial biofilm infections. *Colloids Surf. B Biointerfaces* 206, 111938. doi:10.1016/j.colsurfb.2021.111938

Li, W. R., Ma, Y. K., Shi, Q. S., Xie, X. B., Sun, T. L., Peng, H., et al. (2018). Diallyl disulfide from garlic oil inhibits *Pseudomonas aeruginosa* virulence factors by inactivating key *quorum* sensing genes. *Appl. Microbiol. Biotechnol.* 102 (17), 7555–7564. doi:10.1007/s00253-018-9175-2

Li, W. R., Zeng, T. H., Zhang, Z. Q., Shi, Q. S., and Xie, X. B. (2023). Geraniol attenuates virulence factors by inhibiting *quorum* sensing of *Pseudomonas aeruginosa*. *Front. Microbiol.* 14, 1190619. doi:10.3389/fmicb.2023.1190619

Liu, L., Xiao, X., Li, K., Li, X., Yu, K., Liao, X., et al. (2020). Prevention of bacterial colonization based on self-assembled metal-phenolic nanocoating from rare-earth ions and catechin. *ACS Appl. Mat. Interfaces* 12 (19), 22237–22245. doi:10.1021/acsami.0c06459

Lone, S. A., and Ahmad, A. (2020). Inhibitory effect of novel Eugenol Tosylate Congeners on pathogenicity of Candida albicans. *BMC complementary Med. Ther.* 20 (1), 131. doi:10.1186/s12906-020-02929-0

Loo, C. Y., Rohanizadeh, R., Young, P. M., Traini, D., Cavaliere, R., Whitchurch, C. B., et al. (2016). Combination of silver nanoparticles and curcumin nanoparticles for enhanced anti-biofilm activities. *J. Agric. Food Chem.* 64 (12), 2513–2522. doi:10.1021/acs.jafc.5b04559

Lou, Z., Letsididi, K. S., Yu, F., Pei, Z., Wang, H., and Letsididi, R. (2019). Inhibitive effect of eugenol and its nanoemulsion on *quorum* sensing-mediated virulence factors and biofilm formation by *Pseudomonas aeruginosa*. *J. Food Prot.* 82 (3), 379–389. doi:10.4315/0362-028x.jfp-18-196

Lou, Z., Tang, Y., Song, X., and Wang, H. (2015). Metabolomics-based screening of biofilm-inhibitory compounds against *Pseudomonas aeruginosa* from burdock leaf. *Molecules* 20 (9), 16266–16277. doi:10.3390/molecules200916266

Lu, M., Li, Y., and Wu, M. X. (2021). Bacteria-specific pro-photosensitizer kills multidrug-resistant *Staphylococcus aureus* and *Pseudomonas aeruginosa*. *Commun. Biol.* 4 (1), 408. doi:10.1038/s42003-021-01956-y

Lu, M., Wong, K. I., Li, X., Wang, F., Wei, L., Wang, S., et al. (2022a). Oregano oil and harmless blue light to synergistically inactivate multidrug-resistant pseudomonas aeruginosa. *Front. Microbiol.* 13, 810746. doi:10.3389/fmicb.2022.810746

Lu, M., Wong, K. I., Li, X., Wang, F., Wei, L., Wang, S., et al. (2022b). Oregano oil and harmless blue light to synergistically inactivate multidrug-resistant *Pseudomonas aeruginosa*. *Front. Microbiol.* 13, 810746. doi:10.3389/fmicb.2022.810746

Luciardi, M. C., Blázquez, M. A., Alberto, M. R., Cartagena, E., and Arena, M. E. (2020). Grapefruit essential oils inhibit *quorum* sensing of *Pseudomonas aeruginosa*. *Food Sci. Technol. Int.* 26(3), 231–241. doi:10.1177/1082013219883465

Maisetta, G., Batoni, G., Caboni, P., Esin, S., Rinaldi, A. C., and Zucca, P. (2019). Tannin profile, antioxidant properties, and antimicrobial activity of extracts from two Mediterranean species of parasitic plant Cytinus. *BMC Complement. Altern. Med.* 19 (1), 82. doi:10.1186/s12906-019-2487-7

Marchese, A., Barbieri, R., Coppo, E., Orhan, I. E., Daglia, M., Nabavi, S. F., et al. (2017). Antimicrobial activity of eugenol and essential oils containing eugenol: a mechanistic viewpoint. *Crit. Rev. Microbiol.* 43 (6), 668–689. doi:10.1080/1040841x.2017.1295225

Mechmechani, S., Gharsallaoui, A., El Omari, K., Fadel, A., Hamze, M., and Chihib, N. E. (2022a). Hurdle technology based on the use of microencapsulated pepsin, trypsin and carvacrol to eradicate *Pseudomonas aeruginosa* and *Enterococcus faecalis* biofilms. *Biofouling* 38 (9), 903–915. doi:10.1080/08927014.2022.2151361

Mechmechani, S., Gharsallaoui, A., Fadel, A., El Omari, K., Khelissa, S., Hamze, M., et al. (2022b). Microencapsulation of carvacrol as an efficient tool to fight *Pseudomonas aeruginosa* and *Enterococcus faecalis* biofilms. *PLoS One* 17 (7), e0270200. doi:10.1371/journal.pone.0270200

Mechmechani, S., Gharsallaoui, A., Karam, L., El Omari, K., Fadel, A., Hamze, M., et al. (2023). Pepsin and trypsin treatment combined with carvacrol: an efficient strategy to fight *Pseudomonas aeruginosa* and *Enterococcus faecalis* biofilms. *Microorganisms* 11 (1), 143. doi:10.3390/microorganisms11010143

Mirzahosseinipour, M., Khorsandi, K., Hosseinzadeh, R., Ghazaeian, M., and Shahidi, F. K. (2020). Antimicrobial photodynamic and wound healing activity of curcumin encapsulated in silica nanoparticles. *Photodiagnosis Photodyn. Ther.* 29, 101639. doi:10.1016/j.pdpdt.2019.101639

Mombeshora, M., Chi, G. F., and Mukanganyama, S. (2021). Antibiofilm activity of extract and a compound isolated from Triumfetta welwitschii against *Pseudomonas aeruginosa*. *Biochem. Res. Int.* 2021, 9946183. doi:10.1155/2021/9946183

Namivandi-Zangeneh, R., Yang, Y., Xu, S., Wong, E. H. H., and Boyer, C. (2020). Antibiofilm platform based on the combination of antimicrobial polymers and essential oils. *Biomacromolecules* 21 (1), 262–272. doi:10.1021/acs.biomac.9b01278

Neyestani, Z., Ebrahimi, S. A., Ghazaghi, A., Jalili, A., Sahebkar, A., and Rahimi, H. R. (2019). Review of anti-bacterial activities of curcumin against *Pseudomonas aeruginosa*. *Crit. Rev. Eukaryot. Gene Expr.* 29 (5), 377–385. doi:10.1615/CritRevEukaryotGeneExpr.2019029088

Ni, N., Li, M., Wang, J., and Wang, B. (2009). Inhibitors and antagonists of bacterial *quorum* sensing. *Med. Res. Rev.* 29 (1), 65–124. doi:10.1002/med.20145

Nisar, M. F., Khadim, M., Rafiq, M., Chen, J., Yang, Y., and Wan, C. C. (2021). Pharmacological properties and health benefits of eugenol: a comprehensive review. *Oxid. Med. Cell Longev.* 2021, 2497354. doi:10.1155/2021/2497354

Niu, C., and Gilbert, E. S. (2004). Colorimetric method for identifying plant essential oil components that affect biofilm formation and structure. *Appl. Environ. Microbiol.* 70 (12), 6951–6956. doi:10.1128/aem.70.12.6951-6956.2004

Norizan, S. N., Yin, W. F., and Chan, K. G. (2013). Caffeine as a potential *quorum* sensing inhibitor. *Sensors (Basel)* 13 (4), 5117–5129. doi:10.3390/s130405117

Noumi, E., Merghni, A., M, M. A., Haddad, O., Akmadar, G., De Martino, L., et al. (2018). Chromobacterium violaceum and *Pseudomonas aeruginosa* PAO1: models for evaluating anti-*quorum* sensing activity of melaleuca alternifolia essential oil and its main component terpinen-4-ol. *Molecules* 23, 2672. doi:10.3390/molecules23102672

O'may, C., Ciobanu, A., Lam, H., and Tufenkji, N. (2012). Tannin derived materials can block swarming motility and enhance biofilm formation in *Pseudomonas aeruginosa*. *Biofouling* 28 (10), 1063–1076. doi:10.1080/08927014.2012.725130

Packiavathy, I. A., Priya, S., Pandian, S. K., and Ravi, A. V. (2014). Inhibition of biofilm development of uropathogens by curcumin - an anti-*quorum* sensing agent from Curcuma longa. *Food Chem.* 148, 453–460. doi:10.1016/j.foodchem.2012.08.002

Packiavathy, I. a.S. V., Agilandeswari, P., Musthafa, K. S., Pandian, S. K., and Ravi, A. V. (2012). Antibiofilm and *quorum* sensing inhibitory potential of Cuminum cyminum and its secondary metabolite methyl eugenol against Gram negative bacterial pathogens. *Food Res. Int.* 45 (1), 85–92. doi:10.1016/j.foodres.2011.10.022

Pazarci, O., Tutar, U., and Kilinc, S. (2019). Investigation of the antibiofilm effects of Mentha longifolia essential oil on titanium and stainless steel orthopedic implant surfaces. *Eurasian J. Med.* 51 (2), 128–132. doi:10.5152/eurasianjmed.2019.18432

Pearson, J. P., Passador, L., Iglewski, B. H., and Greenberg, E. P. (1995). A second N-acylhomoserine lactone signal produced by *Pseudomonas aeruginosa*. *Proc. Natl. Acad. Sci. U. S. A.* 92 (5), 1490–1494. doi:10.1073/pnas.92.5.1490

Pejčić, M., Stojanović-Radić, Z., Genčić, M., Dimitrijević, M., and Radulović, N. (2020). Anti-virulence potential of basil and sage essential oils: inhibition of biofilm formation, motility and pyocyanin production of *Pseudomonas aeruginosa* isolates. *Food Chem. Toxicol.* 141, 111431. doi:10.1016/j.fct.2020.111431

Pejin, B., Ciric, A., Glamoclija, J., Nikolic, M., and Sokovic, M. (2015). *In vitro* anti-*quorum* sensing activity of phytol. *Nat. Prod. Res.* 29 (4), 374–377. doi:10.1080/14786419.2014.945088

Persat, A., Nadell, C. D., Kim, M. K., Ingremeau, F., Siryaporn, A., Drescher, K., et al. (2015). The mechanical world of bacteria. *Cell* 161 (5), 988–997. doi:10.1016/j.cell.2015.05.005

Pesci, E. C., Milbank, J. B., Pearson, J. P., Mcknight, S., Kende, A. S., Greenberg, E. P., et al. (1999). Quinolone signaling in the cell-to-cell communication system of *Pseudomonas aeruginosa*. *Proc. Natl. Acad. Sci. U. S. A.* 96 (20), 11229–11234. doi:10.1073/pnas.96.20.11229

Piri-Gharaghie, T., Beiranvand, S., Riahi, A., Shirin, N. J., Badmasti, F., Mirzaie, A., et al. (2022). Fabrication and characterization of thymol-loaded chitosan nanogels: improved antibacterial and anti-biofilm activities with negligible cytotoxicity. *Chem. Biodivers.* 19 (3), e202100426. doi:10.1002/cbdv.202100426

Pourebrahim, M., Nejabatdoust, A., Mirmiran, S. D., Daemi, H. B., Meftahpour, H., and Salehzadeh, A. (2021). Aminoglycosides–loaded glucose-conjugated chitosan nanoparticles for *in vitro* antimicrobial and antibiofilm screening on Klebsiella pneumonia. *BioNanoScience* 11 (3), 901–914. doi:10.1007/s12668-021-00878-7

Prateeksha, Rao, C. V., Das, A. K., Barik, S. K., and Singh, B. N. (2019). ZnO/Curcumin nanocomposites for enhanced inhibition of *Pseudomonas aeruginosa* virulence via LasR-RhlR *quorum* sensing systems. *Mol. Pharm.* 16 (8), 3399–3413. doi:10.1021/acs.molpharmaceut.9b00179

Qais, F. A., Khan, M. S., Ahmad, I., Husain, F. M., Khan, R. A., Hassan, I., et al. (2021). Coumarin exhibits broad-spectrum antibiofilm and anti*quorum* sensing activity against gram-negative bacteria: *in vitro* and *in silico* investigation. *Vitro Silico Investigation* 6 (29), 18823–18835. doi:10.1021/acsomega.1c02046

Quatrin, P. M., Verdi, C. M., De Souza, M. E., De Godoi, S. N., Klein, B., Gundel, A., et al. (2017). Antimicrobial and antibiofilm activities of nanoemulsions containing Eucalyptus globulus oil against *Pseudomonas aeruginosa* and Candida spp. *Microb. Pathog.* 112, 230–242. doi:10.1016/j.micpath.2017.09.062

Radulović, N. S., Blagojević, P. D., Stojanović-Radić, Z. Z., and Stojanović, N. M. (2013). Antimicrobial plant metabolites: structural diversity and mechanism of action. *Curr. Med. Chem.* 20 (7), 932–952. doi:10.2174/092986713805219136

Rahimi, M., Piroozmand, A., Shayestehpour, M., Salamat, S., Peik Falak, F., Shakerimoghaddam, A., et al. (2023). Effect of curcumin nanoparticles and alcoholic extract of Falcaria vulgaris on the growth rate, biofilm, and gene expression in *Pseudomonas aeruginosa* isolated from burn wound infection. *Mol. Biol. Rep.* 50 (8), 6681–6690. doi:10.1007/s11033-023-08559-2

Ramasamy, M., Lee, J. H., and Lee, J. (2017a). Development of gold nanoparticles coated with silica containing the antibiofilm drug cinnamaldehyde and their effects on pathogenic bacteria. *Int. J. Nanomedicine* 12, 2813–2828. doi:10.2147/ijn.s132784

Ramasamy, M., Lee, J. H., and Lee, J. (2017b). Direct one-pot synthesis of cinnamaldehyde immobilized on gold nanoparticles and their antibiofilm properties. *Colloids Surf. B Biointerfaces* 160, 639–648. doi:10.1016/j.colsurfb.2017.10.018

Ramesh, G., Kaviyil, J. E., Paul, W., Sasi, R., and Joseph, R. (2022). Gallium-curcumin nanoparticle conjugates as an antibacterial agent against *Pseudomonas aeruginosa*: synthesis and characterization. *ACS Omega* 7 (8), 6795–6809. doi:10.1021/acsomega.1c06398

Rangel, M. L., De Aquino, S. G., De Lima, J. M., Castellano, L. R., and De Castro, R. D. (2018). *In vitro* effect of cinnamomum zeylanicum blume essential oil on Candida spp. involved in oral infections. *Evid. Based Complement. Altern. Med.* 2018, 4045013. doi:10.1155/2018/4045013

Rathinam, P., Murari, B. M., and Viswanathan, P. (2021). Biofilm inhibition and antifouling evaluation of sol-gel coated silicone implants with prolonged release of eugenol against *Pseudomonas aeruginosa*. *Biofouling* 37 (5), 521–537. doi:10.1080/08927014.2021.1933960

Rathinam, P., Vijay Kumar, H. S., and Viswanathan, P. (2017). Eugenol exhibits anti-virulence properties by competitively binding to *quorum* sensing receptors. *Biofouling* 33 (8), 624–639. doi:10.1080/08927014.2017.1350655

Rathinam, P., and Viswanathan, P. (2018). Anti-virulence potential of eugenol-rich fraction of Syzygium aromaticum against multidrug resistant uropathogens isolated from catheterized patients. *Avicenna J. Phytomed* 8 (5), 416–431.

Reddy, P., and Lokesh, B. R. (1994). Studies on anti-inflammatory activity of spice principles and dietary n-3 polyunsaturated fatty acids on carrageenan-lnduced inflammation in rats. *Ann. Nutr. Metabolism* 38 (6), 349–358. doi:10.1159/000177833

Reichhardt, C., Wong, C., Passos Da Silva, D., Wozniak, D. J., and Parsek, M. R. (2018). CdrA interactions within the *Pseudomonas aeruginosa* biofilm matrix safeguard it from proteolysis and promote cellular packing. *mBio* 9 (5), e01376-18. doi:10.1128/mBio.01376-18

Remold, S. K., Brown, C. K., Farris, J. E., Hundley, T. C., Perpich, J. A., and Purdy, M. E. (2011). Differential habitat use and niche partitioning by Pseudomonas species in human homes. *Microb. Ecol.* 62, 505–517. doi:10.1007/s00248-011-9844-5

Rosi-Marshall, E. J., Kincaid, D. W., Bechtold, H. A., Royer, T. V., Rojas, M., and Kelly, J. J. (2013). Pharmaceuticals suppress algal growth and microbial respiration and alter bacterial communities in stream biofilms. *Ecol. Appl.* 23 (3), 583–593. doi:10.1890/12-0491.1

Roudashti, S., Zeighami, H., Mirshahabi, H., Bahari, S., Soltani, A., and Haghi, F. (2017). Synergistic activity of sub-inhibitory concentrations of curcumin with ceftazidime and ciprofloxacin against *Pseudomonas aeruginosa quorum* sensing related genes and virulence traits. *World J. Microbiol. Biotechnol.* 33 (3), 50. doi:10.1007/s11274-016-2195-0

Rudrappa, T., and Bais, H. P. (2008). Curcumin, a known phenolic from Curcuma longa, attenuates the virulence of *Pseudomonas aeruginosa* PAO1 in whole plant and animal pathogenicity models. *J. Agric. Food Chem.* 56 (6), 1955–1962. doi:10.1021/jf072591j

Ryan, R. P., Fouhy, Y., Lucey, J. F., Crossman, L. C., Spiro, S., He, Y.-W., et al. (2006). Cell–cell signaling in Xanthomonas campestris involves an HD-GYP domain protein that functions in cyclic di-GMP turnover. *Proc. Natl. Acad. Sci.* 103 (17), 6712–6717. doi:10.1073/pnas.0600345103

Sadeghi Mohammadi, S., Vaezi, Z., and Naderi-Manesh, H. (2022). Improvement of anti-biofilm activities via co-delivery of curcumin and gentamicin in lipid-polymer hybrid nanoparticle. *J. Biomater. Sci. Polym. Ed.* 33 (2), 174–196. doi:10.1080/09205063.2021.1982159

Salehi, B., Mishra, A. P., Shukla, I., Sharifi-Rad, M., Contreras, M. D. M., Segura-Carretero, A., et al. (2018). Thymol, thyme, and other plant sources: health and potential uses. *Phytother. Res.* 32 (9), 1688–1706. doi:10.1002/ptr.6109

Salman, A. S. (2022). Antibacterial effect of onion's infusion and garlic's infusion on *Escherichia coli* isolated from urine samples. *science* 10, 11. doi:10.57238/jbb.2022.20107

Sánchez-López, E., Gomes, D., Esteruelas, G., Bonilla, L., Lopez-Machado, A. L., Galindo, R., et al. (2020). Metal-based nanoparticles as antimicrobial agents: an overview. *Nanomater. Basel* 10 (2), 292. doi:10.3390/nano10020292

Sarjit, A., Wang, Y., and Dykes, G. A. (2015). Antimicrobial activity of gallic acid against thermophilic Campylobacter is strain specific and associated with a loss of calcium ions. *Food Microbiol.* 46, 227–233. doi:10.1016/j.fm.2014.08.002

Sawant, S., Baldwin, T. C., Khan, H., and Rahman, A. (2022). Evaluation of the effect of leaf development in Plectranthus amboinicus L. On antimicrobial activity and virulence factors of *Pseudomonas aeruginosa* PAO1 and *Staphylococcus aureus* NCTC8325. *Curr. Microbiol.* 80 (1), 24. doi:10.1007/s00284-022-03126-7

Scandorieiro, S., Teixeira, F., Nogueira, M. C. L., Panagio, L. A., De Oliveira, A. G., Durán, N., et al. (2023). Antibiofilm effect of biogenic silver nanoparticles combined with oregano derivatives against carbapenem-resistant *Klebsiella pneumoniae*. *Antibiot. Basel* 12 (4), 756. doi:10.3390/antibiotics12040756

Schuster, M., Lostroh, C. P., Ogi, T., and Greenberg, E. P. (2003). Identification, timing, and signal specificity of *Pseudomonas aeruginosa quorum*-controlled genes: a transcriptome analysis. *J. Bacteriol.* 185 (7), 2066–2079. doi:10.1128/jb.185.7.2066-2079.2003

Sethupathy, S., Prasath, K. G., Ananthi, S., Mahalingam, S., Balan, S. Y., and Pandian, S. K. (2016). Proteomic analysis reveals modulation of iron homeostasis and oxidative stress response in *Pseudomonas aeruginosa* PAO1 by curcumin inhibiting *quorum* sensing regulated virulence factors and biofilm production. *J. Proteomics* 145, 112–126. doi:10.1016/j.jprot.2016.04.019

Shafiei, M., Abdi-Ali, A., Shahcheraghi, F., Vali, H., Shahbani Zahiri, H., and Akbari Noghabi, K. (2017). Analysis of *Pseudomonas aeruginosa* PAO1 biofilm protein profile after exposure to n-butanolic cyclamen coum extract alone and in combination with ciprofloxacin. *Appl. Biochem. Biotechnol.* 182 (4), 1444–1457. doi:10.1007/s12010-017-2409-4

Shah, S., Gaikwad, S., Nagar, S., Kulshrestha, S., Vaidya, V., Nawani, N., et al. (2019). Biofilm inhibition and anti-*quorum* sensing activity of phytosynthesized silver nanoparticles against the nosocomial pathogen *Pseudomonas aeruginosa*. *Biofouling* 35 (1), 34–49. doi:10.1080/08927014.2018.1563686

Shao, Y., Wu, C., Wu, T., Li, Y., Chen, S., Yuan, C., et al. (2018). Eugenol-chitosan nanoemulsions by ultrasound-mediated emulsification: formulation, characterization and antimicrobial activity. *Carbohydr. Polym.* 193, 144–152. doi:10.1016/j.carbpol.2018.03.101

Shariati, A., Asadian, E., Fallah, F., Azimi, T., Hashemi, A., Yasbolaghi Sharahi, J., et al. (2019). Evaluation of Nano-curcumin effects on expression levels of virulence genes and biofilm production of multidrug-resistant *Pseudomonas aeruginosa* isolated from burn wound infection in Tehran, Iran. *Infect. Drug Resist* 12, 2223–2235. doi:10.2147/idr.s213200

Shariati, A., Didehdar, M., Razavi, S., Heidary, M., Soroush, F., and Chegini, Z. (2022). Natural compounds: a hopeful promise as an antibiofilm agent against Candida species. *Front. Pharmacol.* 13, 917787. doi:10.3389/fphar.2022.917787

Shariff, M., Chatterjee, M., Morris, S. D., Paul, V., Vasudevan, A. K., Mohan, C. G., et al. (2022). Enhanced inhibition of *Pseudomonas aeruginosa* virulence factor production and biofilm development by sublethal concentrations of eugenol and phenyllactic acid. *Lett. Appl. Microbiol.* 75 (5), 1336–1345. doi:10.1111/lam.13803

Sharifian, P., Yaslianifard, S., Fallah, P., Aynesazi, S., Bakhtiyari, M., and Mohammadzadeh, M. (2020). Investigating the effect of nano-curcumin on the expression of biofilm regulatory genes of *Pseudomonas aeruginosa*. *Infect. Drug Resist* 13, 2477–2484. doi:10.2147/idr.s263387

Sharifi-Rad, M., Varoni, E. M., Iriti, M., Martorell, M., Setzer, W. N., Del Mar Contreras, M., et al. (2018). Carvacrol and human health: a comprehensive review. *Phytother. Res.* 32 (9), 1675–1687. doi:10.1002/ptr.6103

Shaw, E., and Wuest, W. M. (2020). Virulence attenuating combination therapy: a potential multi-target synergy approach to treat *Pseudomonas aeruginosa* infections in cystic fibrosis patients. *RSC Med. Chem.* 11 (3), 358–369. doi:10.1039/c9md00566h

Shukla, A., Parmar, P., Rao, P., Goswami, D., and Saraf, M. (2020). Twin peaks: presenting the antagonistic molecular interplay of curcumin with LasR and LuxR *quorum* sensing pathways. *Curr. Microbiol.* 77 (8), 1800–1810. doi:10.1007/s00284-020-01997-2

Shukla, A., Shukla, G., Parmar, P., Patel, B., Goswami, D., and Saraf, M. (2021). Exemplifying the next generation of antibiotic susceptibility intensifiers of phytochemicals by LasR-mediated *quorum* sensing inhibition. *Sci. Rep.* 11 (1), 22421. doi:10.1038/s41598-021-01845-8

Silva, E. C. I., Pratavieira, S., Salvador Bagnato, V., and Alves, F. (2023). Sonophotodynamic inactivation of *Pseudomonas aeruginosa* biofilm mediated by curcumin. *Biofouling* 39 (6), 606–616. doi:10.1080/08927014.2023.2241385

Smith, R. S., and Iglewski, B. H. (2003). *Pseudomonas aeruginosa quorum* sensing as a potential antimicrobial target. *J. Clin. Invest.* 112 (10), 1460–1465. doi:10.1172/jci20364

Spoering, A. L., and Lewis, K. (2001). Biofilms and planktonic cells of *Pseudomonas aeruginosa* have similar resistance to killing by antimicrobials. *J. Bacteriol.* 183 (23), 6746–6751. doi:10.1128/JB.183.23.6746-6751.2001

Sreelatha, S., Kumar, N., Yin, T. S., and Rajani, S. (2021). Evaluating the antibacterial activity and mode of action of thymol-loaded chitosan nanoparticles against plant bacterial pathogen xanthomonas campestris pv. campestris. *Front. Microbiol.* 12, 792737. doi:10.3389/fmicb.2021.792737

S'thebe, N. W., Aribisala, J. O., and Sabiu, S. (2023). Cheminformatics bioprospection of sunflower seeds' oils against *quorum* sensing system of *Pseudomonas aeruginosa*. *Antibiot. Basel.* 12 (3), 504. doi:10.3390/antibiotics12030504

Taganna, J. C., Quanico, J. P., Perono, R. M., Amor, E. C., and Rivera, W. L. (2011). Tannin-rich fraction from *Terminalia catappa* inhibits *quorum* sensing (QS) in Chromobacterium violaceum and the QS-controlled biofilm maturation and LasA staphylolytic activity in *Pseudomonas aeruginosa*. *J. Ethnopharmacol.* 134 (3), 865–871. doi:10.1016/j.jep.2011.01.028

Tang, H. B., Dimango, E., Bryan, R., Gambello, M., Iglewski, B. H., Goldberg, J. B., et al. (1996). Contribution of specific *Pseudomonas aeruginosa* virulence factors to pathogenesis of pneumonia in a neonatal mouse model of infection. *Infect. Immun.* 64 (1), 37–43. doi:10.1128/iai.64.1.37-43.1996

Tanhay Mangoudehi, H., Zamani, H., Shahangian, S. S., and Mirzanejad, L. (2020). Effect of curcumin on the expression of ahyI/R *quorum* sensing genes and some associated phenotypes in pathogenic Aeromonas hydrophila fish isolates. *World J. Microbiol. Biotechnol.* 36 (5), 70. doi:10.1007/s11274-020-02846-x

Tapia-Rodriguez, M. R., Bernal-Mercado, A. T., Gutierrez-Pacheco, M. M., Vazquez-Armenta, F. J., Hernandez-Mendoza, A., Gonzalez-Aguilar, G. A., et al. (2019). Virulence of *Pseudomonas aeruginosa* exposed to carvacrol: alterations of the *quorum* sensing at enzymatic and gene levels. *J. Cell Commun. Signal* 13 (4), 531–537. doi:10.1007/s12079-019-00516-8

Targhi, A. A., Moammeri, A., Jamshidifar, E., Abbaspour, K., Sadeghi, S., Lamakani, L., et al. (2021). Synergistic effect of curcumin-Cu and curcumin-Ag nanoparticle loaded niosome: enhanced antibacterial and anti-biofilm activities. *Bioorg Chem.* 115, 105116. doi:10.1016/j.bioorg.2021.105116

Topa, S. H., Palombo, E. A., Kingshott, P., and Blackall, L. L. (2020). Activity of Cinnamaldehyde on *quorum* Sensing and biofilm susceptibility to antibiotics in *Pseudomonas aeruginosa*. *Microorganisms* 8 (3), 455. doi:10.3390/microorganisms8030455

Topa, S. H., Subramoni, S., Palombo, E. A., Kingshott, P., Rice, S. A., and Blackall, L. L. (2018). Cinnamaldehyde disrupts biofilm formation and swarming motility of *Pseudomonas aeruginosa*. *Microbiology* 164 (9), 1087–1097. doi:10.1099/mic.0.000692

Ultee, A., Bennik, M. H., and Moezelaar, R. (2002). The phenolic hydroxyl group of carvacrol is essential for action against the food-borne pathogen Bacillus cereus. *Appl. Environ. Microbiol.* 68 (4), 1561–1568. doi:10.1128/aem.68.4.1561-1568.2002

Valliammai, A., Selvaraj, A., Yuvashree, U., Aravindraja, C., and Karutha Pandian, S. (2020). sarA-dependent antibiofilm activity of thymol enhances the antibacterial efficacy of rifampicin against *Staphylococcus aureus*. *Front. Microbiol.* 11, 1744. doi:10.3389/fmicb.2020.01744

Vandeputte, O. M., Kiendrebeogo, M., Rajaonson, S., Diallo, B., Mol, A., El Jaziri, M., et al. (2010). Identification of catechin as one of the flavonoids from Combretum albiflorum bark extract that reduces the production of *quorum*-sensing-controlled virulence factors in *Pseudomonas aeruginosa* PAO1. *Appl. Environ. Microbiol.* 76 (1), 243–253. doi:10.1128/aem.01059-09

Velázquez-Carriles, C., Macías-Rodríguez, M. E., Ramírez-Alvarado, O., Corona-González, R. I., Macías-Lamas, A., García-Vera, I., et al. (2022). Nanohybrid of thymol and 2D simonkolleite enhances inhibition of bacterial growth, biofilm formation, and free radicals. *Molecules* 27 (19), 6161. doi:10.3390/molecules27196161

Wagner, V. E., Bushnell, D., Passador, L., Brooks, A. I., and Iglewski, B. H. (2003). Microarray analysis of *Pseudomonas aeruginosa quorum*-sensing regulons: effects of growth phase and environment. *J. Bacteriol.* 185 (7), 2080–2095. doi:10.1128/jb.185.7.2080-2095.2003

Walczak, M., Michalska-Sionkowska, M., Olkiewicz, D., Tarnawska, P., and Warżyńska, O. (2021). Potential of carvacrol and thymol in reducing biofilm formation on technical surfaces. *Molecules* 26 (9), 2723. doi:10.3390/molecules26092723

Walsh, D. J., Livinghouse, T., Goeres, D. M., Mettler, M., and Stewart, P. S. (2019a). Antimicrobial activity of naturally occurring phenols and derivatives against biofilm and planktonic bacteria. *Front. Chem.* 7, 653. doi:10.3389/fchem.2019.00653

Walsh, D. J., Livinghouse, T., Goeres, D. M., Mettler, M., and Stewart, P. S. (2019b). Antimicrobial activity of naturally occurring phenols and derivatives against biofilm and planktonic bacteria. *Front. Chem.* 7, 653. doi:10.3389/fchem.2019.00653

Wang, W. Q., Feng, X. C., Shi, H. T., Wang, Y. M., Jiang, C. Y., Xiao, Z. J., et al. (2023). Biofilm inhibition based on controlling the transmembrane transport and extracellular accumulation of *quorum* sensing signals. *Environ. Res.* 221, 115218. doi:10.1016/j.envres.2023.115218

Wijesinghe, G. K., De Oliveira, T. R., Maia, F. C., De Feiria, S. B., Barbosa, J. P., Joia, F., et al. (2021a). Efficacy of true cinnamon (Cinnamomum verum) leaf essential oil as a therapeutic alternative for Candida biofilm infections. *Iran. J. Basic Med. Sci.* 24 (6), 787–795. doi:10.22038/ijbms.2021.53981.12138

Wijesinghe, G. K., Feiria, S. B., Maia, F. C., Oliveira, T. R., Joia, F., Barbosa, J. P., et al. (2021b). *In-vitro* antibacterial and antibiofilm activity of cinnamomum verum leaf oil against *Pseudomonas aeruginosa*, *Staphylococcus aureus* and *Klebsiella pneumoniae*. *Acad Bras Cienc* 93 (1), e20201507. doi:10.1590/0001-3765202120201507

Wira Septama, A., Arvia Chiara, M., Turnip, G., Nur Tasfiyati, A., Triana Dewi, R., Anggrainy Sianipar, E., et al. (2023). Essential oil of zingiber cassumunar roxb. And zingiber officinale rosc.: a comparative study on chemical constituents, antibacterial activity, biofilm formation, and inhibition of *Pseudomonas aeruginosa quorum* sensing system. *Chem. Biodivers.* 20 (6), e202201205. doi:10.1002/cbdv.202201205

Xue, B., Huang, J., Zhang, H., Li, B., Xu, M., Zhang, Y., et al. (2020). Micronized curcumin fabricated by supercritical CO(2) to improve antibacterial activity against *Pseudomonas aeruginosa*. *Artif. Cells Nanomed Biotechnol.* 48 (1), 1135–1143. doi:10.1080/21691401.2020.1815755

Yan, C., Kim, S. R., Ruiz, D. R., and Farmer, J. R. (2022). Microencapsulation for food applications: a review. *ACS Appl. Bio Mater* 5 (12), 5497–5512. doi:10.1021/acsabm.2c00673

Zangirolami, A. C., Dias, L. D., Blanco, K. C., Vinagreiro, C. S., Inada, N. M., Arnaut, L. G., et al. (2020). Avoiding ventilator-associated pneumonia: curcumin-functionalized endotracheal tube and photodynamic action. *Proc. Natl. Acad. Sci. U. S. A.* 117 (37), 22967–22973. doi:10.1073/pnas.2006759117

Zhang, Y., Sass, A., Van Acker, H., Wille, J., Verhasselt, B., Van Nieuwerburgh, F., et al. (2018). Coumarin reduces virulence and biofilm formation in *Pseudomonas aeruginosa* by affecting *quorum* sensing, type III secretion and C-di-GMP levels. *Front. Microbiol.* 9, 1952. doi:10.3389/fmicb.2018.01952

Zhang, Y., Zhu, Y., Gupta, A., Huang, Y., Murray, C. K., Vrahas, M. S., et al. (2014). Antimicrobial blue light therapy for multidrug-resistant Acinetobacter baumannii infection in a mouse burn model: implications for prophylaxis and treatment of combat-related wound infections. *J. Infect. Dis.* 209 (12), 1963–1971. doi:10.1093/infdis/jit842

Zhong, L., Ravichandran, V., Zhang, N., Wang, H., Bian, X., Zhang, Y., et al. (2020). Attenuation of *Pseudomonas aeruginosa quorum* sensing by natural products: virtual screening, evaluation and biomolecular interactions. *Int. J. Mol. Sci.* 21 (6), 2190. doi:10.3390/ijms21062190

Zhou, L., Zheng, H., Tang, Y., Yu, W., and Gong, Q. (2013). Eugenol inhibits *quorum* sensing at sub-inhibitory concentrations. *Biotechnol. Lett.* 35 (4), 631–637. doi:10.1007/s10529-012-1126-x

Zhu, M., Yang, Y., Wang, M., Li, X., Han, R., Chen, Q., et al. (2021). A deep insight into the suppression mechanism of Sedum alfredii root exudates on *Pseudomonas aeruginosa* based on *quorum* sensing. *Ecotoxicol. Environ. Saf.* 217, 112240. doi:10.1016/j.ecoenv.2021.112240

frontiers | Frontiers in Pharmacology

TYPE Original Research
PUBLISHED 09 May 2024
DOI 10.3389/fphar.2024.1389293

OPEN ACCESS

EDITED BY
Mingkai Li,
Air Force Medical University, China

REVIEWED BY
Michal Szeremeta,
Medical University of Bialystok, Poland
Xudong Gao,
Tianjin University, China

*CORRESPONDENCE
Yunpeng Yi,
yiyp@foxmail.com
Xiaohui Yang,
xiaohuiyang@qlu.edu.cn

†These authors have contributed equally to this work and share first authorship

RECEIVED 21 February 2024
ACCEPTED 24 April 2024
PUBLISHED 09 May 2024

CITATION
Zhang M, Lin S, Han L, Zhang J, Liu S, Yang X, Wang R, Yang X and Yi Y (2024), Safety and efficacy evaluation of halicin as an effective drug for inhibiting intestinal infections. *Front. Pharmacol.* 15:1389293. doi: 10.3389/fphar.2024.1389293

Safety and efficacy evaluation of halicin as an effective drug for inhibiting intestinal infections

Maolu Zhang[1,2†], Shuqian Lin[2†], Lianquan Han[1], Jiaming Zhang[2], Shaoning Liu[3], Xiuzhen Yang[3], Ruiming Wang[1], Xiaohui Yang[1*] and Yunpeng Yi[2*]

[1]State Key Laboratory of Biobased Material and Green Papermaking (LBMP), Qilu University of Technology (Shandong Academy of Sciences), Jinan, Shandong, China, [2]Shandong Provincial Animal and Poultry Green Health Products Creation Engineering Laboratory, Institute of Poultry Science, Shandong Academy of Agricultural Science, Jinan, Shandong, China, [3]Animal Products Quality and Safety Center of Shandong Province, Jinan, Shandong, China

Halicin, the first antibacterial agent discovered by artificial intelligence, exerts broad-spectrum antibacterial effects and has a unique structure. Our study found that halicin had a good inhibitory effect on clinical isolates of drug-resistant strains and *Clostridium perfringens* (*C. perfringens*). The safety of halicin was evaluated by acute oral toxicity, genotoxicity and subchronic toxicity studies. The results of acute toxicity test indicated that halicin, as a low-toxicity compound, had an LD_{50} of 2018.3 mg/kg. The results of sperm malformation, bone marrow chromosome aberration and cell micronucleus tests showed that halicin had no obvious genotoxicity. However, the results of the 90-day subchronic toxicity test indicated that the test rats exhibited weight loss and slight renal inflammation at a high dose of 201.8 mg/kg. Teratogenicity of zebrafish embryos showed that halicin had no significant teratogenicity. Analysis of intestinal microbiota showed that halicin had a significant effect on the intestinal microbial composition, but caused a faster recovery. Furthermore, drug metabolism experiments showed that halicin was poorly absorbed and quickly eliminated *in vivo*. Our study found that halicin had a good therapeutic effect on intestinal infection model of *C. perfringens*. These results show the feasibility of developing oral halicin as a clinical candidate drug for treating intestinal infections.

KEYWORDS

halicin, antimicrobial activities, ames test, safety evaluation, *Clostridium perfringens*

1 Introduction

Since their discovery, antibiotics, have played a crucial role in saving countless lives, and they have become the most effective tools for treating bacterial infections. However, the widespread use of antibiotics has led to an alarming increase in antibiotic-resistant bacteria, with the rapid spread and accumulation of resistance genes among bacterial populations (Crits-Christoph et al., 2022). Unfortunately, the development speed of new antibiotics is significantly lower than the emergence rate of antibiotic-resistant strains. Even antibiotics once hailed as the 'last line of defense' such as vancomycin and colistin, have now been found to have strains resistant to them (Gao et al., 2016). This poses significant challenges in the clinical treatment of bacterial infections. Currently, effective approaches for treating infections caused by antibiotic-resistant bacteria include the development of new antibiotics

10.3389/fphar.2024.1389293

TABLE 1 Antimicrobial activities of halicin (MIC, μg/mL).

Strain and number (G^-)	MIC (μg/mL)	Strain and number (G^+)	MIC (μg/mL)
E. coli (ATCC 25922)	8	*S. aureus* (ATCC 29213)	8
Salmonella (CVCC 3377)	8	*E. faecalis* (ATCC 29212)	4
Proteus (CMCC (B) 49027)	8	*B. subtilis* (ATCC 66333)	128
K. pneumoniae (ATCC 4352)	8	MRSA (ATCC 43300)	8
S. flexneri (CMCC 51572)	8	MRSA (BNCC 337371)	8
R. anatipestifer (ATCC 11845)	4	*S. pneumoniae* (ATCC 49619)	0.5
P. aeruginosa (ATCC 27853)	64	*C. perfringens* (ATCC 13124)	8
A. baumannii (ATCC 19606)	8	*Streptococcus suis* (ATCC 43765)	4
H. parasuis (ATCC 19417)	8		
R. anatipestife (ATCC 11845)	8		

[a]MRSA, Methicillin resistant *S. aureus*.

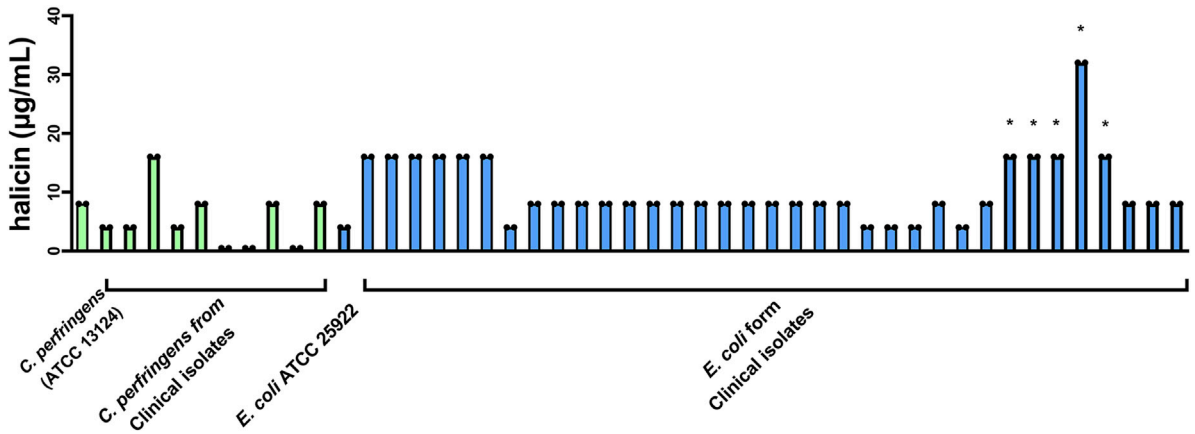

FIGURE 1
Determination of the MIC of halicin against clinical isolates of *C. perfringens* (green) and *E. coli* (blue). *: sulfonamide-resistant *E. coli*. Strain number and MIC are listed in Supplementary Table S1.

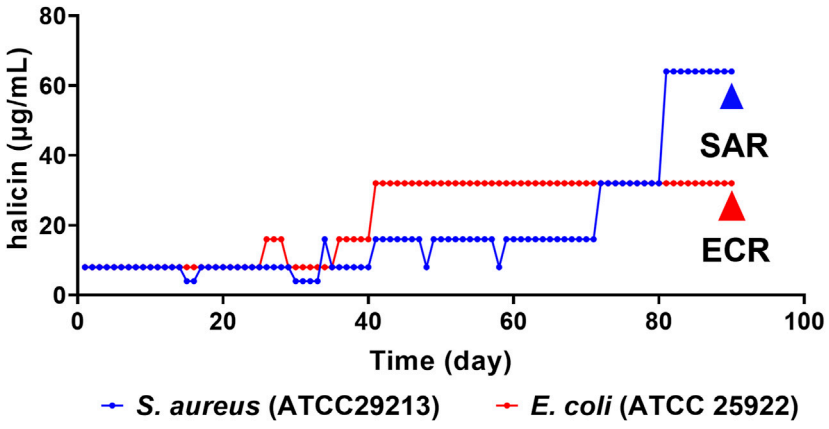

FIGURE 2
Multipassage resistance studies of halicin against *S. aureus* (ATCC 29213, blue) and *E. coli* (ATCC 25922, red). SAR (*S. aureus* ATCC 29213 resistant strains), MIC = 64 μg/mL; ECR (*E. coli* ATCC 25922 resistant strains), MIC = 32 μg/mL.

TABLE 2 Non-synonymous mutations identified in *S. aureus* resistant strains compared with *S. aureus*.

Gene ID	Position	References	Nucleotide variation	AA change	Gene	Annotation
NZ_CP094857.1	89038	C	G	P227A		Glycosyltransferase family 4 protein
NZ_CP094857.1	349779	C	T	V317M	*metC*	Bifunctional cystathionine gamma-lyase/gamma-synthase
NZ_CP094857.1	625195	G	C	E510D		Cation/H^+ exchanger domain-containing protein
NZ_CP094857.1	770810	G	A	R275P		Nucleotide-binding protein NWMN_0733
NZ_CP094857.1	912499	C	G	P20G		Putative undecaprenyl phosphate transporter
NZ_CP094857.1	1176345	C	T	A365V	*priA*	Primosomal protein N′
NZ_CP094857.1	1270992	G	C	G266A	*miaB*	tRNA-2-methylthio-N (6)-dimethylallyladenosine synthase
NZ_CP094857.1	1279253	G	A	G222S		Aquaporin family protein
NZ_CP094857.1	1340970	G	C	G71R	*agcS*	Amino acid carrier protein
NZ_CP094857.1	1396378	G	A	P231L		VWFA domain-containing protein
NZ_CP094857.1	1570973	C	T	E144K	*pbp3*	Penicillin-binding protein 3
NZ_CP094857.1	1595593	C	T	E33K	*prmA*	Ribosomal protein L11 methyltransferase
NZ_CP094857.1	1646174	G	A	T336I	*hisS*	Histidine--tRNA ligase
NZ_CP094857.1	1798638	C	T	R68H	*rot*	HTH-type transcriptional regulator rot
NZ_CP094857.1	1955821	C	T	R189Q	*nadE*	NH(3)-dependent NAD (+) synthetase
NZ_CP094857.1	2058829	G	A	G196R	*ilvD*	Dihydroxy-acid dehydratase
NZ_CP094857.1	2190609	C	T	L301F		Major facilitator superfamily (MFS) profile
NZ_CP094857.1	2550501	G	C	R88A		Putative NAD(P)H nitroreductase

The meaning of the italic values represents the name of the gene encoding the protein.

with diverse mechanisms of action, combination therapies, and antibiotic rotations (Mitcheltree et al., 2021; Selvarajan et al., 2022; Shukla et al., 2023).

In the era of rapid development of science and technology, artificial intelligence (AI) is significantly impacting various fields, especially new drug development and screening (Gupta et al., 2021). AI excels in processing and analyzing complex data, streamlining the drug development process by shortening research times, cutting costs, and enhancing success rates. During drug screening, AI algorithms efficiently search through extensive compound libraries to identify active candidates, improving both the speed and precision of this phase (Deng et al., 2021). To address the problem of drug resistance, AI offers new ways for finding antibiotics with novel action mechanisms. One example is the discovery of halicin, a unique broad-spectrum antibiotic, which was identified using AI from over 6,000 compounds in the Drug Repurposing Hub (Stokes et al., 2020).

Halicin has garnered substantial attention in recent years because of its potential therapeutic applications. As a potential broad-spectrum antibacterial agent, halicin showed remarkable efficacy against both Gram-positive and Gram-negative bacteria (Stokes et al., 2020; Booq et al., 2021; Higashihira et al., 2022). Halicin has a lower likelihood of inducing bacterial resistance than traditional antibiotics. This may be due to its unique mode of action or other factors, making it a promising candidate for further study. It is particularly noted for its effectiveness against *Clostridioides difficile* (*C. difficile*) and *A. baumannii* (*Acinetobacter baumannii*). *In vitro* studies showed that halicin could effectively inhibit the growth of drug-resistant strains. Meanwhile, halicin had antibacterial activity against *C. difficile* *in vivo* (Stokes et al., 2020).

Recently, it has been reported that halicin has exceptional membrane-disrupting effects on *Staphylococcus aureus* (*S. aureus*) (Higashihira et al., 2022). Furthermore, when combined with vancomycin, it exhibited synergistic effects and effectively inhibited the growth of *Enterococcus faecium* (Hussain et al., 2022). These findings highlight the significant research value of halicin in treating infections caused by antibiotic-resistant bacteria. However, current research on halicin mainly focuses on its remarkable antibacterial effect, and there is a lack of systematic evaluation of its drug properties. Additionally, studies on the toxicity of halicin and its potential adverse effects on humans are lacking.

Therefore, we conducted a preliminary pharmacodynamic and toxicological evaluation of halicin. We assessed its antibacterial activity against both common bacteria and clinically isolated drug-resistant strains, and conducted initial safety and efficacy assessments. To further investigate the effect of halicin on the gut microbiota, we collected and analyzed fecal samples from mice treated with halicin, and performed gut microbiota analysis. In addition, a model of intestinal infection with *C. perfringens* was used to evaluate the pharmacodynamics of halicin *in vivo*.

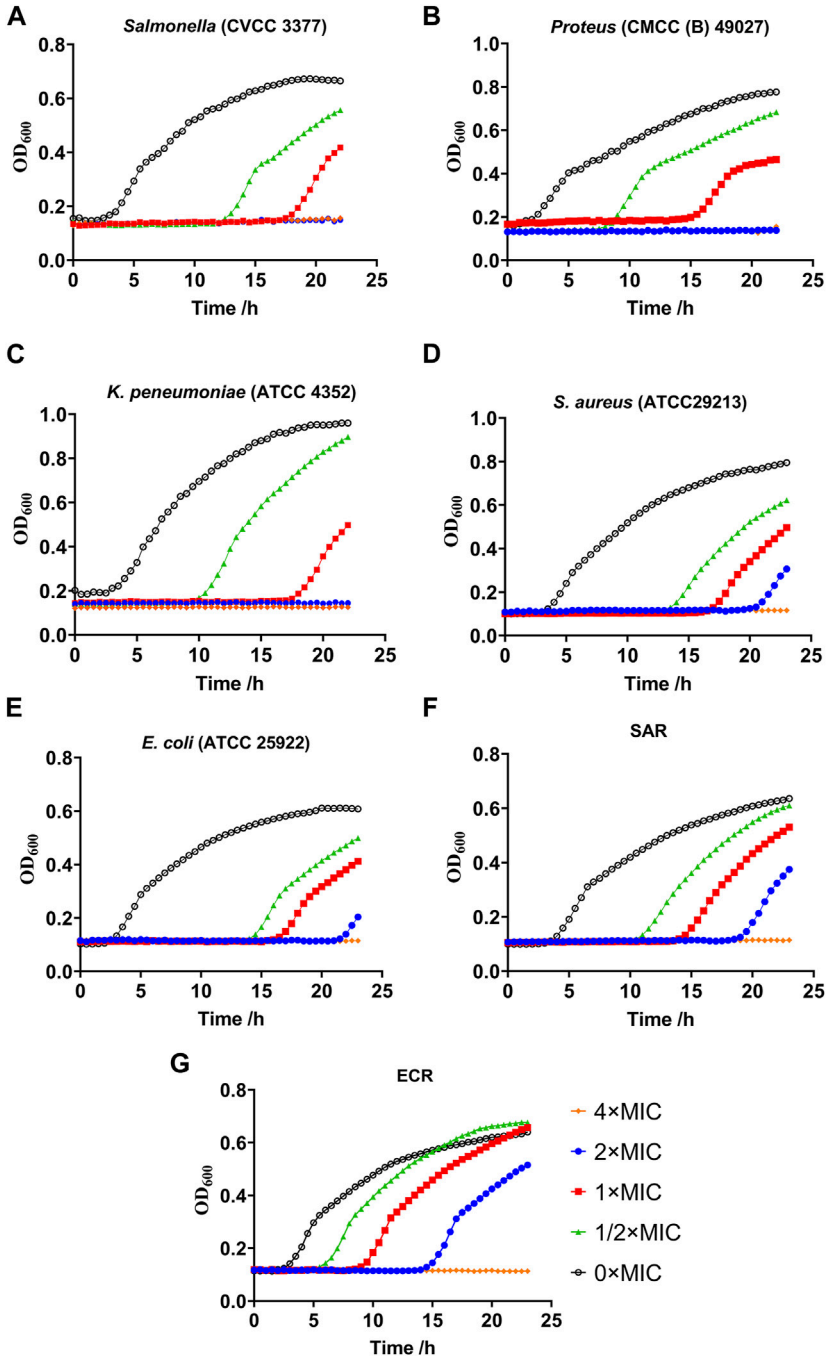

FIGURE 3
Growth kinetics curve assays of resistant *Salmonella* **(A)**, *Proteus* **(B)**, *Klebsiella pneumoniae* **(C)**, *S. aureus* **(D)**, *E. coli* **(E)**, SAR (*S. aureus* ATCC 29213 resistant strains) **(F)** and ECR (*E. coli* ATCC 25922 resistant strains) **(G)**.

2 Materials and methods

2.1 Strains and culture conditions

All bacterial strains used in this experiment were stored at −80°C in culture media containing 25% glycerol. The bacteria were revived in LB agar medium and prepared for experiments. The clinical isolates used in this study were obtained from the Chinese Academy of Agricultural Sciences. Detailed descriptions of these bacteria can be found in Supplementary Table S1.

2.2 Reagents and materials

Halicin was synthesized and identified using NMR in our laboratory (Purity, 99.5%). Carboxymethyl cellulose sodium

TABLE 3 Ames test results of halicin using *Salmonella typhimurium* strains TA97, TA98, TA100, and WP2uvrApKM101.

Treatment	Does (μg/plate)	TA97a		TA98		TA100		WP2uvApKM101	
		+S9	-S9	+S9	-S9	+S9	-S9	+S9	-S9
Vehicle control	0	117 ± 2.8	84 ± 5.7	31 ± 5.7	32 ± 2.8	140 ± 12.7	82 ± 4.2	181 ± 11.3	131 ± 7.1
2-AF	10	2052 ± 91.9	-	3,219 ± 106.1	-	2,234 ± 29.7	-	-	-
DDT	50	-	3,451 ± 53.7	-	2,985 ± 76.4	-	-	-	-
MSM	1	-	-	-	-	-	3,042 ± 69.3	-	926 ± 45.3
2-AT	10	-	-	-	-	-	-	546 ± 26.9	-
Halicin	45	0 ± 0	0 ± 0	0 ± 0	0 ± 0	0 ± 0	0 ± 0	0 ± 0	0 ± 0
	22.5	31 ± 8.5	0 ± 0	53 ± 7.1	55 ± 5.7	0 ± 0	0 ± 0	12 ± 5.7	75 ± 8.5
	11.2	151 ± 11.3	115 ± 8.5	43 ± 8.5	61 ± 14.1	152 ± 12.7	0 ± 0	168 ± 19.8	135 ± 22.6
	5.6	145 ± 5.7	82 ± 14.1	30 ± 12.7	27 ± 2.8	171 ± 11.3	121 ± 9.9	183 ± 15.6	169 ± 15.6

[a]2-AF: 2-Aminofluorene; DDT: fenaminosulf; MSM: methyl methanesulfonate; 2-AT: 2-Aminoanthracene.

(CMC-Na) was purchased from Shanghai Chemical Reagent Co., Ltd. Cyclophosphamide was purchased from Beyotime Biotechnology Co., Ltd. Ciprofloxacin was purchased from Energy Chemical Shanghai Co., Ltd.

2.3 Minimum inhibitory concentration (MIC)

The test strains were inoculated on the corresponding solid medium and incubated overnight at 37°C. A single colony was picked from the medium and inoculated into Luria Broth (LB), and then incubated overnight at 37°C with shaking at 220 rpm. The bacterial suspension was diluted to 0.5 McFarland turbidity with Mueller Hinton broth (MHB), and then dilute 100 times for later use. Halicin was added to the 96-well plate, and diluted it to concentrations of 128, 64, 32, 16, 8, 4, 2, 1, 0.5, 0.25, 0.125, and 0 μg/mL by gradient. The 96-well plate was incubated at 37°C for 16 h, followed by observing and recording the results. The MIC was determined as the concentration at which there was no visible colony growth was observed.

2.4 Continuous induction of antimicrobial resistance in bacteria

According to the determination method of MIC, the bacterial cells were diluted to different concentrations and mixed with halicin, then incubated overnight. Next day, the sample close to the MIC were selected for re-culture, the concentration was adjusted to 1 × 10^6 CFU/mL, and the above steps were repeated. Meanwhile, the strains were preserved daily, and the changes of MIC were recorded.

2.5 Growth kinetics curve

Briefly, *Escherichia coli* (ATCC 25922), *Salmonella* (CVCC 3377), *S. aureus* (ATCC 29213), *Klebsiella pneumoniae* (ATCC 4352) and *Proteus* (CMCC (B) 49027) (1 × 10^6 CFU/mL) were transferred into MHB. Different concentrations of halicin were added to achieve final concentrations of 4 ×, 2 ×, 1 ×, 1/2 ×, and 0 ×MIC. The optical density at 600 nm was determined.

2.6 Ames assay

After dissolving 2 mg of halicin in 1 mL DMSO, the solution was serially diluted in distilled water. The resulting dilutions were mixed with melted top agar to obtain final halicin concentrations of 45, 22.5, 11.2, and 5.6 μg/plate. Positive controls were used with and without the mammalian microsomal enzyme test (S9). The Ames test was conducted as previously described with modifications (Mello Silva Oliveira et al., 2016; Wahab et al., 2018; Fan et al., 2022). The experiments were performed in triplicate.

2.7 Animal source and housing conditions

Both female and male Sprague Dawley (SD) rats and ICR mice were provided by the Shandong Pengyue Experimental Animal Breeding Center. All experimental animals were housed in standard rodent housing conditions, with a temperature of 20°C–24°C, a relative humidity of 55% ± 10%, and a 12/12-h light/dark photoperiod. They had free access to water and food. All animals underwent a 2-week quarantine period and a physical examination before being provided. Prior to the experiment, animals were allowed a 3-day adaptation period. All animals were fasted overnight before the administration of treatment but had free access to water.

2.8 Acute oral toxicity test in ICR mice

Fifty male and female ICR mice weighing 18–22 g were randomly divided into five groups to conduct an acute oral toxicity test and determine the LD_{50}. The mice were given 4,000, 2000, 1,000, 500, and 0 mg/kg (control group) halicin in 0.1 mL per

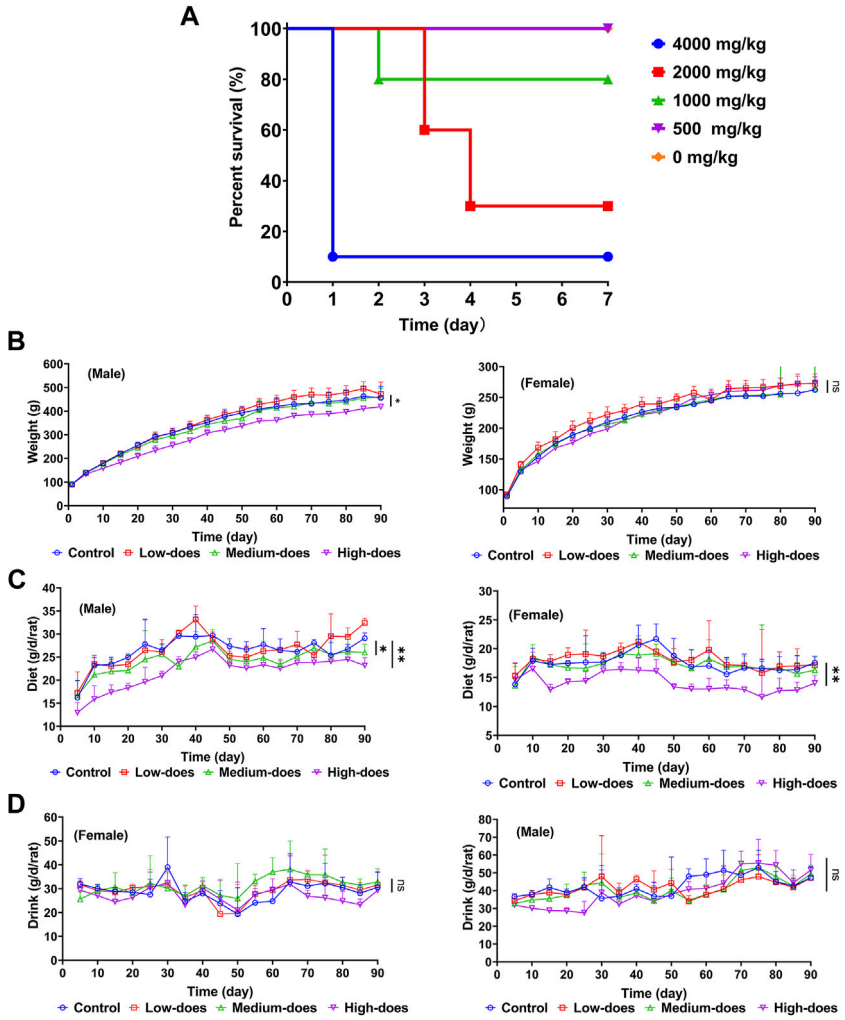

FIGURE 4
Safety evaluation of acute and subchronic toxicity of halicin. **(A)** Acute oral toxicity test of halicin in mice, LD_{50} = 2018.3 mg/kg (95% confidence interval: 1510.0 mg/kg-2738.3 mg/kg). **(B–D)**: 90-day subchronic toxicity test of halicin, assessing changes in rat body weight **(B)**, diet **(C)** and drinking **(D)**. Each dose group contains 5 female and 5 male rats (*, $p < 0.05$; **, $p < 0.01$; ns, $p > 0.05$). High-dose, 201.8 mg/kg; medium-dose, 100.9 mg/kg; low-dose, 50.5 mg/kg.

10 g of body weight using the gavage method. Following administration, their health status was monitored for a period of 7 days. Survival rates and signs of toxicity were recorded. Furthermore, a post-mortem examination was conducted to observe any pathological changes in the organs of deceased animals (Wang et al., 2017).

2.9 Sperm abnormality test in mice

Fifty male ICR mice, aged 6–8 weeks and weighing 25 ± 2 g, were randomly divided into the following five groups (n = 10 mice per group): the high-dose group (1009.2 mg/kg), the medium-dose group (504.6 mg/kg), the low-dose group (252.3 mg/kg), the negative control group (0 mg/kg), and the positive control group (40 mg/kg cyclophosphamide). The mice in the experimental groups were orally administered halicin via gavage. The treatment was conducted every 24 h for five consecutive days. After 35 days from the initial administration, the mice were euthanized by cervical dislocation. Mouse spermatozoa were smeared and then stained using eosin staining solution (Beyotime, China). Under low magnification, non-overlapping areas with a uniform distribution were selected. High magnification was then used to observe and record the percentage of sperm abnormalities and the number of different types of abnormalities present (OECD, 2018; Dong et al., 2022).

2.10 Chromosomal aberration test in mice

Forty ICR mice, with a 1:1 male: female ratio weighing 18–22 g were selected. The dose group settings were the same as 2.9. The mice received three consecutive administrations, spaced 24 h apart. Two to 4 hours before euthanasia, the mice were treated with 2 mM colchicine through intraperitoneal injection. After euthanasia, the bilateral femurs were promptly extracted and cleansed of any blood.

TABLE 4 Sperm abnormality test of halicin in mice.

Parameters	Group (mg/kg)				
	High-dose (1009.1)	Medium-dose (504.6)	Low-dose (252.3)	Negative	Positive
Number of mice	5	5	5	5	5
Number of sperms observed	5 × 1,000	5 × 1,000	5 × 1,000	5 × 1,000	5 × 1,000
Number of sperm abnormality	110	84	78	83	417
Abnormal ratio (%)	2.12 ± 0.38	1.68 ± 0.13	1.56 ± 0.09	1.62 ± 0.15	8.34 ± 0.47
Significance of difference	$p > 0.05$	$p > 0.05$	$p > 0.05$	-	$p < 0.05$
Abnormal sperms counted ratio (%)					
No hook	15.6 ± 5.5	16.7 ± 2.71	16.61 ± 3.11	17.26 ± 4.68	10.07 ± 1.23
Banana shape	42.52 ± 12.57	35.81 ± 4.52	35.98 ± 3.94	28.34 ± 4.12	10.58 ± 1.46
Amorphous	23.6 ± 12.44	29.69 ± 2.67	39.81 ± 3	39.72 ± 4.3	48.33 ± 4.33
Large round head	9.07 ± 4.02	11.96 ± 0.96	3.92 ± 3.58	6.28 ± 4.19	9.37 ± 1.03
Kinks tail	3.05 ± 2.79	2.44 ± 3.37	1.18 ± 2.63	3.61 ± 3.31	5.76 ± 0.94
Two head	3.05 ± 2.79	2.22 ± 3.04	1.33 ± 2.98	2.36 ± 3.24	5.52 ± 1.36
Two tail	3.11 ± 2.84	1.18 ± 2.63	1.18 ± 2.63	2.43 ± 3.33	4.84 ± 1.99

TABLE 5 Summary of chromosomal aberration frequencies in mouse bone marrow cells after halicin administration.

Group (mg/kg)	Number of mice	Number of cells at metaphase	Number of cells with chromosome aberration	Chromosome aberration (%)	*P*
High-does (1009.1)	5	5 × 100	7	1.4 ± 0.55	$p > 0.05$
Medium-does (504.6)	5	5 × 100	8	1.6 ± 0.89	$p > 0.05$
Low-does (252.3)	5	5 × 100	7	1.4 ± 1.14	$p > 0.05$
Negative	5	5 × 100	4	0.8 ± 0.84	-
Positive	5	5 × 100	93	18.6 ± 7.67	$p < 0.05$

Following the guidelines for veterinary drug experiments, bone marrow cells were collected for slide preparation. Samples were stained using Giemsa staining solution (Beyotime, China). A total of 100 cells with well-separated chromosomes in the metaphase stage were randomly selected from each sample for observation. Chromosomal aberrations, such as chromosome or chromatid breaks and chromosome deletions, were documented (OECD, 2016; Akagi et al., 2023).

2.11 Micronucleus experiment of mammalian bone marrow cells

Fifty ICR mice (weight 18–22 g), were divided into the following five groups (n = 10 mice per group). The dose group settings were the same as 2.9. The mice received two consecutive doses, separated by 24 h. All medications were given through tube feeding with 0.5% CMC-Na as the solvent. Six hours after the second administration, the mice were sacrificed. Both femurs were removed, the bone marrow cells were washed with 0.2 mL of calf serum, and the tablets were smeared. Slides were smeared and then stained using eosin staining solution (Beyotime, China). Using a double-blind procedure, 1,000 polychromatic erythrocytes cells were observed from each mouse (OECD, 2016; Guo et al., 2021).

2.12 90-Day subchronic toxicity assay

Forty rats (weight 100 ± 10 g) were randomly divided into four groups (n = 10 rats per group). Each rat was housed in a separate cage. The experiment comprised three treatment groups and one negative control group (0.5% CMC-Na). The dosage concentrations for the treatment groups were determined based on the LD_{50} results obtained from the acute oral toxicity test. The high-dose group received a concentration of 201.8 mg/kg, the medium-dose group received 100.9 mg/kg, and the low-dose group received 50.5 mg/kg. Administration was conducted via oral gavage, with a dosage of 1 mL per 100 g of body weight, for a continuous period of 13 weeks. Throughout the study period, body weight, food intake, and water consumption were recorded daily. Additionally, clinical

TABLE 6 Effects of halicin on bone marrow micronucleus and Polychromatic Erythrocytes/Red Blood Cells (PCE/RBC) ratio in mice.

Sex	Group (mg/kg)	PCE/RBC	PCE micronucleus (‰)	*P*
Female	High-does (1009.1)	0.72 ± 0.08	2.2 ± 0.8	$p < 0.01$
	Medium-does (504.6)	1.06 ± 0.07	0.8 ± 0.4	$p > 0.05$
	Low-does (252.3)	1.09 ± 0.06	1.2 ± 0.4	$p > 0.05$
	Negative	1 ± 0.06	0.6 ± 0.5	-
	Positive	0.5 ± 0.04	18.8 ± 1.9	$p < 0.01$
Male	High-does (1009.1)	0.76 ± 0.03	0.8 ± 0.8	$p < 0.01$
	Medium-does (504.6)	1.08 ± 0.11	1 ± 0.7	$p > 0.05$
	Low-does (252.3)	1.07 ± 0.09	0.6 ± 0.5	$p > 0.05$
	Negative	1 ± 0.05	0.8 ± 0.4	-
	Positive	0.51 ± 0.09	18.8 ± 2.6	$p < 0.01$

Drug toxicity was a crucial factor in determining the viability of a compound as a potential drug candidate. Our study evaluated the toxicity of halicin through various tests, including Ames test, acute oral toxicity, and sperm malformation tests in mice. The results showed that the LD_{50} of halicin was 2018.3 mg/kg, classifying it as a low-toxicity compound (OECD, 2002). Genotoxicity studies showed that halicin did not show significant sperm malformation or chromosomal teratogen damage at doses ranging from 252.3 mg/kg to 1009.1 mg/kg.

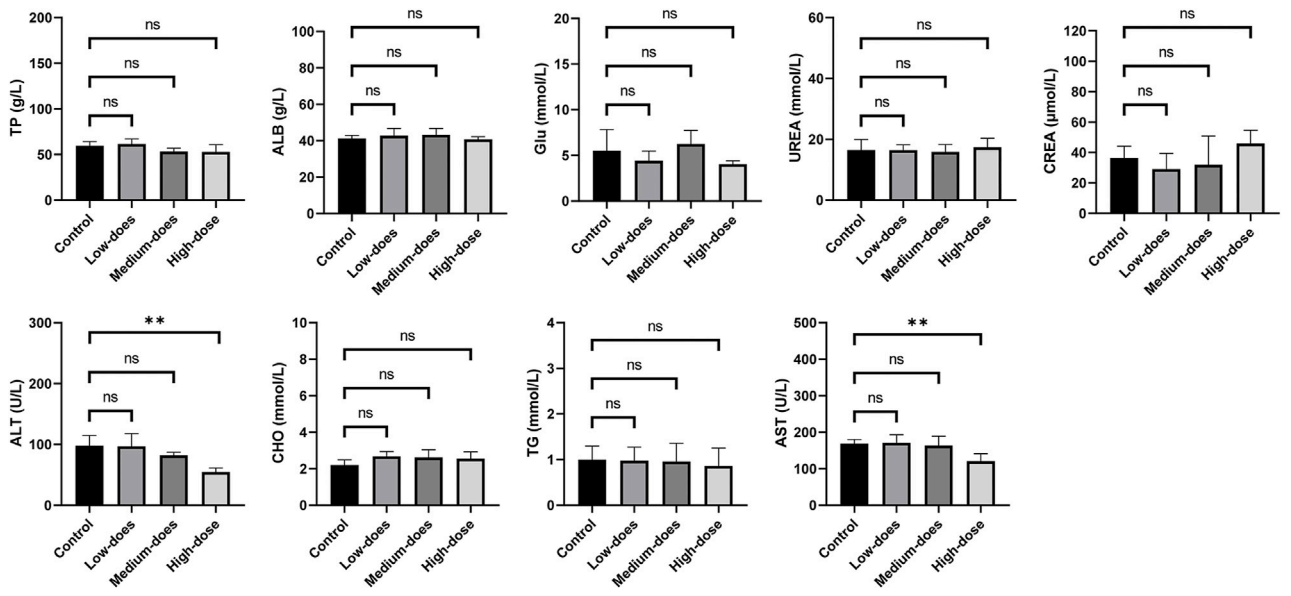

FIGURE 5
Serum biochemical indicators of 90-day subchronic toxicity test. TP: Total protein; ALB: Albumin; Glu: Glucose; UREA: Urea; CREA: Creatinine; ALT: Alanine aminotransferase; CHO: Cholesterol; TG: Triglycerides; AST: Aspartate aminotransferase. High-dose, 201.8 mg/kg; medium-dose, 100.9 mg/kg; low-dose, 50.5 mg/kg. **, $p < 0.01$.

observations and behavioral assessments were conducted. On day 45, which marked the mid-term of the study, blood samples were collected from the rats through the jugular vein. To minimize external interference with the experimental results, the rats were subjected to a 16-h fasting period before blood collection. Whole blood samples were stored in EDTA anticoagulant tubes, and routine hematological parameters were analyzed using a Mindray hematology analyzer.

Clinical chemistry parameters were measured using the ELLIPSE (YSBAERT) clinical chemistry analyzer. At both the mid-term (Day 45) and the end of the experiment (Day 90), five rats from each group were euthanized by cervical dislocation for necropsy. The hearts, livers, spleens, lungs, and kidneys of the rats were embedded in paraffin, stained with eosin and hematoxylin, and observed under a microscope to assess the impact of the treatment on their organs (OECD, 2018; Guefack et al., 2022).

2.13 Zebrafish embryotoxicity test

Under controlled laboratory settings, wild-type zebrafish of strain AB were maintained under a 14/10-h light/dark

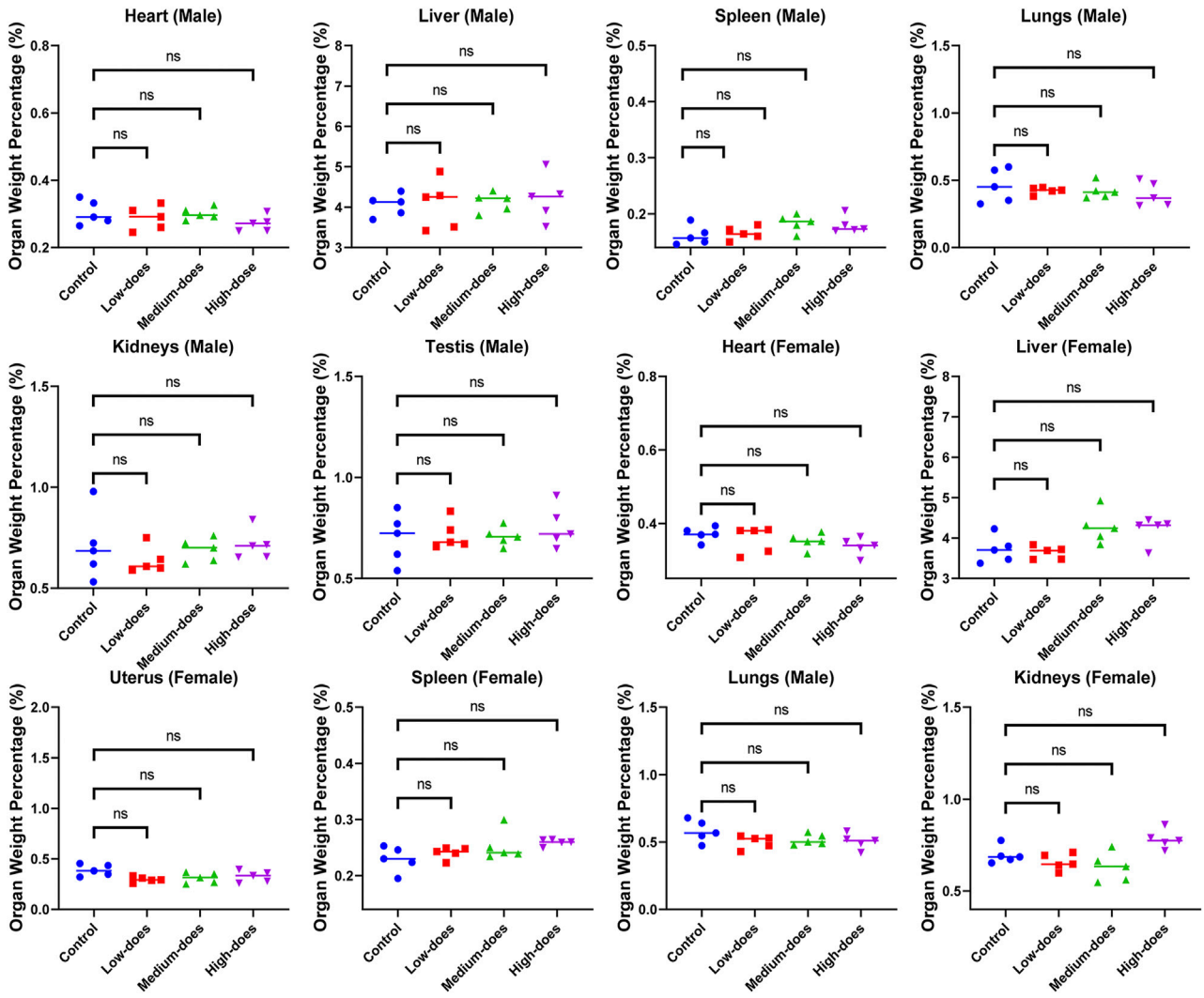

FIGURE 6
Effect of halicin on organ weight ratio of rats at the end of 90-day subchronic toxicity test. High-dose, 201.8 mg/kg; medium-dose, 100.9 mg/kg; low-dose, 50.5 mg/kg.

photoperiod at a constant temperature of 27°C. Approximately 4–5 h prior to the embryotoxicity assay, zebrafish ova were harvested. We primarily utilized ova that had progressed to the blastula stage of embryonic development (OECD, 2013; Adam et al., 2021). Approximately 4–5 h after the fertilization of zebrafish oocytes, halicin was introduced into the culture medium. We employed a 32-well plate format, allocating 20 oocytes to each experimental group. Concentrations of halicin in the culture medium were 128, 64, 32, 16, and 8 μM. As a control, 0.2% DMSO was used. The cultures were maintained at a constant ambient temperature of 27°C. After drug administration, survival of the zebrafish embryos was recorded for 72 h. The LC_{50} of halicin on zebrafish was obtained by this method.

For embryonic malformation studies, groups of 20 zebrafish embryos each were treated with halicin. The concentrations of the drug were set at 4, 2, 1, and 0.5 μM, in accordance with established protocols for zebrafish embryo acute toxicity test. Observations were conducted at 24, 48, and 72 h after fertilization using a microscope. The embryonic assessment focused on six specific teratogenic endpoints: pericardial edema, yolk sac edema, cardiac malformations, morphological body shape deformities, tail deformities, and craniofacial anomalies, as well as otolith abnormalities. To minimize the impact of random variability, these experiments were performed in triplicate (OECD, 1998).

2.14 Microbiological analysis

Six-week-old BALB/c mice, with an equal distribution of males and females ($n = 10$ per group), were selected for the study. The mice were divided into three groups: control group, halicin group, and ciprofloxacin (CIP) group. Administration was conducted via oral gavage at a dose of 10 mg/kg. The treatment was given once daily, with a 24-h interval, for a continuous period of 5 days. Fecal samples

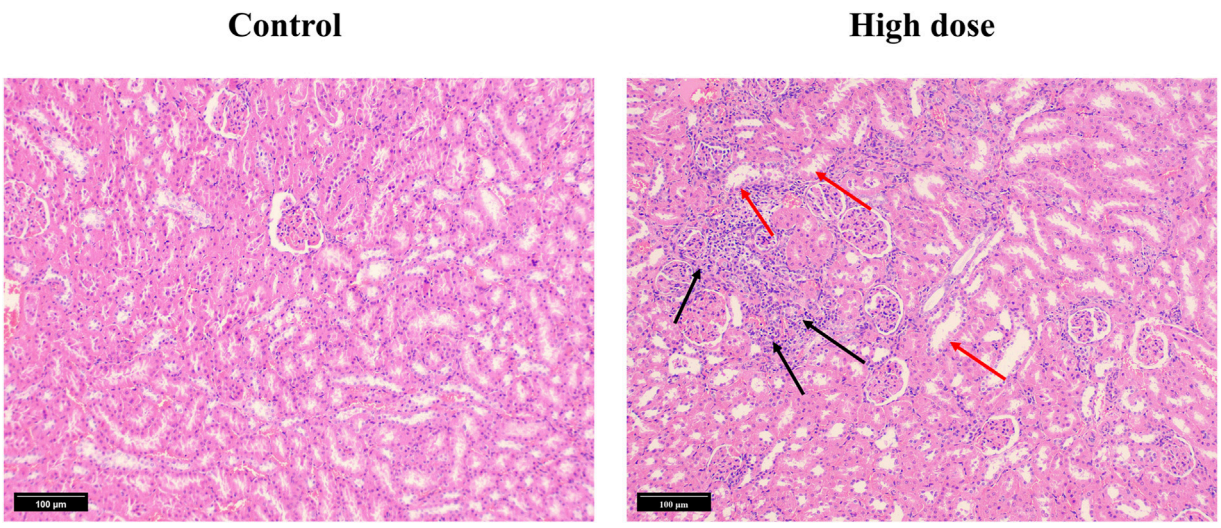

FIGURE 7
Hematoxylin and Eosin (HE) stained section of kidney tissue from the 90-day subchronic toxicity test of halicin. High-dose, 201.8 mg/kg. The black arrow indicates infiltration of inflammatory cells. The red arrow indicates separation of the basement membrane and epithelial cells.

were collected from the mice every day to analyze the changes in the gut microbiota following the drug treatment. The fecal samples were stored at −80°C on day 0, day 4, day 6, day 10, day 18, and day 26 for subsequent 16S rDNA analysis. Genomic DNA from the ground fecal samples was extracted using the Fecal Genomic DNA Extraction Kit (Beijing, Solarbio) for library construction and analysis. Amplification was performed using the primers 515F (5′-GTGCCAGCMGCCGCGGTAA-3′) and 907R (5′-CCGTCA ATTCCTTTGAGTTT-3′). Microbiome bioinformatics analysis was performed using QIIME 2 2019.4 (Bolyen et al., 2019). The sequences were subjected to quality filtering, denoising, merging, and removal of chimeras using the DADA2 plugin (Callahan et al., 2016). The amplicon sequence variants (ASVs) were classified using the classifier (classify-sklearn naive Bayes) from the Feature Classifier plugin, based on the Greengenes 13_8 99% OTU reference sequences (McDonald et al., 2012).

2.15 Pharmacokinetics of halicin

Eight SD rats weighing 200 g on average were used. They were split into two groups, each of which had two males and two females. The drugs were dissolved in a 0.5% CMC-Na aqueous solution to achieve the desired concentration and mixed thoroughly. The medication was given as a single oral gavage at a dose of 1 mL per 100 g body weight. A high-dose group (50 mg/kg) and a low-dose group (10 mg/kg) were set. Blood samples were taken at 0, 1, 2, 4, 8, 12, and 24 h after administration. Liquid chromatography-mass spectrometry (PerkinElmer, Qsight 210) analysis was conducted for the determination of drug levels in the plasma (Q1 262, Q3 133). The 0.1% formic acid in water and acetonitrile were used as the mobile phase. The time-plasma concentration data in the plasma were analyzed and calculated using the PK Solver plugin in Excel, and noncompartmental modeling was employed to calculate various PK parameters.

2.16 Mouse intestinal infection model

We prepared an *in vivo* infection model using 24 BALB/c mice ($n = 6$ per group) weighing 18–22 g. A single colony of *Clostridium perfringens* Type A was inoculated into 10 mL of liver broth gastric digestion medium. The culture was grown in an anaerobic chamber for 16 h, and the pellet was resuspended in PBS buffer. Bacterial counts were determined using the agar plate count method. Based on preliminary experiments, the mouse infection model was established through oral administration (10^9 CFU/mL). One hour after bacterial challenge, halicin was injected intraperitoneally. The mice were divided into four groups: the high-dose group (10 mg/kg), the low-dose group (5 mg/kg), the negative control group (0 mg/kg), and the positive control group (metronidazole, 10 mg/kg). The survival state of mice was observed and recorded.

2.17 Statistical analysis

The LD_{50} of halicin was calculated using the Karber formula and visualized using GraphPad Prism 8.0.2. The data for daily weight gain, food consumption, and organ weights were presented as mean ± standard deviation. Analysis was performed using one-way analysis of variance (ANOVA) to determine significant differences. Pairwise comparisons between all groups and the control group were conducted using the t-test. Significance was reported for results with a $p < 0.05$.

3 Results and discussion

3.1 Evaluation of antibacterial activity of halicin *in vitro*

As shown in Table 1, the *in vitro* activity test results demonstrated that halicin exhibited broad-spectrum

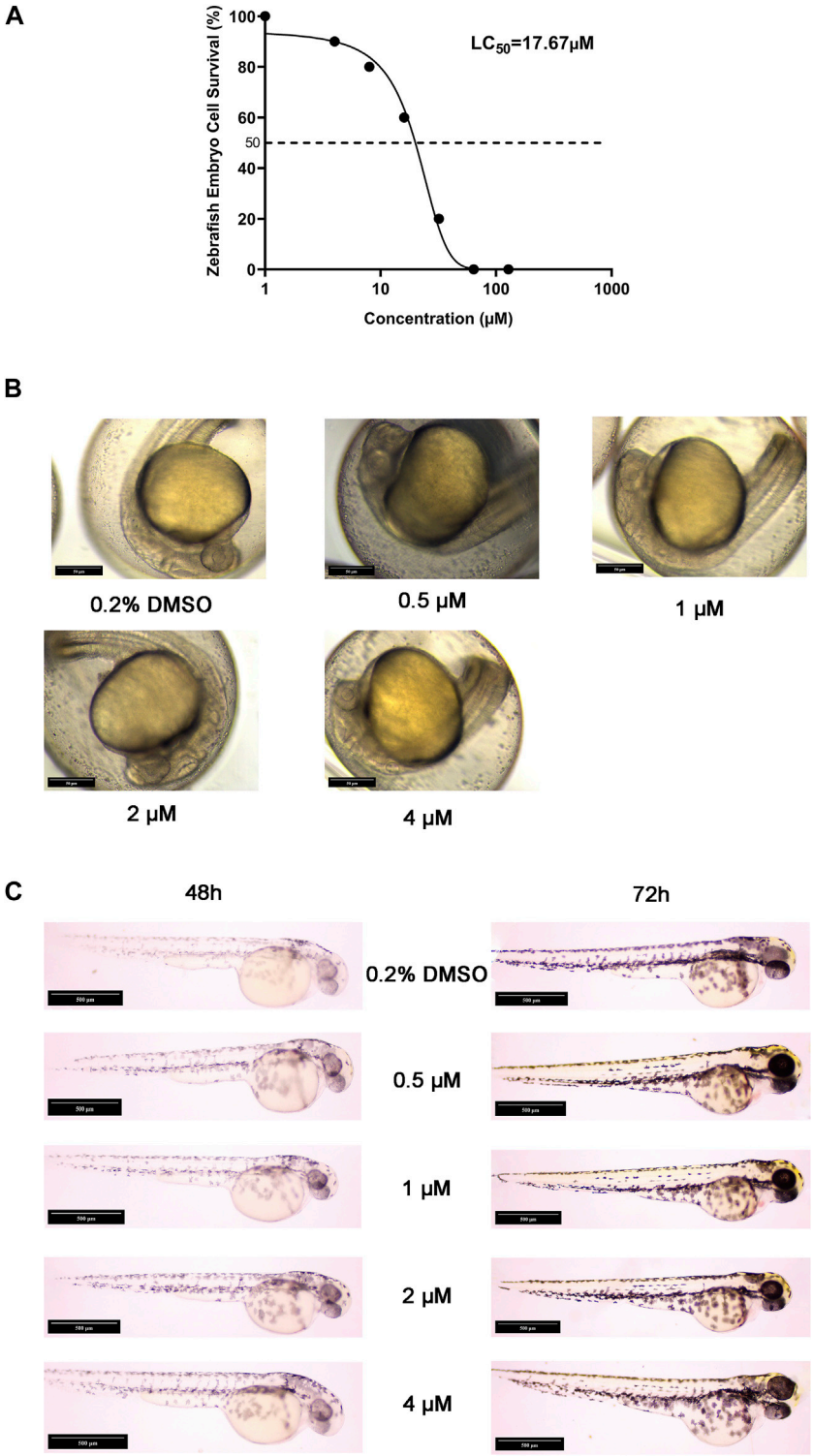

FIGURE 8
Acute embryotoxicity and embryonic malformation studies in zebrafish. **(A)** The LC_{50} value of halicin was determined with a 95% confidence interval ranging from 13.88 to 22.12 μM. **(B)** Zebrafish embryo sections at 24 h after fertilization. **(C)** Zebrafish embryo sections at 48 h (Left) and 72 h (Right) after fertilization.

antibacterial activity. Except for *Bacillus subtilis* and *Pseudomonas aeruginosa*, the MIC of halicin against other bacteria was less than 8 μg/mL.

At the same time, we found that halicin had a good inhibitory effect (MIC, 8 μg/mL) on *C. perfringens*. We conducted *in vitro* antimicrobial experiments using 10 clinical isolates of *C.*

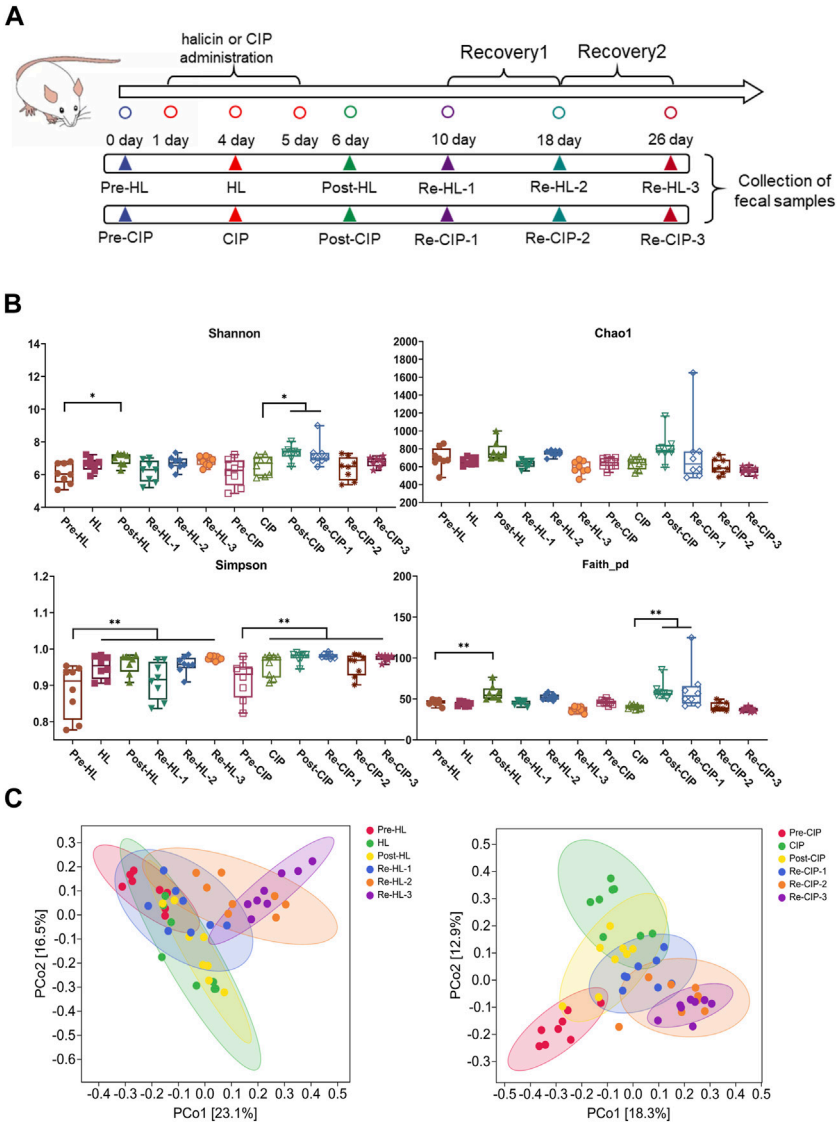

FIGURE 9
Changes in the richness and diversity of the fecal microbiota community of mice after antibiotic treatment. BALB/c mice (n = 10) were treated with halicin and ciprofloxacin for 3 days, respectively, and monitored for recovery after antibiotic withdrawal. **(A)** Experimental grouping and sampling arrangement. The pre-HL represents fecal samples from mice before halicin treatment; HL represents fecal samples from the first day after treatment; Post-HL represents fecal samples from the last day of halicin treatment; RE-HL represents fecal samples after halicin withdrawal; pre-CIP represents fecal samples from mice before ciprofloxacin treatment; CIP represents fecal samples from the first day after treatment; Post-CIP represents fecal samples from the last day of ciprofloxacin treatment; RE-CIP represents fecal samples after ciprofloxacin withdrawal. **(B)** Bacterial α-diversity analysis of fecal samples from different treatment groups. **(C)** β-diversity analysis was performed by PcoA methods.

perfringens strains and 36 clinical isolates of *E. coli* strains. The results showed that the MICs of halicin ranged from 0.5 to 16 μg/mL against clinical isolates of *C. perfringens* strains, and from 4 to 16 μg/mL against clinical isolates of *E. coli* strains (Figure 1). This indicates that halicin has a strong antibacterial activity against both bacteria. Interestingly, we found that *E. coli* with sulfonamide resistance genes showed an increase in the minimum inhibitory concentration (MIC, 16–32 μg/mL) when faced with halicin. This may imply that the mechanism of action of halicin is similar to that of sulfonamide drugs, and that sulfonamide resistance genes affect the sensitivity of resistant strains to halicin.

3.2 Resistance development and growth kinetics curve

After 90 days of continuous exposure to subminimal inhibitory concentration (0.5 × MIC) of halicin (Figure 2), the MIC of *S. aureus* (ATCC 29213) increased from 8 to 64 μg/mL. Resistant strains were isolated and sequenced using a second-generation sequencing scheme to identify the main cause of the increase in MIC. No clear genomic differences were observed between susceptible *S. aureus* (ATCC 29213, MIC 8 μg/mL) and resistant *S. aureus* strains (SAR, MIC 64 μg/mL), indicating that halicin resistance in SAR may be mediated by small chromosomal changes. Compared

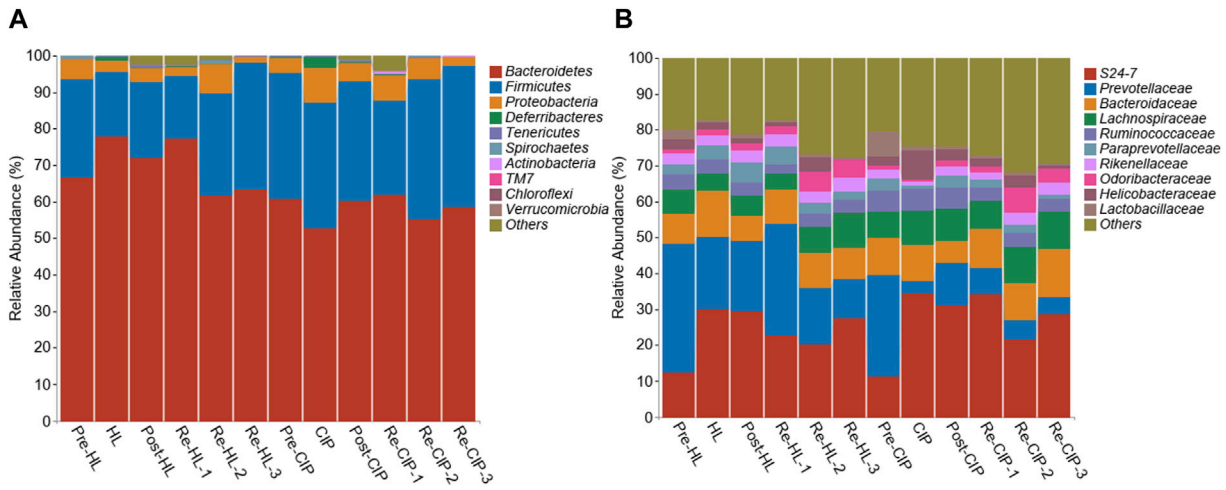

FIGURE 10
Composition of the fecal microbiota of mice before and after halicin or CIP treatment at the phylum **(A)** and genus **(B)** level.

with susceptible *S. aureus* (ATCC 29213), SAR revealed 18 SNPs in the coding regions (Table 2). SNP analysis of SAR suggested that resistance to halcin may be related to bacterial protein synthesis (*priA*, *prmA* and *rot*), transport (*metC and agcS*), methylation regulation (*miaB*) and nitroreduction (*nadE*). *nadE* mutations are important for metronidazole resistance (Danecek et al., 2011). The conversion of cytosine to thymine at nucleotide position 1,955,821 results in the conversion of arginine (codon CGA) to glutaminic acid (codon CAA) at amino acid position 188 of *the nadE* protein.

The main active group of metronidazole is 5-nitro group, and its antibacterial activity largely depends on the reduction reaction (Oliveira et al., 2018). The *nadE* gene encodes the NAD^+ synthase, a crucial enzyme in NAD^+ biosynthesis that is essential for maintaining intracellular NAD^+ levels. NAD^+ is a vital cofactor involved in various biochemical reactions, and affects the cellular reduction environment (Santos et al., 2020). Mutation or expression changes in the *nadE* gene can lead to adjustments in NAD^+ levels, which alters the state of cellular reduction, affects the activity of metronidazole and increases bacterial resistance to metronidazole. Given the structural similarity between the nitro group of halicin and metronidazole, we speculate that this is also the main reason for SAR resistance to halicin. Therefore, before halicin is applied in the clinical treatment of infections with multidrug-resistant pathogens, investigating the effect of altered NAD^+ levels on halicin activity and how variations in the *nadE* gene contribute to the formation of resistance is a key step in developing effective treatment protocols and preventing the development of resistance.

Growth kinetics curve assays showed that *Salmonella*, *Proteus* and *K. pneumoniae* were completely inhibited by halicin at 1/2 × to 4 × MIC (Figures 3A–C). Interestingly, *S. aureus* and *E. coli* still proliferated significantly *in vitro* under halicin treatment at 4 × MIC after 20 h. We compared the growth rates of the induced resistant bacteria (SAR and ECR) and the wild-type strains *S. aureus* (ATCC 29313) and *E. coli* (ATCC 25922) (Figures 3D–G). A specific phenomenon was observed where halicin-treated *S. aureus* started to grow rapidly after 16 h at 1 × MIC. This result confirmed that halicin was a bacteriostatic rather than a bactericidal agent against *S. aureus*. A similar phenomenon was observed in *E. coli* (ATCC 25922) and its resistant strain ECR. However, ECR exhibited a higher bacterial growth rate. At 1/2 × MIC, the growth of *E. coli* (ATCC 25922) was significantly inhibited during the initial 16 h. However, ECR exhibited noticeable growth at the 8 h.

3.3 Toxicity evaluation of halicin

3.3.1 Ames test

The Ames test is a biological assay that assesses the mutagenic potential of chemical compounds by exposing amino acid-requiring organisms to varying concentrations of chemicals and selecting for a reversion event. Only those cells that have undergone reversion to histidine/tryptophan prototrophy survive and grow (Guy, 2024). The halicin induced mutations in *Salmonella typhimurium* with or without S9 metabolic activation are shown in Table 3. The bacterial counts of all positive groups were more than twice that of the solvent control group. Halicin exhibited non-mutagenic characteristics at concentrations below 11.2 μg/plate. However, at 22.5 μg/plate of halicin, the bacterial counts of the four strains significantly decreased due to its antibacterial effect. At 11.2 μg/plate, halicin also significantly reduced the bacterial counts of TA100 (-S9 and +S9). Therefore, the Ames test cannot be used to determine the mutagenic effects of halicin at higher concentrations. This result may be attributed to halicin's bacteriostatic ability.

3.3.2 Acute oral toxicity test in ICR mice

We studied the acute oral toxicity of halicin *in vivo*, as this could provide a dose reference for further toxicity evaluation (Figure 4A). At a dose of 4,000 mg/kg, ICR mice showed clinical symptoms of poisoning such as reduced motor activity, weakness, and drowsiness, and died within 2–24 h with a 7-day survival rate of 10%. At a dose of 2000 mg/kg, the mice died 3–4 days after administration. At a

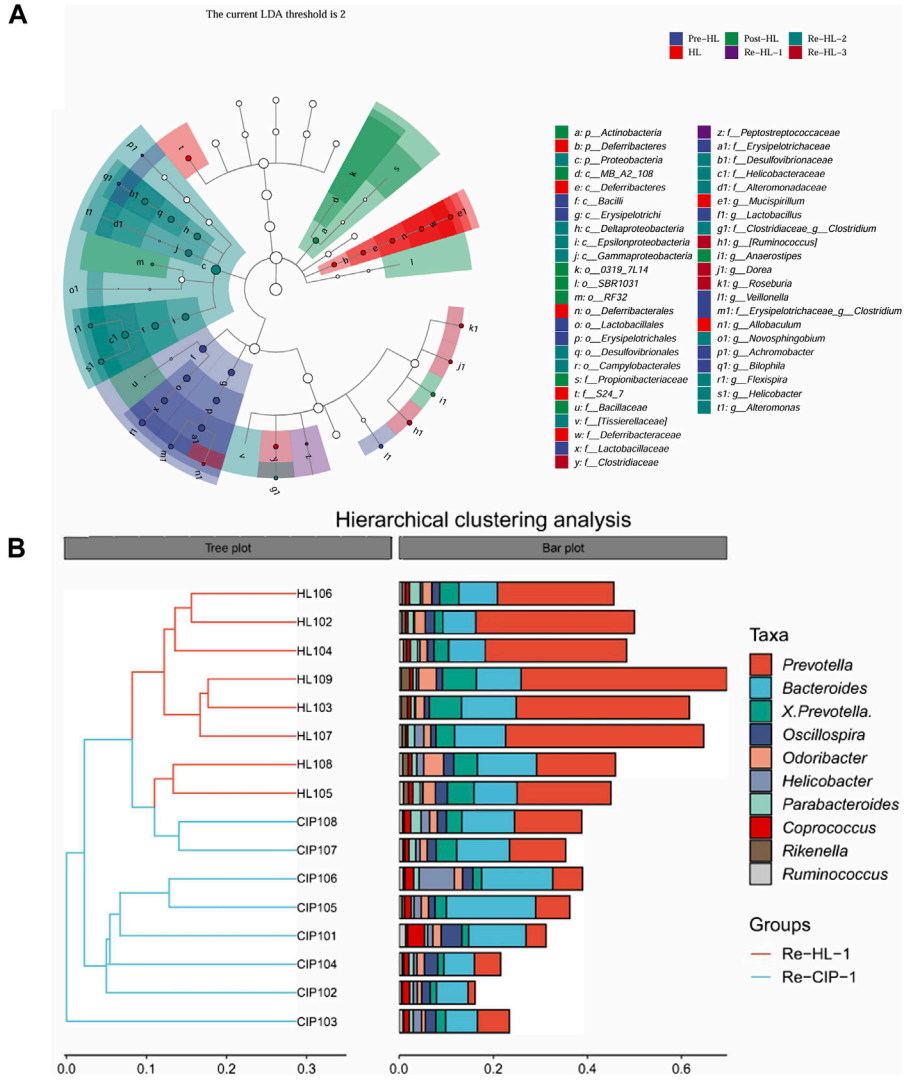

FIGURE 11
Differentially represented bacterial families after antibiotic treatment with halicin or CIP compared to no treatment. **(A)** Lefse analysis identified the microbes that showed significant differences in gut microbiota abundance at different time points of halicin treatment. **(B)** Differences in intestinal flora between the HL and CIP groups on the first day of the recovery period.

TABLE 7 PK parameters of halicin in rat.

PK parameter	Low dose (10 mg/kg)	High dose (50 mg/kg)
λz (1/h)	0.068 ± 0.016	0.085 ± 0.0016
$T_{1/2}$λz (h)	10.32 ± 2.22	8.57 ± 0.22
T_{max} (h)	1.33 ± 1.41	1.33 ± 1.41
C_{max} (ng/mL)	40.99 ± 2.37	64.25 ± 1.98
$AUC_{0\text{-last}}$ (h·ng/mL)	318.05 ± 31.27	459.58 ± 34.53
$AUC_{0\text{-}\infty}$ (h·ng/mL)	395.88 ± 42.41	510.86 ± 46.62
Vd/F (mL/kg)	375074.55 ± 41944.37	828269.08 ± 70840.29
Cl/F (mL/h/kg)	25360.4 ± 2661.85	58983.17 ± 7041.30
MRT_{last} (h)	7.58 ± 0.41	5.85 ± 0.13

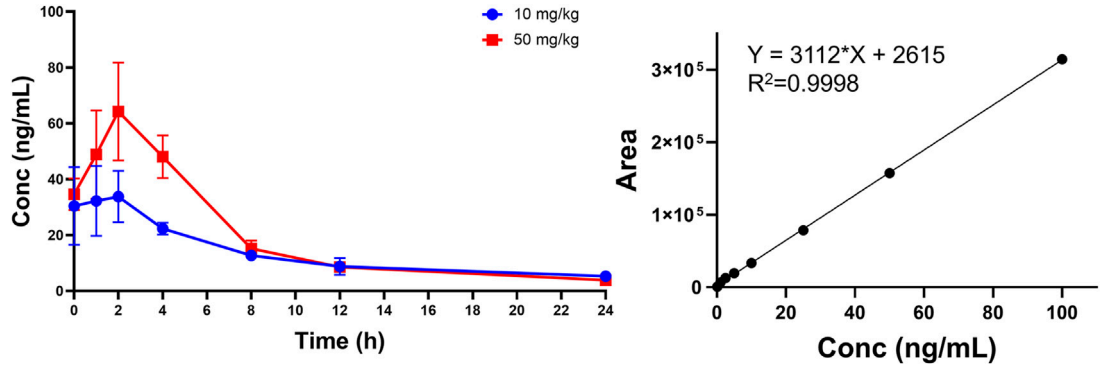

FIGURE 12
Plasma concentration-time curve of halicin after oral administration.

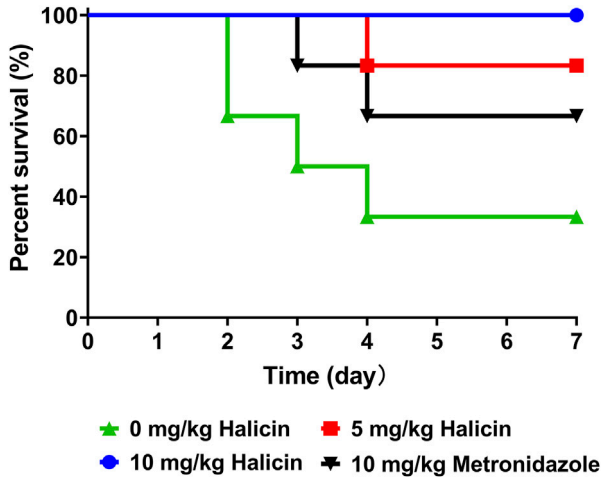

FIGURE 13
Effects of halicin on a mice model of *C. perfringens* infection.

dose of 1,000 mg/kg, only a few mice died on the second day and the survival rate was 80% at 7 days. At a dose of 500 mg/kg, all mice were normal and none died. Based on the dose-mortality relationship, the LD_{50} of halicin in mice was estimated to be 2018.3 mg/kg (95% confidence interval: 1510.0 mg/kg–2738.3 mg/kg) by the Bliss method.

3.3.3 Mice sperm abnormality test

To further assess the genetic toxicity of halicin, we performed a sperm teratogenicity test in mice. The ratio of sperm morphological abnormalities and the proportions of different types of malformations are shown in Table 4 and Supplementary Figure S1A. The proportions of abnormal sperm in halicin treatment groups (high-dose 1009.1 mg/kg, medium-dose 504.6 mg/kg, and low-dose 252.3 mg/kg) were not significantly different from those in the negative control group ($p > 0.05$), and the ratio of sperm abnormalities in the three groups were significantly lower than in the cyclophosphamide group (positive control), indicating that halicin did not cause sperm morphological abnormalities at the three dose levels.

3.3.4 Chromosome aberration test of mammalian bone marrow cells

We further conducted the chromosomal aberration experiment in mouse bone marrow cells (Table 5, Supplementary Figure S1B). There was no significant difference between the negative control group and halicin groups (252.3 mg/kg to 1009.1 mg/kg) ($p > 0.05$). These results indicate that halicin had no significant teratogenic effect on bone marrow cells.

3.3.5 Micronucleus experiment of mammalian bone marrow cells

To further investigate the impact of halicin on the internal structure of chromosomes, and to ensure the reliability of safety experiments, we conducted a bone marrow erythrocyte micronucleus test in addition to the chromosomal aberration assay. The results showed that there was no significant difference in micronucleus ratio between the negative control group and the medium (504.6 mg/kg) and low-dose (252.3 mg/kg) of halicin groups ($p > 0.05$) (Table 6). However, a significant difference was observed between the high-dose (1009.1 mg/kg) and negative control groups ($p < 0.01$). This suggests that halicin, at a concentration of 1009.1 mg/kg, could lead to cellular stress or toxicological effects. The number of micronuclei in all halicin-treated groups and the negative control group were significantly lower than that in the cyclophosphamide group ($p < 0.01$).

3.3.6 90-Day subchronic toxicity assay

We subsequently conducted a 90-day subchronic toxicity test to evaluate the long-term effects of halicin on rats. During the experiment, we monitored the body weight, diet, and water intake of the model animals. The results showed that there was no significant difference in the body weight of female rats between the control group and halicin treatment groups during the experimental period ($p > 0.05$). However, the body weight of male rats in the high-dose group (201.8 mg/kg) was significantly lower than that of the control group ($p < 0.05$) (Figure 4B). This might be related to the different degree of drug metabolism in their bodies. In terms of diet, there were significant differences between the control and the high and medium dose of halicin treatment groups of male rats. No significant differences were noted between the control group and the low-dose group (50.5 mg/kg) ($p > 0.05$)

during the 90-day diet monitoring. In female rats, only the high-dose group (201.8 mg/kg) was significantly different from the control group ($p < 0.01$) (Figure 4C). In addition, it was observed that there were no significant changes in water consumption and mental states across all dosage groups (Figure 4D). No mortality was recorded in any experimental group. Moreover, we examined a large number of blood indicators at 45 and 90 days, most of which did not show significant differences (Figure 5; Supplementary Figure S2–S4). It was found that high-dose halicin treatment significantly reduced the levels of serum alanine aminotransferase (ALT) and aspartate aminotransferase (AST) in rats compared with the control group ($p < 0.01$). The emergence of these results may be related to the renal toxicity caused by halicin. We checked the reference ranges for the hematology and serum biochemistry indices provided by the manufacturer of the purchased rats and found that their values were within the normal range (Kunutsor et al., 2015; Askari et al., 2016). At the end of the experiment, the rats were autopsied and the key organs were weighed (Figure 6). The results showed that there was no significant difference in the weight of organs between the control group and the halicin treatment groups ($p > 0.05$). During autopsy, spotty lesions were found in the kidneys of the high-dose group, and glomerulopathy was present. HE sections of kidney tissue showed that high dose of halicin (201.8 mg/kg) caused kidney lesions in rats, including separation of basement membrane and epithelial cells, and a small amount of inflammatory cell infiltration, which indicated that high dose of halicin had certain renal toxicity (Figure 7).

These findings provide important insight that halicin has a good safety and tolerability at dosages below 50.5 mg/kg, justifying further investigation into its potential therapeutic applications. It is important to note, however, that further research is necessary to fully understand the safety and efficacy of halicin in different animal models and ultimately in human subjects. Nonetheless, these results provide insight into the potential of halicin as a therapeutic agent (Dong et al., 2022a).

3.3.7 Acute embryotoxicity and embryonic malformation studies in zebrafish

Zebrafish were an excellent model organism, especially for the study of drug-induced embryonic teratogenesis, as they allowed for more direct and clear observation of embryonic conditions (Song et al., 2021). To investigate the genotoxicity of halicin, we utilized zebrafish for an embryonic teratogenicity experiment. Our findings indicate that the LC_{50} of halicin in zebrafish embryos is 17.64 μM (Figure 8A). We selected 4 μM as the maximum concentration for teratogenicity studies and observed the yolk sac, heart, body shape, tail, head, and ears of the zebrafish embryos at 24, 48, and 72 h after fertilization (Figures 8B, C). The results demonstrated no any significant teratogenic effects of halicin on the embryos, which is a cause for celebration.

3.4 Microbiological analysis

The *in vitro* activity and toxicity data suggest that halicin is suitable as a potential antibiotic for the treatment of intestinal bacterial infections. However, the effect of halicin on the intestinal microbiota has not been reported. Therefore, we investigated the effects of 15 mg/kg halicin to conduct intestinal microbiota (Figure 9A). The richness and diversity of the microbial community are reflected in its alpha diversity. Ciprofloxacin (CIP), a commonly used drug for the treatment of intestinal bacterial infections, was used as a positive control. We found that halicin and CIP increased Shannon ($p < 0.05$) and Faith_pd levels ($p < 0.01$) 1 day after withdrawal. The results indicated that the diversity and richness of the intestinal microbiota increased significantly after withdrawal, which may be because halicin and CIP are broad-spectrum antibiotics, which have a great impact on the intestinal microbiota after administration, resulting in intestinal microbiota disorder. In the halicin group, the Shannon and Faith_pd values returned to normal levels in the first recovery period, whereas in the CIP group, the Shannon and Faith_pd values recovered in the second recovery period (Figure 9B). We used PCoA methods to analyze beta diversity (Figure 9C). Halicin-treated samples showed no significant separation as the experiment progressed, whereas CIP-treated samples showed significant changes in microbial community. These results indicated that although halicin had a significant effect on gut microbiota, it made them recover faster. CIP treatment caused significant changes in the structure of gut microbiota, which did not return to normal levels 21 days after withdrawal.

The relative proportions of the different taxa were evaluated at the phylum, class, and genus levels (Figure 10). At the phylum level, there was no clear change before and after administration, and phyla mainly included Bacteroidetes, Firmicutes and Proteobacteria, accounting for 94.7%–99.59% of the total proportion, among which Bacteroidetes had the highest proportion (Figure 10A). At the genus level, the main taxon was *S24-7*, *Prevotellaceae*, *Bacteroidaceae*, *Lachnospiraceae*, *Ruminococcaceae*, *Paraprevotellaceae*, *Rikenellaceae*, *Odoribacteraceae*, *Helicobacteraceae*, and *Lactobacillaceae*. Halicin and CIP caused a significant decrease in the content of *Prevotellaceae* and *Lactobacillaceae* after administration. Halicin had less effect on the *Prevotellaceae* and *Lactobacillaceae* abundance than CIP, which did not restore these two genera to normal levels during the third recovery period (Figure 10B).

To further explore the effect of halicin on the intestinal bacterial structure at different time points, we performed Lefse analysis to identify different species at different time points (Figure 11A; Supplementary Figure S5). In the fecal samples collected during administration, there was no significant difference between the CIP-treated and halicin-treated groups at the phylum level; however, we found a special species in each group. In the halicin group, the abundance of *g_Allobaculum*, which has been reported to be associated with beneficial effects in organisms, was increased. In the CIP group administration, we found *g_Mucispirillum*, which has a protective effect on the intestinal mucosa, but mainly attaches to the intestinal epithelial mucosa and is not often found in feces (Supplementary Figure S5). We speculate that this may be related to serious damage to the mouse intestinal mucosal layer after CIP treatment, which affects the colonization of *g_Mucispirillum* in the intestinal mucosal layer. In the halicin group, we identified 15 marker species during the second recovery period, including *p_Proteobacteria, o_Campylobacterales, c_Epsilonproteobacteria, f_Helicobacteraceae, g_Helicobacter, c_Gammaproteobacteria, c_Deltaproteobacteria, f_Desulfovibrionaceae, o_Desulfovibrionales,*

g_Flexispira, g_Novosphingobium, f_Alteromonadaceae, g_Alteromonas, f_Tissierellaceae, f_Clostridiaceae, g_Clostridium. Interestingly, most of these marker species belonged to the phylum *Proteobacteria*. In the first recovery period, the CIP group had more marker species than the halicin group, totaling more than 50 specific species, most of which belonged to the phylum *Proteobacteria*. However, among these marker species, we identified many bacteria that have not been previously reported in the intestinal microbiota. We believe that these bacteria appeared because CIP seriously damaged the mouse intestinal microbiota structure, causing it to lose its resistance to external bacteria colonization. We performed cluster analysis on Re-HL-1 and Re-CIP-1 groups, and showed obvious cluster differences between the two groups (Figure 11B). This result showed that CIP severely disrupted the homeostasis of the gut microbial system in mice during this period.

3.5 Pharmacokinetics in rat

Further studies are necessary to fully elucidate the mechanism of action and the potential clinical applications of halicin. The pharmacokinetics (PK) of a drug determines its method of use and range of applications. Therefore, we performed a preliminary evaluation of the oral PK of halicin.

We used a non-compartmental method (NCA) for PK modeling and PK parameter calculations (Table 7; Figure 12) (Shikov et al., 2020). Halicin had a peak plasma concentration (C_{max}) of 64.25 ± 1.98 ng/mL, and a $T_{1/2}\lambda z$ between 8–10 h. The drug concentration in the blood was ≤5 ng/mL at 24 h after drug administration. The PK parameters indicated that halicin has a high elimination rate and low blood concentration, making it unsuitable for the treatment of systemic infections. Multiple doses may be required to increase the drug concentration in the blood during treatment. According to the PK parameters and *in vitro* activity experiments, halicin is suitable for intestinal treatment.

3.6 Effects of halicin on intestinal infection model in mice

C. perfringens was an anaerobic, gas-producing, spore-forming bacterium that was commonly found in the intestines of humans and animals (Mehdizadeh Gohari et al., 2021). Due to its ability to produce toxins and cause tissue necrosis, *C. perfringens* infections could lead to severe intestinal diseases. *In vitro* studies, we found that *C. perfringens* was sensitive to halicin. We established a mouse intestinal infection model using Ciprofloxacin-resistant *C. perfringens* isolated from clinical samples via gavage (10^9 CFU/mL) and evaluated the therapeutic effect of halicin on it.

The mice in the control group (0 mg/kg halicin) had a high mortality rate and appeared wrinkle and abdominal distension 1 day after administration (Figure 13). Within 4 d, 66% of the mice died, and the intestines of the dead mice were inflated. All mice in the 10 mg/kg halicin group survived, and more than 80% of the mice in the 5 mg/kg halicin group survived, and most of the mice did not show ruffled fur. Halicin was much more effective in treating intestinal anaerobic bacteria infections than 10 mg/kg metronidazole. Considering the dosing and LD_{50} doses, we believe that halicin is a potential drug for the treatment of *C. perfringens* infections.

4 Conclusion

Halicin, an antibiotic that was discovered using artificial intelligence, exhibits broad-spectrum antibacterial activities and can effectively inhibiting both Gram-positive and Gram-negative bacteria, particularly multidrug-resistant strains. Continuous induction experiments demonstrated that bacteria did not easily develop resistance to halicin. Sequencing of halicin-resistant mutants revealed that the primary mutations were concentrated in three functions: bacterial protein synthesis, transport, and nitroreduction. We found that the *nadE* gene, which mediates resistance to metronidazole, may play a significant role in resistance to halicin. Pharmacokinetic parameters in rats indicated that halicin was rapidly eliminated and had low plasma concentration, rendering it unsuitable for treating systemic infections. Given its antibacterial mechanism and activity spectrum, halicin is better suited as a therapeutic agent for intestinal bacterial infections. Oral acute and subchronic toxicity studies indicated that halicin was generally safe but caused some kidney damage at high doses. Halicin did not significantly affect mouse sperm morphology or bone marrow cell chromosomes. However, high doses of halicin (1009.1 mg/kg) influenced the micronucleus ratio in mouse bone marrow erythrocytes. Halicin significantly affected the mouse gut microbiota, but it demonstrated a rapid recovery of these effects. We validated the therapeutic effect of halicin on mice infected with *C. perfringens*. The results showed that halicin had good therapeutic effects at a dose of 5 mg/kg, and no deaths occurred in the group given a dose of 10 mg/kg. In this study, we determined the maximum safe concentration of halicin to be 50.5 mg/kg through an exhaustive safety assessment. It is worth noting that in our study, the effective concentration clinically used to treat intestinal bacterial infections was significantly lower than this value. These results suggest that halicin has a wide range of safety in clinical application, which provides a basis for further optimization of drug dosage and enhancement of efficacy. In summary, halicin is a suitable candidate drug for the treatment of intestinal infections.

Data availability statement

The datasets presented in this study can be found in online repositories. The names of the repository/repositories and accession number(s) can be found below: https://www.ncbi.nlm.nih.gov/, PRJNA1031798 https://www.ncbi.nlm.nih.gov/, PRJNA1031775.

Ethics statement

The animal study was approved by Ethics Committee of Shandong Academy of Agricultural Sciences. The study was conducted in accordance with the local legislation and institutional requirements.

Author contributions

MZ: Methodology, Software, Visualization, Writing–original draft. SL: Funding acquisition, Software, Validation, Writing–original draft. LH: Methodology, Writing–review and editing. JZ: Methodology, Writing–review and editing. SL: Methodology, Writing–review and editing. XuY: Methodology, Writing–review and editing. RW: Writing–original draft. XaY: Conceptualization, Funding acquisition, Project administration, Software, Supervision, Validation, Writing–original draft, Writing–review and editing. YY: Conceptualization, Funding acquisition, Project administration, Supervision, Validation, Writing–review and editing.

Funding

The author(s) declare that financial support was received for the research, authorship, and/or publication of this article. This study was funded by National Key Research and Development Program (2023YFD1800805), National Natural Science Foundation of China (32302929), Shandong Provincial Natural Science Foundation (ZR2021QC123, ZR2020MC049), Special Fund for Agro-scientific Research in the Public Interest (201303038), Shandong Province Science and Technology Achievement Transfer Transformation Subsidy Program Project (Shandong-Chongqing Cooper-ation, 2022LYXZ030), and Shandong Province Science Small and Medium-Sized Sci-Tech Enterprises In-novation Capacity Promotion Project (2023TSGC0265).

Conflict of interest

The authors declare that the research was conducted in the absence of any commercial or financial relationships that could be construed as a potential conflict of interest.

Publisher's note

Supplementary material

The Supplementary Material for this article can be found online at: https://www.frontiersin.org/articles/10.3389/fphar.2024.1389293/full#supplementary-material

References

Adam, A. H. B., de Haan, L. H. J., Louisse, J., Rietjens, I., and Kamelia, L. (2021). Assessment of the *in vitro* developmental toxicity of diethylstilbestrol and estradiol in the zebrafish embryotoxicity test. *Toxicol. Vitro* 72, 105088. doi:10.1016/j.tiv.2021.105088

Akagi, J. I., Mizuta, Y., Akane, H., Toyoda, T., and Ogawa, K. (2023). Oral toxicological study of titanium dioxide nanoparticles with a crystallite diameter of 6 nm in rats. *Part. Fibre Toxicol.* 20 (1), 23. doi:10.1186/s12989-023-00533-x

Askari, H., Seifi, B., and Kadkhodaee, M. (2016). Evaluation of renal-hepatic functional indices and blood pressure based on the progress of time in a rat model of chronic kidney disease. *Nephro-Urology Mon.* 8, e37840. doi:10.5812/numonthly.37840

Bolyen, E., Rideout, J. R., Dillon, M. R., Bokulich, N. A., Abnet, C. C., Al-Ghalith, G. A., et al. (2019). Author Correction: reproducible, interactive, scalable and extensible microbiome data science using QIIME 2. *Nat. Biotechnol.* 37 (9), 1091. doi:10.1038/s41587-019-0252-6

Booq, R. Y., Tawfik, E. A., Alfassam, H. A., Alfahad, A. J., and Alyamani, E. J. (2021). Assessment of the antibacterial efficacy of halicin against pathogenic bacteria. *Antibiot. (Basel, Switz.)* 10 (12), 1480. doi:10.3390/antibiotics10121480

Callahan, B. J., McMurdie, P. J., Rosen, M. J., Han, A. W., Johnson, A. J., and Holmes, S. P. (2016). DADA2: high-resolution sample inference from Illumina amplicon data. *Nat. Methods.* 13 (7), 581–583. doi:10.1038/nmeth.3869

Crits-Christoph, A., Hallowell, H. A., Koutouvalis, K., and Suez, J. (2022). Good microbes, bad genes? The dissemination of antimicrobial resistance in the human microbiome. *Gut Microbes* 14 (1), 2055944. doi:10.1080/19490976.2022.2055944

Danecek, P., Auton, A., Abecasis, G., Albers, C. A., Banks, E., DePristo, M. A., et al. (2011). The variant call format and VCFtools. *Bioinformatics* 27 (15), 2156–2158. doi:10.1093/bioinformatics/btr330

Deng, J., Yang, Z., Ojima, I., Samaras, D., and Wang, F. (2021). Artificial intelligence in drug discovery: applications and techniques. *Briefings Bioinforma.* 23 (1), bbab430. doi:10.1093/bib/bbab430

Dong, Z., Tang, S. S., Ma, X. L., Li, C. H., Tang, Z. S., Yang, Z. H., et al. (2022). Preclinical safety evaluation of macleaya cordata extract: a re-assessment of general toxicity and genotoxicity properties in rodents. *Front. Pharmacol.* 13, 980918. doi:10.3389/fphar.2022.980918

Dong, Z., Tang, S. S., Ma, X. L., Tan, B., Tang, Z. S., Li, C. H., et al. (2022). Acute, chronic, and genotoxic studies on the protopine total alkaloids of the Macleaya cordata (willd.) R. Br. in rodents. *Front. Pharmacol.* 13, 987800. doi:10.3389/fphar.2022.987800

Fan, Y., Fu, Y., Zhou, Y., Liu, Y., Hao, B., and Shang, R. (2022). Acute, subacute oral toxicity and Ames test of Pymulin: an antibacterial drug candidate. *BMC Pharmacol. Toxicol.* 23 (1), 2. doi:10.1186/s40360-021-00543-5

Gao, R., Hu, Y., Li, Z., Sun, J., Wang, Q., Lin, J., et al. (2016). Dissemination and mechanism for the MCR-1 colistin resistance. *PLoS Pathog.* 12 (11), e1005957. doi:10.1371/journal.ppat.1005957

Guefack, M.-G. F., Damen, F., Ngaffo, C. M. N., and Kuete, V. (2022). Acute and subchronic toxicities assessment of methanol bark extract of Hypericum roeperianum in rats. *S. Afr. J. Bot.* 150, 691–701. doi:10.1016/j.sajb.2022.08.006

Guo, X., Qi, Y., Li, J., Fan, H., Yang, L., Wu, X., et al. (2021). A comprehensive study of the genotoxic and anti-genotoxic effects of homocysteine in HUVECs and mouse bone marrow cells. *Food Chem. Toxicol.* 156, 112518. doi:10.1016/j.fct.2021.112518

Gupta, R., Srivastava, D., Sahu, M., Tiwari, S., Ambasta, R. K., and Kumar, P. (2021). Artificial intelligence to deep learning: machine intelligence approach for drug discovery. *Mol. Divers* 25 (3), 1315–1360. doi:10.1007/s11030-021-10217-3

Guy, R. C. (2024). "Ames test," in *Encyclopedia of toxicology*. Editor P. Wexler (Oxford: Academic Press), 377–379.

Higashihira, S., Simpson, S. J., Collier, C. D., Natoli, R. M., Kittaka, M., and Greenfield, E. M. (2022). Halicin Is effective against *Staphylococcus aureus* biofilms *in vitro*. *Clin. Orthop. Relat. Res.* 480 (8), 1476–1487. doi:10.1097/corr.0000000000002251

Hussain, Z., Pengfei, S., Yimin, L., Shasha, L., Zehao, L., Yifan, Y., et al. (2022). Study on antibacterial effect of halicin (SU3327) against *Enterococcus faecalis* and Enterococcus faecium. *Pathog. Dis.* 80 (1), ftac037. doi:10.1093/femspd/ftac037

Kunutsor, S. K., Bakker, S. J., Kootstra-Ros, J. E., Blokzijl, H., Gansevoort, R. T., and Dullaart, R. P. (2015). Inverse linear associations between liver aminotransferases and incident cardiovascular disease risk: the PREVEND study. *Atherosclerosis* 243 (1), 138–147. doi:10.1016/j.atherosclerosis.2015.09.006

McDonald, D., Price, M. N., Goodrich, J., Nawrocki, E. P., DeSantis, T. Z., Probst, A., et al. (2012). An improved Greengenes taxonomy with explicit ranks for ecological and evolutionary analyses of bacteria and archaea. *Isme J.* 6 (3), 610–618. doi:10.1038/ismej.2011.139

Mehdizadeh Gohari, I., Li, J., Shrestha, A., Uzal, F., and A McClane, B. (2021). Pathogenicity and virulence of *Clostridium perfringens*. *Virulence* 12 (1), 723–753. doi:10.1080/21505594.2021.1886777

Mello Silva Oliveira, N., Reis Resende, M., Alexandre Morales, D., Ragão Umbuzeiro, G., and Boriollo, M. F. G. (2016). *In vitro* mutagenicity assay (Ames test) and phytochemical characterization of seeds oil of Helianthus annuus Linné (sunflower). *Toxicol. Rep.* 3, 733–739. doi:10.1016/j.toxrep.2016.09.006

Mitcheltree, M. J., Pisipati, A., Syroegin, E. A., Silvestre, K. J., Klepacki, D., Mason, J. D., et al. (2021). A synthetic antibiotic class overcoming bacterial multidrug resistance. *Nature* 599 (7885), 507–512. doi:10.1038/s41586-021-04045-6

OECD (1998) *Test No. 212: fish, short-term toxicity test on embryo and sac-fry stages*. Paris, France: OECD.

OECD (2002) *Test No. 420: acute oral toxicity - fixed dose procedure*. Paris, France: OECD.

OECD (2013) *Test No. 236: fish embryo acute toxicity (FET) test*. Paris, France: OECD.

OECD (2016) *Test No. 474: mammalian erythrocyte micronucleus test*. Paris, France: OECD.

OECD (2016) *Test No. 475: mammalian bone marrow chromosomal aberration test*. Paris, France: OECD.

OECD (2018) *Test No. 408: repeated dose 90-day oral toxicity study in rodents*. Paris, France: OECD.

OECD (2018) *Test No. 443: extended one-generation reproductive toxicity study*. Paris, France: OECD.

Oliveira, A. A., Oliveira, A. P. A., Franco, L. L., Ferencs, M. O., Ferreira, J. F. G., Bachi, S. M. P. S., et al. (2018). 5-Nitroimidazole-derived Schiff bases and their copper(II) complexes exhibit potent antimicrobial activity against pathogenic anaerobic bacteria. *BioMetals* 31 (4), 571–584. doi:10.1007/s10534-018-0106-6

Santos, A. R. S., Gerhardt, E. C. M., Parize, E., Pedrosa, F. O., Steffens, M. B. R., Chubatsu, L. S., et al. (2020). NAD(+) biosynthesis in bacteria is controlled by global carbon/nitrogen levels via PII signaling. *J. Biol. Chem.* 295 (18), 6165–6176. doi:10.1074/jbc.RA120.012793

Selvarajan, R., Obize, C., Sibanda, T., Abia, A. L. K., and Long, H. (2022). Evolution and emergence of antibiotic resistance in given ecosystems: possible strategies for addressing the challenge of antibiotic resistance. *Antibiot. (Basel)* 12 (1), 28. doi:10.3390/antibiotics12010028

Shikov, A. N., Flisyuk, E. V., Obluchinskaya, E. D., and Pozharitskaya, O. N. (2020). Pharmacokinetics of marine-derived drugs. *Mar. Drugs* 18 (11), 557. doi:10.3390/md18110557

Shukla, R., Peoples, A. J., Ludwig, K. C., Maity, S., Derks, M. G. N., De Benedetti, S., et al. (2023). An antibiotic from an uncultured bacterium binds to an immutable target. *Cell* 186 (19), 4059–4073.e27. doi:10.1016/j.cell.2023.07.038

Song, Y. S., Dai, M. Z., Zhu, C. X., Huang, Y. F., Liu, J., Zhang, C. D., et al. (2021). Validation, optimization, and application of the zebrafish developmental toxicity assay for pharmaceuticals under the ICH S5(R3) guideline. *Front. Cell. Dev. Biol.* 9, 721130. doi:10.3389/fcell.2021.721130

Stokes, J. M., Yang, K., Swanson, K., Jin, W. G., Cubillos-Ruiz, A., Donghia, N. M., et al. (2020). A deep learning approach to antibiotic discovery. *Cell* 181 (2), 475–483. doi:10.1016/j.cell.2020.04.001

Wahab, N., Kannan, T. P., Mahmood, Z., Rahman, I. A., and Ismail, H. (2018). Genotoxicity assessment of biphasic calcium phosphate of modified porosity on human dental pulp cells using Ames and Comet assays. *Toxicol. Vitro* 47, 207–212. doi:10.1016/j.tiv.2017.12.002

Wang, J., Sun, F., Tang, S., Zhang, S., Lv, P., Li, J., et al. (2017). Safety assessment of vitacoxib: acute and 90-day subchronic oral toxicity studies. *Regul. Toxicol. Pharmacol.* 86, 49–58. doi:10.1016/j.yrtph.2017.02.020

frontiers | Frontiers in Pharmacology

TYPE Original Research
PUBLISHED 10 May 2024
DOI 10.3389/fphar.2024.1388150

OPEN ACCESS

EDITED BY
Mingkai Li,
Air Force Medical University, China

REVIEWED BY
Francine Johansson Azeredo,
University of Florida, United States
Fenglei Huang,
Boehringer Ingelheim, Germany

*CORRESPONDENCE
Xingkai Chen,
chxkabc@126.com
Huaijun Zhu,
huaijun.zhu@gmail.com

†These authors have contributed equally to this work and share first authorship

RECEIVED 19 February 2024
ACCEPTED 29 April 2024
PUBLISHED 10 May 2024

CITATION
Chen D, Wu X, Zhang H, Yao H, Jin L, Luo X, Liu J, Wu Z, Li Y, Xu W, Ge W, Chen X and Zhu H (2024), Population pharmacokinetics, dosing optimization and clinical outcomes of biapenem in patients with sepsis.
Front. Pharmacol. 15:1388150.
doi: 10.3389/fphar.2024.1388150

Population pharmacokinetics, dosing optimization and clinical outcomes of biapenem in patients with sepsis

Dayu Chen[1,2†], Xuanyu Wu[1,2,3†], Haixia Zhang[4†], Huimin Yao[5], Lu Jin[1,2], Xuemei Luo[1,2], Jinchun Liu[1,2], Zejun Wu[1,2], Yuanchen Li[6], Wei Xu[5], Weihong Ge[4], Xingkai Chen[1,2*] and Huaijun Zhu[1,2,3*]

[1]Department of Pharmacy, Nanjing Drum Tower Hospital, Nanjing, China, [2]Nanjing Medical Center for Clinical Pharmacy, Nanjing Drum Tower Hospital, Nanjing, China, [3]Department of Pharmacy, Nanjing Drum Tower Hospital, Nanjing Drum Tower Hospital Clinical College of Nanjing University of Chinese Medicine, Nanjing University of Chinese Medicine, Nanjing, China, [4]School of Pharmacy, Faculty of Medicine, Macau University of Science and Technology, Taipa, Macau SAR, China, [5]Department of Cardiology, Nanjing Drum Tower Hospital, Nanjing Drum Tower Hospital Clinical College of Nanjing University of Chinese Medicine, Nanjing University of Chinese Medicine, Nanjing, China, [6]Department of Pharmacy, Nanjing Drum Tower Hospital, School of Basic Medicine and Clinical Pharmacy, China Pharmaceutical University, Nanjing, China

Introduction: Biapenem is a carbapenem antibiotic widely used in Asia, can be used for the treatment of adults and children with infections due to susceptible bacteria. Although biapenem is utilized in the treatment of a diverse range of bacterial infections, current pharmacokinetic data in the context of septic populations remain limited. Consequently, our research aims to evaluate the pharmacokinetics and efficacy of biapenem within a septic population to optimize biapenem therapy.

Methods: In this study, we characterized the pharmacokinetics of biapenem in septic patients using a population pharmacokinetic (PPK) approach. The clinical PK data to develop the PPK model were obtained from 317 septic patients admitted to Nanjing Drum Tower Hospital between 2018 and 2022. All patients were randomized to the modeling and validation cohorts at a 3:1 ratio, with PPK modeling and validation performed utilizing the NONMEM software.

Results: The model found to best describe the available data was a two-compartment PPK model with first-order elimination characterized by the parameters clearance (CL), central volume (V1), peripheral volume (V2), and intercompartmental clearance (Q). A covariate analysis identified that creatinine clearance (CLCR) was a significant covariate influencing biapenem CL, while blood urea nitrogen (BUN) was a significant covariate influencing biapenem Q. Accoding to the clinical outcome analyses, 70% of the time that the free antimicrobial drug concentration exceeds the MIC ($fT_{>MIC}$) is associated with favourable clinical outcomes. The PPK model was then used to perform Monte Carlo simulations to evaluate the probability of attaining 70% $fT_{>MIC}$.

Conclusions: A final PPK model of biapenem was established for patients with sepsis. The current daily dosage regimen of 1.2 g may insufficient to achieve 70% $fT_{>MIC}$ in septic patients. The dosage regimen of 600 mg every 6 h appears to be the optimal choice.

KEYWORDS

biapenem, pharmacokinetics, dosing regimen, sepsis, Monte Carlo simulation

1 Introduction

Biapenem (BPM) is a carbapenem antibiotic, employed in the combat against bacterial infections (Brismar et al., 1996). It exhibits its antibacterial prowess by inhibiting bacterial cell wall synthesis. Comparable to the *in vitro* potency of imipenem and meropenem, BPM possesses a broad-spectrum efficacy, spanning Gram-negative and Gram-positive bacteria, and extending to anaerobic bacteria (Dong et al., 2016). Demonstrations of both clinical and bacteriological effectiveness have been evident in the management of diverse bacterial infections - pneumonia, complicated urinary tract infections, pyelonephritis, peritonitis, and others (Perry and Ibbotson, 2002). Over the past decades, BPM has ascended to become a choice in treating infections precipitated by extended-spectrum β-lactamase-producing Gram-negative bacteria (Alonso et al., 2006).

Alterations in the volume of distribution (Vd) and clearance of antibiotics have been observed in sepsis (van der Poll, 2001; Roberts and Lipman, 2006). Endotoxins induce the synthesis of various endogenous mediators, including cytokines, interleukins, and platelet-activating factor, can influence the vascular endothelium, leading to vasodilation, along with an aberrant distribution of blood flow, endothelial damage, and heightened capillary permeability. This syndrome results in fluid translocation from the intravascular compartment to the interstitial space, consequently increasing the Vd of water-soluble drugs, including carbapenems, and diminishing their serum concentrations (Murínová et al., 2022). It was reported that bipenem has a relatively short elimination half-life of approximately 1 hour. Additionally, it manifests a significant inter-individual variability in its pharmacokinetic characteristics, which leads to substantial disparities in the blood drug concentration amongst patients. Consequently, identical dosing regimens can produce disparate clinical outcomes in different patients. Sole dependence on the suggested dosing regimen outlined in the product label is inadequate for dose adjustments in diverse patient populations, particularly in cases involving sepsis (Evans et al., 2021). Therefore, exploration into the pharmacokinetic profiles of BPM within the septic patient populace is crucial in order to predict the pharmacokinetic parameters of this specific populace, and to effectively enhance or refine the dosage for improved patient outcomes.

BPM exhibits a time-dependent bactericidal action, where its antimicrobial effectiveness is contingent upon the duration for which serum drug levels surpass the minimal inhibitory concentration (MIC). In the current clinical practice, BPM is commonly administered twice or three times a day, with a dose of 300mg–600 mg per administration (Griffith et al., 2023). However, due to its relatively brief elimination half-life and time-dependent nature, achieving the pharmacokinetics/pharmacodynamics (PK/PD) target remains challenging with dosing intervals of either 8 or 12 h (Ikawa et al., 2008a; Ikawa et al., 2008b; Rao et al., 2023).

Currently, there is a notable gap in the literature, as population pharmacokinetic studies focusing on BPM in septic patients are lacking. This is particularly significant considering the frequent prescription of BPM within this patient population. Thus, the primary objective of this study is to investigate the pharmacokinetics of BPM in septic individuals utilizing a population pharmacokinetic (PPK) approach. This investigation is intended to facilitate dosing optimization, thereby enhancing the achievement of the PK/PD target in this patient cohort.

2 Materials and methods

2.1 Study design, patient enrollment and data collection

This was a retrospective, single center study performed in Nanjing Drum Tower hospital, a university-affiliated tertiary medical center with 3,800 beds. The study was performed in accordance with the ethical standards of the Declaration of Helsinki. The study was approved by the Ethics Committee of Nanjing Drum Tower Hospital Affiliated Hospital of Nanjing University Medical School, Nanjing, China (2022-504-01) and was registered at the Chinese Clinical Trial Registry (ChiCTR2300073976). The need for informed consent was waived by the ethics committee in view of the observational and retrospective nature of the study. Adult patients (over 18 years of age) with sepsis who treated by BPM in Nanjing Drum Tower Hospital (China) from January 2018 to May 2022 were included. Sepsis was defined by criteria according to the Third International Consensus Definitions for Sepsis and Septic Shock (Singer et al., 2016). The exclusion criteria were as follows: patients who received BPM for less than 48 h; patients received renal replacement therapy or extracorporeal membrane oxygenation during BPM therapy; patients did not receive therapeutic drug monitoring (TDM) and patients with incomplete medical record. Given the nature of this retrospective observational study, no intervention was made to standardize care. According to the clinical practice, samples were usually collected after the third dose interval of BPM and were measured for serum concentration.

Clinical records of all included patients were reviewed and evaluated. BPM dosing regimens, including administration times and infusion rates were collected. The initiation and termination times of each drug infusion, along with the timing for blood sampling, were meticulously documented within the hospital's electronic medical records system via an automated information system, with time entries recorded with minute-level precision. The gender, age, body weight, alanine aminotransferase (ALT), aspartate transaminase (AST), alkaline phosphatase (AKP), glutamyltransferase (GGT), total bilirubin (TB), direct bilirubin (DB), total protein (TP), albumin

(ALB), blood urea nitrogen (BUN), serum creatinine (SCR), white blood cell count (WBC), hemoglobin (HB), platelet (PLT) of included patients during BPM therapy were recorded. The estimated glomerular filtration rate (eGFR) was calculated according to the Modification of Diet in Renal Disease formula and creatinine clearance (CLCr) was calculated according to the Cockcroft-Gault formula (Cockcroft and Gault, 1976). Body mass index (BMI) was calculated as body weight (kg) divided by the square of height (m). Immunocompromised patients, severity of sepsis and primary infection site were also included for analysis. All patients were randomly divided into a modeling cohort and an validation cohort in a ratio of 3:1.

2.2 Dosing, sampling schedule, bioanalytical method and determination of BPM concentration

TDM of BPM is performed routinely in septic patients according to the clinical practice at the participating site. According to the product label, the dose of BPM for adults was 300–600 mg per administration, given 2–4 times per day, with a daily dose not exceeding 1.2 g. BPM was intravenously administered to all patients with 100 mL of sodium chloride or glucose injection as a solvent. BPM were infused over 1 h according to the clinical practice.

Blood samples were obtained via an indwelling cannula, collected into EDTA tubes, and immediately placed on ice during transferring to the drug monitoring laboratory. In order to stabilize BPM, all blood samples were then pretreatmented by adding an equal volume of 1 M 3- (*N*-morpholino) propanesulfonic acid (MOPS) buffer (pH 7.0) as a stabilizer after centrifugation. The samples were then frozen and stored prior to assay at −20°C. After samples were mixed with their internal standard (50 mg/mL 5-hydroxyindole-3-acetic acid) and transferring to an ultrafiltration device and centrifuged, the plasma concentration of BPM was then measured by a Shimadzu LC-2030C 3D High-Performance Liquid Chromatography Analyzer (Shimadzu Corporation, Tokyo, Japan) with a reversed-phase column (TSKgel ODS-100V, 4.6 mm × 250 mm, 5μm; Tosoh Corporation, Yamaguchi-ken, Japan). The ultraviolet absorbance was detected at 300 nm. The mobile phase was a mixture of potassium dihydrogen phosphate (pH 6.5–7.0) and methanol (94:6). To investigate the linear relationship, 270 μL of blank plasma was taken and subsequently fortified with BPM standard solutions at concentrations of 3, 6, 18, 60, 180, and 300 mg/L, each at a volume of 30 μL. This resulted in final BPM plasma concentrations of 0.3, 0.6, 1.8, 6.0, 18.0, and 30.0 mg/L. The samples were processed according to the method described before, and the chromatographic peaks were recorded. The concentration of BPM (x) was plotted on the *x*-axis, while the ratio of the peak area of BPM (A_s) to the internal standard peak area (A_i) was plotted on the *y*-axis. Weighted least squares regression [with the weight coefficient being (1/C2 was employed for linear regression to establish the standard curve. The resulting regression equation was (y = 0.4094x - 0.0665) (with r = 0.9999), indicating a strong linear relationship between the plasma concentration of BPM and the peak area within the range of 0.3–30 μg/mL, with 0.3 μg/mL as the lower limit of quantitation. To assess the precision and accuracy of the method, blank plasma samples were prepared with BPM concentrations of 0.3, 0.6, 3, and 24 mg/L. Each concentration level had a set of 5 samples. These samples were processed and analyzed as per the protocol outlined before. The chromatographic peak areas were recorded, and the concentrations of each sample were calculated using the established standard curve. This process was repeated across three batches to evaluate the method's precision and accuracy. For the stability assessment, 270 μL of blank plasma was fortified with BPM standard solutions to achieve concentrations of 0.3, 0.6, 3, and 24 mg/L. Additionally, 100 μL of stabilizer and 20 μL of internal standard solution were added to each sample. The stability of BPM in plasma was examined under various conditions: room temperature storage for 2 h, room temperature storage for 6 h, three freeze-thaw cycles, and storage at −80°C for 60 days. Concentrations of BPM in plasma were calculated using the standard curve and compared with theoretical concentrations. The relative deviations of all measurements were within 15%, indicating that the plasma samples remained stable under the tested conditions of room temperature storage for both 2 and 6 h, three freeze-thaw cycles, and long-term storage at −80°C for 60 days. The intra- and inter-day coefficients of variation (CVs) were all <15%.

2.3 Population pharmacokinetic model development

The non-linear mixed effect modeling software NONMEM Ver. 7.3 (Icon Inc., Mayfield, PA, United States) compiled with gFortran (Version 4.6; http://www.gfortran.org) was used to perform the population pharmacokinetic analysis of BPM with the first-order method throughout the model-building procedure. GraphPad Prism 9.2 (GraphPad Software, La Jolla, CA, United States), R (Version 3.6.1; http://www.r-project.org) and the Xpose package (Version 4.5.3; http://xpose.sourceforge.net)were used for visual diagnosis.

2.3.1 Basic model

The structural pharmacokinetics model composed of the one or two compartment with first-order elimination were compared. The variability among subjects was quantified by assuming that individual parameters followed a multivariate log-normal distribution, and the inter-individual variability of patients was described using an exponential model (Eq. 1):

$$\boldsymbol{Pi} = \boldsymbol{TV}(\boldsymbol{P}) * \boldsymbol{exp}(\boldsymbol{\eta i}) \tag{1}$$

where P *i* is the individual parameter estimate for the *i*-th patient, TV(P) represents the typical population value of pharmacokinetic parameters. ηi is the inter-individual variability with a mean of 0 and variance of ω^2.

The intra-individual variability of pharmacokinetic parameters in patients is described using an additive model (Eq. 2), exponential model (Eq. 3), or a combined additive and exponential model (Eq. 4):

$$\boldsymbol{Y} = \boldsymbol{IPRED} + \boldsymbol{\varepsilon} \tag{2}$$

$$\boldsymbol{Y} = \boldsymbol{IPRED} \times (\boldsymbol{1} + \boldsymbol{\varepsilon}) \tag{3}$$

$$\boldsymbol{Y} = \boldsymbol{IPRED} \times (\boldsymbol{1} + \boldsymbol{\varepsilon 1}) + \boldsymbol{\varepsilon 2} \tag{4}$$

where Y represents the observed blood drug concentration, IPRED is the individual predicted concentration, and ε is the residual variable with a mean of 0 and variance of σ^2.

2.3.2 Covariate models and model selection criteria

All covariates were introduced into the basic model in both linear and nonlinear methods, and the significance of each covariate was evaluated through likelihood ratio tests and visual inspection of diagnostic goodness-of-fit plots. The continuous covariates, including age, weight, ALT, AST, AKP, GGT, TB, DB, TP, ALB, BUN, SCR, eGFR, CLCr, WBC, HB, PLT, WBC,HB, PLT and categorical covariate gender, immunocompromisation, septic shock and primary infection site were screened for their influence on clearance and the volume of distribution. A model was established using a forward inclusion approach, with each covariate being individually added to the basic model for analysis. After that, a backward elimination approach was used. If the introduction of a covariate to the model decreased the objective function value (OFV) more than 3.84 ($df = 1, p < 0.05$), the covariate was considered to have a significant impact on the model and was included. Conversely, if the OFV did not significantly decrease, the covariate was excluded. This process was repeated until the covariate model was initially established with no significant reduction in the OFV. The backward elimination step was applied to examine the covariates included in the model. If the removal of a covariate resulted in an increase in the OFV less than 6.63 ($df = 1, p < 0.01$), the covariate was considered to have no statistical significance and was removed from the full regression model. The final model was established after this process was repeated for each covariate until the change in the OFV value was greater than 6.63.

2.3.3 Model evaluation

Internal evaluation of the model was then performed. The goodness-of-fit (GOF) plots of the model including: the observed concentrations (DV) versus population prediction (PRED), DV versus individual prediction (IPRED), conditional weighted residuals (CWRES) versus PRED and CWRES versus time were plotted (Hooker et al., 2007). A prediction corrected visual predictive check (pcVPC) was used to describe the predictive performance of the model based on the distribution characteristics of observed and predicted concentrations in the graph, as well as the proportion of observed concentrations falling within the 95% confidence interval (CI) of the predicted concentrations. To evaluate the stability and reliability of the final model, 1,000 independent repeated samples were performed by using the non-parametric bootstrap method, comparing the 95% CI of the sampling results with the parameter estimates of the model.

One-quarter of the patients were included in the validation cohort. The PRED were estimated and compared with the corresponding observations by estimating the relative prediction error (PE) using Eq. 5. The median prediction error (MDPE) (Eq. 6), median absolute prediction error (MAPE) (Eq. 7) were used to evaluate the predictive accuracy and precision. PE within ±20% (F_{20}) (Eq. 8) and PE within ±30% (F_{30}) (Eq. 9) were calculated to evaluate the accuracy and precision of the model. In this study, when the standards of MDPE ≤±15%, MAPE ≤30%, $F_{20} > 35\%$, and $F_{30} > 50\%$ were attained after evaluated by validation cohort, the model was considered to be satisfactory, clinically acceptable and have decent predictive performance (Bleeker et al., 2003; Nguyen et al., 2017).

$$PEi = \frac{PREDi - DVi}{DVi} \times 100\% \quad (5)$$

$$MDPE = Median\left(\frac{PREDi - DVi}{DVi}\right) \times 100\% \quad (6)$$

$$MAPE = Median\left(\left|\frac{PREDi - DVi}{DVi}\right|\right) \times 100\% \quad (7)$$

$$F_{20} = \frac{N(|PE| \le 20\%)}{N(DV)} \times 100\% \quad (8)$$

$$F_{30} = \frac{N(|PE| \le 30\%)}{N(DV)} \times 100\% \quad (9)$$

2.4 Microbial efficacy and clinical outcomes

All antimicrobial susceptibility tests were conducted at the Microbiology Laboratory at Nanjing Drum Tower Hospital. The MIC values of all isolates were determined following the recommendations of The Clinical and Laboratory Standards Institute by means of agar dilution method in our bacteriological laboratory for each patient in whom the microorganism was identified.

Clinical outcomes were compared in patients with at least one pathogen was identified. The primary treatment outcome was the clinical response, which was classified as either success or failure. Clinical success was defined as the resolution or improvement of infection-related clinical signs and symptoms as well as the microbial eradication at the end of BPM therapy with no need to add or change the antibacterial therapy. Clinical failure was defined as the persistence or worsening of any clinical signs or symptoms of infection, the emergence of any new clinical signs or symptoms of infection, or the need for additional systemic antibacterial medication, or the failure to achieve microbial eradication at the end of BPM therapy.

2.5 Dosing regimen optimization based on a pharmacokinetic model

Carbapenems are classified as time-dependent antimicrobial agents, characterized by the pharmacodynamic parameter of time exceeds the MIC ($fT_{>MIC}$). The PK/PD index associated with optimal carbapenem activity is the % $fT_{>MIC}$ (40%–70%) according to current guidelines (Li et al., 2007; McKinnon et al., 2008; Abdul-Aziz et al., 2020). Monte Carlo simulations (n = 10,000) were performed using the NONMEM in order to optimize the dose strategy of BPM. The final PPK model was used to perform Monte Carlo simulations to evaluate the probability of target attainment (PTA). From the simulated concentration-time profiles, $fT_{>MIC}$ was determined for each virtual patient over a range of MIC values, from 0.0625 to 2.0 mg/L. Then, the PTA was calculated as the percentage of patients who achieved 70% $fT_{>MIC}$ targets, in order to optimize BPM therapy.

Subsequent deescalation to other narrow-spectrum antibiotics, according to microbiological results, was considered a standard of care and did not imply treatment failure. The secondary treatment outcome was ICU mortality.

3 Results

3.1 Patients

According to the predetermined patient inclusion criteria of this study, a total of 466 BPM measurements collected from 317 adult

TABLE 1 Clinical characteristics.

Variable	Modeling cohort (n = 245)			External evaluation cohort (n = 72)		
	Mean ± SD	Median (range)	N (%)	Mean ± SD	Median (range)	N (%)
Gender						
Male			156 (63.7)			46 (63.9)
Female			89 (36.3)			26 (36.1)
Age (years)	59.13 ± 19.01	63 (18–97)		58.18 ± 14.53	60 (18–85)	
Weight (kg)	63.40 ± 11.34	62 (36.8–100)		63.78 ± 15.90	60.5 (45–148)	
ALT (U/L)	51.23 ± 161.04	20.5 (0.8–2,813.3)		46.19 ± 89.92	19.8 (4.7–842.3)	
AST (U/L)	69.05 ± 342.55	22.3 (4.9–6,598)		58.70 ± 176.25	24.4 (4.6–2002.2)	
AKP (U/L)	104.62 ± 83.65	79.1 (14.9–816)		141.14 ± 174.57	87.2 (35.5–1,576.1)	
GGT (U/L)	76.21 ± 89.59	45.7 (5.1–758.8)		123.24 ± 228.58	51.05 (9.1–1,536.7)	
TB (μmol/L)	20.88 ± 40.76	11.2 (1.6–453.7)		37.64 ± 63.84	16.2 (2.7–393.1)	
DB (μmol/L)	9.84 ± 26.13	3.3 (0.1–320.7)		22.35 ± 45.05	5.5 (0.3–277)	
TP (g/L)	59.90 ± 9.82	59.8 (21.1–116.4)		59.66 ± 10.31	59.3 (39.7–123.7)	
ALB (g/L)	34.68 ± 5.30	34.85 (3.5–55.1)		34.67 ± 4.52	34.9 (19.1–44.7)	
BUN (mmol/L)	9.84 ± 8.90	6.2 (0.4–66.9)		10.31 ± 9.38	7.1 (1–49.4)	
SCR (μmol/L)	153.86 ± 214.21	66 (28–1,655)		155.52 ± 244.11	65 (24–1949)	
eGFR (mL/min/1.73 m^2)	104.16 ± 65.24	108.1 (2.6–332.9)		103.5 ± 62.32	106.1 (2.6–276.2)	
CLCr (mL/min)	88.91 ± 60.14	84.92 (3.5–295.5)		87.95 ± 58.66	82.72 (5.2–316.63)	
WBC (10^9/L)	8.80 ± 16.56	5.7 (0.1–154.2)		6.96 ± 6.03	5.35 (0.1–35.6)	
HB (g/L)	85.88 ± 20.71	84 (12–161)		84.33 ± 20.83	80 (28–162)	
PLT (10^9/L)	126.56 ± 124.88	85.5 (1–759)		144.02 ± 133.13	105 (7–605)	
Time after the last dose of biapenem administration (h)	6 ± 2.23	6 (0.5–20.73)		5.83 ± 2.84	5.95 (1–20.3)	
Immunocompromisation			34 (13.9)			11 (15.3)
Septic shock			66 (26.9)			20 (27.8)
Primary infection site						
Respiratory			108 (44.1)			29 (40.3)
Intra-abdominal			119 (48.6)			36 (50.9)
Other			18 (7.3)			7 (9.7)

ALT, alanine aminotransferase; AST, aspartate transaminase; AKP, alkaline phosphatase; GGT, glutamyltransferase; TB, total bilirubin; DB, direct bilirubin; TP, total protein; ALB, albumin; BUN, blood urea nitrogen; SCR, serum creatinine; eGFR, estimated glomerular filtration rate; CLCr, creatinine clearance; WBC, white blood cell count; HB, hemoglobin; PLT, platelet.

patients were included. Among them, 351 blood concentration samples collected from 245 patients were defined as the modeling cohort, while the other 115 BPM concentration samples collected from 72 patients were defined as the external evaluation cohort. Each participant received an average of 1.5 samples. Supplementary Figure S1 in the Supplementary Material presents the scatter plots of time versus BPM concentration. The median trough drug concentration (C_{min}) from the modeling and external evaluation datasets was 2.1 mg/L and 1.8 mg/L, respectively. Clinical characteristics of the patients included in the analysis are summarized in Table 1.

3.2 Model building

The minimum OFV indicated that the a two-compartment model (679.233) better described the data than a one-

TABLE 2 Population pharmacokinetic parameter estimates of the final model and bootstrap.

Parameter	Final model		Bootstrap		
	Esteimate	RSE (%)	Median	5th-95th	Bias (%)
CL (L/h)					
$CL = \theta_1 \times [1+\theta_5 \times (CLCr - 78.2)]$					
θ_1	8.33	6.4	8.331	7.48–9.92	0.01
θ_5	0.0046	11.9	0.0049	0.0034–0.0064	6.52
$V1(L) = \theta_2$					
θ_2	13.4	15	13.23	10.94–23.55	−1.27
$Q\ (L/h) = \theta_3 \times [1+\theta_6 \times (BUN - 6.8)]$					
θ_3	3.75	13.6	3.58	2.26–5.73	−4.53
θ_6	0.112	1.9	0.114	0.034–0.15	1.79
$V2(L) = \theta_4$					
θ_4	60.4	17.5	64.72	23.38–169.07	7.15
Inter-individual variability					
ω_{CL}	0.0591	19.8	0.057	0.031–0.088	−3.55
ω_Q	1.12	25.2	1.10	0.26–2.94	−1.79
Residual variability					
ε	0.591	17.1	0.59	0.39–0.85	−0.17

RSE, relative standard error; CL, clearance (L/h); Q, inter-compartmental clearance (L/h), V1, volume of distribution of central compartment (L), V2, volume of distribution of the peripheral compartment (L); CLCr, creatinine clearance (mL/min), BUN, blood urea nitrogen (mmol/L); Bias(%)= (bootstrap estimated value-final model estimated value)/final model estimated value ×100%.

compartment model (734.914), so the pharmacokinetics of BPM were described by a two-compartment model with first-order elimination. Detailed covariate screening process is presented in Supplementary Table S1 in the Supplementary Material. The residual unexplained variability was best described by an additive residual error model. During the forward inclusion process of covariate screening, it was found that CLCr and ALB had a significant impact on total clearance (CL), while BUN was a significant covariate for intercompartment clearance (Q). In the backward elimination process, ALB was removed from the model. The OFV of the final model was 550.508, which was 132.991 lower than the basic model. The PPK parameters of the base and final models are summarized in Table 2. The final model for BPM is represented by the following equation:

$$CL(L/h) = 8.33 \times \{1 + 0.046 \times [CLCr(ml/min) - 78.2]\}$$
$$V1(L) = 13.4$$
$$Q(L/h) = 3.75 \times \{1 + 0.112 \times [BUN(mmol/L) - 6.8]\}$$
$$V2(L) = 60.4$$

3.3 Model evaluation

3.3.1 Internal evaluation

The diagnostic plots demonstrated acceptable goodness of fit for the final PPK model of BPM. As depicted in Figure 1, there is no apparent systematic bias. Figure 1A shows the DV versus PRED scatter plot and Figure 1B shows the DV versus IPRED scatter plot. The diagnostics of WRES versus time as well as PRED are presented in Figures 1C, D, showing no obvious bias. The red solid line is the trend line of the scatter plot, and the black solid line is the reference line. As shown in Figures 1A, B, the trend lines of population predictions and individual predictions of the model are close to the reference line of Y = X, and the scattered points are evenly distributed on both sides of the reference line, indicating that the model individual predicted values are basically the same as the observed values. The scatter plot of weighted residuals is evenly distributed on both sides of 0, and most of the values are within ±2, indicating a good fit of the final model. The VPC results of the final model are shown in Figure 2. The curves from top to bottom represent the 95th, 50th, and 5th percentiles of observed concentrations, and the shaded area represents the 95% CI of simulated concentrations. The scatter points represent the observed values. According to the analysis, the proportion of observed concentrations falling within the predicted concentration 95% CI of the final model was 93.73%, and the percentile distribution of observed concentrations was similar to the 95% CI of the simulated data. Therefore, the final model has good predictive performance.

3.3.2 External evaluation

A total of 115 BPM concentration samples from 72 adult patients were included in the external evaluation cohort of the final model. The results of the prediction error test method were as follows: MDPE = 6.75%, MAPE = 26.25%, F_{20} = 42.61%, and F_{30} = 53.04%. The prediction error results were within the target range of standards, indicating that the final model has good predictive performance.

3.4 Microbiology and clinical outcomes

Of the 317 patients, at least on major pathogen was identified in 211 patients (67%) and included in the microbiology and clinical

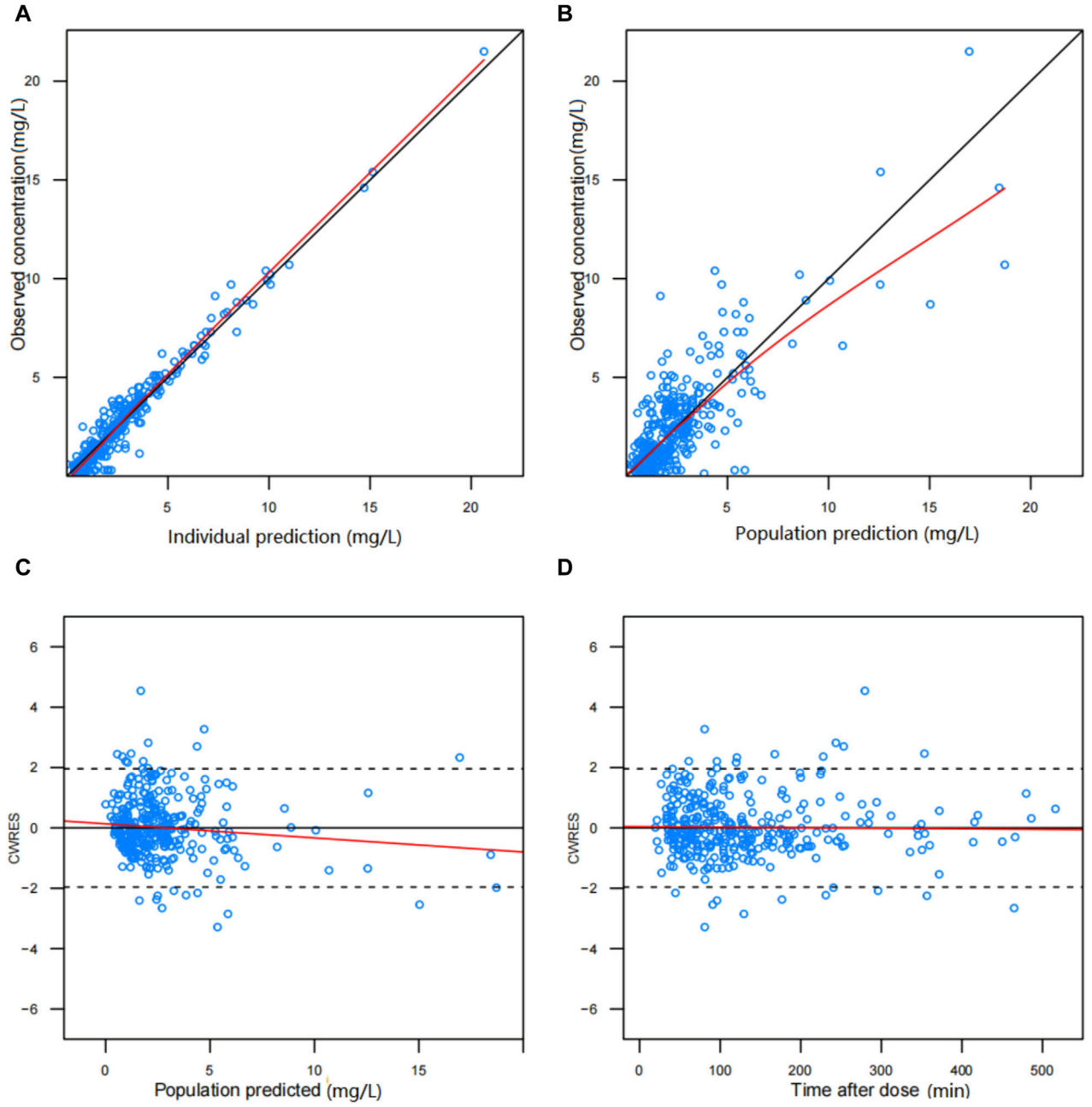

FIGURE 1
Diagnostic scatter plots of final population PK model for biapenem: **(A)** predicted vs. observed concentration, **(B)** individual predicted vs. observed concentration, **(C)** conditional weighted residual (CWRES) vs. predicted concentration, and **(D)** CWRES vs. time.

outcome analysis. A total of 265 pathogens were identified and the microbiological findings are presented in Table 3. The most commonly isolated microorganisms were *Escherichia coli* (25%), *Klebsiella pneumoniae* (15%), *Pseudomonas aeruginosa* (15%), and *Acinetobacter baumannii* (12%). The median MIC values of BPM for *Enterobacteriaceae*, *P. aeruginosa*, and *A. baumannii* were 0.25, 1.0, and 8.0 mg/L, respectively.

Overall, 125 (59%) patients achieved successful clinical cure after BPM treatment. The baseline clinical characteristics are shown in Table 4. Among all the patients, 85% (179/211) of them achieved 40% $fT_{>MIC}$ and 60% (127/211) of them achieved 70% $fT_{>MIC}$. The proportion of patients reaching the $fT_{>MIC}$ targets were higher in the clinical success group than in the failure group. The results of the multivariable logistic analyses of clinical success are presented in Table 5. According to the analyses, 70% $fT_{>MIC}$ was associated with an increasing possibility to achieve clinical cure when treating septic patients with BPM. The Odds Ratio (OR) was resulted to be 7.07 with a 95% confidence interval

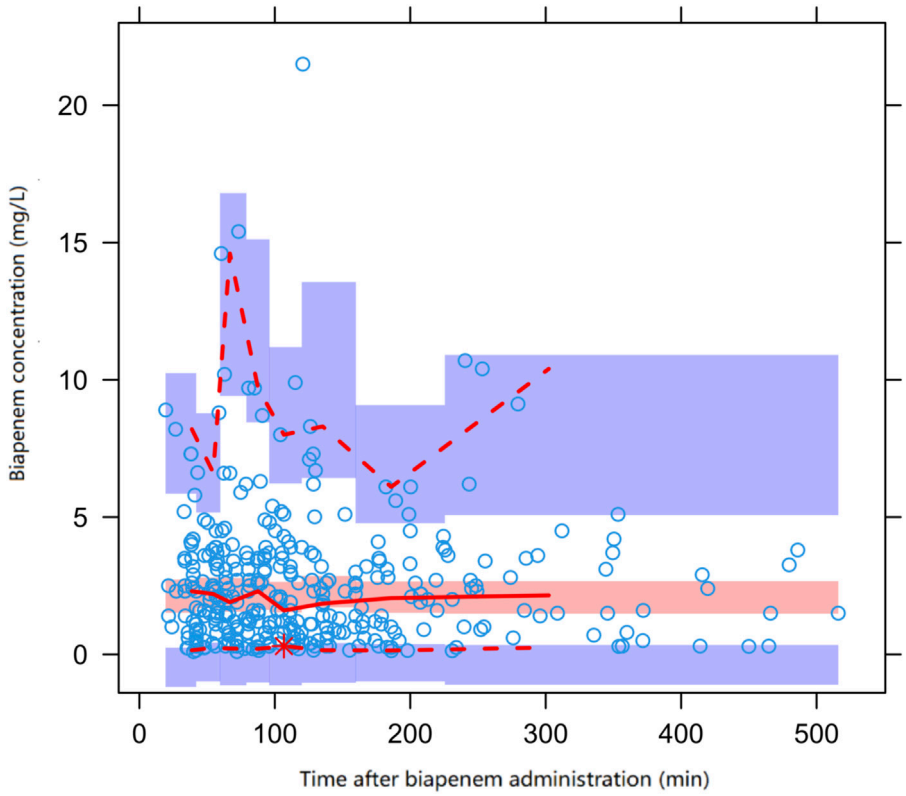

FIGURE 2
Prediction corrected visual predictive check (pcVPC) of biapenem concentration vs. time for the final model. Open circles represent observed concentrations, the solid line and the dashed line represent the median and the 95% CI of observations, respectively. The middle red shadow areas represent the 95% CI of the median for the results of 1,000 simulations of the final model and the blue shadow areas represent the 95% CI of the 10th and 90th percentiles of the results of 1,000 simulations of the pharmacokinetic final model.

of 2.45–20.37 and a p-value <0.001. Also, hypoalbuminemia is a risk factor for treatment failure (OR: 0.33, 95% CI: 0.12–0.91, p-value: 0.03).

3.5 Dosing regimen optimization

The target attainment (70% $fT_{>MIC}$) rate as functions of the simulated dose for different MIC susceptibility breakpoints are shown in Figure 3. The results of the simulation revealed that the existing standard dosage regimens, as delineated in the product label (up to a maximum of 1.2 g per day), are insufficient to achieve a PTA of 70% $fT_{>MIC}$ in more than 60% septic patients when MIC is higher than 1 mg/L. Within the dosage regimen recommended by the current product label, the administration regimen of 300 mg every 6 hours appears to be the optimal choice for patients with sepsis. However, this regimen may not provide adequate antimicrobial activity when there is an increase in the MIC. When BPM is administered 300 mg every 6 h, only 60.22% of the septic patients achieved the pharmacodynamic target for MIC of 1 mg/L, showing that this was an underdose. When a maximum dose of 2.4 g per day was administered (600 mg every 6 h), 81.47% of the septic patients achieved the pharmacodynamic target for MIC of 1 mg/L. In summary, the BPM regimens needed to achieve optimal PTA for 70% $fT_{>MIC}$ is 600 mg every 6 h, the recommended daily dose of product label may not be sufficient in septic patients.

4 Discussion

Life-threatening sepsis and severe nosocomial bacterial infections in hospitalized patients represent a significant clinical challenge (Evans et al., 2021). A robust correlation exists between the $fT_{>MIC}$ of carbapenems and their clinical efficacy (Zhanel et al., 2007). Deviations from optimal dosage, whether insufficient or excessive, can lead to adverse effects, consequently influencing the overall clinical efficacy of these antimicrobial agents (Boonpeng et al., 2022; Dinh et al., 2022). Consequently, this research endeavors to develop a BPM PPK model specifically for adult patients suffering from sepsis. This initiative is intended to furnish empirical support for the optimization of clinical administration strategies of this antimicrobial agent.

At present, there are many methods evaluating the influence of covariates on PK model parameters. In spite of the selected method, the intention of such evaluations is usually to describe inter- and intra-subject variability in PK parameters with patient factors. These factors may be those patient characteristics that are recorded for each subject at a baseline study visit and describe patient-specific factors such as the subject's gender, age, weight, and height, for

TABLE 3 Microbiologic characteristics (265 isolates from 211 patients) and biapenem susceptibility.

Pathogen	No. of isolates	Biapenem MIC range (mg/L)
Escherichia coli	66	0.1–2
Klebsiella pneumoniae	31	0.5–2
Klebsiella pneumoniae (CRE)	9	≥16
Pseudomonas aeruginosa	37	1–8
Pseudomonas aeruginosa (CR-GNB)	3	≥16
Acinetobacter baumannii	9	1–2
Acinetobacter baumannii (CR-GNB)	23	≥16
Enterobacter cloacae	13	0.25–0.5
Enterococcus faecalis	29	1–2
Enterococcus faecium	10	ND
Stenotrophomonas maltophilia	5	ND
Staphylococcus aureus	5	ND
Staphylococcus spp.	4	ND
Serratia marcescens	5	0.25
Other *Enterobacteriaceae*	11	0.1–2
Other *Acinetobacter* spp.	2	1–8
Other *Pseudomonas* spp.	3	1–4

CRE, carbapenem-resistant *Enterobacteriaceae*; CR-GNB, carbapenem-resistant Gram-negative bacteria; ND, not determined.

TABLE 4 Comparison of baseline characteristics between clinical success and failure groups.

Characteristics	Success (n = 125)	Failure (n = 86)	*p*-value
Male (%)	82 (66)	59 (69)	0.65
Age (years)	62.12 ± 16.62	60.05 ± 15.88	0.52
Body weight (kg)	62.91 ± 13.61	63.93 ± 7.63	0.61
Albumin (g/L)	30.00 ± 3.54	28.13 ± 3.39	0.02
Septic shock (%)	30 (24)	28 (33)	0.17
Serum creatinine (μmol/L)	93.50 (61.00, 450.25)	120.50 (67.75, 409.75)	0.67
White blood cell count (10^9/L)	10.40 (7.13, 14.58)	12.30 (8.85, 18.58)	0.15
C-reactive protein (mg/L)	88.09 (35.50, 129.85)	71.55 (44.75, 116.78)	0.93
Target attainment (%)			
40% *fT* > MIC	108 (86)	71 (83)	0.45
70% *fT* > MIC	96 (77)	31 (36)	<0.001
Therapy regimens (%)			
Concomitant antimicrobials	59 (47)	44 (51)	0.57
Biapenem monotherapy	66 (53)	42 (49)	
Primary infection site (%)			
Respiratory	55 (44)	38 (44)	0.81
Intraabdominal	56 (45)	36 (42)	
Other	14 (11)	12 (14)	

instance. Covariates that describe something about the current disease status and/or medical history for each patient may also be collected (Mould and Upton, 2013). In longer term studies, the extent to which a covariate, such as renal function, measured by creatinine clearance, may be changing could be particularly important to capture, especially BPM elimination is largely renal

TABLE 5 Multivariable Logistic analysis of factors associated with biapenem treatment clinical success.

Variables	Odds ratio	95% Confidence interval	*p*-value
70% *fT* > MIC	7.07	2.45–20.37	<0.001
Hypoalbuminemia	0.33	0.12–0.91	0.03

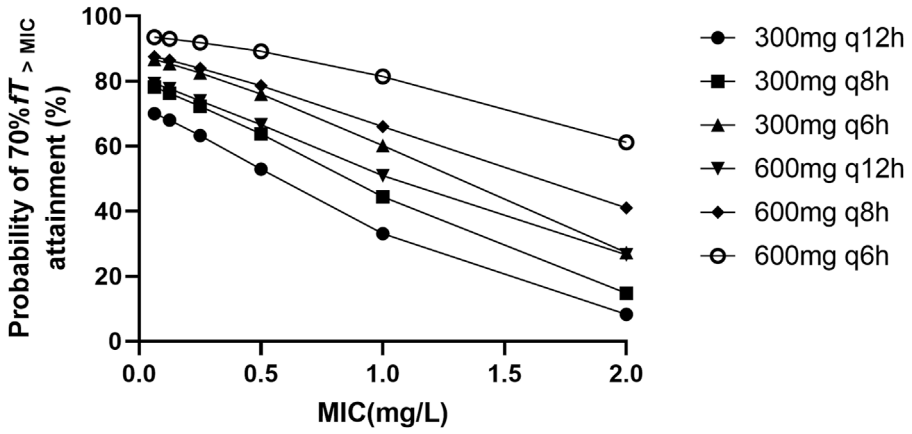

FIGURE 3
Probability of ≥70% fT > MIC attainment for different biapenem dosage regimens with different MIC values ranging from 0.0625 to 2 mg/L.

(Perry and Ibbotson, 2002). Other covariates that are sometimes studied as time-varying factors include laboratory measures of hepatic function, which may be measured at multiple study visits, as well as concomitant medications of interest with the potential to induce a drug–drug interaction. So the above covariates were introduced in the model building in this study.

The present study used a two-compartment model to describe the pharmacokinetic data of BPM, which is consistent with previous study (Ikawa et al., 2008b). To assess the pharmacokinetic characteristics of the adult patients with sepsis, we examined the impact of covariates on pharmacokinetic parameters. The previous study of Ikawa et al. found that the average CL of BPM in adult patients was 8.13 L/h for CLCr of 77.5 mL/min (Ikawa et al., 2008b). In this study, an average CL was observed, the mean CL of BPM in patients with sepsis was 8.33 L/h for CLCr of 78.2 mL/min. Hang et al. reported an average CL BPM in critically ill patients was 20.9 L/h, higher than the CL observed from this study (Hang et al., 2018). Although ALB was included as a covariate affecting CL during the model building process using forward inclusion method, it was eventually eliminated from the final model. Therefore, it was found through the study that CLCr was the most significant influencing factor on BPM CL. However, we speculate that a low ALB level may also have a potential impact on CL of BPM. Patients with lower level of ALB was often related with impaired renal or liver function. A previous study has also shown that, under the same renal function level, patients with decompensated cirrhosis have relatively lower meropenem trough concentrations, suggesting that alteration of pharmacokinetics was common in patients with impaired liver function, which could be similar in pharmacokinetics of BPM (Bastida et al., 2020).

Also, the volume of distribution of BPM differs significantly from previous studies. Ikawa et al. reported an average V (V_1+V_2) of 14.3 L in adult patients (Ikawa et al., 2008b) while Hang et al. found the V was 46.43 L in critically ill patients (Hang et al., 2018). In the current investigation, the V (V_1+V_2) of BPM was observed to reach a notable 73.8 L among patients suffering from sepsis, approximately four to five times higher than that observed in other patient populations in previous studies. Although only a few studies have investigated the population pharmacokinetics of carbapenems in septic patients, an increase in the volume of distribution is common. Fukumoto et al. revealed the volume of distribution of meropenem V (V_1+V_2) in patients with sepsis was 39.7L (Fukumoto et al., 2023), while Murínová et al. reported an average V of 55L in patients with serious infection (Murínová et al., 2022), respectively. Both studies reported higher V of meropenem in patients with sepsis comparing with other patients, which may be caused by the increase in V of hydrophilic drugs, which is quite common in critically ill patients (Roberts and Lipman, 2006). In this study, the observed elevation in the V of BPM among septic patients, also a hydrophilic drug, is consistent with the theory established in previous research.

In the present study, we found that the Q of BPM in septic patients is affected by the levels of BUN. It has been reported that BUN levels are significantly correlated with the prognosis of sepsis patients (Li et al., 2021; Harazim et al., 2023), with even a mild elevation in BUN being associated with an increased mortality in these patients. While the association between elevated BUN levels and neurohormonal response has predominantly been established within populations of patients experiencing cardio-renal issues, we contend that elevated BUN, irrespective of eGFR, may intricately signify intricate underlying pathological processes directly involved in the pathophysiology of sepsis. Although the link between elevated BUN and neurohormonal response has almost exclusively been derived from population of patients with cardio-renal problems

we believe that elevated BUN independent of GFR may sensitively reflect complex underlying pathological processes directly implicated in the pathophysiology of sepsis. In the context of sepsis, arterial underfilling arising from systemic inflammation-induced arterial vasodilation serves as a robust trigger for the activation of the sympathetic nervous system (SNS), the renin–angiotensin–aldosterone axis (RAAS), and the non-osmotic release of vasopressin (AVP) (Gomes et al., 2020). While the SNS, RAAS and AVP all constitute pivotal adaptive responses to stress, there is a compelling inclination to hypothesize that excessive and prolonged activation during sepsis may transition into a maladaptive state, eliciting adverse effects. Moreover, sepsis is distinguished by a profound and frequently enduring catabolic state, culminating in the depletion of muscle mass and neuromuscular weakness. In this context, elevated BUN may additionally function as an indicator of severe catabolism in sepsis. Substantiating this concept, Haines et al. recently recognized the urea-to-creatinine ratio as a promising biomarker of catabolism associated with critical illness (Haines et al., 2019). The aforementioned alterations may signify the undiscovered prognostic value of BUN in the pathophysiology of sepsis, potentially entwined with systemic metabolism and inflammatory levels, which influence the pharmacokinetics of BPM.

According to our analyses, achieving a 70% $fT_{>MIC}$ significantly enhances the likelihood of clinical cure in patients with sepsis treated with BPM. This finding underscores the critical role of optimizing antimicrobial exposure to improve therapeutic outcomes. Additionally, the analysis identified hypoalbuminemia as a significant risk factor for treatment failure. The implications of these findings are twofold. Firstly, they highlight the importance of individualized dosing strategies based on PK/PD principles to maximize the efficacy of BPM in treating septic patients. Secondly, the identification of hypoalbuminemia as a risk factor suggests that addressing underlying nutritional deficits or managing the protein distribution profiles may be crucial in enhancing treatment efficacy. These insights pave the way for targeted interventions and optimized therapeutic strategies in the management of sepsis, potentially improving patient outcomes through tailored therapeutic approaches.

Carbapenems demonstrate time-dependent antibacterial activity, wherein their efficacy is most closely associated with the % $fT_{>MIC}$. It is generally recommended that the %$fT_{>MIC}$ of carbapenems should reach a threshold of 40%–50% to achieve optimal bactericidal effects, and the position paper of European Society of Intensive Care Medicine recommended a clinical PK/PD target for efficacy of 50%–100%$fT_{>MIC}$ (Abdul-Aziz et al., 2020). In this study, we chose a target of 70% $fT_{>MIC}$. Although there are limited pharmacodynamic data of BPM beyond this study, a goal of 70% $fT_{>MIC}$ would represent a more conservative endpoint. As shown in the results of Monte Carlo simulations, in the population of patients with sepsis, it appears that the recommended dosage as per the product label may not adequately achieve the clinical efficacy targets. Under the daily total dose regimen of 1.2 g, probability was lower than 80% to attain 70% $fT_{>MIC}$ in patients with pathogens exhibiting a MIC of 1.0 mg/L. Only the 300 mg q6h regimen demonstrates a probability exceeding 60% for attaining 70% $fT_{>MIC}$ in this microbial subset. The probability drop to less than 30% in patients with pathogens exhibiting a MIC of 2.0 mg/L under the daily total dose regimen of 1.2 g. This implies that a higher daily dosage of BPM is required in septic patients to achieve therapeutic goals. To improve PK/PD target attainment, an optimized dosing regimen of 600 mg q6h was required for pathogens with a MIC of 1.0 mg/L because of a higher PD parameter attainment (81.47%). In septic patients, the BPM regimen of 600 mg q8h appears to exhibit no significant increase in the probability of achieving PK/PD targets compared to the 300 mg q6h regimen. The difference in target attainment probabilities between the two dosage regimens exceeds 10% only when the MIC is 2 mg/L (41.08% vs. 27.32%). Currently, there are no recommendations published by CLSI and EUCAST regarding bacterial susceptibility breakpoints for BPM. According to the antimicrobial susceptibility report from the bacteriological laboratory in China, *Escherichia coli* and *Enterobacter cloacae* exhibited susceptibility to BPM, with MIC_{90} values of 0.25 mg/L and 0.5 mg/L, respectively, while *Klebsiella pneumoniae* has an MIC_{90} of 2 mg/L (Dong et al., 2016). Therefore, based on our research findings, it is suggested that BPM may necessitate a daily dosage higher than the current clinical standard (1.2 g per day) in septic patients to achieve sufficient clinical efficacy while infections are caused by *Klebsiella pneumoniae*. This calls for further exploration through meticulously designed prospective randomized controlled clinical studies.

At the same time, we must confess that the current study's limitation to a single-center cohort restricts its external validity. Extending the future study to include multiple centers, especially those in different geographic locations, would not only enhance the robustness of the pharmacokinetic model but also improve its generalizability across broader patient populations. While the study effectively identifies creatinine clearance and blood urea nitrogen as significant predictors of biapenem clearance, these findings scratch the surface of the complex interplay of factors impacting drug metabolism in septic patients. Investigating additional covariates, such as genetic factors, could uncover nuances in pharmacokinetic parameters that standard analyses might overlook. The inclusion of a validation cohort in the study is commendable; however, validation through an independent cohort from diverse demographics or geographic areas would solidify the pharmacokinetic model's utility and reliability. This approach would mitigate the cohort-specific bias and confirm the model's efficacy across various clinical settings. The manuscript delineates the inter-individual variability observed in the pharmacokinetic parameters of biapenem. Identifying the sources of this variability is crucial for optimizing dosing strategies. Moreover, exploring inter-occasion variability, which accounts for changes in pharmacokinetic parameters between different visits of the same patient, could enhance the model's accuracy. This variability might be attributed to changes in disease state, concomitant medications, or recovery phase, and its inclusion in the analysis could refine dose adjustments over the course of treatment. However, due to the retrospective nature of the study, we were not able to discover the variability more specifically. This study fail to integrate microbiological efficacy data, such as bacterial load dynamics and susceptibility changes, to enhance the pharmacokinetic model's utility by linking drug exposure to microbial response. This approach should be utilized in future prospective study to provide a more holistic understanding of biapenem's therapeutic impact, particularly in modifying treatment strategies based on microbiological feedback. Lastly, while the manuscript adeptly discusses pharmacokinetic-driven dose optimization using Monte Carlo simulations, and

compare the clinical outcomes of the, integrating these theoretical dosing schemes with real-world clinical outcomes would vastly improve the practical value of the study. Prospective clinical trials designed to evaluate the correlation between optimized dosing regimens and patient-centric outcomes such as infection resolution and survival rates are essential for translating pharmacokinetic insights into clinical practice.

This study represents the first exploration of the PK parameters of BPM in septic patients. The considerable sample size included in this study can be attributed to the routine implementation of TDM in clinical practice for BPM therapy. There are limitations in our present study. The use of data collected during routine TDM limiting the number of BPM concentrations measured for each patient. Due to the substantial heterogeneity in microbiota among septic patients and the complexity of clinical conditions during treatment, integrating PPK models, actual clinical efficacy, and PK/PD index is challenging and complicated. Ultimately, the optimal dose regimen based on modeling and simulation should be evaluated in clinical practice to confirm its clinical benefits.

5 Conclusion

The PPK model of BPM was developed in patients with sepsis and elucidated the significant effects of CLCr and BUN on BPM pharmacokinetics. The target of 70%$fT_{>MIC}$ is associated with favorable clinical outcomes. The current daily dosage regimen of 1.2 g may potentially fall short of achieving sufficient clinical efficacy in septic patients when treating pathogens with MIC>1 g/L. To attaian 70%$fT_{>MIC}$, the dosage regimen of 600 mg every 6 h appears to be the optimal choice. These results better define the pharmacokinetics of BPM and help in the choice of the appropriate dosage regimens of BPM for patients with sepsis.

Data availability statement

The raw data supporting the conclusion of this article will be made available by the authors, without undue reservation.

Ethics statement

The study was approved by the Ethics Committee of Nanjing Drum Tower Hospital Affiliated Hospital of Nanjing University Medical School, Nanjing, China (2022-504-01) and was registered at the Chinese Clinical Trial Registry (ChiCTR2300073976). The need for informed consent was waived by the ethics committee in view of the observational and retrospective nature of the study.

Author contributions

DC: Conceptualization, Data curation, Funding acquisition, Project administration, Writing–original draft, Writing–review and editing. XW: Conceptualization, Data curation, Software, Visualization, Writing–original draft, Writing–review and editing. HaZ: Conceptualization, Data curation, Funding acquisition, Writing–original draft, Writing–review and editing. HY: Data curation, Formal Analysis, Writing–original draft. LJ: Investigation, Methodology, Writing–original draft. XL: Investigation, Writing–original draft. JL: Investigation, Writing–original draft. ZW: Investigation, Writing–original draft. YL: Software, Writing–original draft. WX: Resources, Writing–original draft. WG: Resources, Writing–original draft. XC: Project administration, Supervision, Validation, Writing–review and editing, Writing–original draft. HuZ: Project administration, Supervision, Validation, Writing–review and editing, Writing–original draft.

Funding

The author(s) declare that financial support was received for the research, authorship, and/or publication of this article. This study was supported by Project of Modern Hospital Management and Development Institute, Nanjing University and Aid Project of Drum Tower Hospital Health, Education and Research Foundation (NDYG2021044), Nanjing Pharmaceutical Association—Changzhou Si Yao Research Foundation of Hospital Pharmacy (2023YX013) and Nanjing Medical Center for Clinical Pharmacy (NWKJ 2020–1).

Acknowledgments

The authors thank all the patients participated in the study. The authors thank all the doctors, residents, pharmacists, and nurses directly involved in the management of these patients. We thank Xiaoyuan Chen, Jinglin Wang, and Haozhen Ren for their valuable suggestions in manuscript drafting. We thank Yao Du, Xiao Du, Simin Yan, Dan Han, Yunxing Liu, Huanyu Ni, Min Xue, Huiyan Jiang, and Yanran Zhao (Nanjing Drum Tower Hospital) for supporting our research during this pandemic in the context of such a difficult health crisis. They did not receive funding for this assistance.

Conflict of interest

The authors declare that the research was conducted in the absence of any commercial or financial relationships that could be construed as a potential conflict of interest.

Publisher's note

Supplementary material

The Supplementary Material for this article can be found online at: https://www.frontiersin.org/articles/10.3389/fphar.2024.1388150/full#supplementary-material

References

Abdul-Aziz, M. H., Alffenaar, J. C., Bassetti, M., Bracht, H., Dimopoulos, G., Marriott, D., et al. (2020). Antimicrobial therapeutic drug monitoring in critically ill adult patients: a Position Paper<sub/>. *Med* 46, 1127–1153. doi:10.1007/s00134-020-06050-1

Alonso, R., Fernández-Aranguiz, A., Colom, K., Morla, A., Suinaga, E., Umaran, A., et al. (2006). *In vitro* activity of biapenem against beta-lactamase producing Enterobacteriaceae. *Eur. J. Clin. Microbiol. Infect. Dis.* 13, 820–822. doi:10.1007/BF02111342

Bastida, C., Hernández-Tejero, M., Aziz, F., Espinosa, C., Sanz, M., Brunet, M., et al. (2020). Meropenem population pharmacokinetics in patients with decompensated cirrhosis and severe infections. *J. Antimicrob. Chemother.* 75, 3619–3624. doi:10.1093/jac/dkaa362

Bleeker, S. E., Moll, H. A., Steyerberg, E. W., Donders, A. R., Derksen-Lubsen, G., Grobbee, D. E., et al. (2003). External validation is necessary in prediction research: a clinical example. *J. Clin. Epidemiol.* 56 (9), 826–832. doi:10.1016/s0895-4356(03)00207-5

Boonpeng, A., Jaruratanasirikul, S., Jullangkoon, M., Samaeng, M., Wattanavijitkul, T., Bhurayanontachai, R., et al. (2022). Population pharmacokinetics/pharmacodynamics and clinical outcomes of meropenem in critically ill patients. *Antimicrob. Agents. Chemother.* 66, e0084522. doi:10.1128/aac.00845-22

Brismar, B., Akerlund, J. E., Sjöstedt, S., Johansson, C., Törnqvist, A., Bäckstrand, B., et al. (1996). Biapenem versus imipenem/cilastatin in the treatment of complicated intra-abdominal infections: report from a Swedish Study Group. *Scand. J. Infect. Dis.* 28, 507–512. doi:10.3109/00365549609037949

Cockcroft, D. W., and Gault, M. H. (1976). Prediction of creatinine clearance from serum creatinine. *Nephron.* 16, 31–41. doi:10.1159/000180580

Dinh, T. D., Nguyen, H. N., Le, B. H., Nguyen, T. T. T., and Nguyen, H. T. L. (2022). Population-based pharmacokinetics and dose optimization of imipenem in Vietnamese critically-ill patients. *Infect. Drug. Resist.* 15, 4575–4583. doi:10.2147/IDR.S373348

Dong, J., Chen, Y. C., Xiong, W., Zhao, Y. F., Sun, Y. B., Lu, Y., et al. (2016). Efficacy and safety of biapenem against lower respiratory tract infections in elderly Chinese patients and optimal dosing regimen based on pharmacokinetic/pharmacodynamic analysis. *J. Chemother.* 28, 403–410. doi:10.1179/1973947815Y.0000000078

Evans, L., Rhodes, A., Alhazzani, W., Antonelli, M., Coopersmith, C. M., French, C., et al. (2021). Surviving sepsis campaign: international guidelines for management of sepsis and septic shock 2021. *Intensive. Care. Med.* 47, 1181–1247. doi:10.1007/s00134-021-06506-y

Fukumoto, S., Ohbayashi, M., Okada, A., Kohyama, N., Tamatsukuri, T., Inoue, H., et al. (2023). Population pharmacokinetic model and dosing simulation of meropenem using measured creatinine clearance for patients with sepsis. *Ther. Drug. Monit.* 45, 392–399. doi:10.1097/FTD.0000000000001040

Gomes, D. A., de Almeida Beltrão, R. L., de Oliveira Junior, F. M., da Silva Junior, J. C., de Arruda, E. P. C., Lira, E. C., et al. (2020). Vasopressin and copeptin release during sepsis and septic shock. *Peptides* 136, 170437. doi:10.1016/j.peptides.2020.170437

Griffith, D. C., Morgan, E. E., Dudley, M. N., and Loutit, J. S. (2023). A phase 1 study of the safety, tolerability, and pharmacokinetics of biapenem in healthy adult subjects. *Antimicrob. Agents. Chemother.* 65, e02612. doi:10.1128/AAC.02612-20

Haines, R. W., Zolfaghari, P., Wan, Y., Pearse, R. M., Puthucheary, Z., and Prowle, J. R. (2019). Elevated urea-to-creatinine ratio provides a biochemical signature of muscle catabolism and persistent critical illness after major trauma. *Intensive. Care. Med.* 45 (12), 1718–1731. doi:10.1007/s00134-019-05760-5

Hang, Y., Chen, Y., Xue, L., Sun, S., Liu, L., Gao, J., et al. (2018). Evaluating biapenem dosage regimens in intensive care unit patients with *Pseudomonas aeruginosa* infections: a pharmacokinetic/pharmacodynamic analysis using Monte Carlo simulation. *Int. J. Antimicrob. Agents.* 51, 484–487. doi:10.1016/j.ijantimicag.2017.07.005

Harazim, M., Tan, K., Nalos, M., and Matejovic, M. (2023). Blood urea nitrogen - independent marker of mortality in sepsis. *Biomed. Pap. Med. Fac. Univ. Palacky. Olomouc. Czech. Repub.* 167, 24–29. doi:10.5507/bp.2022.015

Hooker, A. C., Staatz, C. E., and Karlsson, M. O. (2007). Conditional weighted residuals (CWRES): a model diagnostic for the FOCE method. *Pharm. Res.* 24, 2187–2197. doi:10.1007/s11095-007-9361-x

Ikawa, K., Morikawa, N., Ikeda, K., Miki, M., Nishimura, S., and Kobayashi, M. (2008a). Population pharmacokinetics and pharmacodynamics of biapenem in paediatric patients. *J. Clin. Pharm. Ther.* 33, 203–210. doi:10.1111/j.1365-2710.2008.00908.x

Ikawa, K., Morikawa, N., Ikeda, K., Ohge, H., Sueda, T., Suyama, H., et al. (2008b). Pharmacokinetic-pharmacodynamic target attainment analysis of biapenem in adult patients: a dosing strategy. *Chemotherapy* 54, 386–394. doi:10.1159/000152459

Li, C., Du, X., Kuti, J. L., and Nicolau, D. P. (2007). Clinical pharmacodynamics of meropenem in patients with lower respiratory tract infections. *Chemother* 51, 1725–1730. doi:10.1128/AAC.00294-06

Li, X., Zheng, R., Zhang, T., Zeng, Z., Li, H., and Liu, J. (2021). Association between blood urea nitrogen and 30-day mortality in patients with sepsis: a retrospective analysis. *Ann. Palliat. Med.* 10, 11653–11663. doi:10.21037/apm-21-2937

McKinnon, P. S., Paladino, J. A., and Schentag, J. J. (2008). Evaluation of area under the inhibitory curve (AUIC) and time above the minimum inhibitory concentration (T>MIC) as predictors of outcome for cefepime and ceftazidime in serious bacterial infections. *Int. J. Antimicrob. Agents.* 31, 345–351. doi:10.1016/j.ijantimicag.2007.12.009

Mould, D. R., and Upton, R. N. (2013). Basic concepts in population modeling, simulation, and model-based drug development-part 2: introduction to pharmacokinetic modeling methods. *CPT pharmacometrics Syst. Pharmacol.* 2 (4), e38. doi:10.1038/psp.2013.14

Murínová, I., Švidrnoch, M., Gucký, T., Řezáč, D., Hlaváč, J., Slanař, O., et al. (2022). Meropenem population pharmacokinetics and model-based dosing optimisation in patients with serious bacterial infection. *Eur. J. Hosp. Pharm. ejhpharm-2022-003535* 31, 253–258. doi:10.1136/ejhpharm-2022-003535

Nguyen, T. H., Mouksassi, M. S., Holford, N., Al-Huniti, N., Freedman, I., Hooker, A. C., et al. (2017). Model evaluation of continuous data pharmacometric models: metrics and graphics. *CPT Pharmacometrics Syst. Pharmacol.* 6 (2), 87–109. doi:10.1002/psp4.12161

Perry, C. M., and Ibbotson, T. (2002). Biapenem. *Drugs* 62, 2221–2234. ; discussion 2235. doi:10.2165/00003495-200262150-00005

Rao, Q., Yang, Y., Wang, S., Zhu, H., Jin, L., Zhang, J., et al. (2023). Optimal dosing regimen of biapenem based on population pharmacokinetic/pharmacodynamic modelling and Monte Carlo simulation in patients with febrile neutropenia and haematological malignancies. *Int. J. Antimicrob. Agents.* 62, 106841. doi:10.1016/j.ijantimicag.2023.106841

Roberts, J. A., and Lipman, J. (2006). Antibacterial dosing in intensive care: pharmacokinetics, degree of disease and pharmacodynamics of sepsis. *Clin. Pharmacokinet.* 45, 755–773. doi:10.2165/00003088-200645080-00001

Singer, M., Deutschman, C. S., Seymour, C. W., Shankar-Hari, M., Annane, D., Bauer, M., et al. (2016). The third international Consensus Definitions for sepsis and septic shock (Sepsis-3). *JAMA* 315, 801–810. doi:10.1001/jama.2016.0287

van der Poll, T. (2001). Immunotherapy of sepsis. *Lancet. Infect. Dis.* 1, 165–174. doi:10.1016/S1473-3099(01)00093-7

Zhanel, G. G., Wiebe, R., Dilay, L., Thomson, K., Rubinstein, E., Hoban, D. J., et al. (2007). Comparative review of the carbapenems. *Drugs* 67, 1027–1052. doi:10.2165/00003495-200767070-00006

frontiers | Frontiers in Pharmacology

TYPE Review
PUBLISHED 20 May 2024
DOI 10.3389/fphar.2024.1385261

OPEN ACCESS

EDITED BY
Nikolaos E. Labrou,
Agricultural University of Athens, Greece

REVIEWED BY
Sarunyou Chusri,
Prince of Songkla University, Thailand
Shanmugaraj Gowrishankar,
Alagappa University, India
Md. Sharifull Islam,
Chinese Academy of Sciences (CAS), China
Pir Tariq Shah,
Dalian University of Technology, China

*CORRESPONDENCE
Rui Zhang,
ruizhang@szu.edu.cn
Bin Liu,
liubin@szu.edu.cn

RECEIVED 12 February 2024
ACCEPTED 16 April 2024
PUBLISHED 20 May 2024

CITATION
Khan FM, Rasheed F, Yang Y, Liu B and Zhang R (2024), Endolysins: a new antimicrobial agent against antimicrobial resistance. Strategies and opportunities in overcoming the challenges of endolysins against Gram-negative bacteria. *Front. Pharmacol.* 15:1385261. doi: 10.3389/fphar.2024.1385261

Endolysins: a new antimicrobial agent against antimicrobial resistance. Strategies and opportunities in overcoming the challenges of endolysins against Gram-negative bacteria

Fazal Mehmood Khan[1,2], Fazal Rasheed[3], Yunlan Yang[2], Bin Liu[2]* and Rui Zhang[2,4]*

[1]College of Civil and Transportation Engineering, Shenzhen University, Shenzhen, China, [2]Institute for Advanced Study, Shenzhen University, Shenzhen, China, [3]Institute of Microscale Optoelectronics, Shenzhen University, Shenzhen, China, [4]Southern Marine Science and Engineering Guangdong Laboratory, Zhuhai, China

Antibiotic-resistant bacteria are rapidly emerging, and the increasing prevalence of multidrug-resistant (MDR) *Acinetobacter baumannii* poses a severe threat to humans and healthcare organizations, due to the lack of innovative antibacterial drugs. Endolysins, which are peptidoglycan hydrolases encoded by a bacteriophage, are a promising new family of antimicrobials. Endolysins have been demonstrated as an effective therapeutic agent against bacterial infections of *A. baumannii* and many other Gram-positive and Gram-negative bacteria. Endolysin research has progressed from basic *in vitro* characterization to sophisticated protein engineering methodologies, including advanced preclinical and clinical testing. Endolysin are therapeutic agent that shows antimicrobial properties against bacterial infections caused by drug-resistant Gram-negative bacteria, there are still barriers to their implementation in clinical settings, such as safety concerns with outer membrane permeabilizers (OMP) use, low efficiency against stationary phase bacteria, and stability issues. The application of protein engineering and formulation techniques to improve enzyme stability, as well as combination therapy with other types of antibacterial drugs to optimize their medicinal value, have been reviewed as well. In this review, we summarize the clinical development of endolysin and its challenges and approaches for bringing endolysin therapies to the clinic. This review also discusses the different applications of endolysins.

KEYWORDS

antimicrobial resistance, antimicrobial agent, *A. baumannii*, Gram-negative bacteria, endolysin

1 Antimicrobial resistance

The discovery of antibiotics transformed medicine, greatly increasing the quality of life, extending human lifespans, and enabling numerous complicated medical procedures and medicines, all while maintaining healthy lives and boosting public health. Unfortunately, genetically encoded antimicrobial resistance (AMR) has increased as discoveries have

reduced, particularly in the early part of this century. Nonetheless, there have always been infectious factors when antibiotics have failed, and these keep outnumbering antibiotic resistance as a cause of morbidity and mortality (de la Fuente-Nunez et al., 2023). The resistance to antibiotics is a result of bacterial evolution, which protects bacteria from drugs that are harmful to their survival. It is a subset of AMR, a broader term for the evolution of resistance to naturally occurring agents or targeted medications in bacteria. AMR is linked to antibiotic use and becomes worse by antibiotic misuse and overuse in the medical sector. Increased resistance in pathogenic bacteria poses several critical public health problems, including severe and protracted illness, more hospitalizations and complications, and higher rates, all of which result in a significant cost burden (Behling et al., 2023). In recent decades, worldwide use of veterinary antibiotics has decreased, although worldwide clinical use of antibiotics remains high, and overuse exists in low- and middle-income nations. Although the majority of countries have implemented national action plans (NAPs) to actively address antibiotic resistance, actual AMR measures range significantly (Ding et al., 2023). In 2015, the 68th World Health Organization (WHO) assembly passed the global action plan on AMR to support action against resistance to antibiotics, and as a result, several nations and regions have implemented AMR mitigation strategies. The library of AMR NAPs was evaluated on 31 January 2023, and 134 countries (of which 40 were written in a language other than English) had officially approved NAPs, which includes 69% of the world's 194 countries (Ding et al., 2023). As a result of antibiotic overuse and misuse, an increasing number of resistant bacteria have been isolated from the healthcare system and the environment. The rapid genetic material and resistance genes exchange among bacterial strains encourages the spread of AMR (Loh et al., 2021). Antibiotic resistance has been a worldwide challenge that could make a massive impact on both healthcare systems and the economic system. To fill the significant gap left by a high rate of resistance development and an inadequately filled antibiotic development pipeline, the WHO has called for the urgent development of novel antibacterial agents (Abdelkader et al., 2022). A novel alternative antimicrobial agent must be developed immediately to combat the severe threat of MDR bacterial infections due to the decline in antibiotic efficacy and the lack of novel antibiotics, pushing us closer to a post-antibiotic era (Chu et al., 2022). The bacteria that are part of ESKAPE (*Enterococcus faecium, Staphylococcus aureus, Kleibsiella pneumoniae, A. baumannii, P. aeruginosa* and *Enterobacter species*) are important drug-resistant pathogens. Among these, *Acinetobacter baumannii* is regarded as a global problem because of its potential to gain antibiotic resistance at a staggering rate (Rai and Kumar, 2022). *A. baumannii* is a significant nosocomial and opportunistic Gram-negative bacterium, causing infections worldwide, especially in intensive care units (ICU). It can cause numerous hospital- and community-acquired infections, such as ventilator-associated pneumonia, bacteremia, wound infections, and meningitis. It is clinically significant because of its capacity to survive for long periods on the substrate surface and its resistance to multiple drugs, making it the most prevalent and high alert pathogen on the WHO list of critical pathogens. This bacterium has been recognized to flout available therapeutic options. Alternative approaches to medicating *A. baumannii* infections are vitally important (Oyejobi et al., 2022a). The WHO has classified carbapenem-resistant *A. baumannii* (CRAB) as an urgently needed pathogen with limited therapy choices, thus there is an urgent need for research and development of new antibiotics as well as various alternative treatment strategies (Jansen et al., 2018). AMR highlighted that the present therapeutic pipeline is insufficient to address the AMR issue, particularly for three Gram-negative carbapenem-resistant, important priority pathogens: *Pseudomonas aeruginosa, A. baumannii,* and Enterobacteriaceae. Despite an increase in the number of antibiotics targeting Gram-negative infections in the clinical pipeline, most of them are variants of existing ones, serving as a temporary remedy because resistance to these evolved medications is likely to emerge quickly. Out of forty-two novel drugs for treatment that target priority pathogens, just two drugs from the same class (siderophore-cephalosporins) target the three Gram-negative critical priority pathogens (Gutiérrez and Briers, 2021). With a novel mode of action, bacteriophage-encoded endolysin has developed into the most effective class of bactericidal biological agents currently undergoing clinical testing (WHO (Organization, 2019). Endolysin were initially denied from use against Gram-negative pathogens due to their impermeable outer membrane, but they are now being developed as effective therapeutic agent against these critical priority pathogens. In principle, the three routes of investigation have been recently explored and advanced to varying degrees, including the use of endolysin that possess intrinsic activity due to a positively charged C-terminus that destabilizes the outer membrane, the use of physical or chemical methods to disrupt the outer membrane integrity, and protein engineering to provide the endolysin with the tools it needs to overcome the outer membrane (Gutiérrez and Briers, 2021). In this review article, we have specifically addressed the use of endolysin against *A. baumannii* and we have addressed and presented *A. baumannii* as a case study model of the use of endolysin as a new therapeutic agent. We have also highlighted the issues and barriers of transforming endolysin from the lab to the clinic and the strategies to overcome these issues of endolysin to be used as a novel therapeutic drug.

1.1 Endolysins' structure and enzymatic activity

Endolysins are proteins that are expressed late in the bacteriophage virus's lytic cycle. After the bacteriophage completes its lytic cycle within the host, endolysins break down the host's cell wall by splitting the host's peptidoglycan to release offspring virions (Abdelrahman et al., 2021b). Gram-positive bacteriophage endolysins have a modular structure, with EADs at the N-terminus and CBDs attached at the C-terminus via a linker. Endolysins have enzymatic hydrolysis and substrate identification capabilities due to the presence of EADs and CBDs. Typically, modular endolysins have one or two EADs at the N-terminal and CBD at the C-terminal connected by a flexible region known as the linker (Gondil et al., 2021b). The N-terminal EAD of modular endolysins cleaves certain peptidoglycan bonds in the host bacterium's murein layer, while the C-terminal CBD identifies and connects to numerous epitopes in the cell wall for optimal

binding of the EAD's catalytic actions (Wang et al., 2023). The bacteriophage-derived endolysins of Gram-negative hosts can be structured in different kinds of ways, although most of them have a basic globular EAD domain without a CBD. The latest study also discovered Gram-negative endolysins with globular structures, one or two CBDs at the N-terminus, and the EAD module at the end of the C-terminal region (Briers et al., 2007). Endolysins are categorized based on their cleavage site. These enzymes include lysozymes (N-acetylmuramidases), glycosidases (N-acetyl--d-glucosamidases), N-acetylmuramoyl-l-alanine amidases, and L-alanoyl-d-glutamate endopeptidases (Khan et al., 2023b). Endolysins, which are composed of one of these four N-terminals connected to a distinct cell wall-binding domain, also be known as bacteriophage-encoded cell wall hydrolases (Murray et al., 2021).

Glycosidases: The polymeric structures of N-acetylmuramic acids (MurNAc) and N-acetylglucosamines (GlcNAc) are linked by −1,4 glycosidic linkages that are split by glycosidases. N-acetyl--D-muramidase's split bonds within GlcNAc and MurNAc residues. N-acetyl--D-glucosidases split bonds within GlcNAc and MurNAc residues (Matamp and Bhat, 2019). Like the other two glycosidases, transglycosylases cleave −1,4 bonds within GlcNAc and MurNAc, but they additionally play a role in an intramolecular mechanism that results in the production of a 1,6-anhydro ring at the MurNAc residue (Rodríguez-Rubio et al., 2016a). Lysozymes, also known as N-acetylmuramidases, eradicate bacteria by specialized hydrolysis. Glycosidases, or N-acetyl-β-d-glucosamidases, control the hydrolysis of the glycosidic link. Glycosidic linkages β-1,4 bind the NAG (N-acetylglucosamine) and NAM (N-acetylmuramic acid) monomers of peptidoglycan polymers together. Lysozyme acts to break the structural integrity of the peptidoglycan cell wall by hydrolyzing these connections. This results in an imbalance in the turgor pressure, which kills the bacterial cell (Ragland and Criss, 2017).

Amidases: The mechanism by which N-acetylmuramoyl-L-alanine amidases, also referred to as peptidoglycan amidases act is to break the amide bond that separates the glycan strand from the stem peptide that is located between the L-alanine and N-acetylmuramic acid residues (Abdelrahman et al., 2021b).

Endopeptidases: Enzymes called endopeptidases dissolve the bonds that hold two amino acids together in the stem peptide. Both L-alanoyl-d-glutamate endopeptidases and interpeptide bridge-specific endopeptidases target the peptide that makes up the L-alanoyl-d-glutamate link. Between stem peptides or inside an interpeptide bridge, bonds can break (Rodríguez-Rubio et al., 2016a).

1.2 *A. baumannii* resistance and a lack of therapeutic alternatives

Treatment of *A. baumannii* infections is complex due to its high capacity for acquiring resistance genes and its natural resistance to a wide range of antibiotics (Poirel et al., 2011). *Acinetobacter baumannii* infections are frequently treated with colistin as a last-line antibiotic. Still, an increasing number of reports on colistin-resistant strains indicate that the era of antibiotics is challenging (Lim et al., 2019). Carbapenems were once the primary therapy for MDR *A. baumannii* infections, but their use has resulted in an increase in carbapenem resistance in recent years (Nordmann and Poirel, 2019). Polymyxins are currently routinely used as the antibiotics of choice for treating MDR *A. baumannii* infections, despite initially being prohibited due to systemic toxicities (nephrotoxicity and neurotoxicity) (Piperaki et al., 2019). Extensive drug-resistant (XDR) *A. baumannii* is classified as an isolate resistant to three or more of the antibiotic classes (penicillin's and cephalosporins, which include inhibitor combinations, fluoroquinolones, and aminoglycosides, with carbapenem resistance in the majority of cases). In contrast, pan-drug-resistant (PDR) *A. baumannii* is an XDR isolate resistant to polymyxins and tigecycline (Mulani et al., 2019). Antibiotic resistance mechanisms fall into three categories. First, resistance can be developed by decreasing membrane permeability or increasing antibiotic efflux, thereby blocking access to the target. Secondly, bacteria can safeguard the antibiotic receptor through genetic mutation or post-translational modification. Finally, antibiotics can be immediately inactivated through hydrolysis or alteration (Blair et al., 2015). One of *Acinetobacter's* most powerful weapons is its remarkable genetic adaptation, which allows for rapid genetic changes and rearrangements, as well as the incorporation of foreign determinants carried by mobile genetic components. Insertion sequences are regarded as one of the primary mechanisms shaping bacterial genomes and, ultimately, evolution (Vrancianu et al., 2020). Furthermore, *A. baumannii* can form biofilms, extending its ability to survive on healthcare equipment, such as ventilators in intensive care units (ICUs) (Pakharukova et al., 2018). However, the link between biofilm development and antibiotic resistance is currently unclear (Yang et al., 2019). Many therapeutic options have been failed by *A. baumannii*, making treatment of these infections difficult and, in some circumstances, impossible. Given the scarcity of treatment alternatives, there is a need for an innovative strategy and rethinking of remedies for combating this bacterium (Oyejobi et al., 2022b).

1.3 Endolysins are a new class of therapeutic products against *A. baumannii* infections

The emergence of antibiotic-resistant *A. baumannii* necessitates the development of alternative treatment options, with many global pharmaceutical industry players strategically choosing to discontinue or outsource novel antibiotic discovery programs. One of the most promising methods is endolysin therapy, which uses endolysin to combat bacterial pathogens (Khan et al., 2021). Endolysins are peptidoglycan hydrolytic enzymes encoded by bacteriophages that have great potential as a new class of antimicrobial therapeutic agents for multidrug-resistant bacteria (Gondil et al., 2021a). Due to the widespread emergence of antibiotic resistance, endolysins have drawn more attention as an alternative therapy. There is strong evidence that endolysins can externally degrade peptidoglycan without the aid of a bacteriophage. Their incorporation into therapeutic approaches has consequently created new opportunities for treating bacterial infections in the human, veterinary, agricultural, and biotechnology fields (Abdelrahman et al., 2021a). Endolysins are a desirable alternative due to their lytic potential against various bacterial

TABLE 1 Endolysin against *A. baumannii*.

Endolysin	Antibacterial activity spectrum	Outcome	References
AbLys2	*A. baumannii*	• AbLys2 has a strong affinity for *A. baumannii*	Premetis et al. (2023a)
		• AbLys2 has effective lytic and antibacterial activity	
lysAB-vT2	*A. baumannii*	• lysAB-vT2 disrupts the mature bacterial biofilm	Sitthisak et al. (2023a)
LysAB54	*A. baumannii*	• LysAB54 is encoded by a novel *A. baumannii* bacteriophage p54, which showed a broad range of antibacterial activity against Gram-negative bacteria	Khan et al. (2021)
		• Shows a 4-log reduction activity against *A. baumannii* without the use of OMPs	
		• LysAB54 exhibited antibacterial activity against both the logarithmic and stationary phases of *A. baumannii*	
LysP53	*A. baumannii*	• LysP53 is active against a wide range of antibiotic-resistant Gram-negative bacteria, including *A. baumannii*	Li et al. (2021)
		• LysP53, 100 μg/mL showed a 5-log reduction of *A. baumannii* viable number	
LysSS	*A. baumannii*	• LysSS inhibits the growth of *A. baumannii* and *P. aeruginosa*	Kim et al. (2020)
	P. aeruginosa	• A549 human lung cells are not cytotoxic to LysSS.	
		• An intraperitoneal administration of LysSS protects mice infected with *A. baumannii* from systemic infection	
LysAB2P3	*A. baumannii*	• LysAB2 P3 reduced the bacterial burden by 13 times in ascites and 27 times in blood in a mouse intraperitoneal infection model	Peng et al. (2017)
		• LysAB2 P3 prevented deadly bacteremia in 60% of mice with severe *A. baumannii* infections	
LysAB2-KWK	*A. baumannii*	• LysAB2-KWK showed disruption of bacterial biofilms	Chen et al. (2021)
		• Showed activity against the stationary phase of *A. baumannii*	
		• LysAB2-KWK protects the larvae of *Galleria mellonella* from infection with *A. baumannii*	
		• It exhibits a long storage life, moderate serum tolerance, and a broad antibacterial spectrum against Gram-negative bacteria	
Ablysin	*A. baumannii*	• Strong antimicrobial activity in the absence of an outer membrane permeabilizer	Vasina et al. (2021)
		• Lysis activity against multi-drug resistant clinical strains of *A. baumannii*	
		• Antibacterial and biofilm-removing activities against *A. baumannii*	
LysAB3 and LysAB4	*A. baumannii*	• LysAB3 and LysAB4 100 μg/mL disrupt the *A. baumannii* cell shape	Lai et al. (2013)
Abtn-4	*A. baumannii*	• Showed a 3-log reduction against *A. baumannii*	Yuan et al. (2021)
		• Anti-biofilmactivity against bacterial biofilm	
		• Antimicrobial activity against phage-resistant bacterial mutants	
DS-PA90	*A. baumannii*	• It can completely lysis the *A. baumannii* at 0.25 μM concentration	Lim et al. (2022)
Artilysin Art-175	*A. baumannii*	• High antibacterial activity against multidrug-resistant *A. baumannii* stationary-phase cells	Defraine et al. (2016)
		• It can eliminate huge inoculum (10^8 CFU/mL)	

(Continued on following page)

TABLE 1 (*Continued*) Endolysin against *A. baumannii*.

Endolysin	Antibacterial activity spectrum	Outcome	References
LysMK34	*A. baumannii*	• LysMK34 exhibited intrinsic antibacterial activity against *A. baumannii* strains up to 4.8 log units in the presence of turgor pressure • Tolerate temperatures up to 55°C, as well as a wide pH activity range (4–10)	Abdelkader et al. (2020)
LysABP-01	*A. baumannii*	• LysABP-01 can denature the rough cell wall of the *A. baumannii* strain • It showed synergist activity with colistin	Thummeepak et al. (2016a)
AbLys1	*A. baumannii*	• AbLys1 have high specificity for *A. baumannii* • It is most active at pH values of 7–8	Premetis et al. (2023b)
LysAB2	*A. baumannii*	• LysAB2 lysis the *A. baumannii* peptidoglycan	Lai et al. (2011a)
PlyF307	*A. baumannii*	• It can efficiently kill more than >5-log-unit reduction of *A. baumannii* clinical strains • PlyF307 treatment disrupted the biofilm of *A. baumannii* • PlyF307 saved mice from potentially deadly *A. baumannii* bacteremia	Lood et al. (2015)
P307 and P307Q-8C	*A. baumannii*	• P307 and P307SQ-8C both exhibited strong *in vitro* efficacy against biofilms of *A. baumannii* • P307SQ-8C diminished the bacterial burden in a mouse model of *A. baumannii* superficial infection by 2 logs	Thandar et al. (2016)
PlyAB1	*A. baumannii*	• PlyAB1 has lytic activity against the *A. baumannii* AB1 strain • It did lysis of 48 *A. baumannii* isolates that are resistant to drugs	Huang et al. (2014)
Ply6A3	*A. baumannii*	• The intraperitoneal injections of endolysin Ply6A3 rescue deadly *A. baumannii* sepsis mice *in vivo*	Wu et al. (2019)

species that cause human infections. Endolysins are the most successful alternative therapy for treating and curing MDR bacteria. According to reports numerous endolysins have been used successfully to treat bacteria resistant to antibiotics. The antibacterial treatment through bacteriophage-derived endolysin is tested in animal experiment models. Due to their extraordinary therapeutic potential against multidrug-resistant bacteria, endolysin has attracted much attention in recent years (Mehmood Khan et al., 2023). Endolysin are bacteriophage-derived proteins which have high specificity for bacteria, they have no detrimental effects on human or animal cells. Endolysin lacks many features that make antibiotics superior to them, such as no resistance and high specificity (Abdelrahman et al., 2021a; Gondil et al., 2021b). Most bacteriophage endolysins indicate near-species specificity, which is thought to be one of their most beneficial features in this age of broad-range resistance to antibiotics as it avoids selective pressure on naturally occurring beneficial microbiota. Furthermore, resistance to endolysins is improbable for a variety of reasons, Endolysins have evolved to attach to and break highly conserved components in the cell wall of the pathogenic bacteria, secondly, as the bacteriophage and host bacteria coevolution occurs so there are fewer chances of resistance development to endolysin. Furthermore, because endolysins are applied externally and act on the cell wall rather than entering the bacterial cell, they avoid the majority of possible resistance mechanisms (e.g., active efflux from the cell or decreased membrane permeability) that contribute to resistance to most conventional antibiotics. Several endolysins include two catalytic domains that hydrolyze distinct bonds in the peptidoglycan, which is thought to limit the likelihood of resistance formation (Haddad Kashani et al., 2018).

Endolysin LysAB1245 showed broad lytic range efficacy against *A. baumannii* isolates from various capsular variants. Furthermore, LysAB1245 exhibited quick antibacterial activity and stability under different ranges of pH and temperature conditions. This study tested the possibility of LysAB1245 as a novel therapeutic agent for the treatment of MDR A. baumannii bacterial infections (Soontarach et al., 2024). Table 1 shows the summary of the therapeutic potentials of bacteriophage derived endolysins against *A. baumannii*.

1.4 Evaluation of endolysin against *A. baumannii*

Establishing the *in vivo* safety and efficacy of phage-encoded endolysin as medicinal products is an essential step in their development (Lai et al., 2020a). Endolysin can be administered by various methods, such as intravenously and intraperitoneal

injections, topical treatments (creams, ointments, and gels), and trans nasal, vaginal, and oral delivery systems (Abdelrahman et al., 2021b). Endolysins, which target pathogens in various tissues and organs, are currently in clinical trials. Schmelcher et al. have briefly addressed the systemic use of endolysins to treat bacteria-related infections of the bloodstream, organs, and tissues (Schmelcher M. and Loessner M. J. J. C. O. I. B., 2021). In an *A. baumannii* mouse model of burn wound infection, a single dosage of 14 μg/mouse of endolysin LysP53 resulted in a 3-log reduction in bacterial load. The findings suggested that LysP53 can be a promising choice for the treatment of topical infections caused by *A. baumannii* and other Gram-negative bacteria (Li et al., 2021). ElyA1 was used to treat skin infections of *A. baumannii* in *Galleria mellonella*. ElyA1 showed a confirmed significant reduction in the number of bacteria (Blasco et al., 2020a). The $P307_{SQ-8C}$ reduced the bacterial burden by two logs in a mice model of *A. baumannii* cutaneous infection in 2 h (Thandar et al., 2016). LysAB2 P3 reduced bacterial burden in ascites and blood by 13-fold and 27-fold, respectively, in a mouse intraperitoneal infection model 4 h after bacterial injection. Furthermore, LysAB2 P3 saved 60% of mice infected with *A. baumannii* from deadly bacteremia (Peng et al., 2017). Repeated exposure to endolysins LysAm24, LysAp22, LysECD7, and LysSi3 that target Gram-negative bacteria are tested to determine the development of resistance. These endolysins function well in animal models of wound and burn skin infections, have a broad spectrum of activity, and are active against both planktonic bacteria and bacterial biofilms. Regarding safety, these enzymes do not cause cytotoxicity, do not contribute to the development of resistance, and do not disrupt the natural intestinal microbiota *in vivo* (Vasina et al., 2021). Endolysins specifically prevent specific species or subspecies of pathogenic bacteria, without disrupting the surrounding normal microbiota (Yoong et al., 2004). The endolysin PlyV12 causes less disruption of the normal microbiota when used to treat antibiotic-resistant bacterial strains and they do not transfer resistance genes or bacterial toxins and do not eliminate the colonized beneficial normal flora of mucous membranes (Rahimzadeh et al., 2018).

1.5 Endolysin against *A. baumannii* biofilm

Due to several resistance mechanisms, including biofilm formation, *A. baumannii* can survive and spread in the hospital environment (Salmani et al., 2020). Endolysin chemotherapy has a significant antibacterial effect on biofilm-associated bacteria, which are difficult to eliminate due to their minimal metabolic activity (Chang et al., 2022). Endolysin Abtn-4 treatment inhibited *A. baumannii* biofilm growth by more than 30%, suggesting that endolysin is a possibly effective antibacterial agent in regulating biofilm development (Yuan et al., 2021). The pre-treatment of catheters with endolysin PlyF307 decreased *A. baumannii* biofilm on the surface by 1.6 log10, resulting in a substantial decrease in total biofilm growth (Lood et al., 2015a). In an additional *in vivo* study, Lood et al. investigated the efficiency of PlyF307 in eliminating biofilm from subcutaneously implanted catheters colonized with 2-day-old *A. baumannii* biofilms in the intestines of mice. Their findings revealed that mice with fatal *A. baumannii* bacteremia were saved by PlyF307 (Lood et al., 2015a). Endolysin anti-biofilm activity should be evaluated in future studies implementing more clinically relevant models such as multispecies biofilm matrices and flow cell-based biofilm models, as well as pre-treatment processes on diverse substrates and surfaces in hospitals (Chang et al., 2022). The endolysin LysAB1245 showed broad lytic spectrum efficacy against MDR *A. baumannii* isolates from various main capsular types. Furthermore, LysAB1245 has the potential for use with nosocomial MDR *A. baumannii* infections and can control the biofilms in the clinical healthcare environment (Soontarach et al., 2024).

1.6 Synergistic effects of endolysin and antibiotic against *A. baumannii*

The outer membrane of Gram-negative bacteria acts as a barrier for many endolysins, and very few endolysins with exogenous activity against Gram-negative bacteria have been observed. Endolysins can target Gram-negative bacteria if the outer membrane is first permeated with chemicals such as Ethylenediaminetetraacetic acid (EDTA), which destabilizes the lipopolysaccharides of the outer membrane; but the combined use of endolysin and EDTA is restricted to superficial treatment of localized infection (Briers et al., 2011; Thummeepak et al., 2016b). Several studies have tried enhancing the muralytic effect of endolysins by using them with different antibiotics to take on their combined synergistic effects (Thummeepak et al., 2016b; Letrado et al., 2018). Using endolysin and antibiotics together to target Gram-negative bacteria has shown some promising outcomes (Lai et al., 2020a). The synergistic effect of LysABP-01 endolysin with seven commonly prescribed antibiotics against the MDR strain of *A. baumannii* was assessed. LysABP-01 and colistin together had a synergistic effect *in vitro*, with a fractional inhibitory concentration index ranging from 0.156 to 0.188. The encouraging findings demonstrated that colistin and LysABP-01's minimum inhibitory concentrations (MICs) were lowered by up to 8 and 32 fold, respectively (Thummeepak et al., 2016a). Colistin, a 'last-resort' antibiotic, is commonly used to treat infections caused by MDR Gram-negative bacteria. However, due to its nephrotoxicity and neurotoxicity, the dose of colistin is extremely restrictive (Nation and Li, 2009). As a result, combining colistin with lysins may help optimize the clinical use of colistin at a lower dose. Blasco et al. recently demonstrated the synergistic effects of the endolysin ElyA1 and colistin in targeting various MDR Gram-negative bacteria including *A. baumannii*, in both *in vitro* and *in vivo* conditions. When colistin was combined with ELyA1, the MIC of colistin was lowered by at least 4-fold for all tested *A. baumannii* strains (Blasco et al., 2020a). In both skin and lung infection models, the *in vivo* survival rate for *A. baumannii* infected *G. mellonella* and bacterial reduction of infected mice treated with ELyA1 and colistin combination was considerably greater than that of the colistin-alone. Colistin can operate as an OMPto break the integrity of the OM, allowing lysin access to the PG substrates. Simultaneously, peptidoglycan cleavage by endolysin may increase antibiotic absorption and hence promote antibiotic action (Gerstmans et al., 2018a). These positive results show that combining endolysin and antibiotics has the potential to resensitize bacterial pathogens with drug resistance to antibiotics. And to slow the spread of antibiotic resistance by using fewer antibiotic treatments of low

dosages (Lai et al., 2020a). Combined use of endolysin LysAB-vT2-fusion with colistin, polymyxin B, or copper showed synergistic against *A. baumannii*, which may be used for the control of *A. baumannii* infection (Sitthisak et al., 2023b).

2 Clinical development of endolysin

Protein prescription drugs are a rapidly growing sector of the pharmaceutical industry. According to THPdb, a curated database of FDA-approved therapeutic proteins and peptides, there are 239 approved proteins and peptides, as well as 380 recognized variants of these proteins/peptides (Usmani et al., 2017; Wishart et al., 2018). Protein enzymes have significant advantages as medications because of their high selectivity, proteinaceous composition, which eliminates chemical toxicity, and tremendous potential for modification and consequent development (Labrou, 2019). Endolysins have been recognized by the WHO as a novel, non-traditional antimicrobial (WHO (Organization, 2022). Several biotechnology and pharmaceutical companies have been performing human clinical trials utilizing endolysins. ContraFect, a biotech company located at Rockefeller University, obtained ownership rights to nine phage-derived endolysin. This company particularly focuses on endolysin therapy for bacterial infectious diseases. ContraFect conducts a phase III clinical medicine trial on endolysin (identifier#: NCT04160468). At the same time, iNtRON Biopharma completed a phase III clinical trial of N-Rephasin Sal200 in 2021. (clinicalTrials.gov, accessed on 21 June 2022, identifier#: NCT03089697). In February 2020, the FDA recognized endolysin innovations as antibacterial biological drugs by recognizing the ContraFect endolysin in the phase III study as "Breakthrough Therapy." Pre-clinical development of additional endolysins is now underway in both industries and universities (Harhala et al., 2022). Exebacase "Endolysin CF-301" is a recombinant endolysin developed by ContraFects for use against a variety of *Streptococcus* and *Staphylococcus* species in the treatment of infective endocarditis in humans. This endolysin was the first of its class to enter human clinical trials in the United States. In phase II clinical studies, endolysin enhanced the recovery rate of methicilin-resistant *S. aureus* (MRSA) induced infectious endocarditis by 42.8% when used in combination with regular antibiotic treatment (Watson et al., 2019). Another phage-derived endolysin that has shown clinical efficacy is SAL200. SAL200, also known as N-Rephasin® SAL200, was found to be an acceptable medication for intravenous administration in this trial. Thirty-four healthy male volunteers received SAL200 at varying doses, There were no significant adverse effects noted during the endolysin pharmacokinetics study in the human body and its tolerance to intravenous administration (Jun et al., 2017).

3 Challenges of endolysin therapy transferring from the lab to the clinic

Totté et al. reported three clinical cases in which patients with persistent and recurring *S. aureus*-related skin infections were successfully treated with Staphefekt SA.100. Staphefekt SA.100 is a synthetic phage endolysin designed for topical skin application. Staphefekt is currently registered as a (class 1) medical device in Europe and is readily accessible over the counter as a cetomacrogol-based cream and gel (Totté et al., 2017). Although increased interest has been directed to investigating the potential of endolysin to target MDR Gram-negative bacteria, there are several challenges to its clinical application. These include questions about the safety of OMPs with endolysin, the application of outcomes from animal models of acute infection to clinical practice, and the effectiveness and stability of endolysin. Protein engineering and formulation design for effective distribution and stabilization of Gram-negative endolysin could be some options for advancing Gram-negative endolysin development for clinical testing before regulatory authorization (Lai et al., 2020a).

Figure 1 describes the current challenges of endolysin use in the clinic and healthcare market.

3.1 Concerns about the safety of OMPs with endolysin

In Gram-negative bacteria, the outer membrane functions as a barrier to several endolysins.

Few endolysins with exogenous activity against Gram-negative bacteria have been reported and the majority are synthetically engineered endolysins (Lai et al., 2011b; Briers et al., 2014a; Briers et al., 2014b; Lim et al., 2014; Lood et al., 2015; Soontarach et al., 2024).

OMPs have the potential to significantly increase the antibacterial activity of endolysin while also broadening their host spectrum. However, the *in-vivo* study of the efficacy of endolysin and OMPs in combination is rarely described in the literature. The harmful effects of the most often used OMPs such as EDTA through various delivery routes, such as oral, intravenous, intraperitoneal, topical, and inhalation, have been investigated (Lanigan and Yamarik, 2002). EDTA is cytotoxic, slightly genotoxic, and has an anticoagulant effect. It has been observed that the low EDTA dose required to cause toxicity in rats was 750 mg/kg/day. As a result, the use of EDTA with endolysin should be restricted to topical applications because it cannot affect the skin and does not produce skin hypersensitivity (Lanigan and Yamarik, 2002). Citric acid is also used as an OMP, but despite having a much better safety profile than EDTA, more testing is required because citric acid also has hazardous consequences, When used in combination with endolysin, particularly for the inhalation route, as it has been linked to animal obstruction of the airway and cause reactions in humans coughing (Allott et al., 1980). With further work being done on combining endolysin with polycationic peptides to enable them to target Gram-negative bacteria, their therapeutic use should be carefully evaluated. This is because endolysin with OM-disrupting characteristics or those coupled with peptide OMPs may also interact with eukaryotic cell membranes, raising safety issues (Schmelcher et al., 2012).

3.2 Weak effectiveness against the stationary phase of Gram-negative bacteria

The log-growth phase bacteria are more susceptible to endolysin treatments than the stationary phase bacteria. Oliveira et al. presented that the lower bactericidal efficiency against the bacterial stationary cells is due to modifications to the

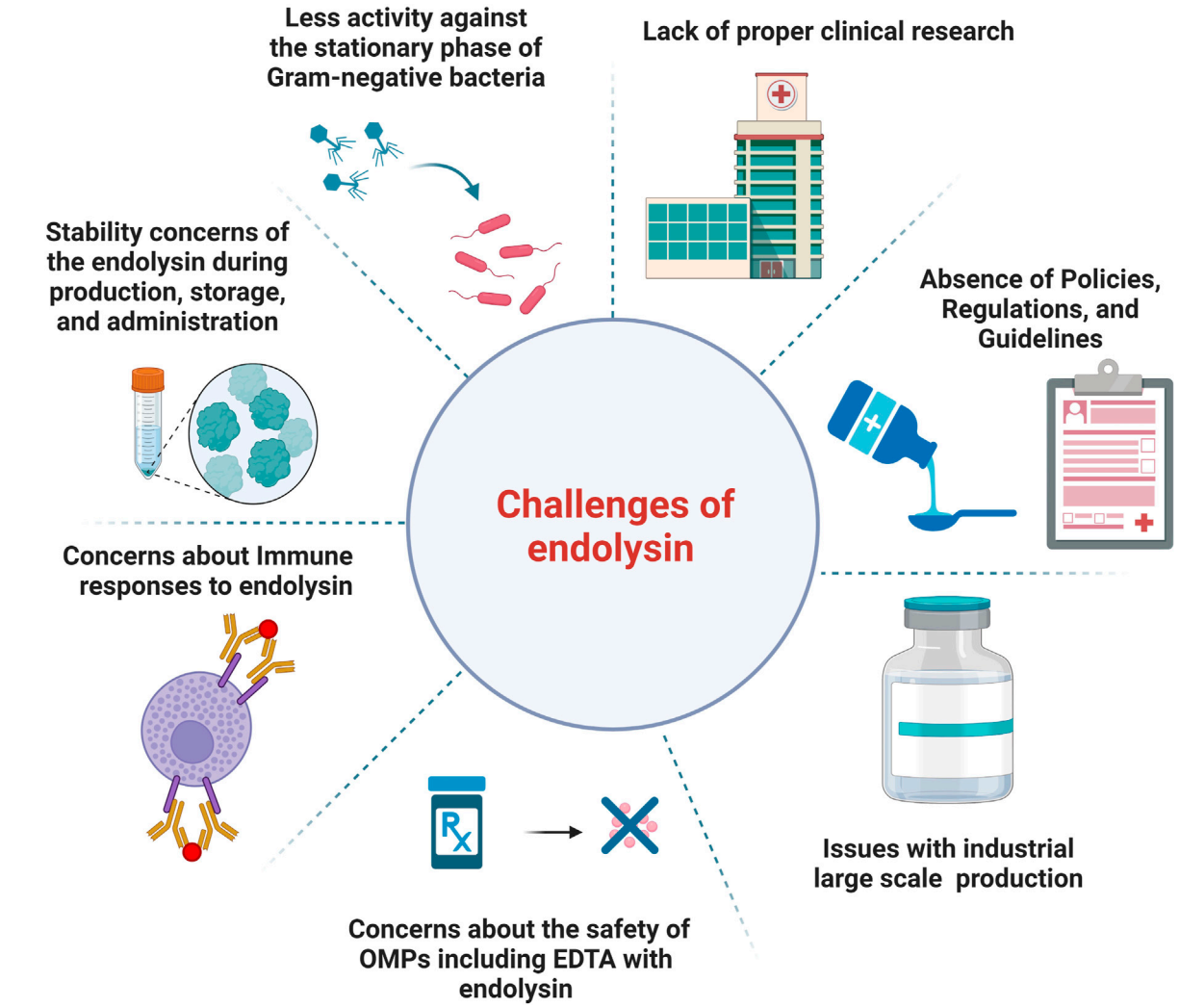

FIGURE 1
An illustration of the current challenges of endolysins use in the clinic and healthcare market.

structure in the outer membrane, such as LPS biosynthesis, which affects endolysin permeability that even in the presence of OMPs, or chemical modifications of the peptidoglycan compositions (Oliveira et al., 2014). These alterations could aid bacterial cells in coping with endolysins *via* acetylation, N-deacetylation, and amidation (Typas et al., 2012). A significant number of findings show anti-bacterial efficacy against the log-phase bacteria. To overcome this research gap, and to completely investigate the potency of endolysin against Gram-negative bacteria, further research is required to evaluate the antibacterial efficiency of endolysins against the stationary phase bacteria. Regarding the concern of the resistance of bacteria to endolysin; The resistance development of endolysin was evaluated in which bacterial strains were repeatedly challenged with subinhibitory doses of endolysins or artilysins failed to give rise to resistant mutants, although bacterial strains exposed to control antibiotics got resistance. The probability of developing resistance against endolysins and artilysins is thus regarded as minimal, especially when compared to standard antibiotics (Fischetti, 2005; Briers et al., 2014a).

3.3 Concerns about stability

The stability of the endolysin during production, storage, and administration is essential for its prospective use as an antibacterial agent. Several stability concerns of Gram-negative endolysins have been observed in preclinical studies and must be solved for further research and development (Lai et al., 2020a). The oral delivery route is the most widely used for gut-targeted medicines and is also the most well-liked by patients. Most medications available on the market are used orally and come in tablet or liquid form. This is not without its challenges, though. Because medications of this kind have to pass through the stomach and digestive tract, they are instantly exposed to a variety of enzymes, varying pH levels, and mechanical digestion. All of these may have an impact on the drug's molecular integrity and systemic bioavailability (Murray et al., 2021). Endolysins are proteinaceous, therefore they can be swiftly damaged by these processes, rendering them ineffective. Stomach acid has the potential to damage the structure of several endolysins. Proteases such as trypsin, chymotrypsin, pepsin, and peptidase degrade proteins. Many endolysins contain cleavage sites that these enzymes can target (Bruno et al., 2013).

3.3.1 Inactivation of endolysin in physiological conditions

Environmental conditions such as salts and proteins are well recognized to have a major impact on the activity of Gram-negative endolysins. Khan et al. reported that the *A. baumannii* endolysins LysAB54 entirely loses its antibacterial efficacy in the serum, limiting its use to topical infections such as burn wounds or joint infections. One possible explanation for the reduction of LysAB54 activity in the serum is endolysin ion exchange, which might potentially neutralize endolysin antibacterial activity (Khan et al., 2021). Endolysin inactivation in human serum could be associated with the conjugation and passivation of positively charged peptides on endolysin by negatively charged serum molecules. The neutralized cationic domain may result in the lack of intrinsic OM permeabilizing activity (Yang et al., 2015).

3.3.2 Thermostability

Because of their proteinaceous composition, endolysins are temperature-sensitive. Temperature effects on endolysin activity have been extensively studied since protein thermostability can affect functionality and storage stability. Most endolysin perform best activities between 30°C and 40 °C, making them useful for clinical use (Lai et al., 2020b).

3.3.3 Storage stability

Drugs with a moderately extended shelf life (12 months) under refrigeration (2°C–8°C) or at room temperature (20°C–25°C) are preferable for commercial viability. Products for freezer storage (−20°C ± 5°C) should have at least a 12-month shelf-life (Guideline, 2003). However, there is a lack of information regarding the Gram-negative endolysin storage stability, and what little that is available only covers short-term storage—from 1 week to six months—under various storage environments (Lai et al., 2020b).

3.4 Concerns about immune responses to endolysins

One of the limitations of endolysin is its short *in vivo* half-life, caused by the inflammatory response of cytokines and neutralizing antibodies. Endolysin elicits an immune system response when used repeatedly, and as a result of the immune response, it loses its enzyme-mediated lytic activity *in vivo* (Nau and Eiffert, 2002; Jado et al., 2003; Abdelrahman et al., 2021a). Raz et al. described a novel approach to discovering immune-derived engineered endolysins. The engineering of CBDs of different endolysins fusions to the Fc receptor of human IgG antibodies. The engineered lysin called Lysibodies binds to *S. aureus* cells and opsonizes them, causing immune complement system activation, which can cause phagocytosis and clearance of the bacteria. Through this approach, endolysin can be used to target an immune response toward pathogenic bacteria (Raz et al., 2018). A similar approach without using antibody fragments was described for a protein derived from the CBD of the endolysin PlyV12 (Yang et al., 2018). As some of the Gram-negative endolysin enter preclinical development, concerns about immunogenicity, toxicity from lipopolysaccharide release during the bactericidal process, and pharmacokinetic issues due to the complexity of the Gram-negative cell wall must be addressed (Ghose and Euler, 2020). We suggested a strategy to minimize the body's immune responses to endolysin. Engineered endolysins should be designed with human immune cells. When such proteins are expressed, the immune cells will recognize them as their body proteins, so there will be fewer immune reactions to these foreign proteins and less chance of the clearance of such foreign proteins in the body.

3.5 Lack of proper clinical research

In February 2020, the FDA recognized endolysin innovations as antibacterial biological drugs in the phase iii study as "Breakthrough Therapy" (Harhala et al., 2022). However, the fundamental obstacle to the use of endolysins as a therapeutic agent is the lack of proper clinical research to provide an excellent scientific fundamental basis for approval. We suggested that additional research on endolysins affecting their safety in humans will be beneficial to get past the reservations point of view on endolysins' usage and create the legal framework for the approval of endolysins. Preclinical trials of more endolysins are needed to bring endolysin into the medical market for treatment purposes.

3.6 Absence of policies, regulations, and guidelines

Numerous potential endolysin applications are currently being reported in medicine, but there are no published guidelines and regulations for endolysins. Early and effective communication with the relevant authorities is essential to establish endolysin regulatory pathways in their use as a medicine in the health sector and medicine industry. However, there are currently no clear legal principles or laws governing the use of endolysins.

3.7 Issues with large-scale industrial production

Endolysins have made great progress towards clinical application as novel antibacterial treatments. Another major problem that must be addressed is the large-scale industrial manufacture of endolysin. The present cost of endolysin production is projected to be expensive, which may be a major barrier to the use of endolysins as antibacterial replacements (Oliveira et al., 2012). The high cost arises mostly from the necessity for the development of recombination engineering, effective, and safe expression platforms for endolysin expression and purification. As a result, technical techniques to increase the solubility and expression levels of target endolysins, as well as cost-effective expression systems, are required to make endolysins commercially acceptable antibacterial agents worth investing in (Lee et al., 2023). When transferring the therapeutic endolysin expression and purification from the lab to the industrial scale, manufacturing costs and safety concerns must be addressed. This applies to the entire manufacturing process, from the selection of the expression host. From the beginning of protein expression until the last

stages of processing, there are numerous chances to lower production costs and improve safety. Cell harvesting, cell lysis, and purification are examples of downstream processing procedures that are carried out once endolysins have been engineered and reassembled in a particular expression system. Toxic effects must be avoided, especially when it comes to protein expression in bacteria where endotoxin must be eliminated. Furthermore, early in the production process, choosing the best expression hosts—such as bacteria, yeast, or plants—is a crucial step toward achieving overexpression and cheap expression costs. Because they are inexpensive to produce, plants have been suggested as potential hosts for recombinant protein production. Furthermore, plant-produced proteins are likely safer than those made from bacteria or animal cells (Magnusdottir et al., 2013).

3.7.1 High dose of endolysin needed for efficient killing of Gram-negative bacteria

The majority of Gram-negative bacteria require dosages of 100–500 μg/mL of endolysin to be eradicated, which is significantly higher than that of their Gram-positive counterparts, which commonly need doses of less than 10 μg/mL (Abouhmad et al., 2016; Gerstmans et al., 2018b). The development of commercially viable products might encounter production and formulation issues due to the high concentration of endolysin needed. Reducing the amount of endolysin dose by boosting the potency of Gram-negative endolysin is an efficient way to deal with this problem. Protein engineering could be able to perform this higher lytic activity, meaning that, in comparison to natural lysins, a lower concentration (<100 μg/mL) of modified endolysin is needed to exert effective bacterial killing. The logical design of engineered endolysin is crucial for successful modification to improve activity and stability. To attain this goal, knowledge of the endolysin tertiary or crystal structures will be required (Lai et al., 2020b).

3.8 Limited availability of *in vivo* data

So far, the effectiveness of Gram-negative endolysin *in vivo* has only been assessed using acute infection models. There are fewer documented chronic *in vivo* models for endolysin assessment, except for topical infection research investigations (Lai et al., 2020b). The current *in vivo* research on Gram-negative endolysin has been focused on assessing the rates of survival and/or reduction of bacterial burden to validate their effectiveness. Before continued research, issues with immunogenicity, pharmacokinetics, and the production of proinflammatory components during bacteriolysis must be resolved for the systemic use of Gram-negative endolysin. Many Gram-positive endolysins had problems being cleared by neutralizing antibodies because they were proteinaceous, which resulted in a relatively short half-life in vivo—between 4 and 40 min, depending on the type of endolysin (Gerstmans et al., 2018b).

4 Overcoming challenges of Gram-negative endolysins through genetic engineering

The majority of naturally occurring endolysins are lytic against Gram-positive bacteria. In Gram-negative bacteria, the outer membrane inhibits endolysin from accessing the target peptidoglycan. Various scientific and formulation solutions have been developed throughout the years for tackling the outer membrane barrier (De Maesschalck et al., 2020). Modular endolysins offer a unique opportunity for scientists to engineer proteins to change bacteriolytic activity, solubility, specificity, and various other physicochemical properties (Haddad Kashani et al., 2018). The shortening of a full-length enzyme, site-directed mutagenesis, or different fusions such as EADs with cell wall binding domain CBDs of distinct endolysin, virion-associated endolysin with CBD of a different endolysin, endolysin fusion with antimicrobial peptides are examples of engineering techniques (Love et al., 2018).

4.1 Formulation strategies

Formulation techniques include the use of different carrier systems. The use of OMP (chelators such as citric acid, lactic acid, malic acid, acetic acid, benzoic acid and EDTA in the formulation is useful in permeabilizing the outer membrane of Gram-negative bacteria to endolysins (Oliveira et al., 2016a). Using OMP is the simplest way to get over the outer membrane barrier. The most often utilized permeabilizer in this scenario is EDTA, which works by chelating the outer membrane stabilizing divalent cations (Kocot et al., 2023).

4.2 Endolysin encapsulation system

Despite their therapeutic effects, bacteriophages and endolysins face some practical challenges posed by the host system, such as low bioavailability, losing activity, non-targeted delivery, rapid elimination by the retinal endothelial system, and antibody-mediated deactivation. Against this context, there has been an increase of interest among scientists to investigate the possibilities of delivery systems for encapsulating bacteriophages and endolysins. In recent years, a multitude of bacteriophage and endolysin encapsulation strategies have been reported (Loh et al., 2021). Similarly, nanoencapsulation can help improve the therapeutic potential by not only shielding endolysin from degradation but also allowing for continuous release, potentially boosting stability, shelf life, and therapeutic efficacy (Gondil and Chhibber, 2021). Liposomes' ability to penetrate bacterial outer membranes through membrane fusion is also a viable way for delivering endolysin to Gram-negative bacteria. The authors achieved successful lysis of both *Salmonella typhimurium* and *E. coli* with endolysin BSP16Lys-containing liposomes without the need for a membrane permeabilizer (Bai et al., 2019b). These examples highlight the need to utilize these existing strategies to improve the potential of endolysin as an effective and sustainable therapy.

4.3 Endolysin delivery using liposomes

It has been observed that endolysin encapsulated in liposomes enhances the efficacy of endolysins against Gram-negative bacteria (Bai et al., 2019a). The method of packing lytic proteins derived from bacteriophage in the structure of liposomes appears to be a promising weapon against Gram-negative bacteria. Like

dendrimers, liposomes can also have a protective role that maintains the endolysin activity (Kocot et al., 2023).

4.4 Endolysin delivery using chitosan nanoparticles

Encapsulation in alginate-chitosan nanoparticles is another strategy for increasing the efficacy of endolysin, particularly for use in therapy (Gondil and Chhibber, 2021). Chitosan-based formulations provide benefits over alternative delivery systems in that they boost therapeutic agent bioavailability while also properly removing from the host after the release of the agent (Gondil and Chhibber, 2021).

4.5 Breaching the barrier of the outer membrane of Gram-negative bacteria

Because the outer membrane (OM) of Gram-negative bacteria prevents externally applied endolysins from accessing peptidoglycan, controlling the growth of these Gram-negative pathogenic bacteria is difficult (Sisson et al., 2024b).

4.5.1 Synergy through permeabilizing molecules

Chemical permeabilizers are a useful tool for facilitating endolysins' entry into the periplasm. Divalent metal ion (Mg2+ and Ca2+) chemical chelate stabilizes the lipopolysaccharide (LPS) layer, degrades and permeabilizes the OM, and makes the peptidoglycan accessible to endolysins (Oliveira et al., 2016b). Citric and malic acids are examples of organic acids that permeabilize the OM and improve endolysins' ability to kill Gram-negative bacteria (Sisson et al., 2024a). Endolysins work in combination with additional compounds that disrupt the OM. Oregano and thyme essential oils, carvacrol, have been shown to enhance endolysin activity against Gram-negative bacteria and could cause the breakdown of lipopolysaccharides. Moreover, colistin, polymyxin B, and ε-poly-L-lysine, which are cationic chemicals, work in combination with endolysins by either dissolving or competitively displacing OM cations. In summary, many chemicals allow endolysins to access peptidoglycan and promote cell lysis by damaging or permeabilizing the OM (Blasco et al., 2020b; Ning et al., 2021; Hong and Myung, 2022).

4.5.2 Synergy through bacterial receptors

An alternate method for increasing endolysin activity is to enhance its attachment to and permeation of the OM. Adding endolysins to proteins allows them to attach to bacterial cell surface receptors. For example, 'Lysocins' are endolysin-bacteriocin fusions (Martínez et al., 2016; Heselpoth et al., 2019). Some bacteriocins produce pores in a membrane by binding to OM phospholipids and specific surface components, such as receptors and transporters, allowing the endolysin to pass through to the peptidoglycan (Martínez et al., 2016). Innolysins include the attachment of endolysin EADs to phage receptor-binding proteins (RBPs) and provide a second way of breaking through the OM (Zampara et al., 2020).

4.6 Engineering of endolysin with antimicrobial peptide

Some endolysins contain peptides, typically at their C-terminus, that have a strong antibacterial activity that is not dependent on peptidoglycan breakdown. These antimicrobial peptides (AMPs) are responsible for some endolysins natural capacity to penetrate the outer membrane of Gram-negative bacteria (Szadkowska et al., 2022; Kocot et al., 2023). Predicting AMP-like regions is a good technique for designing endolysin with an intrinsic antibacterial activity that can serve as a framework for further engineering (Kocot et al., 2023).

However, Gram-negative bacteria are difficult to regulate due to the presence of an outer membrane that protects the peptidoglycan layer from enzymatic breakdown. To surpass this threshold, the fusion of endolysin with a sensitizer peptide is known to extend efficacy by disrupting the outer membrane of Gram-negative bacteria (Son et al., 2023). The sensitizer peptide-fused endolysin Lys1S-L9P has highly effective bactericidal activity against various MDR Gram-negative bacteria. Lys1S-L9P displayed strong antibacterial action against MDR Gram-negative bacteria in the *G. mellonella in vivo* model, with no harmful effect. Sensitizer peptide-fused endolysin could be a useful biocontrol agent against MDR Gram-negative bacteria (Son et al., 2023).

5 Applications of endolysins

5.1 Endolysin is a disinfectant agent in the healthcare environment

A. baumannii is a leading contributor to nosocomial infections; it is becoming more and more linked to different epidemics and is a serious worry in intensive care units of hospitals across the globe (Almasaudi, 2018). Nosocomial infections resulting from multidrug-resistant bacteria are life-threatening (Choi et al., 2022). Secondly, the formation of bacterial biofilms on medical equipment is one of the biggest problems in the healthcare system (Gutiérrez et al., 2012). Bacteria trapped in biofilms are less sensitive because they grow more slowly and have restricted access to antibiotics and disinfectants (Davies, 2003). The bacteria-reduced susceptibility to antimicrobial agents within the biofilm that exhibited a more resistant phenotypic condition has also been linked to recurring infections (Lewis, 2007). Endolysins break down the bacterial cell wall peptidoglycan and could potentially help in controlling the spread of infections of MDR bacteria seen in hospitals (Choi et al., 2022). This revealed the endolysin potential as an environmentally friendly replacement for hospital-use harmful chemical disinfectants (Choi et al., 2022).

5.2 Role of endolysin in therapeutic protein delivery

Vaccination, which stimulates the immune system to enhance adaptive immunity through the injection of antigenic material, is one of the greatest public health achievements. Viral

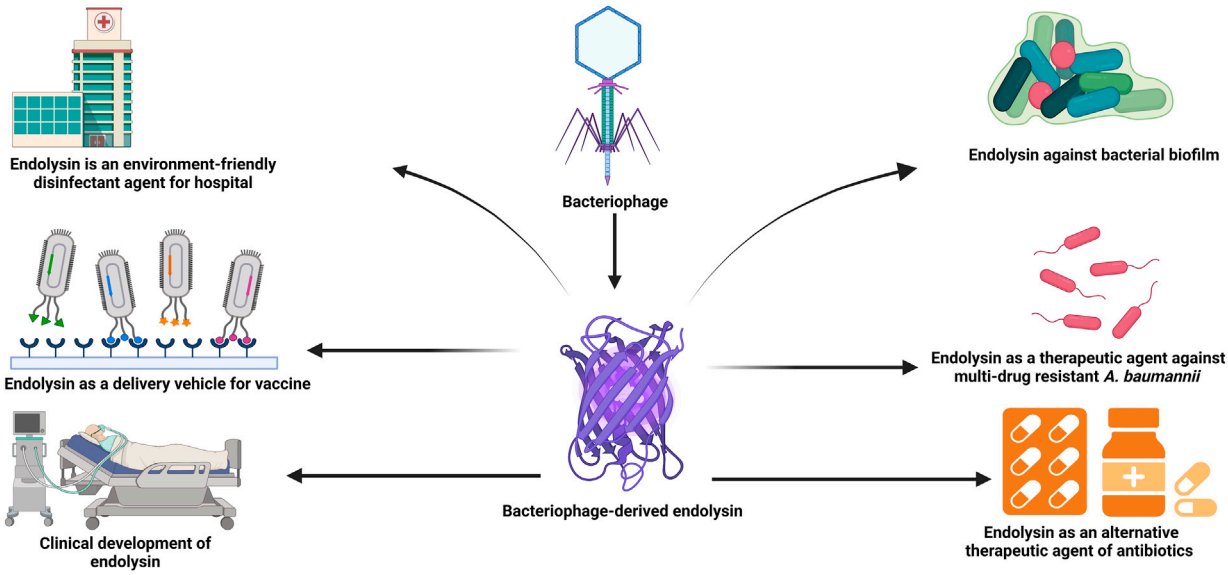

FIGURE 2
The figure illustrates the different applications of bacteriophage-derived endolysins.

nanoparticles (VNPs) have been a focus of recent research as delivery vehicles for protein and peptide-based vaccinations (Rodríguez-Rubio et al., 2016b). Bacteriophage-derived nanoparticles have drawn the attention of researchers since foreign peptides or proteins can be expressed on the surface of phages as fusion proteins. As a result, phage-displayed peptides or proteins have been proven to be functionally and immunologically active, making them appropriate for vaccine development (Hamzeh-Mivehroud et al., 2013). Endolysin can also be employed as a binding agent for displaying heterologous proteins on the surfaces of bacteria in the hunt for live vaccination delivery systems. The endolysin CBDs, can be fused with various other proteins such as antigens to show them at the bacterial surface while retaining their structure and activity (Loessner et al., 2002). Surface display technology based on bacteriophage-derived endolysins has been developed using lactic acid bacteria (Hu et al., 2010; Ribelles et al., 2013). It has been shown that the external addition of the E7 antigen from human papillomavirus type-16 (HPV-16) when fixed on the surface of lactic acid bacteria by the CBD of *Lactobacillus* casei A2 phage endolysin, secure mice from an HPV-16 attack and its associated tumors. After being immunized *via* intranasal vaccination with lactic acid bacteria expressing E7 antigen, more than 60% of the mice remained tumor-free. Thus, the surface display of endolysins CBDs is a fascinating method for effectively and safely delivering therapeutic proteins (Ribelles et al., 2013). Figure 2, illustrates the applications of bacteriophage-derived endolysin.

6 Conclusion

Due to the lack of antibiotic development for Gram-negative bacterial infections, in a scenario in which no curative therapies are available, there is an urgent need to find innovative antibacterial drugs. While bacteriophage-encoded endolysin has been regarded as an alternative therapeutic agent against bacterial infections. For Gram-positive bacteria, there are various ongoing clinical trials in Phase I and Phase III, while endolysin development against Gram-negative bacterial infections is lagging. The presence of an outer membrane on the Gram-negative bacteria is a key barrier to its development because it prevents endolysin from accessing the underlying peptidoglycan substrates, limiting their potency. For this reason, increasing interest has been focused on permeabilizing endolysin that exerts lytic activity against Gram-negative bacteria throughout the outer membrane. Endolysin with synergistic effects with other antibacterial drugs against *A. baumannii* are summarized and described. To move clinical development forward, several challenges must be overcome, including safety concerns about the Gram-negative bacteria membrane-disrupting permeabilizers including EDTA, a lack of knowledge about immunogenicity and pharmacokinetics, lower potency against the stationary phase of Gram-negative bacteria and stability issues in serum and blood. While further *in vivo* research is needed to understand the safety and distribution profiles of endolysin after administration, protein engineering and formulation sciences are promising ways to improve the efficacy and stability of Gram-negative endolysin.

Author contributions

FK: Writing–review and editing, Writing–original draft, Investigation, Funding acquisition, Conceptualization. FR: Writing–review and editing, Writing–original draft, Software, Investigation, Conceptualization. YY: Writing–review and editing, Software, Investigation, Formal Analysis. BL: Writing–review and

editing, Supervision, Investigation, Funding acquisition, Conceptualization. RZ: Writing–review and editing, Supervision, Resources, Project administration, Funding acquisition, Conceptualization.

Funding

The author(s) declare that financial support was received for the research, authorship, and/or publication of this article. This work is financially supported by the Research Fund for International Young Scientists, Grant number 32250410292, from the National Natural Science Foundation of China (NSFC) to FK. This study was also supported by the Southern Marine Science and Engineering Guangdong Laboratory (Zhuhai) (SML2023SP218), the Guangdong Major Project of Basic and Applied Basic Research (2023B0303000017) and the Innovation Team Project of Universities in Guangdong Province (No. 2023KCXTD028).

Acknowledgments

BioRender.com was used to generate figures.

Conflict of interest

The authors declare that the research was conducted in the absence of any commercial or financial relationships that could be construed as a potential conflict of interest.

Publisher's note

References

Abdelkader, K., Gutiérrez, D., Grimon, D., Ruas-Madiedo, P., Lood, C., Lavigne, R., et al. (2020). Lysin LysMK34 of Acinetobacter baumannii bacteriophage PMK34 has a turgor pressure-dependent intrinsic antibacterial activity and reverts colistin resistance. *Appl. Environ. Microbiol.* 86, e01311-20–e01320. doi:10.1128/AEM.01311-20

Abdelkader, K., Gutiérrez, D., Tamés-Caunedo, H., Ruas-Madiedo, P., Safaan, A., Khairalla, A. S., et al. (2022). Engineering a lysin with intrinsic antibacterial activity (LysMK34) by cecropin a fusion enhances its antibacterial properties against Acinetobacter baumannii. *Appl. Environ. Microbiol.* 88, 01515211. doi:10.1128/AEM.01515-21

Abdelrahman, F., Easwaran, M., Daramola, O. I., Ragab, S., Lynch, S., Oduselu, T. J., et al. (2021a). Phage-encoded endolysins. *Antibiotics* 10, 124. doi:10.3390/antibiotics10020124

Abdelrahman, F., Easwaran, M., Daramola, O. I., Ragab, S., Lynch, S., Oduselu, T. J., et al. (2021b). Phage-encoded endolysins. *Antibiot. (Basel).* 10, 124. doi:10.3390/antibiotics10020124

Abouhmad, A., Mamo, G., Dishisha, T., Amin, M., and Hatti-Kaul, R. J. J. O. a.M. (2016). T4 lysozyme fused with cellulose-binding module for antimicrobial cellulosic wound dressing materials. *J. Appl. Microbiol.* 121, 115–125. doi:10.1111/jam.13146

Allott, C., Evans, D., and Marshall, P. (1980). A model of irritant-induced bronchoconstriction in the spontaneously breathing Guinea-pig. *Br. J. Pharmacol.* 71, 165–168. doi:10.1111/j.1476-5381.1980.tb10921.x

Almasaudi, S. B. (2018). Acinetobacter spp. as nosocomial pathogens: epidemiology and resistance features. *Saudi J. Biol. Sci.* 25, 586–596. doi:10.1016/j.sjbs.2016.02.009

Bai, J., Jeon, B., and Ryu, S. (2019a). Effective inhibition of Salmonella Typhimurium in fresh produce by a phage cocktail targeting multiple host receptors. *Food Microbiol.* 77, 52–60. doi:10.1016/j.fm.2018.08.011

Bai, J., Yang, E., Chang, P.-S., and Ryu, S. (2019b). Preparation and characterization of endolysin-containing liposomes and evaluation of their antimicrobial activities against gram-negative bacteria. *Enzyme Microb. Technol.* 128, 40–48. doi:10.1016/j.enzmictec.2019.05.006

Behling, A. H., Wilson, B. C., Ho, D., Virta, M., O'sullivan, J. M., and Vatanen, T. J. C. O. I. M. (2023). Addressing antibiotic resistance: computational answers to a biological problem? *Curr. Opin. Microbiol.* 74, 102305. doi:10.1016/j.mib.2023.102305

Blair, J. M., Webber, M. A., Baylay, A. J., Ogbolu, D. O., and Piddock, L. J. J. N. R. M. (2015). Molecular mechanisms of antibiotic resistance. *Nat. Rev. Microbiol.* 13, 42–51. doi:10.1038/nrmicro3380

Blasco, L., Ambroa, A., Trastoy, R., Bleriot, I., Moscoso, M., Fernández-Garcia, L., et al. (2020a). *In vitro* and *in vivo* efficacy of combinations of colistin and different endolysins against clinical strains of multi-drug resistant pathogens. *Sci. Rep.* 10, 7163. doi:10.1038/s41598-020-64145-7

Blasco, L., Ambroa, A., Trastoy, R., Bleriot, I., Moscoso, M., Fernández-Garcia, L., et al. (2020b). *In vitro* and *in vivo* efficacy of combinations of colistin and different endolysins against clinical strains of multi-drug resistant pathogens. *Sci. Rep.* 10, 7163. doi:10.1038/s41598-020-64145-7

Briers, Y., Volckaert, G., Cornelissen, A., Lagaert, S., Michiels, C. W., Hertveldt, K., et al. (2007). Muralytic activity and modular structure of the endolysins of *Pseudomonas aeruginosa* bacteriophages phiKZ and EL. *Mol. Microbiol.* 65, 1334–1344. doi:10.1111/j.1365-2958.2007.05870.x

Briers, Y., Walmagh, M., Grymonprez, B., Biebl, M., Pirnay, J.-P., Defraine, V., et al. (2014a). Art-175 is a highly efficient antibacterial against multidrug-resistant strains and persisters of *Pseudomonas aeruginosa*. *Antimicrob. Agents Chemother.* 58, 3774–3784. doi:10.1128/AAC.02668-14

Briers, Y., Walmagh, M., and Lavigne, R. J. J. O. a.M. (2011). Use of bacteriophage endolysin EL188 and outer membrane permeabilizers against *Pseudomonas aeruginosa*. *J. Appl. Microbiol.* 110, 778–785. doi:10.1111/j.1365-2672.2010.04931.x

Briers, Y., Walmagh, M., Van Puyenbroeck, V., Cornelissen, A., Cenens, W., Aertsen, A., et al. (2014b). Engineered endolysin-based "Artilysins" to combat multidrug-resistant gram-negative pathogens. *mBio* 5, e01379–e01314. doi:10.1128/mBio.01379-14

Bruno, B. J., Miller, G. D., and Lim, C. S. J. T. D. (2013). Basics and recent advances in peptide and protein drug delivery. *Ther. Deliv.* 4, 1443–1467. doi:10.4155/tde.13.104

Chang, R. Y. K., Nang, S. C., Chan, H.-K., and Li, J. (2022). Novel antimicrobial agents for combating antibiotic-resistant bacteria. *Adv. Drug Deliv. Rev.* 187, 114378. doi:10.1016/j.addr.2022.114378

Chen, X., Liu, M., Zhang, P., Leung, S. S. Y., and Xia, J. (2021). Membrane-permeable antibacterial enzyme against multidrug-resistant Acinetobacter baumannii. *ACS Infect. Dis.* 7, 2192–2204. doi:10.1021/acsinfecdis.1c00222

Choi, Y.-J., Kim, S., Bae, S., Kim, Y., Chang, H.-H., and Kim, J. (2022). Antibacterial effects of recombinant endolysins in disinfecting medical equipment: a pilot study. *Front. Microbiol.* 12, 773640. doi:10.3389/fmicb.2021.773640

Chu, J. J. K., Poh, W. H., Hasnuddin, N. T. B., Hew, E. Y., Dam, L. C., Sahili, A. E., et al. (2022). Novel phage lysin Abp013 against Acinetobacter baumannii. *Antibiotics* 11, 169. doi:10.3390/antibiotics11020169

Davies, D. (2003). Understanding biofilm resistance to antibacterial agents. *Nat. Rev. Drug Discov.* 2, 114–122. doi:10.1038/nrd1008

Defraine, V., Schuermans, J., Grymonprez, B., Govers, S. K., Aertsen, A., Fauvart, M., et al. (2016). Efficacy of artilysin Art-175 against resistant and persistent Acinetobacter baumannii. *Antimicrob. agents Chemother.* 60, 3480–3488. doi:10.1128/AAC.00285-16

De La Fuente-Nunez, C., Cesaro, A., and Hancock, R. E. J. D. R. U. (2023). *Antibiotic failure: beyond antimicrobial resistance*, 101012.

De Maesschalck, V., Gutiérrez, D., Paeshuyse, J., Lavigne, R., and Briers, Y. (2020). Advanced engineering of third-generation lysins and formulation strategies for clinical applications. *Crit. Rev. Microbiol.* 46, 548–564. doi:10.1080/1040841X.2020.1809346

Ding, D., Wang, B., Zhang, X., Zhang, J., Zhang, H., Liu, X., et al. (2023). The spread of antibiotic resistance to humans and potential protection strategies. *Ecotoxicol. Environ. Saf.* 254, 114734. doi:10.1016/j.ecoenv.2023.114734

Fischetti, V. a.J. T. I. M. (2005). Bacteriophage lytic enzymes: novel anti-infectives. *Trends Microbiol.* 13, 491–496. doi:10.1016/j.tim.2005.08.007

Gerstmans, H., Criel, B., and Briers, Y. (2018a). Synthetic biology of modular endolysins. *Biotechnol. Adv.* 36, 624–640. doi:10.1016/j.biotechadv.2017.12.009

Gerstmans, H., Criel, B., and Briers, Y. J. B. A. (2018b). Synthetic biology of modular endolysins. *Biotechnol. Adv.* 36, 624–640. doi:10.1016/j.biotechadv.2017.12.009

Ghose, C., and Euler, C. W. J. A. (2020). Gram-negative bacterial lysins. *Antibiot. (Basel).* 9, 74. doi:10.3390/antibiotics9020074

Gondil, V. S., and Chhibber, S. (2021). Bacteriophage and endolysin encapsulation systems: a promising strategy to improve therapeutic outcomes. *Front. Pharmacol.* 12, 675440. doi:10.3389/fphar.2021.675440

Gondil, V. S., Khan, F. M., Mehra, N., Kumar, D., Khullar, A., Sharma, T., et al. (2021a). "Clinical potential of bacteriophage and endolysin based therapeutics: a futuristic approach," in *Microbial products for health, environment and agriculture* (Springer), 39–58.

Gondil, V. S., Khan, F. M., Mehra, N., Kumar, D., Khullar, A., Sharma, T., et al. (2021b). *Clinical potential of bacteriophage and Endolysin based therapeutics: a futuristic approach*, 39–58. Environment, and Agriculture.

Guideline, I. J. Q. A. (2003). Stability testing of new drug substances and products. 4.

Gutiérrez, D., and Briers, Y. J. C. O. I. B. (2021). Lysins breaking down the walls of Gram-negative bacteria, no longer a no-go. *Curr. Opin. Biotechnol.* 68, 15–22. doi:10.1016/j.copbio.2020.08.014

Gutiérrez, D., Delgado, S., Vázquez-Sánchez, D., Martínez, B., Cabo, M. L., Rodríguez, A., et al. (2012). Incidence of *Staphylococcus aureus* and analysis of associated bacterial communities on food industry surfaces. *Appl. Environ. Microbiol.* 78, 8547–8554. doi:10.1128/AEM.02045-12

Haddad Kashani, H., Schmelcher, M., Sabzalipoor, H., Seyed Hosseini, E., and Moniri, R. (2018). Recombinant endolysins as potential therapeutics against antibiotic-resistant *Staphylococcus aureus*: current status of research and novel delivery strategies. *Clin. Microbiol. Rev.* 31, e00071. doi:10.1128/CMR.00071-17

Hamzeh-Mivehroud, M., Alizadeh, A. A., Morris, M. B., Church, W. B., and Dastmalchi, S. (2013). Phage display as a technology delivering on the promise of peptide drug discovery. *Drug Discov. today* 18, 1144–1157. doi:10.1016/j.drudis.2013.09.001

Harhala, M. A., Gembara, K., Nelson, D. C., Miernikiewicz, P., and Dąbrowska, K. (2022). Immunogenicity of endolysin PlyC. *Antibiotics* 11, 966. doi:10.3390/antibiotics11070966

Heselpoth, R. D., Euler, C. W., Schuch, R., Fischetti, V. a.J. a.A., and Chemotherapy (2019). Lysocins: bioengineered antimicrobials that deliver lysins across the outer membrane of Gram-negative bacteria. *Antimicrob. Agents Chemother.* 63, e00342. doi:10.1128/AAC.00342-19

Hong, H.-W., Myung, H. J. F. I. M., Jang, J., Kim, M. S., and Song, M. (2022). Combination effect of engineered endolysin EC340 with antibiotics. *Front. Microbiol.* 13, 821936. doi:10.3389/fmicb.2022.821936

Hu, S., Kong, J., Kong, W., Guo, T., and Ji, M. (2010). Characterization of a novel LysM domain from Lactobacillus fermentum bacteriophage endolysin and its use as an anchor to display heterologous proteins on the surfaces of lactic acid bacteria. *Appl. Environ. Microbiol.* 76, 2410–2418. doi:10.1128/AEM.01752-09

Huang, G., Shen, X., Gong, Y., Dong, Z., Zhao, X., Shen, W., et al. (2014). Antibacterial properties of acinetobacter baumanniiphage Abp1 endolysin (PlyAB1). *BMC Infect. Dis.* 14, 681–688. doi:10.1186/s12879-014-0681-2

Jado, I., López, R., García, E., Fenoll, A., Casal, J., García, P., et al. (2003). Phage lytic enzymes as therapy for antibiotic-resistant Streptococcus pneumoniae infection in a murine sepsis model. *J. Antimicrob. Chemother.* 52, 967–973. doi:10.1093/jac/dkg485

Jansen, M., Wahida, A., Latz, S., Krüttgen, A., Häfner, H., Buhl, E. M., et al. (2018). Enhanced antibacterial effect of the novel T4-like bacteriophage KARL-1 in combination with antibiotics against multi-drug resistant Acinetobacter baumannii. *Sci. Rep.* 8, 14140. doi:10.1038/s41598-018-32344-y

Jun, S. Y., Jang, I. J., Yoon, S., Jang, K., Yu, K.-S., Cho, J. Y., et al. (2017). Pharmacokinetics and tolerance of the phage endolysin-based candidate drug SAL200 after a single intravenous administration among healthy volunteers. *Antimicrob. agents Chemother.* 61, e02629. doi:10.1128/AAC.02629-16

Khan, F. M., Chen, J.-H., Zhang, R., and Liu, B. J. F. I. M. (2023a). A comprehensive review of the applications of bacteriophage-derived endolysins for foodborne bacterial pathogens and food safety: recent advances, challenges, and future perspective. *Front. Microbiol.* 14, 1259210. doi:10.3389/fmicb.2023.1259210

Khan, F. M., Chen, J.-H., Zhang, R., and Liu, B. J. F. I. M. (2023b). A comprehensive review of the applications of bacteriophage-derived endolysins for foodborne bacterial pathogens and food safety: recent advances, challenges, and future perspective. *Front. Microbiol.* 14, 1259210. doi:10.3389/fmicb.2023.1259210

Khan, F. M., Gondil, V. S., Li, C., Jiang, M., Li, J., Yu, J., et al. (2021). A novel Acinetobacter baumannii bacteriophage endolysin LysAB54 with high antibacterial activity against multiple Gram-negative microbes. *Front. Cell. Infect. Microbiol.* 11, 637313. doi:10.3389/fcimb.2021.637313

Kim, S., Lee, D.-W., Jin, J.-S., and Kim, J. (2020). Antimicrobial activity of LysSS, a novel phage endolysin, against Acinetobacter baumannii and *Pseudomonas aeruginosa*. *J. Glob. Antimicrob. Resist.* 22, 32–39. doi:10.1016/j.jgar.2020.01.005

Kocot, A. M., Briers, Y., and Plotka, M. (2023). Phages and engineered lysins as an effective tool to combat Gram-negative foodborne pathogens. *Compr. Rev. Food Sci. Food Saf.* 22, 2235–2266. doi:10.1111/1541-4337.13145

Labrou, N. (2019). *Therapeutic enzymes: function and clinical implications*. Springer.

Lai, M.-J., Lin, N.-T., Hu, A., Soo, P.-C., Chen, L.-K., Chen, L.-H., et al. (2011a). Antibacterial activity of Acinetobacter baumannii phage ϕAB2 endolysin (LysAB2) against both gram-positive and gram-negative bacteria. *Appl. Microbiol. Biotechnol.* 90, 529–539. doi:10.1007/s00253-011-3104-y

Lai, M.-J., Lin, N.-T., Hu, A., Soo, P.-C., Chen, L.-K., Chen, L.-H., et al. (2011b). Antibacterial activity of Acinetobacter baumannii phage ϕAB2 endolysin (LysAB2) against both gram-positive and gram-negative bacteria. *Appl. Microbiol. Biotechnol.* 90, 529–539. doi:10.1007/s00253-011-3104-y

Lai, M.-J., Soo, P.-C., Lin, N.-T., Hu, A., Chen, Y.-J., Chen, L.-K., et al. (2013). Identification and characterisation of the putative phage-related endolysins through full genome sequence analysis in Acinetobacter baumannii ATCC 17978. *Int. J. Antimicrob. agents* 42, 141–148. doi:10.1016/j.ijantimicag.2013.04.022

Lai, W. C. B., Chen, X., Ho, M. K. Y., Xia, J., and Leung, S. S. Y. (2020a). Bacteriophage-derived endolysins to target gram-negative bacteria. *Int. J. Pharm.* 589, 119833. doi:10.1016/j.ijpharm.2020.119833

Lai, W. C. B., Chen, X., Ho, M. K. Y., Xia, J., and Leung, S. S. Y. J. I. J. O. P. (2020b). Bacteriophage-derived endolysins to target gram-negative bacteria. *Int. J. Pharm.* 589, 119833. doi:10.1016/j.ijpharm.2020.119833

Lanigan, R. S., and Yamarik, T. A. (2002). Final report on the safety assessment of EDTA, calcium disodium EDTA, diammonium EDTA, dipotassium EDTA, disodium EDTA, TEA-EDTA, tetrasodium EDTA, tripotassium EDTA, trisodium EDTA, HEDTA, and trisodium HEDTA. *Int. J. Toxicol.* 21, 95–142. doi:10.1080/10915810290096522

Lee, C., Kim, H., Ryu, S. J. C. R. I. F. S., and Nutrition (2023). Bacteriophage and endolysin engineering for biocontrol of food pathogens/pathogens in the food: recent advances and future trends. *Crit. Rev. Food Sci. Nutr.* 63, 8919–8938. doi:10.1080/10408398.2022.2059442

Letrado, P., Corsini, B., Díez-Martínez, R., Bustamante, N., Yuste, J. E., and García, P. J. F. M. (2018). Bactericidal synergism between antibiotics and phage endolysin Cpl-711 to kill multidrug-resistant pneumococcus. *Future Microbiol.* 13, 1215–1223. doi:10.2217/fmb-2018-0077

Lewis, K. (2007). Persister cells, dormancy and infectious disease. *Nat. Rev. Microbiol.* 5, 48–56. doi:10.1038/nrmicro1557

Li, C., Jiang, M., Khan, F. M., Zhao, X., Wang, G., Zhou, W., et al. (2021). Intrinsic antimicrobial peptide facilitates a new broad-spectrum lysin LysP53 to kill Acinetobacter baumannii *in vitro* and in a mouse burn infection model. *ACS Infect. Dis.* 7, 3336–3344. doi:10.1021/acsinfecdis.1c00497

Lim, J., Jang, J., Myung, H., and Song, M. (2022). Eradication of drug-resistant Acinetobacter baumannii by cell-penetrating peptide fused endolysin. *J. Microbiol.* 60, 859–866. doi:10.1007/s12275-022-2107-y

Lim, J.-A., Shin, H., Heu, S., Ryu, S. J. J. O. M., and Biotechnology (2014). Exogenous lytic activity of SPN9CC endolysin against gram-negative bacteria. *J. Microbiol. Biotechnol.* 24, 803–811. doi:10.4014/jmb.1403.03035

Lim, S. M. S., Abidin, A. Z., Liew, S., Roberts, J., and Sime, F. (2019). The global prevalence of multidrug-resistance among Acinetobacter baumannii causing hospital-acquired and ventilator-associated pneumonia and its associated mortality: a systematic review and meta-analysis. *J. Infect.* 79, 593–600. doi:10.1016/j.jinf.2019.09.012

Loessner, M. J., Kramer, K., Ebel, F., and Scherer, S. (2002). C-terminal domains of Listeria monocytogenes bacteriophage murein hydrolases determine specific recognition and high-affinity binding to bacterial cell wall carbohydrates. *Mol. Microbiol.* 44, 335–349. doi:10.1046/j.1365-2958.2002.02889.x

Loh, B., Gondil, V. S., Manohar, P., Khan, F. M., Yang, H., and Leptihn, S. (2021). Encapsulation and delivery of therapeutic phages. *Appl. Environ. Microbiol.* 87, e01979-20–e01920. doi:10.1128/AEM.01979-20

Lood, R., Winer, B. Y., Pelzek, A. J., Diez-Martinez, R., Thandar, M., Euler, C. W., et al. (2015a). Novel phage lysin capable of killing the multidrug-resistant gram-negative bacterium Acinetobacter baumannii in a mouse bacteremia model. *Antimicrob. agents Chemother.* 59, 1983–1991. doi:10.1128/AAC.04641-14

Love, M. J., Bhandari, D., Dobson, R. C., and Billington, C. (2018). Potential for bacteriophage endolysins to supplement or replace antibiotics in food production and clinical care. *Antibiotics* 7, 17. doi:10.3390/antibiotics7010017

Magnusdottir, A., Vidarsson, H., Björnsson, J. M., and Örvar, B. L. J. T. I. B. (2013). Barley grains for the production of endotoxin-free growth factors. *Trends Biotechnol.* 31, 572–580. doi:10.1016/j.tibtech.2013.06.002

Martínez, B., Rodríguez, A., and Suárez, E. J. N. W. T. C. B. G. (2016). *Antimicrobial peptides produced by bacteria: the bacteriocins*, 15–38.

Matamp, N., and Bhat, S. G. J. M. (2019). Phage endolysins as potential antimicrobials against multidrug resistant Vibrio alginolyticus and Vibrio parahaemolyticus: current status of research and challenges ahead. *Microorganisms* 7, 84. doi:10.3390/microorganisms7030084

Mehmood Khan, F., Manohar, P., Singh Gondil, V., Mehra, N., Kayode Oyejobi, G., Odiwuor, N., et al. (2023). The applications of animal models in phage therapy: an update. *Hum. Vaccines Immunother.* 19, 2175519. doi:10.1080/21645515.2023.2175519

Mulani, M. S., Kamble, E. E., Kumkar, S. N., Tawre, M. S., and Pardesi, K. R. J. F. I. M. (2019). Emerging strategies to combat ESKAPE pathogens in the era of antimicrobial resistance: a review. *Front. Microbiol.* 10, 539. doi:10.3389/fmicb.2019.00539

Murray, E., Draper, L. A., Ross, R. P., and Hill, C. J. V. (2021). The advantages and challenges of using endolysins in a clinical setting. *Viruses* 13, 680. doi:10.3390/v13040680

Nation, R. L., and Li, J. (2009). Colistin in the 21st century. *Curr. Opin. Infect. Dis.* 22, 535–543. doi:10.1097/QCO.0b013e328332e672

Nau, R., and Eiffert, H. (2002). Modulation of release of proinflammatory bacterial compounds by antibacterials: potential impact on course of inflammation and outcome in sepsis and meningitis. *Clin. Microbiol. Rev.* 15, 95–110. doi:10.1128/cmr.15.1.95-110.2002

Ning, H.-Q., Lin, H., and Wang, J.-X. J. I. J. O. F. M. (2021). Synergistic effects of endolysin Lysqdvp001 and ε-poly-lysine in controlling Vibrio parahaemolyticus and its biofilms. *Int. J. Food Microbiol.* 343, 109112. doi:10.1016/j.ijfoodmicro.2021.109112

Nordmann, P., and Poirel, L. J. C. I. D. (2019). Epidemiology and diagnostics of carbapenem resistance in gram-negative bacteria. *Clin. Infect. Dis.* 69, S521–S528. doi:10.1093/cid/ciz824

Oliveira, H., Azeredo, J., Lavigne, R., and Kluskens, L. D. J. T. I. F. S. (2012). Bacteriophage endolysins as a response to emerging foodborne pathogens. *Bacteriophage endolysins as a response Emerg. foodborne pathogens* 28, 103–115. doi:10.1016/j.tifs.2012.06.016

Oliveira, H., Thiagarajan, V., Walmagh, M., Sillankorva, S., Lavigne, R., Neves-Petersen, M. T., et al. (2014). A thermostable Salmonella phage endolysin, Lys68, with broad bactericidal properties against gram-negative pathogens in presence of weak acids. *PLoS One* 9, e108376. doi:10.1371/journal.pone.0108376

Oliveira, H., Vilas Boas, D., Mesnage, S., Kluskens, L. D., Lavigne, R., Sillankorva, S., et al. (2016a). Structural and enzymatic characterization of ABgp46, a novel phage endolysin with broad anti-gram-negative bacterial activity. *Front. Microbiol.* 7, 208. doi:10.3389/fmicb.2016.00208

Oliveira, H., Vilas Boas, D., Mesnage, S., Kluskens, L. D., Lavigne, R., Sillankorva, S., et al. (2016b). Structural and enzymatic characterization of ABgp46, a novel phage endolysin with broad anti-gram-negative bacterial activity. *Front. Microbiol.* 7, 208. doi:10.3389/fmicb.2016.00208

Organization, W. H. (2019). *2019 Antibacterial agents in clinical development: an analysis of the antibacterial clinical development pipeline*.

Organization, W. H. (2022). *2021 antibacterial agents in clinical and preclinical development: an overview and analysis*.

Oyejobi, G. K., Olaniyan, S. O., Yusuf, N.-A., Ojewande, D. A., Awopetu, M. J., Oyeniran, G. O., et al. (2022a). Acinetobacter baumannii: more ways to die. *Microbiol. Res.* 261, 127069. doi:10.1016/j.micres.2022.127069

Oyejobi, G. K., Olaniyan, S. O., Yusuf, N.-A., Ojewande, D. A., Awopetu, M. J., Oyeniran, G. O., et al. (2022b). Acinetobacter baumannii: More ways to die. *Microbiol. Res.* 261, 127069. doi:10.1016/j.micres.2022.127069

Pakharukova, N., Tuittila, M., Paavilainen, S., Malmi, H., Parilova, O., Teneberg, S., et al. (2018). Structural basis for Acinetobacter baumannii biofilm formation. *Proc. Natl. Acad. Sci. U. S. A.* 115, 5558–5563. doi:10.1073/pnas.1800961115

Peng, S.-Y., You, R.-I., Lai, M.-J., Lin, N.-T., Chen, L.-K., and Chang, K.-C. (2017). Highly potent antimicrobial modified peptides derived from the Acinetobacter baumannii phage endolysin LysAB2. *Sci. Rep.* 7, 11477. doi:10.1038/s41598-017-11832-7

Piperaki, E.-T., Tzouvelekis, L., Miriagou, V., Daikos, G. J. C. M., and Infection (2019). Carbapenem-resistant Acinetobacter baumannii: in pursuit of an effective treatment. *Clin. Microbiol. Infect.* 25, 951–957. doi:10.1016/j.cmi.2019.03.014

Poirel, L., Bonnin, R. A., and Nordmann, P. (2011). Genetic basis of antibiotic resistance in pathogenic Acinetobacter species. *IUBMB life* 63, 1061–1067. doi:10.1002/iub.532

Premetis, G. E., Georgakis, N. D., Stathi, A., and Labrou, N. E. (2023a). Metaviromics analysis of marine biofilm reveals a glycoside hydrolase endolysin with high specificity towards Acinetobacter baumannii. *Biochimica Biophysica Acta (BBA)-Proteins Proteomics* 1871, 140918. doi:10.1016/j.bbapap.2023.140918

Premetis, G. E., Stathi, A., Papageorgiou, A. C., and Labrou, N. E. (2023b). Characterization of a glycoside hydrolase endolysin from Acinetobacter baumannii phage Ab TZA1 with high antibacterial potency and novel structural features. *FEBS J.* 290, 2146–2164. doi:10.1111/febs.16686

Ragland, S. A., and Criss, A. K. J. P. P. (2017). From bacterial killing to immune modulation: recent insights into the functions of lysozyme. *PLoS Pathog.* 13, e1006512. doi:10.1371/journal.ppat.1006512

Rahimzadeh, G., Gill, P., and Rezai, M. S. J. J. O. P. R. (2018). Endolysins of bacteriophages as an anti-methicillin resistant staphylococcus aureus infection in children: a narrative review. *J. Pediatr. Rev.* 6, 36–43. doi:10.5812/jpr.11562

Rai, S., and Kumar, A. J. E. M. R. (2022). Bacteriophage therapeutics to confront multidrug-resistant Acinetobacter baumannii-a global health menace. *Environ. Microbiol. Rep.* 14, 347–364. doi:10.1111/1758-2229.12988

Raz, A., Serrano, A., Thaker, M., Alston, T., and Fischetti, V. A. (2018). Lysostaphin lysibody leads to effective opsonization and killing of methicillin-resistant *Staphylococcus aureus* in a murine model. *Antimicrob. Agents Chemother.* 62, e01056. doi:10.1128/AAC.01056-18

Ribelles, P., Benbouziane, B., Langella, P., Suárez, J. E., Bermúdez-Humarán, L. G., and Riazi, A. (2013). Protection against human papillomavirus type 16-induced tumors in mice using non-genetically modified lactic acid bacteria displaying E7 antigen at its surface. *Appl. Microbiol. Biotechnol.* 97, 1231–1239. doi:10.1007/s00253-012-4575-1

Rodríguez-Rubio, L., Gerstmans, H., Thorpe, S., Mesnage, S., Lavigne, R., Briers, Y. J. A., et al. (2016a). DUF3380 domain from a Salmonella phage endolysin shows potent N-acetylmuramidase activity. *Appl. Environ. Microbiol.* 82, 4975–4981. doi:10.1128/AEM.00446-16

Rodríguez-Rubio, L., Gutiérrez, D., Donovan, D. M., Martínez, B., Rodríguez, A., and García, P. (2016b). Phage lytic proteins: biotechnological applications beyond clinical antimicrobials. *Crit. Rev. Biotechnol.* 36, 542–552. doi:10.3109/07388551.2014.993587

Salmani, A., Mohsenzadeh, M., Pirouzi, A., and Khaledi, A. (2020). A comprehensive meta-analysis of antibiotic resistance pattern among biofilm production strains of Acinetobacter baumannii recovered from clinical specimens of patients. *Gene Rep.* 19, 100664. doi:10.1016/j.genrep.2020.100664

Schmelcher, M., Donovan, D. M., and Loessner, M. J. (2012). Bacteriophage endolysins as novel antimicrobials. *Future Microbiol.* 7, 1147–1171. doi:10.2217/fmb.12.97

Schmelcher, M., and Loessner, M. J. (2021a). Bacteriophage endolysins—extending their application to tissues and the bloodstream. *Curr. Opin. Biotechnol.* 68, 51–59. doi:10.1016/j.copbio.2020.09.012

Schmelcher, M., and Loessner, M. J. J. C. O. I. B. (2021b). Bacteriophage endolysins—extending their application to tissues and the bloodstream. *Curr. Opin. Biotechnol.* 68, 51–59. doi:10.1016/j.copbio.2020.09.012

Sisson, H. M., Fagerlund, R. D., Jackson, S. A., Briers, Y., Warring, S. L., Fineran, P. C. J. A., et al. (2024a). Antibacterial synergy between a phage endolysin and citric acid against the Gram-negative kiwifruit pathogen *Pseudomonas syringae* pv. *Actinidiae*. *e01846-01823*. doi:10.1128/aem.01846-23

Sisson, H. M., Jackson, S. A., Fagerlund, R. D., Warring, S. L., and Fineran, P. C. J. C. O. I. M. (2024b). Gram-negative endolysins: overcoming the outer membrane obstacle. *Curr. Opin. Microbiol.* 78, 102433. doi:10.1016/j.mib.2024.102433

Sitthisak, S., Manrueang, S., Khongfak, S., Leungtongkam, U., Thummeepak, R., Thanwisai, A., et al. (2023a). Antibacterial activity of vB_AbaM_PhT2 phage hydrophobic amino acid fusion endolysin, combined with colistin against Acinetobacter baumannii. *Sci. Rep.* 13, 7470. doi:10.1038/s41598-023-33822-8

Sitthisak, S., Manrueang, S., Khongfak, S., Leungtongkam, U., Thummeepak, R., Thanwisai, A., et al. (2023b). Antibacterial activity of vB_AbaM_PhT2 phage hydrophobic amino acid fusion endolysin, combined with colistin against Acinetobacter baumannii. *Sci. Rep.* 13, 7470. doi:10.1038/s41598-023-33822-8

Son, S. M., Kim, J., and Ryu, S. J. F. I. M. (2023). Development of sensitizer peptide-fused endolysin Lys1S-L9P acting against multidrug-resistant gram-negative bacteria. *Front. Microbiol.* 14, 1296796. doi:10.3389/fmicb.2023.1296796

Soontarach, R., Srimanote, P., Arechanajan, B., Nakkaew, A., Voravuthikunchai, S. P., and Chusri, S. J. P. O. (2024). Characterization of a novel bacteriophage endolysin (LysAB1245) with extended lytic activity against distinct capsular types associated with Acinetobacter baumannii resistance. *PLoS One* 19, e0296453. doi:10.1371/journal.pone.0296453

Szadkowska, M., Olewniczak, M., Kloska, A., Jankowska, E., Kapusta, M., Rybak, B., et al. (2022). A novel cryptic clostridial peptide that kills bacteria by a cell membrane permeabilization mechanism. *Microbiol. Spectr.* 10, 01657222. doi:10.1128/spectrum.01657-22

Thandar, M., Lood, R., Winer, B. Y., Deutsch, D. R., Euler, C. W., and Fischetti, V. A. (2016). Novel engineered peptides of a phage lysin as effective antimicrobials against multidrug-resistant Acinetobacter baumannii. *Antimicrob. agents Chemother.* 60, 2671–2679. doi:10.1128/AAC.02972-15

Thummeepak, R., Kitti, T., Kunthalert, D., and Sitthisak, S. (2016a). Enhanced antibacterial activity of acinetobacter baumannii bacteriophage øabp-01 endolysin (LysABP-01) in combination with colistin. *Front. Microbiol.* 7, 1402. doi:10.3389/fmicb.2016.01402

Thummeepak, R., Kitti, T., Kunthalert, D., and Sitthisak, S. J. F. I. M. (2016b). Enhanced antibacterial activity of Acinetobacter baumannii bacteriophage ØABP-01 endolysin (LysABP-01) in combination with colistin. *Front. Microbiol.* 7, 1402. doi:10.3389/fmicb.2016.01402

Totté, J. E., Van Doorn, M. B., and Pasmans, S. G. J. C. R. I. D. (2017). Successful treatment of chronic Staphylococcus aureus-related dermatoses with the topical endolysin Staphefekt SA.100: a report of 3 cases. *100 a Rep. 3 cases* 9, 19–25. doi:10.1159/000473872

Typas, A., Banzhaf, M., Gross, C. A., and Vollmer, W. (2012). From the regulation of peptidoglycan synthesis to bacterial growth and morphology. *Nat. Rev. Microbiol.* 10, 123–136. doi:10.1038/nrmicro2677

Usmani, S. S., Bedi, G., Samuel, J. S., Singh, S., Kalra, S., Kumar, P., et al. (2017). THPdb: database of FDA-approved peptide and protein therapeutics. *PloS one* 12, e0181748. doi:10.1371/journal.pone.0181748

Vasina, D. V., Antonova, N. P., Grigoriev, I. V., Yakimakha, V. S., Nikiforova, M. A., Pochtovyi, A. A., et al. (2021). Discovering the potentials of four phage endolysins to combat gram-negative infections. *Front. Microbiol.* 12, 748718. doi:10.3389/fmicb.2021.748718

Vrancianu, C. O., Gheorghe, I., Czobor, I. B., and Chifiriuc, M. C. J. M. (2020). Antibiotic resistance profiles, molecular mechanisms and innovative treatment strategies of Acinetobacter baumannii. *Microorganisms* 8, 935. doi:10.3390/microorganisms8060935

Wang, M., Zhang, J., Wei, J., Jiang, L., Jiang, L., Sun, Y., et al. (2023). *Phage-inspired strategies to combat antibacterial resistance*, 1–16.

Watson, A., Oh, J. T., Sauve, K., Bradford, P. A., Cassino, C., and Schuch, R. (2019). Antimicrobial activity of exebacase (lysin CF-301) against the most common causes of infective endocarditis. *Antimicrob. Agents Chemother.* 63, e01078. doi:10.1128/AAC.01078-19

Wishart, D. S., Feunang, Y. D., Guo, A. C., Lo, E. J., Marcu, A., Grant, J. R., et al. (2018). DrugBank 5.0: a major update to the DrugBank database for 2018. *Nucleic acids Res.* 46, D1074-D1082–D1082. doi:10.1093/nar/gkx1037

Wu, M., Hu, K., Xie, Y., Liu, Y., Mu, D., Guo, H., et al. (2019). A novel phage PD-6A3, and its endolysin Ply6A3, with extended lytic activity against Acinetobacter baumannii. *Front. Microbiol.* 9, 3302. doi:10.3389/fmicb.2018.03302

Yang, C.-H., Su, P.-W., Moi, S.-H., and Chuang, L.-Y. J. M. (2019). Biofilm formation in Acinetobacter Baumannii: genotype-phenotype correlation. *Molecules* 24, 1849. doi:10.3390/molecules24101849

Yang, H., Wang, M., Yu, J., and Wei, H. J. F. I. M. (2015). Antibacterial activity of a novel peptide-modified lysin against Acinetobacter baumannii and *Pseudomonas aeruginosa*. *Front. Microbiol.* 6, 1471. doi:10.3389/fmicb.2015.01471

Yang, H., Xu, J., Li, W., Wang, S., Li, J., Yu, J., et al. (2018). *Staphylococcus aureus* virulence attenuation and immune clearance mediated by a phage lysin-derived protein. *EMBO J.* 37, e98045. doi:10.15252/embj.201798045

Yoong, P., Schuch, R., Nelson, D., and Fischetti, V. a.J. J. O. B. (2004). Identification of a broadly active phage lytic enzyme with lethal activity against antibiotic-resistant *Enterococcus faecalis* and Enterococcus faecium. *J. Bacteriol.* 186, 4808–4812. doi:10.1128/JB.186.14.4808-4812.2004

Yuan, Y., Li, X., Wang, L., Li, G., Cong, C., Li, R., et al. (2021). The endolysin of the Acinetobacter baumannii phage vB_AbaP_D2 shows broad antibacterial activity. *Microb. Biotechnol.* 14, 403–418. doi:10.1111/1751-7915.13594

Zampara, A., Sørensen, M. C. H., Grimon, D., Antenucci, F., Vitt, A. R., Bortolaia, V., et al. (2020). Exploiting phage receptor binding proteins to enable endolysins to kill Gram-negative bacteria. *Sci. Rep.* 10, 12087. doi:10.1038/s41598-020-68983-3

frontiers | Frontiers in Pharmacology

TYPE Brief Research Report
PUBLISHED 30 October 2024
DOI 10.3389/fphar.2024.1347306

OPEN ACCESS

EDITED BY
Mingkai Li,
Air Force Medical University, China

REVIEWED BY
Zhihong Peng,
Hubei University, China
Mohamed Said,
University of Pretoria, South Africa
Wasan Katip,
Chiang Mai University, Thailand

*CORRESPONDENCE
Romaric Larcher,
romaric.larcher@chu-nimes.fr

RECEIVED 30 November 2023
ACCEPTED 18 September 2024
PUBLISHED 30 October 2024

CITATION
Laffont-Lozes P, Naciri T, Pantel A, Martin A, Pruvot-Occean A-S, Haignere V, Loubet P, Sotto A and Larcher R (2024) First case report of a vertebral osteomyelitis caused by carbapenem-resistant *Enterobacter cloacae* treated with imipenem/cilastatin/relebactam prolonged infusion then meropenem/vaborbactam in continuous infusion. *Front. Pharmacol.* 15:1347306. doi: 10.3389/fphar.2024.1347306

First case report of a vertebral osteomyelitis caused by carbapenem-resistant *Enterobacter cloacae* treated with imipenem/cilastatin/relebactam prolonged infusion then meropenem/vaborbactam in continuous infusion

Paul Laffont-Lozes[1], Tayma Naciri[2], Alix Pantel[3,4], Aurélie Martin[2], Anne-Sophie Pruvot-Occean[5], Vincent Haignere[6], Paul Loubet[2,4], Albert Sotto[2,4] and Romaric Larcher [2,7]*

[1]Department of Pharmacy, Nimes University Hospital, Nîmes, France, [2]Department of Infectious and Tropical Diseases, Nimes University Hospital, Nîmes, France, [3]Department of Microbiology and Hospital Hygiene, Nimes University Hospital, Nîmes France, [4]VBIC (Bacterial Virulence and Chronic Infection), INSERM (French Institute of Health and Medical Research), Montpellier University, Montpellier, France, [5]Department of Neurosurgery, Nimes University Hospital, Nîmes, France, [6]Department of Orthopaedic Surgery and Traumatology, Nimes University Hospital, Nîmes, France, [7]PhyMedExp (Physiology and Experimental Medicine), INSERM (French Institute of Health and Medical Research), CNRS (French National Centre for Scientific Research), University of Montpellier, Montpellier, France

Introduction: Bone and joint infections (BJIs) caused by multidrug-resistant bacteria are becoming more frequent. However, data on the use of novel β-lactam/β-lactamase inhibitors, such as imipenem/cilastatin/relebactam (I-R) and meropenem/vaborbactam (MVB), to treat BJIs is lacking. Furthermore, prolonged infusions of these β-lactams should theoretically optimize pharmacokinetic/pharmacodynamics target in these indications, but there are currently no reports on this type of infusions, especially in the setting of BJI.

Case Presentation: We report a case of a vertebral osteomyelitis caused by carbapenem-resistant *Enterobacter cloacae* successfully treated with extended-infusion of I-R (1.25 g q6h over 2 h), then with continuous infusion of MVB (2 g q4h as over 4 h). Therapeutic drug monitoring confirmed that extended-infusion of I-R and continuous infusion of MVB achieved serum concentrations up to 12 mg/L of imipenem and 19 mg/L of meropenem, respectively.

Conclusion: The favourable outcome of this patient treated for a vertebral osteomyelitis caused by carbapenem-resistant *E. cloacae* suggest that extended- and continuous infusions of I-R and MVB, are promising regimens for treatment of BJIs caused by carbapenem-resistant Enterobacterales.

KEYWORDS

bone and joint infection, vertebral osteomyelitis, meropenem/vaborbactam, continuous infusion, imipenem/cilastatin/relebactam, extended infusion, therapeutic drug monitoring

1 Introduction

The incidence of multidrug resistance (MDR) is increasing worldwide, leading to higher mortality and longer hospital stays (Murray et al., 2022). In response to this issue, new antimicrobials have recently been developed. Novel β-lactam/β-lactamase inhibitors are now the first treatment option for carbapenem-resistant Gram-negative bacteria (Tamma et al., 2022). Meropenem/vaborbactam (MVB) and imipenem/cilastatin/relebactam (I-R) are antimicrobials combining a carbapenem and a new β-lactamase inhibitor active against carbapenemase. They are approved by the European Medicines Agency and/or the US Food and Drug Administration (Summary of product characteristics: Vaborem, 2018; Summary of product characteristics: Recarbrio, 2020), for the treatment of bacteraemia, hospital-acquired pneumonia including ventilator associated pneumonia, complicated urinary tract infection and complicated intra-abdominal infection. However, the use of these molecules in more complex infections such as bone and joint infections (BJIs) has not been studied.

Data on the use of these novel antimicrobials for treating BJIs are needed, as they represent a promising therapeutic option for managing BJIs caused by MDR bacteria, which are an increasing concern (Rebold et al., 2021; Rempenault et al., 2021; Larcher et al., 2022; Davido et al., 2023). In addition, previous data (Roberts et al., 2016; Rebold et al., 2021; Larcher et al., 2022; Le Vavasseur and Zeller, 2022) have suggested that it could be interesting to use these new β-lactams in prolonged or continuous infusion, to improve pharmacokinetic, bacteriological eradication and clinical success in BJIs caused by carbapenem-resistant *Enterobacterales*.

We aimed to report the first case of vertebral osteomyelitis caused by carbapenem-resistant *Enterobacter cloacae* successfully treated with extended infusion of I-R then continuous infusion of MVB. This case provides important data on using novel antimicrobials for BJIs and offers insights into their optimized administration for effective management.

2 Case description

In November 2022, a 77-year-old man, weighing 78 kg, was admitted to a French tertiary hospital for opiate-resistant back pain. He had a medical history of hypertension, Parkinson's disease and atrial fibrillation. Two months prior, he had also been treated with ofloxacin for 21 days, for prostatitis caused by extended spectrum beta-lactamase (ESBL) producing-*E. cloacae*. On admission to the emergency room, a neutrophil count of 8.3 G/L (N = 1.5–7 G/L) and C reactive protein (CRP) level at 87.5 mg/L (N < 0.5 mg/L) prompted the physicians to perform a lumbar magnetic resonance imaging (MRI). A T11-T12 vertebral osteomyelitis with a significant infiltration of the surrounding soft tissues and an epiduritis was found (Figure 1). The patient was admitted to the infectious disease department and a couple of days later, ertapenem 1 g q12 h was started when blood cultures flagged positive for Gram-negative bacilli. An ESBL-producing-*E. cloacae* (Table 1) was identified. After 8 days of ertapenem therapy, the patient still had fever and CRP level remained at a plateau of 70 mg/L. Blood cultures drawn at this point were positive for carbapenem-resistant *E. cloacae* (Table 1). No carbapenemase enzyme was found (Xpert® Carba-R test, Cepheid, CA, United States and β CARBA test®, Bio-Rad, CA,USA) and resistance to ertapenem was explained by a combination of impermeability with ESBL and AmpC-beta-lactamase. Extended-infusion meropenem 2 g q8h over 3 h was started according to the 2022 Infectious Diseases Society of America (IDSA) guidelines (Tamma et al., 2022) for infections caused by non-carbapenemase producing carbapenem-resistant *Enterobacterales* (non-CP-CRE) resistant to ertapenem, that remain susceptible to meropenem (Table 1). On the first day of treatment, a single dose of amikacin (30 mg/kg) was also administered. Blood cultures were negative after 5 days of treatment. However, back pain and fever persisted, the patient became disoriented, and CRP level rose to 99 mg/L. Clinical failure and drug neurotoxicity related to the use of a high dose of meropenem despite reduced renal clearance (estimated

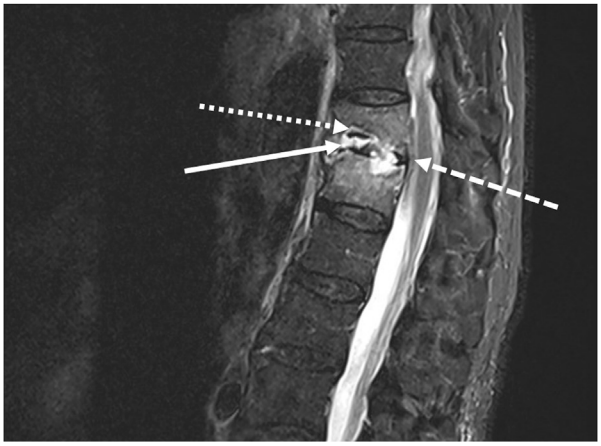

FIGURE 1
Medullar magnetic resonance imaging: Decreased height and STIR hypersignal of disc (white arrow) with irregularity and erosion of T11-T12 vertebral body endplates (white dotted arrow), and epidural collections (white dashed arrow).

TABLE 1 Antibiotic susceptibility testing (AST) of *Enterobacter cloacae* isolates.

Antibiotics	*Enterobacter cloacae* Strain 1		*Enterobacter cloacae* Strain 2		2022 EUCAST breakpoints (mg/L)
	AST	MIC (mg/L)	AST	MIC (mg/L)	
Piperacillin/tazobactam	R	-	R	-	
Cefepime	R	-	R	-	
Ertapenem	S	-	R	2[a]	0.5
Imipenem	S	-	S	0.25[a]	4
Meropenem	S	-	S	0.25[a]	8
Ceftazidime/Avibactam	-	-	S	0.5[a]	8
Meropenem/Vaborbactam	-	-	S	0.06[a]	8
Imipenem/Relebactam	-	-	S	0.06 [b]	2
Tigecycline	-	-	R	1.5[a]	0.5
Fosfomycin	R	-	R	-	
Sulfamethoxazole-trimethoprim	R	-	R	-	
Ofloxacin	R	-	R	-	
Ciprofloxacin	R	-	R	-	
Amikacin	S	-	S	-	
Gentamicin	R	-	R	-	
Tobramycin	R	-	R	-	

MIC: minimum inhibitory concentration. S: Sensitive. R: Resistant. EUCAST: European Committee on Antimicrobial Susceptibility Testing. [a]MICs determined with Etest® (bioMérieux, Marcy-l'Etoile, France), [b]MICs determined with MIC test strip (MTS) (Liofilchem, Inc., Waltham, MA).

glomerular filtration rate, eGFR, at around 40 mL/min/1.73 m^2 at this point) were suspected. Therefore, we decided to change the antibiotic therapy.

Among the available therapeutic options tested, only the novel β-lactam-β-lactamase inhibitor agents, namely, ceftazidime/avibactam (CZA), I-R and MVB remained active against the carbapenem-resistant *E. cloacae* strain (Table 1). On the one hand, given the presumed toxicity of meropenem, we initially decided not to use MVB. On the other hand, I-R had the lowest minimum inhibitory concentration (MIC), at 0.06 mg/L, more than four times lower than the MIC of meropenem (0.25 mg/L) and eight time lower than the MIC of CZA (0.5 mg/L), see Table 1. A treatment with I-R was therefore administered at 1.25 g (*i.e.* 500 mg of imipenem, 500 mg of cilastatin and 250 mg of relebactam) as a 2 h infusion every 8 h. As the renal function improved (eGFR = 65 mL/min) we performed a therapeutic drug monitoring (TDM) of imipenem 7 days after I-R initiation. Blood samples for imipenem plasma concentration measurement were collected 15–30 min prior to the start of the subsequent infusion (trough or Cmin levels), then imipenem concentration were assessed utilizing an ultra-high performance liquid chromatography technique combined with high-resolution mass spectrometry as previously described (Bouglé et al., 2019). Plasma trough concentration were at 0.4 mg/L (Figure 2; Table 2). We then increased the I-R dose at 1.25 g q6h over 2 h, which allowed plasma through concentration of imipenem to reach 12 mg/L at day 12 (Figure 2; Table 2). The patient was afebrile, and the CRP level decreased to 37 mg/L. He was discharged to a rehabilitation centre.

During his stay in the rehabilitation centre, I-R dosing regimen was changed in 1.25 g as a 30 min infusion every 6 h and the TDM performed at day 20 days found an imipenem plasma through concentration of 2.3 mg/L (Figure 2; Table 2). At day 25, as the patient experienced a relapse in thoracic back pain, and CRP levels rose to 130 mg/L, he was readmitted to the infectious diseases department (Figure 2). A new spinal CT-scan showed severe osteolysis of T11-T12 with a significant posterior wall recession, resulting in a 60% central canal stenosis. At this time, we discussed two antimicrobial strategies: restarting the extended-infusion I-R over 2 h or modifying the treatment in favor of continuous infusion of MVB. As the patient renal function continued to improve (eGFR = 85 mL/min), we selected MVB 2 g (meropenem 1 g and vaborbactam 1 g) q4h as a 4-h infusion, resulting in a continuous infusion of 12 g/day of MVB. Surgical laminectomy of T11-T12 and percutaneous osteosynthesis of T9-T10 and L1-L2 were performed on day 36, to relieve central canal stenosis responsible for the pain the patient. No surgical debridement could be performed due to the spinal instability caused by the extensive osteolysis of T11-12 and no orthopaedic hardware was implanted in T11-T12 to limit the risk of bacterial biofilm formation on such implants, which would hinder antimicrobial therapy. Microbiological cultures of

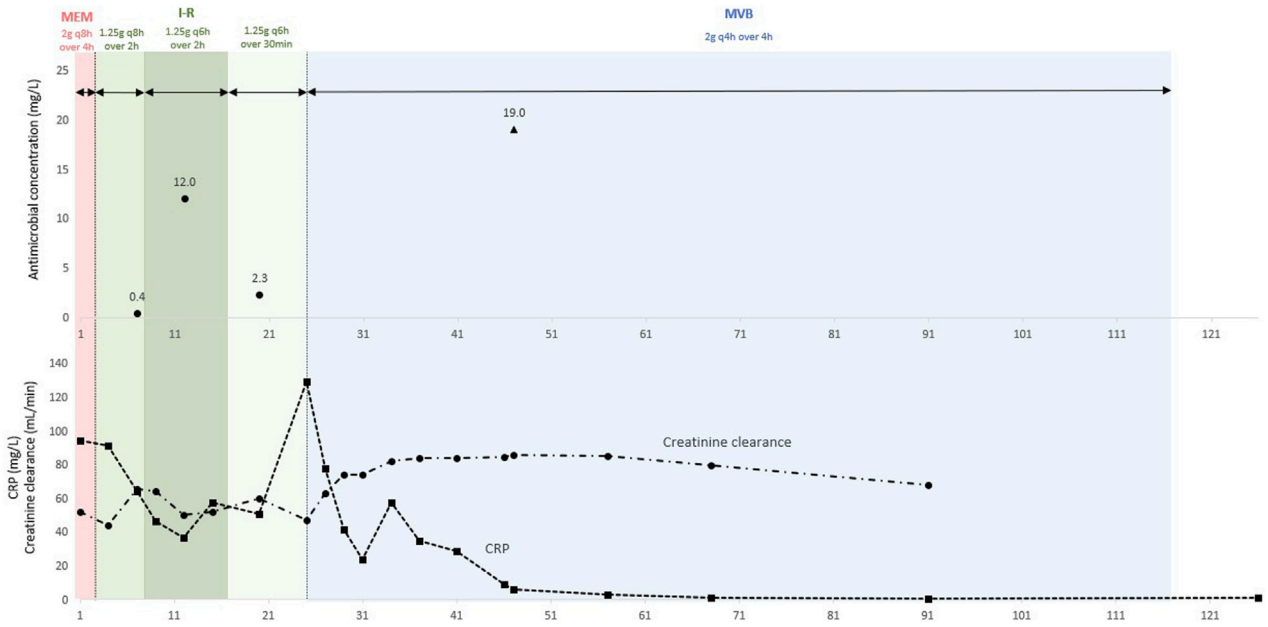

FIGURE 2
Therapeutic drug monitoring of imipenem and meropenem plasma concentrations in the patient. Imipenem through concentrations are represented by black circles and meropenem steady-state concentrations are represented by black triangles. Creatinine clearance is represented by black circles and dotted line, and C-reactive protein (CRP) is represented by black squares and dotted line.

TABLE 2 Pharmacokinetic models parameter estimates.

	Plasma concentration (mg/L)	Clearance (L/h)	Distribution volume (L)
I-R sample 1	0.4	9.39	12.6
I-R sample 2	12	8.19	12.6
I-R sample 3	2.3	9	12.6
MVB	19	13.04	12.02

PK parameters were estimated using R software version 4.2.0 (The R Foundation for Statistical Computing, Vienna, Austria) with PKPDsim version 1.3.0 and tidyverse version packages. I-R: imipenem/cilastatin/relebactam; MVB: meropenem/vaborbactam

the biopsies of the affected bone and intervertebral disc were sterile. Pain gradually decreased after the surgery. At day 47, 20 days after MVB initiation, CRP levels were at 6 mg/L. At the time, plasma concentration of meropenem was measured at 19 mg/L (Figure 2; Table 2), in a blood sample collected at steady-state using high-performance liquid chromatography coupled with Ultraviolet Detection as previously described (Larcher et al., 2023). Importantly, no sign of clinical or biological toxicity was evidenced during I-R or MVB treatment course. At day 50, the patient was afebrile with normal CRP levels and was discharged to a rehabilitation centre. One month after an antibiotic course of 90 days, the clinical outcome was favourable, and the CRP decreased to 0.5 mg/L (Figure 2).

3 Discussion

To the best of our knowledge, this is the first case of successful treatment of a vertebral osteomyelitis caused by carbapenem-resistant *E. cloacae* with continuous infusion of MVB at 2 g q4h as a 4-h infusion in a patient with normal renal clearance. This dosing regimen achieved plasma steady-state concentrations of meropenem up to 19 mg/L. In addition, our data also suggest the feasibility of extended-infusion of I-R as 1.25 g q6h over 2 h to achieve plasma through concentration of imipenem up to 12 mg/L. There were no adverse effects associated to prolonged treatment with I-R and MVB.

The treatment strategies reported herein were based on limited evidence. Few cases reported successful treatment of BJIs with novel antibiotics such as CZA (Rempenault et al., 2021; Davido et al., 2023) and I-R (Rebold et al., 2021; Larcher et al., 2022). Data on bone diffusion of ceftazidime, meropenem, and imipenem encourage their use in BJI treatments (Landersdorfer et al., 2009; Thabit et al., 2019), but no data on beta-lactamase inhibitors diffusion in bones and joints are available. However, β-lactamase inhibitors appear to have the same pharmacokinetics as the beta-lactam with which they are associated (Nicolau et al., 2015; Wenzler et al., 2017; Rizk

et al., 2018) suggesting novel β-lactam/β-lactamase inhibitors could be used in treatment of BJIs. Additionally, these new antimicrobials offer the advantage of being less nephrotoxic compared to treatment regimens based on colistin (Wunderink et al., 2018; Brown et al., 2020). Recent data indicate that while colistin monotherapy for treating BJIs caused by MDR bacteria is associated with high toxicity and mortality rates, these rates are even higher when colistin is combined with fosfomycin (Katip et al., 2024). This highlights the challenges of managing colistin and underscores the urgent need to explore more effective and less toxic alternatives, such as I-R and MVB.

As β-lactams and β-lactamase inhibitors displays mainly time-dependent killing, either extended or continuous infusion are recognized options for optimizing the time during which the antimicrobials concentration is maintained above the MIC of the treated bacteria (Abdul-Aziz et al., 2020). Optimized administrations of antimicrobial aim to improve microbiological and clinical outcome in the setting of severe diseases caused by difficult to treat bacteria (Roberts et al., 2016; Abdul-Aziz et al., 2020; Le Vavasseur and Zeller, 2022). However, few data have been published on MVB administration by continuous infusion (Larcher et al., 2023) and none on the use of I-R extended infusion. This case report therefore represents the first data available in the literature, especially in the setting of BJIs.

To improve the safety and the efficiency of off-label use of I-R and MVB in extended or prolonged infusion, we complied with the product stabilities recommended by the manufacturers (2 h for I-R and 6 h for MVB) (Summary of product characteristics: Vaborem, 2018; Summary of product characteristics: Recarbrio, 2020), and carried out therapeutic monitoring of plasma concentrations of imipenem and meropenem using a high performance liquid chromatography method (Larcher et al., 2023). We report optimized dosing regimens of I-R and MVB that achieved plasma concentrations above the MIC of most susceptible pathogens throughout the whole dosing interval (and more than 100%*f* T>4xMIC for many pathogens) (Abdul-Aziz et al., 2020). These dosing regimens enable sufficiently high plasma concentrations to be achieved, making it possible to treat infections at sites where antibiotic distribution is limited, such as BJIs (Landersdorfer et al., 2009; Thabit et al., 2019). It should be noted that surgical debridement plays an important part in achieving clinical cure, in addition to antimicrobials, especially in case of MDR bacteria, in order to reduce bacterial inoculum (Papadopoulos et al., 2019). However, in our case, surgical intervention was necessary due to spinal instability. The surgery was not specifically intended to control the source of infection but rather for mechanical reasons, as the infection was considered controlled prior to the intervention. It is also important to note that the surgical bone biopsy was negative in culture, which provides further evidence of the microbiological effectiveness of the treatments used in this case report.

Our work has limitations. First, this is a single case report, and larger-scale studies are needed to confirm our results. Second, TDM of I-R and MVB was based solely on the plasma concentration of beta-lactams (namely, imipenem and meropenem). However, as beta-lactamase inhibitors have the same pharmacokinetics as the beta-lactam with which they are associated (Nicolau et al., 2015; Wenzler et al., 2017; Rizk et al., 2018), the plasma concentration of the later can be used as a surrogate. Nonetheless, we did not obtain I-R and MVB concentrations in bone biopsies to confirm the diffusion of these new antibiotics in the affected bone, which would have been the preferred method of TDM. Last, TDM of beta-lactam is not performed every day in our hospital, and due to this fact, we were unable to confirm the meropenem overdose suspected at the beginning of the patient care.

Despite the limitations inherent to the level of evidence provided by case reports, we believe that documenting novel treatment strategies (Tamma et al., 2022) is urgently needed to address the growing challenge of antimicrobial resistance (Murray et al., 2022). This case report, in particular, illustrates how healthcare professionals, through interdisciplinary collaboration, can pave the way for novel therapeutic approaches and propose innovative solutions for managing the most challenging infections caused by MDR bacteria. Nonetheless, it remains necessary to validate these strategies on a larger scale through well-conducted clinical studies, ideally randomized controlled trials.

In conclusion, the case reported here suggest that I-R extended infusion and MVB continuous infusion are promising options for treatment of BJI caused by non-CP-CRE and CPE, provided that susceptibility to these agents is confirmed by antibiotic susceptibility testing. Further studies are essential to assess the pharmacokinetics of these β-lactam-β-lactamase inhibitor associations in BJIs. Notably, data on simultaneous measurements of β-lactam and β-lactamase inhibitor concentrations in both plasma and bone, using various administration strategies, particularly extended or continuous infusions, are needed. Additionally, clinical studies are required to validate the use of I-R and MVB for treating BJIs caused by MDR bacteria and to confirm that protocols derived from pharmacokinetic studies are effective and safe in such indications.

Data availability statement

The original contributions presented in the study are included in the article/supplementary material, further inquiries can be directed to the corresponding author.

Ethics statement

Written informed consent was obtained from the individual(s) for the publication of any potentially identifiable images or data included in this article.

Author contributions

PL-L: Writing–original draft, Writing–review and editing. TN: Writing–review and editing. AP: Writing–review and

editing. AM: Writing–review and editing. A-SP-O: Writing–review and editing. VH: Writing–review and editing. PL: Supervision, Validation, Writing–review and editing. AS: Supervision, Validation, Writing–review and editing. RL: Methodology, Supervision, Validation, Writing–original draft, Writing–review and editing.

Funding

The author(s) declare that no financial support was received for the research, authorship, and/or publication of this article.

Conflict of interest

The authors declare that the research was conducted in the absence of any commercial or financial relationships that could be construed as a potential conflict of interest.

Publisher's note

All claims expressed in this article are solely those of the authors and do not necessarily represent those of their affiliated organizations, or those of the publisher, the editors and the reviewers. Any product that may be evaluated in this article, or claim that may be made by its manufacturer, is not guaranteed or endorsed by the publisher.

References

Abdul-Aziz, M. H., Alffenaar, J.-W. C., Bassetti, M., Bracht, H., Dimopoulos, G., Marriott, D., et al. (2020). Antimicrobial therapeutic drug monitoring in critically ill adult patients: a Position Paper<sub/>. *Intensive Care Med.* 46, 1127–1153. doi:10.1007/s00134-020-06050-1

Bouglé, A., Dujardin, O., Lepère, V., Ait Hamou, N., Vidal, C., Lebreton, G., et al. (2019). PHARMECMO: therapeutic drug monitoring and adequacy of current dosing regimens of antibiotics in patients on Extracorporeal Life Support. *Anaesth. Crit. Care and Pain Med.* 38, 493–497. doi:10.1016/j.accpm.2019.02.015

Brown, M. L., Motsch, J., Kaye, K. S., File, T. M., Boucher, H. W., Vendetti, N., et al. (2020). Evaluation of renal safety between imipenem/relebactam and colistin plus imipenem in patients with imipenem-nonsusceptible bacterial infections in the randomized, phase 3 RESTORE-IMI 1 study. *Open Forum Infect. Dis.* 7, ofaa054. doi:10.1093/ofid/ofaa054

Davido, B., Crémieux, A.-C., Vaugier, I., Gatin, L., Noussair, L., Massias, L., et al. (2023). Efficacy of ceftazidime-avibactam in various combinations for the treatment of experimental osteomyelitis due to *Klebsiella pneumoniae* carbapenemase (KPC)-producing *Klebsiella pneumoniae*. *Int. J. Antimicrob. Agents* 61, 106702. doi:10.1016/j.ijantimicag.2022.106702

Katip, W., Rayanakorn, A., Oberdorfer, P., Taruangsri, P., Nampuan, T., and Okonogi, S. (2024). Comparative effectiveness and mortality of colistin monotherapy versus colistin-fosfomycin combination therapy for the treatment of carbapenem-resistant Enterobacteriaceae (CRE) infections: a propensity score analysis. *J. Infect. Public Health* 17, 727–734. doi:10.1016/j.jiph.2024.03.010

Landersdorfer, C. B., Bulitta, J. B., Kinzig, M., Holzgrabe, U., and Sörgel, F. (2009). Penetration of antibacterials into bone: pharmacokinetic, pharmacodynamic and bioanalytical considerations. *Clin. Pharmacokinet.* 48, 89–124. doi:10.2165/00003088-200948020-00002

Larcher, R., Laffont-Lozes, P., Naciri, T., Bourgeois, P.-M., Gandon, C., Magnan, C., et al. (2023). Continuous infusion of meropenem–vaborbactam for a KPC-3-producing *Klebsiella pneumoniae* bloodstream infection in a critically ill patient with augmented renal clearance. *Infection* 51, 1835–1840. doi:10.1007/s15010-023-02055-2

Larcher, R., Laffont-Lozes, P., Roger, C., Doncesco, R., Groul-Viaud, C., Martin, A., et al. (2022). Last resort beta-lactam antibiotics for treatment of New-Delhi Metallo-Beta-Lactamase producing Enterobacterales and other Difficult-to-Treat Resistance in Gram-negative bacteria: a real-life study. *Front. Cell. Infect. Microbiol.* 12, 1048633. doi:10.3389/fcimb.2022.1048633

Le Vavasseur, B., and Zeller, V. (2022). Antibiotic therapy for prosthetic joint infections: an overview. *Antibiotics* 11, 486. doi:10.3390/antibiotics11040486

Murray, C. J., Ikuta, K. S., Sharara, F., Swetschinski, L., Robles Aguilar, G., Gray, A., et al. (2022). Global burden of bacterial antimicrobial resistance in 2019: a systematic analysis. *Lancet* 399, 629–655. doi:10.1016/S0140-6736(21)02724-0

Nicolau, D. P., Siew, L., Armstrong, J., Li, J., Edeki, T., Learoyd, M., et al. (2015). Phase 1 study assessing the steady-state concentration of ceftazidime and avibactam in plasma and epithelial lining fluid following two dosing regimens. *J. Antimicrob. Chemother.* 70, 2862–2869. doi:10.1093/jac/dkv170

Papadopoulos, A., Ribera, A., Mavrogenis, A. F., Rodriguez-Pardo, D., Bonnet, E., Salles, M. J., et al. (2019). Multidrug-resistant and extensively drug-resistant Gram-negative prosthetic joint infections: role of surgery and impact of colistin administration. *Int. J. Antimicrob. Agents* 53, 294–301. doi:10.1016/j.ijantimicag.2018.10.018

Rebold, N., Morrisette, T., Lagnf, A. M., Alosaimy, S., Holger, D., Barber, K., et al. (2021). Early multicenter experience with imipenem-cilastatin-relebactam for multidrug-resistant gram-negative infections. *Open Forum Infect. Dis.* 8, ofab554. doi:10.1093/ofid/ofab554

Recarbrio (2020). Summary of product characteristics: Recarbrio. Available at: https://www.ema.europa.eu/en/documents/product-information/recarbrio-epar-product-information_en.pdf (Accessed May 28, 2023).

Rempenault, C., Pagis, V., Noussair, L., Berbescu, S., Duran, C., Bouchand, F., et al. (2021). Treatment of bone and joint infections by ceftazidime/avibactam and ceftolozane/tazobactam: a cohort study. *J. Glob. Antimicrob. Resist.* 25, 282–286. doi:10.1016/j.jgar.2021.04.003

Rizk, M. L., Rhee, E. G., Jumes, P. A., Gotfried, M. H., Zhao, T., Mangin, E., et al. (2018). Intrapulmonary pharmacokinetics of relebactam, a novel β-lactamase inhibitor, dosed in combination with imipenem-cilastatin in healthy subjects. *Antimicrob. Agents Chemother.* 62, e01411–e01417. doi:10.1128/aac.01411-17

Roberts, J. A., Abdul-Aziz, M.-H., Davis, J. S., Dulhunty, J. M., Cotta, M. O., Myburgh, J., et al. (2016). Continuous versus intermittent β-lactam infusion in severe sepsis. A meta-analysis of individual patient data from randomized trials. *Am. J. Respir. Crit. Care Med.* 194, 681–691. doi:10.1164/rccm.201601-0024OC

Tamma, P. D., Aitken, S. L., Bonomo, R. A., Mathers, A. J., van Duin, D., and Clancy, C. J. (2022). Infectious diseases society of America 2022 guidance on the treatment of extended-spectrum β-lactamase producing Enterobacterales (ESBL-E), carbapenem-resistant Enterobacterales (CRE), and *Pseudomonas aeruginosa* with difficult-to-treat resistance (DTR-P. aeruginosa). *Clin. Infect. Dis.* 75, 187–212. doi:10.1093/cid/ciac268

Thabit, A. K., Fatani, D. F., Bamakhrama, M. S., Barnawi, O. A., Basudan, L. O., and Alhejaili, S. F. (2019). Antibiotic penetration into bone and joints: an updated review. *Int. J. Infect. Dis.* 81, 128–136. doi:10.1016/j.ijid.2019.02.005

Vaborem (2018). Summary of product characteristics: Vaborem. Available at: https://www.ema.europa.eu/en/documents/product-information/vaborem-epar-product-information_en.pdf (Accessed July 16, 2023).

Wenzler, E., Ellis-Grosse, E. J., and Rodvold, K. A. (2017). Pharmacokinetics, safety, and tolerability of single-dose intravenous (ZTI-01) and oral fosfomycin in healthy volunteers. *Antimicrob. Agents Chemother.* 61, 00775-17–e817. doi:10.1128/AAC.00775-17

Wunderink, R. G., Giamarellos-Bourboulis, E. J., Rahav, G., Mathers, A. J., Bassetti, M., Vazquez, J., et al. (2018). Effect and safety of meropenem–vaborbactam versus best-available therapy in patients with carbapenem-resistant enterobacteriaceae infections: the TANGO II randomized clinical trial. *Infect. Dis. Ther.* 7, 439–455. doi:10.1007/s40121-018-0214-1

Frontiers in Pharmacology

Explores the interactions between chemicals and living beings

The most cited journal in its field, which advances access to pharmacological discoveries to prevent and treat human disease.

Discover the latest Research Topics

See more →

Frontiers

Avenue du Tribunal-Fédéral 34
1005 Lausanne, Switzerland
frontiersin.org

Contact us

+41 (0)21 510 17 00
frontiersin.org/about/contact